Model Configuration and Results

Klamath River Model for TMDL Development

Fourth Revision: December 2009
Third Revision: June 2009
Second Revision: September 2008
First Revision: September 2007
Original: September 2005

Prepared for:
U.S. Environmental Protection Agency Region 9
U.S. Environmental Protection Agency Region 10
North Coast Regional Water Quality Control Board
Oregon Department of Environmental Quality

Prepared by:
Tetra Tech, Inc.

Contents

Acknowledgments

Completion of the Klamath River Hydrodynamic and Water Quality Model for TMDL development was made possible by the generous support and responsiveness of many people. The authors would like to acknowledge the following professionals, in particular, for their contributions:

Ben Cope	U.S. Environmental Protection Agency, Region 10
Clayton Creager	North Coast Regional Water Quality Control Board
Michael Deas	Watercourse Engineering, Inc.
Mark Filippini	U.S. Environmental Protection Agency, Region 10
Susan Keydel	U.S. Environmental Protection Agency, Region 9
Steve Kirk	Oregon Department of Environmental Quality
David Leland	North Coast Regional Water Quality Control Board
Gail Louis	U.S. Environmental Protection Agency, Region 9
Bryan McFadin	North Coast Regional Water Quality Control Board
Matt St. John	North Coast Regional Water Quality Control Board
Daniel Turner	Oregon Department of Environmental Quality

Andrew Parker, Rui Zou, and Mustafa Faizullabhoy led Tetra Tech's model development and application effort.

1.0 Introduction

The Klamath River watershed traverses the states of Oregon and California, encompassing an area of approximately 15,722 square miles. The headwaters of the Klamath River originate in the Cascade Mountains and the river flows to the southwest from Oregon into northern California toward its confluence with the Pacific Ocean (Figure 1-1). Major tributaries to the Klamath River include the Lost River Diversion Channel and the Shasta, Scott, Salmon, and Trinity Rivers.

The watershed includes portions of Jackson, Josephine, Klamath, and Lake Counties in Oregon, and Del Norte, Humboldt, Modoc, Siskiyou, and Trinity Counties in California. Nearly 63 percent of the watershed (approximately 9,933 square miles) lies in California, while 37 percent (5,727 square miles) is in Oregon. The Klamath River watershed includes twelve U.S. Geological Survey (USGS) 8-digit hydrologic cataloging units, numbers 18010201 through 18010212.

The Oregon Department of Environmental Quality (ODEQ) and California's North Coast Regional Water Quality Control Board (NCRWQCB) have both included the Klamath River on their corresponding Clean Water Act section 303(d) lists as a result of observed water quality criteria exceedances. Impairments include dissolved oxygen (DO), chlorophyll *a*, temperature, pH, and ammonia for various portions of the Klamath River and its tributaries in Oregon and nutrients, temperature, and organic enrichment/low DO for segments of the river and its tributaries in California.

The states are required to develop total maximum daily loads (TMDLs) for applicable water quality parameters. The TMDL process identifies the maximum load of a pollutant a waterbody is able to assimilate and still fully support its designated uses. The TMDL process also allocates portions of the allowable load to all sources, identifies the necessary controls that may be implemented voluntarily or through regulatory means, and describes a monitoring plan and associated corrective feedback loop to ensure that uses are fully supported. Watershed and water quality modeling is often used during the development of TMDLs to help with one or more of these tasks. Modeling is a quantitative approach to better understand complex environmental processes and relationships. Models can be used to help fill in gaps in observed water quality data, estimate existing pollutant sources throughout a watershed, calculate allowable loads, and assess the potential effectiveness of various control options.

The first steps in the TMDL development process were previously conducted, including compiling available data; evaluating monitoring data to identify the extent, location, and timing of water quality impairments; and developing a technical approach to analyze the relationship between source pollutant loading contributions and in-stream response. These steps were detailed in *Data Review and Modeling Approach—Klamath and Lost Rivers TMDL Development* (Tetra Tech, Inc. 2004). Subsequent steps include model configuration, model testing (calibration), and scenario analysis. This document discusses the configuration of the Klamath River model and presents modeling results for the Klamath River from Upper Klamath Lake (UKL) to the river's outlet at the Pacific Ocean for the river and reservoir segments (2000 and 2002) and estuarine segment (2004).

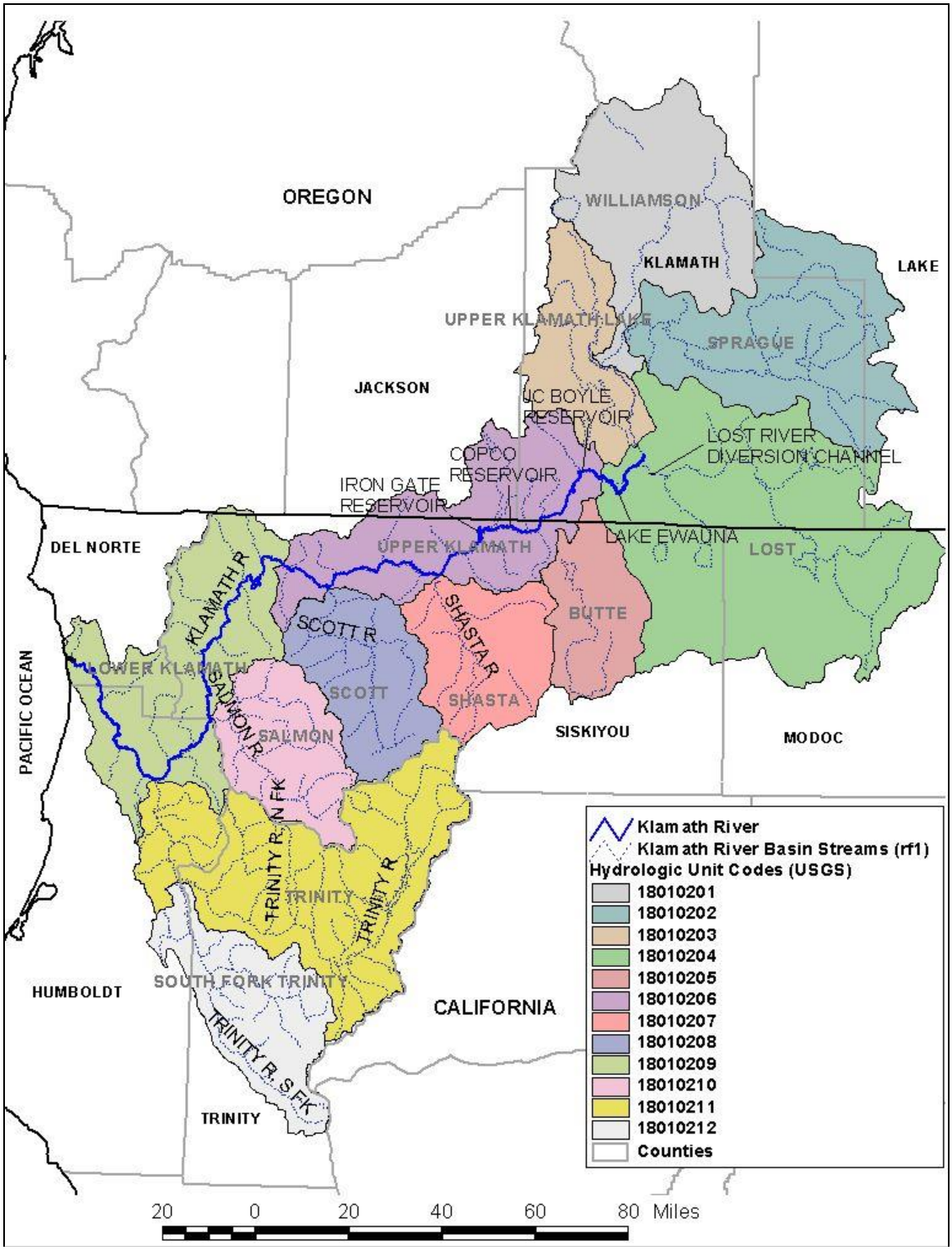

Figure 1-1. Extent of the Klamath River watershed

2.0 Modeling Approach

2.1 Model Selection

To support TMDL development for the Klamath River system, the need for an integrated receiving water hydrodynamic and water quality modeling system was identified. The following model capabilities were identified as being necessary to support TMDL development. The model must be

- Capable of predicting hydrodynamics, nutrient cycles, DO, temperature, pH, and other parameters and processes pertinent to the TMDL development effort;
- Capable of simulating the multiple flow control structures along the length of the Klamath River;
- Dynamic (time-variable) and thus capable of representing the highly variable flow and water quality conditions within years and between years;
- Capable of considering the steep channel slope of the Klamath River; and
- Capable of representing conditions in the Klamath Estuary.

A model for the Klamath River had already been developed by PacifiCorp to support studies for the Federal Energy Regulatory Commission Hydropower relicensing process (Watercourse Engineering, Inc. 2004) when this project began. The version of the model available in 2004 is hereafter referred to as the *PacifiCorp Model*. The PacifiCorp Model and other models, including the operational models MODSIM and CALSIM, were evaluated for applicability to Klamath River TMDL development (Tetra Tech, Inc. 2004). NCRWQCB, ODEQ, and the U.S. Environmental Protection Agency (EPA) determined that the existing PacifiCorp Model would provide the optimal basis, after making some enhancements, for TMDL model development. Section 2.2 provides a description of the enhancements made to the PacifiCorp Model. It should be noted that PacifiCorp has since updated the model after receiving comments from reviewers (PacifiCorp 2005).

The original PacifiCorp Model consisted of Resource Management Associates (RMA) RMA-2 and RMA-11 models and the CE-QUAL-W2 model. Specifically, the RMA-2 and RMA-11 models were applied for Link River (which is the stretch of the Klamath River from UKL to Keno Dam), Keno Dam to J.C. Boyle Reservoir, Bypass/Peaking Reach (hereafter referred to as the Bypass/Full Flow Reach), and Iron Gate Dam to Turwar. RMA-2 simulates hydrodynamics, while RMA-11 represents water quality processes. The CE-QUAL-W2 model was applied for Lake Ewauna-Keno Dam, J.C. Boyle Reservoir, Copco Reservoir, and Iron Gate Reservoir. In addition to addressing the model needs identified above, the PacifiCorp Model

- Uses hydrodynamic and water quality models with a proven track record in the environmental arena, including historical application to the Klamath River;
- Has already been reviewed by most stakeholders in the watershed;
- Can be directly compared to ODEQ, NCRWQCB and tribal water quality criteria;
- Has been preliminarily calibrated for the Klamath River and its applicability demonstrated; and
- Uses the public domain model CE-QUAL-W2 and a version of RMA that can be distributed to the public for purposes of TMDL application.

Because the estuarine portion of the Klamath River (Turwar to the Pacific Ocean) was not included in the original PacifiCorp Model, it was necessary to identify a model appropriate for modeling that portion of the river. After reviewing a 2004 bathymetric survey and grab, multiprobe, and cross-sectional profile data, it was determined that a laterally averaged 2-D model, such as CE-QUAL-W2, was not the ideal choice for modeling the estuarine portion of the Klamath River.

Hydrodynamics and water quality within the estuary are highly variable spatially and throughout the year and are greatly influenced by time of year, river flow, tidal cycle, and location of the estuary mouth (which changes because of sand bar movement). Additionally, transect temperature and salinity data in the lower estuary showed significant lateral variability, as did DO to a lesser extent. The Environmental Fluid Dynamics Code (EFDC), which is a full 3-D hydrodynamic and water quality model, was selected to model the complex estuarine environment instead.

EFDC is an EPA-endorsed and widely applied 3-D model (particularly for TMDL development). EFDC allows for representing the complex geometry of the Klamath Estuary with a boundary-fitted, curvilinear grid. The model is capable of simulating important physical processes and features, such as the circulation pattern near the funnel-shaped mouth and islands. The mouth of the estuary is very wide; however, it does not open to the Pacific Ocean completely because of the presence of a sand bar. As a result, the estuary can communicate with the ocean only through a very narrow opening in the sand bar. Configuring a CE-QUAL-W2 grid for this portion of the system would likely result in a very wide segment at the downstream end of the river. The wide segment would be linked to a very narrow segment representing the opening in the sand bar. This configuration runs the risk of resulting in computational error because of the sudden change in segment width at the most dynamic portion of the system (Cole and Wells, 2003). Although it is impossible to simulate the evolution of the existing sand bar at the estuary mouth with available technology, EFDC can potentially be used to efficiently evaluate the implications of mouth locations on hydrodynamics and water quality.

Hydrodynamics and water quality in the estuary are also highly variable throughout the year and are greatly influenced by time of year, river flow, tidal cycle, and location of the mouth. Hydrodynamic data also show significant lateral variability, as does DO to a lesser extent. It is desirable to apply a model that has the potential to represent this variability and EFDC is capable.

Additional factors leading to the choice of EFDC for modeling the estuary include the following:

- EFDC is capable of predicting hydrodynamics, nutrient cycles, DO, temperature, and other parameters and processes pertinent to the TMDL development effort for the estuarine section.
- The EFDC model is dynamic (time-variable) and thus capable of representing the highly variable flow and water quality conditions within years and between years.
- EFDC has a proven track record in the environmental arena—particularly with regard to TMDLs.
- Model results can be directly compared to ODEQ, NCRWQCB and tribal water quality criteria.
- EFDC is EPA-endorsed and supported and is included in the EPA TMDL Modeling Toolbox. It is a public domain model, fully transparent (i.e., model code), and is available free of charge. EPA also provides training and support on the application free of charge.

- EFDC has a function for blocking flows between computational cells, and this allows for efficiently evaluating the effect of the location and size of the sand bar opening, with a single grid configuration.
- The EFDC water quality module possesses a fully numerical sediment diagenesis module to predict sediment oxygen demand (SOD) and benthic nutrient flux based on organic loading to the waterbody. This improves the reliability of the model for DO and nutrient TMDLs. Although this component was not used in this study because of time and data limitations, it can be implemented in the future using the existing framework when sufficient data become available.

The combination of the enhanced PacifiCorp Model (RMA and CE-QUAL-W2) and EFDC resulted in the Klamath River model used for TMDL development. Table 2-1 identifies the modeling elements applied to each river segment.

Table 2-1. Model components applied to each Klamath River segment

Modeling segment	Segment type	Model(s)	Dimensions
Link River	River	RMA-2/RMA-11	1-D
Lake Ewauna-Keno Dam	Reservoir	CE-QUAL-W2	2-D
Keno Dam to J.C. Boyle Reservoir	River	RMA-2/RMA-11	1-D
J.C. Boyle Reservoir	Reservoir	CE-QUAL-W2	2-D
Bypass/Full Flow Reach	River	RMA-2/RMA-11	1-D
Copco Reservoir	Reservoir	CE-QUAL-W2	2-D
Iron Gate Reservoir	Reservoir	CE-QUAL-W2	2-D
Iron Gate Dam to Turwar	River	RMA-2/RMA-11	1-D
Turwar to Pacific Ocean	Estuary	EFDC	3-D

The linkages between the riverine and reservoir/estuary models identified in Table 2-1 were made by transferring time-variable flow and water quality from one model to the next (e.g., output from the Link River model became input for the Lake Ewauna-Keno Dam model). This modeling framework is consistent with available models appropriate for application to riverine/reservoir systems and is based on the PacifiCorp Model's existing modeling approach for the river system.

Each model type included (RMA, CE-QUAL-W2, and EFDC) is discussed in more detail below.

RMA

The hydrodynamic component of the RMA modeling suite, RMA-2, is a model specifically designed to assess flow response in complex river systems (Deas 2000). RMA-2 solves the full-flow equations, known as the St. Venant Equations. These equations use all terms of the conservation of momentum formulation and provide a complete description of dynamic flow conditions. The model has been widely applied (it is one of the most used full hydrodynamic models in the United States) to a variety of river and estuary systems in the United States as well as internationally.

The water quality component, RMA-11, is a general-purpose water quality model, compatible in geometry with the configuration of the RMA-2 hydrodynamic model. The model simulates advective heat transport and air-water heat exchange processes, as well as fate and transport of water quality parameters (e.g., nutrients), to produce dynamic descriptions of temperature and constituent concentration along the river reach. Input requirements include temperatures and quality of boundary flows, and meteorological data defining atmospheric conditions governing heat exchange at the air-water interface. Model output is in the form of longitudinal profiles of temperature and water quality parameters along river reaches, or time series at fixed locations.

CE-QUAL-W2

The U.S. Army Corps of Engineers' CE-QUAL-W2 is a 2-D, longitudinal/vertical (laterally averaged), hydrodynamic and water quality model (Cole and Wells, 2003). The model allows for application to streams, reservoirs, and estuaries with variable grid spacing, time-variable boundary conditions, and multiple inflows and outflows from point/nonpoint sources and precipitation.

The two major components of the model include hydrodynamics and water quality kinetics, which simulate changes in constituent concentrations. Both of these components are coupled (i.e., the hydrodynamic output is used to drive the water quality at every timestep). The hydrodynamic portion of the model predicts water surface elevations, velocities, and temperature. The ULTIMATE-QUICKEST numerical scheme used in the CE-QUAL-W2 model is designed to reduce the numerical diffusion in the vertical direction to a minimum and in areas of high gradients, reduce the undershoots and overshoots that could produce small negative concentrations. The water quality kinetics portion can simulate 21 water quality parameters including DO, nutrients, phytoplankton interactions, and pH.

EFDC

EFDC is a general purpose modeling package for simulating 1-D, 2-D, and 3-D flow, transport, and biogeochemical processes in surface water systems including rivers, lakes, estuaries, reservoirs, wetlands, and coastal regions. The EFDC model was originally developed at the Virginia Institute of Marine Science for estuarine and coastal applications. This model is now being supported by EPA and has been used extensively to support TMDL development throughout the country. In addition to hydrodynamic, salinity, and temperature transport simulation capabilities, EFDC is capable of simulating cohesive and non-cohesive sediment transport, near-field and far-field discharge dilution from multiple sources, eutrophication processes, the transport and fate of toxic contaminants in the water and sediment phases, and the transport and fate of various life stages of finfish and shellfish. Cohesive sediment refers to silt and clay particles while non-cohesive refers to anything larger than silt (e.g., sand, gravel). The EFDC model has been extensively tested, documented, and applied to environmental studies worldwide by universities, governmental agencies, and environmental consulting firms.

The structure of the EFDC model includes four major modules: (1) a hydrodynamic model, (2) a water quality model, (3) a sediment transport model, and (4) a toxics model. The water quality portion of the model simulates the spatial and temporal distributions of 22 water quality parameters including DO, suspended algae (3 groups), attached algae, various components of carbon, nitrogen, phosphorus and silica cycles, and fecal coliform bacteria. Salinity, water temperature, and total suspended solids are needed for computation of the 22 water quality parameters, and they are simulated by the hydrodynamic model.

EFDC's water quality model also includes a sediment process model, which uses a slightly modified version of the Chesapeake Bay 3-D model (Park et al. 1995). Upon receiving the particulate organic matter (OM) deposited from the overlying water column, it simulates its diagenesis and the resulting fluxes of inorganic substances (ammonium, nitrate, phosphate and silica) and SOD back to the water column. The coupling of the sediment process model with the water quality model not only enhances the model's predictive capability of water quality parameters, but also enables it to simulate the long-term changes in water quality conditions in response to changes in nutrient loads.

2.2 Model Enhancements

Although the original PacifiCorp Model (Watercourse Engineering, Inc. 2004) is capable of addressing the identified water quality issues, a number of enhancements to the model were necessary to expedite and strengthen the model for the rigors of TMDL development for the Klamath River.

Selected algorithms in the PacifiCorp Model were considered for augmentation of the modeling framework to address specific processes and support TMDL development. Enhancements were made in the following areas:

- BOD/OM unification
- Two-state algae transformation algorithm in Lake Ewauna
- Monod-type continuous SOD and OM decay
- pH simulation in RMA
- OM-dependent light extinction simulation in RMA
- Reaeration formulations
- Dynamic OM partitioning
- Periphyton carrying capacity
- Additional shading in RMA
- Second order polynomial spillway representation

2.2.1 BOD/OM Unification

It was determined that biochemical oxygen demand (BOD) should not be modeled in addition to OM because BOD itself is a surrogate for OM. The BOD compartment in the modeling system was eliminated for both the riverine (RMA model component) and reservoir (CE-QUAL-W2 model component) sections. To maintain consistency between the new version of the model and the original version in terms of organic loading, the BOD concentration in the original version was converted to an OM component by using a stoichiometric ratio of BOD:OM = 1.4. This stoichiometric coefficient was derived on the basis of the original RMA-11 model and is also consistent with representation in the CE-QUAL-W2 model. This converted OM was combined with the OM in the original version to form the total OM in the new version. This conversion allowed the model to represent consistent amounts of OM in the original and new versions.

Additionally, in the original CE-QUAL-W2 models for the reservoirs, particulate OM was not included in the tributary boundary condition files. This is expected to result in an underestimation of particulate OM into the system. Therefore, for the major tributaries that are highly productive, such as the Lost River Diversion Channel, particulate OM loading was represented on the basis of data and appropriate assumptions. Concentration boundary condition files were modified using a labile particulate OM (LPOM) to labile dissolved OM (LDOM) ratio of 4.0 (LPOM:LDOM = 0.8:0.2), which is same as for the Link River boundary condition. Labile OM refers to the portion that is decomposed relatively quickly.

2.2.2 Two-state Algae Transformation Algorithm in Lake Ewauna

Very low levels of phytoplankton were observed in lower Lake Ewauna, as shown in the year 2000 monitoring data for the Highway (Hwy) 66 station. Phytoplankton biomass in Lake Ewauna also shows significant variability from upstream (Miller Island water quality station) to downstream (Hwy 66 water quality station). In addition, observed data show that there was a sharp drop in algae concentration at the Miller Island station during the summer. These phenomena were not predicted by the existing PacifiCorp Model, although it is configured to simulate all algae-DO-nutrient interactions represented in the W2 model code.

Simulated algae biomass in the existing PacifiCorp Model is similar at both locations, and algae concentrations remained high throughout the summer period. This is due to the dominant upstream inflow (from UKL) that causes water to flow quickly from upstream to downstream. The inability to accurately predict the temporal and spatial distribution of phytoplankton has significant implications on the water quality dynamics. Therefore, model refinement was needed to better represent the algae dynamics in this lake.

It appears that with the existing kinetic structure in the model, it is not possible to reproduce this type of spatial distribution of algae biomass. During the model testing process, which is described later in this report, the algae growth and mortality parameters were varied significantly in an attempt to reproduce the observed spatial algae pattern in Lake Ewauna. Regardless of the parameter combinations used, the model predicted similar algae magnitudes and patterns at the Miller Island and Hwy 66 stations (due in large part to the rapid transport of algae in Lake Ewauna). It is believed that the summer hypoxia/anoxia in the lake influences the spatial variability of algae biomass in Lake Ewauna. Data show that sometimes during the summer, the entire Lake Ewauna water column becomes hypoxic (exhibiting very low DO concentrations), and even anoxic (exhibiting DO concentrations near zero). Figure 2-1 shows the observed DO data, along with chlorophyll *a*, at the Miller Island and Hwy 66 locations for 2000 (at approximately 1 meter from the surface). Algal mortality has been causally linked with low DO in UKL (National Research Council 2004) and found to be related to anoxic conditions in other systems (Baric et al. 2003). Available data show no other explanation for the observed phenomenon.

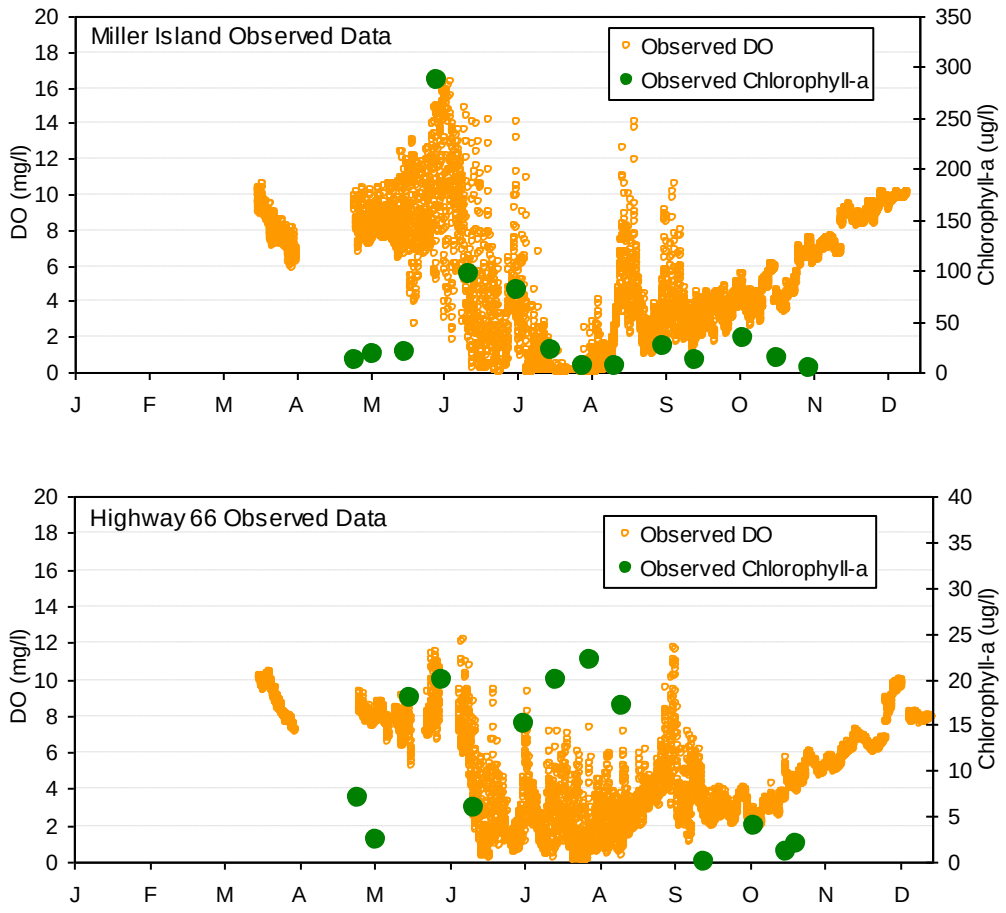

Figure 2-1. Observed DO and Algae at sites in Lake Ewauna (2000)

Algae need oxygen to respire. Thus, when oxygen levels become low or depleted, algae metabolism might be affected. Growth is likely to be slowed down, and death/excretion is likely to increase. In addition to directly affecting algae metabolism, the hypoxia/anoxic condition from top to bottom in the lake can result in excessive concentration of undesirable chemicals such as H2S in the water column, which is highly toxic to phytoplankton. Previous scientific investigations do not indicate whether DO or other undesirable chemicals directly cause the observed pattern, however the impacts of all these factors (since they are manifested under low DO conditions) can be mathematically represented through DO concentration alone. Therefore, DO-dependent algae kinetics representation was deemed the most appropriate approach for representing the phenomenon.

The major assumptions associated with the DO-dependent algae kinetics are the following:

- Low DO concentrations can restrict algae growth and enhance algae death due to either the directly effect on metabolism or indirect effect through chemical toxicity.
- The longer algae are exposed to hypoxia/anoxia or toxic water environment associated with these conditions, the more the algae mortality is enhanced.

Using these assumptions, a model capable of simulating the impact of hypoxic/anoxic conditions on algae dynamics not only needs to represent the dependence of algae on DO concentrations, but

it needs to track the duration of exposure of algae to these conditions. For example, a cluster of algae in Link River (before entering hypoxic Lake Ewauna) is free of the effects of low DO concentrations. However, after this cluster enters Lake Ewauna, it is subjected to local hypoxic conditions (while being transported downstream). The effect of the hypoxic/anoxic conditions on the algae becomes more severe with distance downstream because the exposure time to these conditions increases. This exposure time is hereby referred to as *ET*, and it is not the same as the time that the DO is hypoxic/anoxic at a specific location, which is referred to as *THA*.

CE-QUAL-W2, like most numerical hydrodynamic and water quality models, is based on the Eulerian system that does not track the history of travel of particles. Therefore, it is very difficult to directly track the ET of a specific cluster of algae. The PacifiCorp Model was unable to reproduce the sharp algae decline from upstream to downstream in Lake Ewauna, in part because it was unable to consider exposure time. In this study, a two-state algae transformation approach was applied to the model as a surrogate for representing the effect of the ET. The approach involves defining two states of algae, where one state represents the *healthy* group which is free of the hypoxic/anoxic impact and the other state represents the *unhealthy* group (for which the physiological condition is severely disturbed because of hypoxia/anoxia). The healthy group is represented using typical algae growth and respiration rates; however, the unhealthy algae growth and respiration rates are very low or 0.0 (because of the hypoxic/anoxic condition's effect on the algae's physiology).

The ET is indirectly represented through conversion of healthy algae to unhealthy algae using a first-order transformation mechanism when the algae are in the presence of low-DO conditions. The longer the algae are exposed to hypoxia/anoxia, the higher the fraction of algae transformed into the unhealthy state becomes. Thus, the overall growth and respiration rate of the entire algae cluster is reduced because of the larger amount of unhealthy algae. In the following equations, *A* denotes the healthy group and *B* denotes the unhealthy group:

$$\frac{dC_A}{dt} = L_A - K_1 C_A + K_2 C_B \qquad (1)$$

$$\frac{dC_B}{dt} = L_B + K_1 C_A - K_2 C_B \qquad (2)$$

where

C_A = concentration of algae group A
C_B = concentration of algae group B
L_A = total sources and sinks including kinetics for algae group A as represented in the original model
L_B = total sources and sinks including kinetics for algae group B as represented in the original model
K_1 = transformation rate from algae group A to B
K_2 = recovering rate from algae group B to A

The effect of low DO on the kinetic parameters K_1 and K_2 is represented as:

$$K_1 = K_{1(0)} \frac{HDO_1}{HDO_1 + DO} \qquad (3)$$

$$K_2 = K_{2(0)} \frac{DO}{HDO_2 + DO} \quad (4)$$

where

$K_{1(0)}$ = the base transformation rate from algae group A to B
$K_{2(0)}$ = the base recovering rate from algae group B to A
DO = the DO concentration in the water column
HDO_1 = the half saturation coefficient in mg oxygen /L for K_1
HDO_2 = the half saturation coefficient in mg oxygen/L for K_2

The mechanisms described in Equations (1) through (4) were incorporated into the CE-QUAL-CE-QUAL-W2 source code. The model was then run for Lake Ewauna, and the results indicated that the model was capable of explaining the observed algae patterns reasonably well. It should be noted that the assumptions, mathematical formulations, and code development for algae kinetics are based on general scientific knowledge of algae metabolism. It is recommended that further research be conducted to investigate the impact and response relationships among DO, water chemistry changes, and algae metabolism to better understand this complex phenomenon.

2.2.3 Monod-Type SOD and OM Decay

The PacifiCorp Model used the CE-QUAL-W2 code, which represents SOD and OM decay as a delta function. With the delta function, the SOD and OM decay are activated when DO is greater than a pre-specified value (generally close to zero), and deactivated when DO is lower than the value. This leads to abruptly turning SOD and OM decay on and off when DO is low or fluctuates around the pre-specified value. A Monod-type continuous SOD and OM decay formulation was thus incorporated into the CE-QUAL-W2 code to represent a smoother transition of SOD and OM decay effects when DO is low.

$$SOD = \frac{DO}{DO + HDO} SOD_s$$

$$Kd = \frac{DO}{DO + HDM} Kd_s$$

where

SOD = effective SOD (g O_2/m^2/day)
DO = DO concentration in the water column for Kd, or in the bottom water for SOD (milligrams per liter [mg/L])
HDO = half saturation DO concentration (mg/L)
SOD_s = SOD before being adjusted by the water column DO (g O_2/m^2/day)
Kd = effective OM decay rate (1/day)
HDM = half saturation DO concentration for OM decay rate adjustment (mg/L)
Kd_s = OM decay rate before DO adjustment (1/day)

2.2.4 pH Simulation Module in RMA

The standard RMA modeling framework does not have the capability of simulating interactions among nutrients, phytoplankton/benthic algae, and pH. Because pH is a key water quality target for Klamath TMDL development, the modeling framework was enhanced to dynamically simulate pH dynamics.

A pH simulation module was developed and incorporated into the RMA framework to simulate the pH in the river, considering the impact of boundary conditions, phytoplankton, periphyton, benthic sources, and atmospheric-water exchange. The state variables for the pH module include Total Inorganic Carbon (TIC) and Alkalinity (Alk). Their transport is simulated using the same algorithms used for transporting other dissolved constituents in RMA. While Alk is assumed to be conservative in the water column, TIC changes due to several physical (water-air interface exchange), chemical (OM decay and benthic sources), and biological (phytoplankton and benthic algae metabolism) factors. The mathematical equations for the pH module are based on those described in Chapter 39 of Chapra (1997), and are detailed in Appendix A.

2.2.5 OM-dependent Light Extinction Formulation in RMA

The existing RMA model does not have the capability of representing the effect of OM on light conditions. Thus, it can inaccurately predict periphyton or phytoplankton growth in the presence of OM. OM can reduce sunlight and limit aquatic vegetation growth. An OM-dependent light extinction formulation was developed using the same formulation in the CE-QUAL-W2 model and incorporated into the RMA code to provide a more realistic representation of the system:

$$Ke = Ke' + OM \times KEOM$$

where

Ke = effective light extinction coefficient
Ke' = light extinction coefficient before OM adjustment
OM = OM concentration
KEOM = light extinction coefficient adjustment factor related to OM concentration

2.2.6 Reaeration Formulation Modification

In the existing RMA-11 model, the flow velocity used for reaeration calculation was forced to be greater than or equal to 0.5 meters per second (m/s). This resulted in excessive reaeration when the flow velocity was actually slower (e.g., during low-flow conditions). A modification was made to this formulation to set the lower bound of the velocity to 0.03 m/s based on Chapra (1997). This modification results in more reasonable DO predictions under low flow, critical conditions.

A scaling factor was also introduced into the RMA-11 model to enhance reaeration just downstream of Iron Gate Dam. At this location, the observed summer DO concentration is much higher than what can be predicted by RMA-11 using the available empirical formulas. In the model, the DO concentration of water exiting Iron Gate Reservoir during the summer is low due to vertical stratification in the reservoir (and thus low DO concentrations at depths from which water is drawn). Significant reaeration is necessary over a very short distance to increase the low DO concentrations to the significantly higher observed concentrations. The RMA-11 formulas,

however, are unable to replicate this phenomenon, which is caused by the presence of significant turbulence downstream of Iron Gate Dam. To account for this observed phenomenon, a scaling factor (or multiplier) was introduced into the RMA-11 model. After multiple iterations during model testing, a value of 100.0 was selected. Application of this scaling factor results in a significantly higher coefficient than what is typically used with the RMA-11 formulas, however, it is necessary (and justifiable) to simulate the observed DO concentrations.

2.2.7 Dynamic OM Partitioning

Key updates were made to the original PacifiCorp Model to transfer model results between segments represented using CE-QUAL-W2 and those represented using RMA. Originally, the upstream boundary conditions for a CE-QUAL-W2 reservoir model were based on model results from the upstream riverine RMA model. In RMA all the OM is represented as a lumped parameter, while in W2 they are partitioned into four different components: LPOM, RPOM, LDOM, and RDOM. Therefore, when transferring the RMA OM results to W2, the OM output must be partitioned into the four components for W2. In the existing PacifiCorp Model, a static partitioning ratio of 0.8:0.2 was used to partition the OM into LPOM and LDOM, respectively. This static conversion factor does not account for the change in OM composition that occurs throughout the system. Therefore, a dynamic OM partitioning scheme was implemented that calculates and tracks the time-variable partitioning ratio in the reservoir models and applies the ratios to downstream segments. Using this approach, different ratios are implemented for J.C. Boyle and Copco reservoirs. For J.C. Boyle Reservoir, the OM in the upstream river flow is partitioned in such a way that, on average, LDOM accounts for 62 percent, LPOM 36 percent, RDOM 1 percent, and RPOM 1 percent. For Copco Reservoir, the corresponding values are: 67 percent, 30 percent, 2 percent, and 1 percent. These values demonstrate that the fraction of dissolved OM increases with downstream distance, while the fraction of particulate OM decreases (because of the effect of settling).

2.2.8 Periphyton Carrying Capacity

In the RMA-11 model code used in the PacifiCorp Model, the carrying capacity of periphyton biomass was implemented such that when the simulated periphyton biomass exceeds a prescribed maximum value, the simulated biomass is set to that value. This method of handling the periphyton carrying capacity results in unbalanced nutrient representation in the system. When the simulated biomass exceeds the prescribed maximum value, additional nutrients are not utilized by the periphyton biomass (as they would be should no maximum be set). The PacifiCorp Model predicts that the periphyton biomass remains constant for an extended period of time during the summer. Not only is this unrealistic, but it is equivalent to artificially removing nutrients from the system.

A more reasonable way of reflecting the growth limitation when the simulated periphyton approaches the carrying capacity is to relate the growth rate to the biomass itself. Thus growth is depressed when biomass is high, but it has no impact when biomass is low. The formula is:

$$G_e = G \times (1 - C/Cmax)$$

where

G_e = effective growth rate of periphyton (day^{-1})
G = growth rate before adjusting for carrying capacity (self-limiting) effects

C = periphyton biomass (g/m^2)
C_{max} = periphyton carrying capacity (g/m^2)

When the periphyton biomass increases, the corresponding effective growth rate decreases. When the biomass reaches the carrying capacity, the effective growth rate becomes 0.0. Since nutrient uptake is coupled with periphyton growth in water quality models, formulating the effect of carrying capacity in this manner guarantees a balanced nutrient budget in the system.

2.2.9 Additional Shading in RMA

Temperature simulated by the PacifiCorp Model for the Bypass/Full Flow Reach downstream of J.C. Boyle Reservoir was significantly higher than the observed data. Therefore, during the model testing process one of the most influential factors, the representation of solar radiation, was explored. RMA-11 uses empirical equations to internally calculate solar radiation for the thermal and bio-chemical simulations. These equations are based on longitude, altitude, sunrise and sunset time, and cloud condition. To evaluate whether or not RMA-11 was appropriately estimating solar radiation in this area, the RMA-11-estimated solar radiation was compared to the solar radiation data used in the Copco Reservoir CE-QUAL-W2 model. It was found that the solar radiation estimated using RMA-11 is approximately 20% higher than that used in the Copco Reservoir CE-QUAL-W2 model. This apparent over-estimation of solar radiation likely caused the overprediction of temperature noted above. To account for this discrepancy and to reduce the solar radiation calculated by RMA-11, additional shading was configured in the model. A value of 20% was selected based on the comparison made. To maintain consistency among all the RMA-11 models used for the Klamath River, this 20% additional shading was applied to all RMA-11 models. No changes were necessary for the CE-QUAL-W2 or EFDC models since solar radiation is handled differently for those models and because temperature predictions were not uniformly over- or under-estimated.

2.2.10 Second Order Polynomial Spillway Representation

To support TMDL development, The Klamath River model will not only be used to represent the current condition, but it will be used to represent conditions prior to the creation of Keno Dam. Based on information provided by the U.S. Bureau of Reclamation (USBR), a version of the CE-QUAL-W2 model for Lake Ewauna-Keno Dam was developed to represent the historical presence of Keno Reef (McGlashan and Dean 1913). The approach taken to represent the reef required modification of the CE-QUAL-W2 model code. Specifically, Keno Reef was represented in the model using a second-order spillway equation derived by USBR from historical data. The formulation of the spillway equation is:

$$Q=101.265(H-1244.5)^2-15.030(H-1244.5)+12.35$$

where

Q = flow rate over Keno Reef (cms)
H = water surface elevation (m)
1244.5 = the Keno Reef datum (m).

2.3 Model Configuration

Model configuration involved setting up the model computational grid (bathymetry) using available geometric data, designating the model's state variables, setting boundary conditions, and setting initial conditions. This section describes briefly the configuration process and key components of the model in greater detail.

2.3.1 Segmentation/Computational Grid Setup

The computational grid setup defines the process of segmenting the entire Klamath River into smaller computational segments for application of the model. In general, bathymetry is the most critical component in developing the grid for the system.

The Klamath River model includes the entire Klamath River from Link Dam (at the outlet of the UKL) to the Pacific Ocean. The river is impounded by five dams along its length: Keno, J.C. Boyle, Copco, Copco 2, and Iron Gate Dam. For this modeling study, the Klamath River was divided into nine waterbodies (or Model Segments). Figures 2-2 and 2-3 show each of the waterbodies from upstream to downstream. Note that distances for each waterbody are approximate. Appendix B presents an excerpt (verbatim) from *Klamath River Water Quality Model Implementation, Calibration, and Validation* (PacifiCorp 2005) that summarizes geometric information for all waterbodies. Each of these waterbodies was represented using unique geometric and hydrological characteristics in the model and is detailed in subsequent sections.

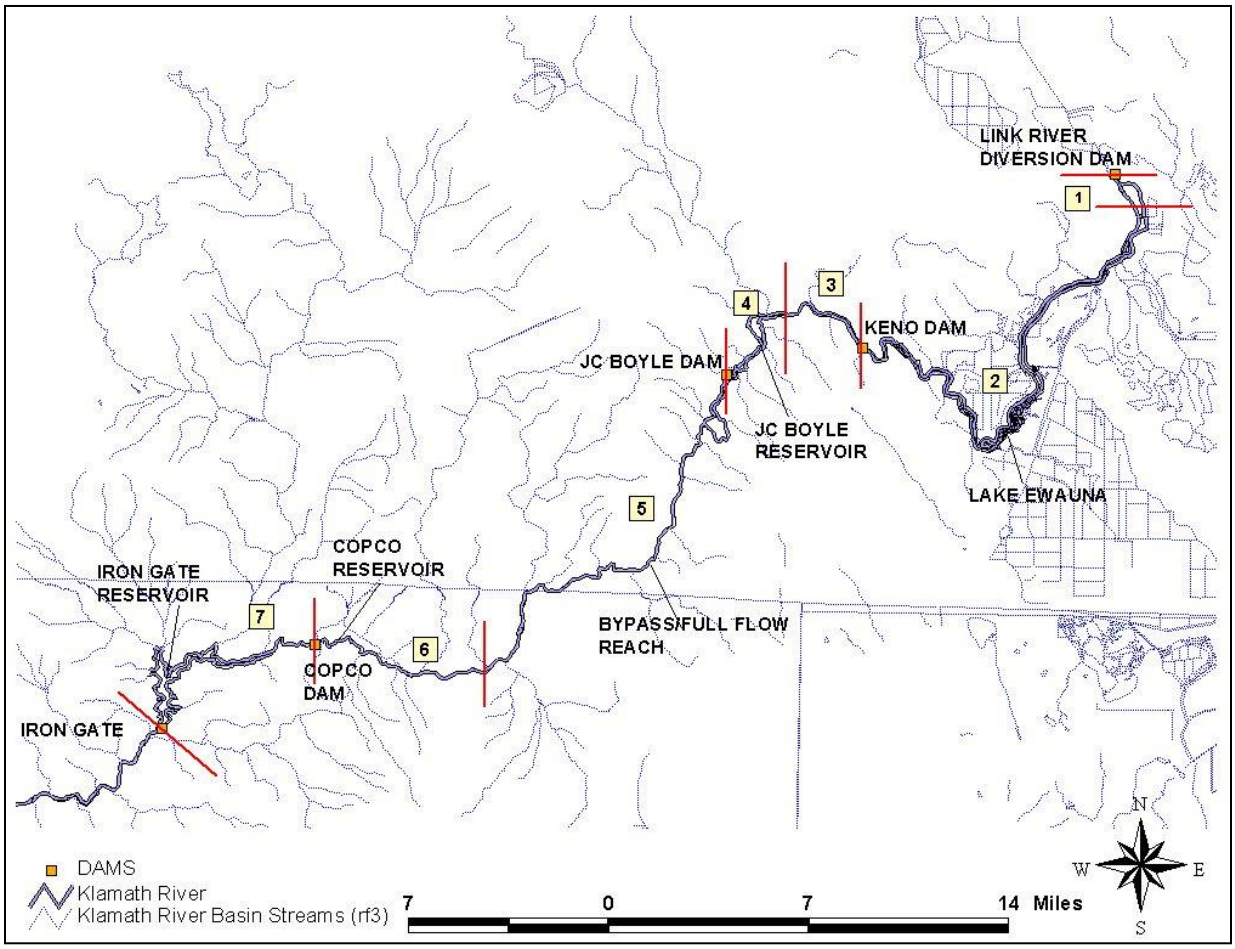

Figure 2-2. Location of waterbodies 1 through 7 along the Klamath River

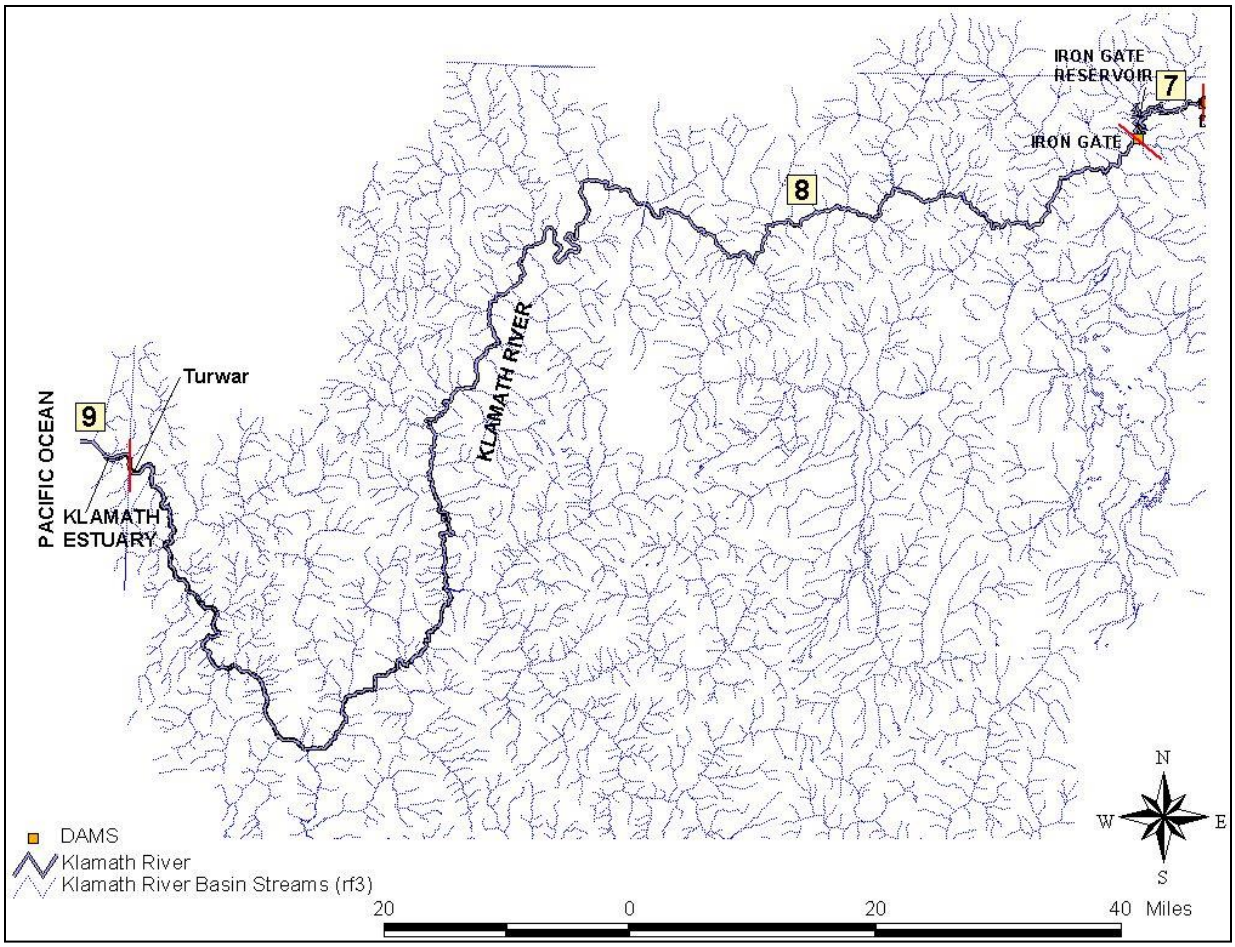

Figure 2-3. Location of waterbodies 7 through 9 along the Klamath River

2.3.1.1 Segmentation of River and Reservoir Segments

Within each of these separate Model Segments (excluding the Klamath Estuary) the primary waterbody (either a Klamath River section or a reservoir) was subdivided into higher resolution elements for greater detail in modeling. The TMDL modeling framework components were segmented similarly to the existing PacifiCorp Model. For the reservoir/lake models in the existing PacifiCorp Model (Lake Ewauna, J.C. Boyle Reservoir, Copco Reservoir, and Iron Gate Reservoir), the corresponding CE-QUAL-W2 models have layer thicknesses (depths) ranging from 0.61 to 1.0 meters and segment lengths ranging from 37 to 714 meters. For the riverine reaches (Link River, Keno reach, Bypass/Full Flow Reach downstream of J.C. Boyle Reservoir, and Klamath River from Iron Gate Dam to Turwar), the corresponding finite element model RMA has node distances ranging from 75 to approximately 300 meters (and are assumed to be homogeneous in the vertical direction). For greater detail on model segmentation in the river and reservoir segments of the Klamath River model, see Section 2.3 of the *PacifiCorp Report.*

Only the mainstem Klamath River and its reservoirs were simulated with the Klamath River model. All tributaries to the river were represented as boundary conditions (i.e., they were not

explicitly modeled). More detailed information regarding the specific tributaries to be included or inflows to the model are included in Section 2.3.3 of this report.

2.3.1.2 Segmentation of the Klamath Estuary Segment

The tidal portion of the Klamath River from Turwar to the Pacific Ocean, which was not included in the existing PacifiCorp Model, was modeled using EFDC. The first step to configure EFDC was to discretize the waterbody into a computational grid. A boundary-fit curvilinear grid was developed to accurately represent the shape of the river. Significant hydraulic features (channels, shorelines, and major bathymetric variability) and their locations were considered in preparation of the grid. The grid consists of 138 curvilinear grid cells, with widths ranging from 99 to 209 meters and lengths from 192 to 1590 meters. Within the modeling domain, each cell is represented by four vertical layer(s), therefore a 3-D spatial representation represents the estuary portion.

The open boundary at the downstream end of the estuary was extended into the Pacific Ocean to reduce the effect of boundary reflection. This would likely occur if the open boundary was set directly at the opening of the sand bar. Appendix C presents the computational grid for the Klamath Estuary EFDC model. The bold red line in Appendix C represents the impermeable barriers added to the EFDC grid. The barriers allow for the water to flow through the outlet, as seen in the 2004 bathymetry data. These barriers may be reconfigured in the future, if needed, to simulate the sandbar opening at a different location. It should be noted that this grid was developed and refined through an iterative process wherein model resolution, accuracy, and simulation time were optimized. The number of layers was determined by configuring a model with eight vertical layers in addition to the version with four vertical layers and comparing predictions. The comparison indicated that refining the vertical resolution beyond four vertical layers would not lead to significantly improved model predictions with regard to vertical variability in salinity and water quality. The four layer representation reduced computational time without compromising model accuracy.

Bathymetry data for the Klamath Estuary were obtained from the NCRWQCB and represent bathymetric conditions in the year 2004. These data contain xyz format coordinate elevation data relative to North American Datum of 1988 (NAVD88) and were directly incorporated into the grid generation process. Bathymetry data were available from the outlet of the Klamath at the Pacific Ocean upstream to the Rt. 101 Bridge (Hwy 101 @ Klamath). No bathymetry data were available from the Rt. 101 Bridge upstream to the USGS Klamath River near Klamath station (USGS 11530500) (a distance of approximately 3,300 meters). To address this data gap, a constant bed slope similar to the upstream portion of the bathymetry data (where the bathymetry was measured) was assumed. This slope was refined until tidal impacts were properly represented (i.e., no tidal effect was observed at Turwar).

River bank boundaries for the grid were defined using digital orthophotography obtained from the California Spatial Information Library (CaSIL) (http://gis.ca.gov/). Orthophotography was used instead of USGS quadrangle images due to the age of the USGS quadrangles. For example, the Requa, CA USGS quadrangle was last revised in 1966, while Requa orthophotography represents conditions in 1998. The images were georeferenced to a Universal Transverse Mercator (UTM) Zone 10 projection, using a NAD 1927 horizontal datum. This coordinate system was then used to develop the horizontal dimensions of the grid and calculate the dimensions of the computational cells.

2.3.2 State Variables

Selection of appropriate model state variables to represent water quality processes of concern is a critical factor in model configuration. For this study, state variables were selected to most accurately predict TMDL impairments and related physical, chemical, and biological processes. State variables varied for each model type in the Klamath River model (RMA, CE-QUAL-W2, and EFDC). Note that pH is not a state variable. It is computed from alkalinity and TIC. Alkalinity and TIC are transported by the model and are thus state variables. The following state variables were configured for the riverine segments of the Klamath River model (for the RMA portions of the model):

1. Arbitrary Constituent (configured as a tracer to evaluate the mass balance)
2. DO
3. Organic matter (OM)
4. Orthophosphorus (PO_4)
5. Ammonium (NH_4)
6. Nitrite (NO_2)
7. Nitrate (NO_3)
8. Phytoplankton
9. Temperature
10. Periphyton
11. Total inorganic carbon (TIC)
12. Alkalinity (Alk)

The reservoir segments of the Klamath River, where the CE-QUAL-W2 model was applied, were configured using the following active state variables:

1. Labile dissolved organic matter (LDOM)
2. Refractory dissolved organic matter (RDOM)
3. Labile particulate organic matter (LPOM)
4. Refractory particulate organic matter (RPOM)
5. Inorganic Suspended Solids (ISS)
6. PO_4
7. NH_4
8. NO_2/NO_3
9. DO
10. Phytoplankton
11. Alk
12. TIC
13. Temperature
14. Tracer
15. TDS
16. Age (to track detention time at different locations)
17. Coliform bacteria

The estuarine portion of the Klamath River, which was modeled using EFDC, was configured with the following constituents as state variables:

1. Phytoplankton
2. Labile particulate organic carbon (LPOC)
3. Labile dissolved organic carbon (LDOC)
4. Labile particulate organic phosphorous (LPOP)
5. Labile dissolved organic phosphorous (LDOP)

6. PO_4
7. Labile particulate organic nitrogen (LPON)
8. Labile dissolved organic nitrogen (LDON)
9. NH_4
10. NO_2/NO_3
11. DO
12. Temperature
13. Salinity
14. Periphyton

The RMA model considers a single, lumped OM constituent while the CE-QUAL-W2 model contains four compartments (LDOM, RDOM, LPOM, and RPOM). Because available data are insufficient to accurately partition between labile and refractory components and because RMA only considers lumped OM, all the OM boundary conditions configured for the reservoir models were partitioned between only dissolved and particulate components. Further partitioning between labile and refractory components was not implemented. It's important to note that the state variable slots in the CE-QUAL-W2 models for labile OM (i.e., LDOM and LPOM) were used to represent the all dissolved OM and particulate OM, respectively. Therefore, even though the terms "LDOM" and "LPOM" are used when referring to model results, the values essentially represent all OM, without differentiating between labile and refractory components. Because average values are used in the model to represent characteristics such as decay rate, the model can be considered to inherently include some amount of both fast- and slow-decaying OM material (i.e., some amount of labile and refractory material). The model was configured such that a small amount of true refractory OM can be generated through algal metabolism, however, this amount is typically negligible. For the EFDC model of the estuary, the organic nutrients were not partitioned between labile and refractory components either. Rather ,they were lumped together and represented using the labile state variable slots.

The schematic below (Figure 2-4) shows the flow of OM to and from each of the models. The 0.8:0.2 ratio for partitioning OM was used in the existing PacifiCorp Model and was based on the CE-QUAL-W2 algae partition coefficient (APOM = 0.8). The RMA to W2 conversion shown in Figure 2-4 does not apply to the upstream boundary conditions for J.C. Boyle and Copco reservoirs, because dynamic OM partitioning was implemented (as previously discussed). For Link River, where no upstream dynamic reservoir model was available, the static partitioning shown in Figure 2-4 was implemented.

For model calibration, the EFDC upstream boundary condition was derived using 2004 monitoring data. Therefore, no OM conversion from the upstream RMA model was necessary. When modeling scenarios were run (which are not addressed in this report), the upstream RMA model representing Irongate to Turwar was linked to the estuary EFDC model. For this case, OM from the RMA model was converted into organic nitrogen (ON), organic phosphorous (OP), and organic carbon (OC) components for the EFDC model. This conversion is based on the stoichiometric ratio used in the upstream W2 and RMA models, where OM multipliers are the following: ON = 0.07, OP = 0.0055, and OC = 0.45 (Cole and Wells 2003). To further partition the ON, OP, and OC into particulate/dissolved components, the ratios presented in Figure 2-4 were used.

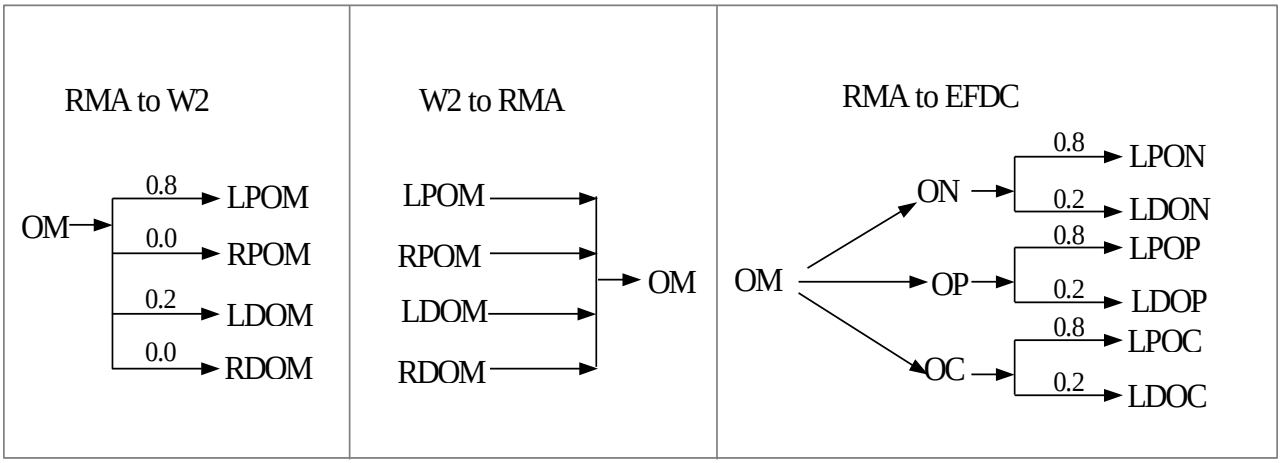

Note: The RMA to W2 conversion shown above does not apply to the upstream boundary conditions for J.C. Boyle and Copco reservoirs, where dynamic OM partitioning was applied. The RMA to EFDC representation does not reflect calibration conditions, rather it summarizes transfer used during scenario analysis.

Figure 2-4. Schematic showing the transfer of OM between models

2.3.3 Boundary Conditions

To run the Klamath River model, external forcing factors known as boundary conditions must be specified for the system. These forcing factors are a critical component in the modeling process and have direct implications on the quality of the model's predictions. External forcing factors include a wide range of dynamic information:

- Upstream Inflow Boundary Conditions: Upstream external inflows, temperature, and constituent boundary conditions
- Tributary (or Lateral) Inflow Boundary Conditions: Tributary inflows, temperature, and constituent boundary conditions
- Withdrawal Boundary Conditions
- Surface Boundary Conditions: Atmospheric conditions (including wind, air temperature, solar radiation)

Upstream external inflows essentially represent the inflow at the model's *starting* point. Tributary inflows represent the major tributaries that feed into the Klamath River. All water removed from the system is combined within the withdrawals category.

The surface boundary conditions are determined by the meteorological or atmospheric conditions and include air temperature, dew point temperature, wind speed, wind direction, and cloud cover. The meteorological file from the original PacifiCorp Model was maintained since it was based on real data and was intensively reviewed. Data obtained from station KFLO near Klamath Falls were used to represent the conditions from Link Dam to J.C. Boyle Dam. Data from Brazie Ranch represent the boundary conditions from J.C. Boyle Dam to Seiad Valley. For the reach from Seiad Valley to Turwar, the weather data from Hoopa and Somes Bar were used to represent the meteorological boundary conditions. Data from the Arcata Eureka Airport were applied to the estuarine portion of the Klamath River (Turwar to the Pacific Ocean), as described later in Section 2.3.3.9.

The following subsections provide a detailed description of the boundary conditions used to represent each modeled segment. The descriptions begin upstream at the Link River segment and continue downstream to the Klamath Estuary segment. In the existing PacifiCorp Model, boundary conditions were set as time series at each location on the basis of observed data or other assumptions where data were not available. For periods when no data were available, the model internally estimates the boundary on the basis of linearly interpolating the time series provided in the boundary condition files. In some situations, boundary conditions were updated using more recently acquired monitoring data. Both types of modification are further described in this section.

The upper and middle segments of the model (Model Segments 1 through 8) were tested (calibrated) using data from the year 2000. In addition, the calibration of the upper segments (Model Segments 1 through 5) was further corroborated (validated) with observed data for 2002. The estuarine portion (Model Segment 9), which was modeled with EFDC, was calibrated using data from the year 2004. As described in Section 3.0, these periods were selected because of data availability. In subsequent discussions, boundary condition descriptions are first described for the year 2000. Any deviations from the year 2000 representation for the year 2002 are then noted.

2.3.3.1 Model Segment 1: Link River

The Link River segment begins at the outlet of UKL (Link Dam) and ends at Lake Ewauna. Four types of boundary conditions were included in this model segment: upstream inflow boundary conditions, tributary boundary conditions, downstream stage-discharge boundary conditions, and surface boundary conditions (discussed above).

Upstream Inflow Boundary Conditions: The inflow to Link River is from UKL through releases from Link Dam. Since there were no observed data available at the head of Link River for 2000, observed water quality data at Pelican Marina (in UKL) were used as the basis for upstream boundary conditions. This representation is different than that in the existing PacifiCorp Model which used multiple year composite data for Link River at Fremont Bridge as the basis of boundary condition. Considering the significant inter-year variability in water quality in UKL, it is preferable to use data collected during the modeling year rather than other years to represent the external forces at boundaries. Monitoring data for NH_4, NO_2/NO_3, phytoplankton, DO, and temperature were directly applied to the boundary conditions using a linear interpolation method to obtain daily values for dates without data. OM boundary conditions were derived using observed total phosphorus (TP), dissolved PO_4, and chlorophyll *a* data and following these steps:

Step 1: derive algal P as: $OP_{alg} = Chla \times CCHA / AGP$
Step 2: derive non-algal P as: $OP_{non\text{-}alg} = TP$ – dissolved $PO_4 - OP_{alg}$
Step 3: derive OM as: $OM = OP_{non\text{-}alg} \times OMP$

where

Chla = observed chlorophyll *a* concentration (µg/L)
CCHA = 0.067 (mg-algae per µg-chlorophyll *a*); derivation: Algae = Chla × 67 × (1 mg/1000 ug), where 67 represents the Algae:Chla ratio defined as 30/0.45 (on the basis of the WASP model default ratio of 30 for Algae-C:Chla and the CE-QUAL-W2 model default ratio of 0.45 for Algae-C:Algae)
AGP = algal P content coefficient (mg-algae / mg-P)
OMP = organic matter P content coefficient (mg-OM / mg-P)

OMP was determined to be 180.0 based on 2002 data for Link River at Fremont Bridge (where the average organic carbon:organic phosphorus ratio is 81, and thus the OM:OP ratio is 81 / 0.45 = 180.0). AGP was assumed to be the same as OMP because phytoplankton is the major source of OM in UKL. BOD was not configured for the model because all OM are represented using a single state variable (as previously noted).

Initially, the total PO_4 boundary condition was represented using the dissolved PO_4 monitoring data at Pelican Marina. It was found, however, that setting the PO_4 boundary concentration at Link River to the observed dissolved PO_4 value resulted in a significant underprediction of PO_4 concentration at Miller Island, in Lake Ewauna. Because Link River flow is dominant in upper Lake Ewauna, the PO_4 concentration at Miller Island should be similar in magnitude and pattern to that at the head of Link River. Several model sensitivity analyses confirmed this. The difference between the dissolved PO_4 data at Pelican Marina and the PO_4 data at Miller Island suggests that the dissolved PO_4 at Pelican Marina is likely not a good representation of conditions at the head of Link River. Therefore, the observed PO_4 data at Miller Island were used as the basis for configuring the PO_4 boundary condition at Link Dam.

The alkalinity boundary condition was configured on the basis of alkalinity monitoring data at Link River and Miller Island. In 2000 there was a limited amount of alkalinity data at Link River (on seven discrete dates). These data were insufficient to accurately predict alkalinity concentrations at Miller Island. Therefore, Miller Island data were used to supplement the Link River data in constructing the boundary condition. The first step in doing this was to compare the flow from Link River and the Lost River Diversion Channel to determine the period during which Link River flow was dominant. For this period the alkalinity at Miller Island would be similar in magnitude to that at Link River. Therefore, data at Miller Island were incorporated into the Link River data to form an expanded data set. The upstream boundary condition for alkalinity was then configured using this expanded data set. There were no data available for TIC; therefore, the TIC boundary condition was obtained through the pH calibration process for Miller Island. Initially, TIC at the Link River boundary was derived on the basis of pH at Miller Island and alkalinity at Link River. These estimates were refined to achieve a better calibration of pH at Miller Island in Lake Ewauna.

The upstream boundary condition for the 2002 model was derived using a method similar to that used for 2000. Available data at both the head of Link River (Fremont Bridge) and at Pelican Marina were combined to form a composite data set for 2002 boundary condition derivation. Monitoring data for PO_4, NH_4, NO_2/NO_3, phytoplankton, DO, and temperature were directly applied to the boundary conditions using a linear interpolation method to obtain daily values for dates without data. The OM boundary condition was derived using the same approach used for the 2000 model. The alkalinity boundary condition was derived on the basis of monitoring data at Fremont Bridge. And the TIC boundary condition was derived on the basis of alkalinity data and pH data at the same location.

Tributary Boundary Conditions: There are two diversions from UKL at Link Dam. These diversions are two powerhouses that discharge water from UKL into the Link River segment (East Side and West Side). USGS gage 11507500 (Link River at Klamath Falls, Oregon) is between the powerhouse discharges.

The constituent concentrations for the tributary boundary conditions were set to be the same as the upstream boundary conditions because the powerhouses have the same water source as the upstream boundary (UKL).

Downstream Boundary Conditions: Downstream boundary conditions were configured using a stage-discharge relationship. Although this type of boundary condition does not allow for representation of the backflow condition that occasionally occur at the mouth of Link River, it is a better predictive tool than using the Lake Ewauna elevation as the downstream boundary condition. The backflow condition does not have a significant impact on the loading rate from Link River to Lake Ewauna, thus, it does not significantly impact the water quality in the lake.

2.3.3.2 Model Segment 2: Lake Ewauna to Keno Dam

This segment extends from the point where Link River enters Lake Ewauna to the outlet at Keno Dam. Five types of boundary conditions were included in the Klamath River model for the Lake Ewauna segment. They are upstream inflow boundary conditions, tributary boundary conditions, withdrawal boundary conditions, downstream outflow boundary conditions, and surface boundary conditions.

Upstream Inflow Boundary Conditions: The upstream boundary condition was defined as the water flowing into Lake Ewauna from Link River (Model Segment 1). Link River's flow was determined by using the observed flows at USGS flow gage 11507500 minus the flow from the PacifiCorp West Turbine (powerhouse) gage, which is downstream of the USGS gage.

The upstream boundary conditions for water quality constituent concentrations were based on the model results in the downstream region of the Link River Model Segment. PO_4, NH_4, NO_2/NO_3, DO, phytoplankton, Alk, TIC, and temperature were directly transferred from the RMA-11 model (from Link River) to the CE-QUAL-W2 input data file for Lake Ewauna. Output for OM from Link River was applied to the Lake Ewauna segment and partitioned into four components: LDOM, RDOM, LPOM, and RPOM with partition ratios as 0.2, 0.0, 0.8, and 0.0, respectively. These ratios were based on the CE-QUAL-W2 ALPOM value and the decision not to further partition OM between labile and refractory components. These assumptions were justified because the majority of the organic matter from UKL are likely generated by phytoplankton blooms and metabolism. Therefore, the CE-QUAL-W2 ALPOM value can be used to represent partitioning. In reality significant spatial and temporal variability associated with organic matter composition may exist, however insufficient data are available to more accurately represent the organic matter boundary conditions. In addition, CE-QUAL-W2 isn't capable of representing seasonal variability of OM composition for the boundary conditions.

Tributary Boundary Conditions: There are 18 tributary discharges in the Lake Ewauna to Keno Dam river segment. These discharges include 11 stormwater locations, Columbia Plywood discharge, Klamath Falls Wastewater Treatment Plant, South Suburban Sanitation District, two discharges at Collins Forest Products, Lost River Diversion Channel, and Klamath Straits Drain (KSD).

The inflow from the stormwater locations was calculated as an average percentage of total stormwater runoff. The flow from Columbia Plywood was calculated from the discharger's monthly monitoring reports as an average of 0.01 cubic feet per second (cfs). Variable daily flows were used for the Klamath Falls Wastewater Treatment Plant and ranged from approximately 4 to 12 cfs. Variable daily flows were also used for South Suburban Sanitation District and generally ranged from 1 to 4 cfs. The two discharges at Collins Forest Products had average daily flows of approximately 1.4 cfs and 0.1 cfs. Daily flows from Lost River Diversion Channel and KSD into Lake Ewauna were obtained from USBR's flow gages at these locations.

The water quality constituent concentrations of the tributary boundary conditions were set to be the same as in the previous PacifiCorp Model except for the major tributaries and point sources, including KSD, Klamath Falls Wastewater Treatment Plant, and South Suburban Sanitation District. For these major tributaries and point sources, available data for 2000 and 2002 were used to update the boundary conditions. The details of updating these boundary conditions are summarized as follows:

a) KSD

The concentration boundary condition at KSD was represented using data at station Pump F in the KSD. The formulas used to convert observed data to model boundary conditions are listed below. For each constituent notation, the one on the left-hand side corresponds to the model boundary condition, while the one on the right-hand side corresponds to observed data. For parameters not listed, observed values were used directly.

- Algae [mg/L] = Chlorophyll *a* [µg/L] × 0.067, where 0.067 was derived similarly to CCHA for the UKL boundary condition (previously described)
- LDOM [mg/L] = (TP [mg/L] – PO_4 [mg/L]) × 180.0 × 0.7, where 180.0 was derived similarly to OMP for the UKL boundary condition (previously described), and 0.7 was derived on the basis of 2002 data at KSD (Dissolved TP / TP)
- RDOM [mg/L] = 0.0
- LPOM [mg/L] = (TP – PO_4) × 180.0 × 0.3, where the ratio 0.3 was derived from (1.0–0.7, where 0.7 represents LDOM).
- RPOM [mg/L] = 0.0
- ISS [mg/L] = TSS [mg/L]
- TIC [mg/L] = *f*(Alk, temperature, pH), where *f* represents the functional form relating TIC to Alkalinity [mg/L], temperature [^oC], and pH. Detailed equations can be found in Chapra 1997.

b) Klamath Falls Wastewater Treatment Plant and South Suburban Sanitation District

The water quality constituent concentrations for both the Klamath Falls Wastewater Treatment Plant and South Suburban Sanitation District were set to be the same as in the previous PacifiCorp Model, except for where more recent facility discharge monitoring report data were available. The formulas used to derive the boundary conditions based on data are as follows:

- BODu [mg/L] = BOD5 [mg/L] × 3.386, where the ratio 3.386 is based on the assumption that the treatment plants provide secondary treatment, thus the BOD has a decay rate around 0.07/day (Chapra, 1997)
- LDOM [mg/L] = BODu / 1.4 × 0.2, where the ratio 1.4 is based on the W2 stoichiometric ratio, and 0.2 is the same as that used for the UKL boundary condition
- LPOM [mg/L] = BODu / 1.4 × 0.8, where the ratio 1.4 is based on the W2 stoichiometric ratio, and 0.8 is the same as that used for the UKL boundary condition
- OM [mg/L] = LPOM + LDOM, which is based on the conservative assumption that all OM are labile for boundary inputs
- ISS [mg/L] = TSS [mg/L]
- PO_4 [mg/L] = TP [mg/L] – BODu / 1.4 / 180.0
- Org-P [mg/L] = OM × 0.0055, where the coefficient 0.0055 is the stoichiometric ratio used in the model
- TP [mg/L] = Org-P + PO_4

- Org-N [mg/L] = OM × 0.07 where the coefficient 0.07 is the stoichiometric ratio used in the model
- TN [mg/L] = Org-N + NH4 [mg/L] + NO2/NO3 [mg/L]

The 2000 boundary conditions for LDOM, LPOM, and DO at the Klamath Falls Wastewater Treatment Plant were updated using data from 2000. No data were available for ISS, PO_4, or NH4 for 2000, therefore data from 2002 were used for the 2000 model. For the 2002 model, LDOM, LPOM, DO, ISS, PO_4 and NH4 were all based on the 2002 data.

The 2000 and 2002 boundary conditions for LDOM, LPOM, DO, ISS, PO_4, and NH4 at South Suburban Sanitation District were configured based on data available for the corresponding year. For dates when PO_4 data were not available and thus could not be directly applied, PO_4 was derived based on the TP and BOD data using the formulas listed above.

Withdrawal Boundary Conditions: Three withdrawals in this segment are explicitly represented, including the Lost River, North Canal, and ADY Canal. Daily flows at all three of these withdrawals are gaged by USBR.

There is a lack of available daily withdrawal rates for a few non-USBR irrigation diversions, therefore they are not explicitly represented. Water diversion is grossly represented in the distributed flow, which was derived through a flow balance analysis.

The hourly flow rate at Keno Dam was available from USGS gage 11509500 (Klamath River near Keno, Oregon). The flows ranged from less than 500 cfs to more than 4,000 cfs. All these boundary conditions were kept the same as in the previous PacifiCorp Model.

Downstream Outflow Boundary Conditions: For Lake Ewauna, the downstream boundary condition was set as the outflow at the point before entering Keno Reach (Keno Dam to J.C. Boyle Reservoir). The downstream boundary condition was set to be outflow; therefore, no water quality concentration boundary condition was needed.

2.3.3.3 Model Segment 3: Keno Dam to J.C. Boyle Reservoir (Keno Reach)

There were three types of boundary conditions included in this section of the model: upstream inflow boundary conditions, downstream outflow boundary conditions, and surface boundary conditions.

Upstream Inflow Boundary Conditions: The upstream inflow to this reach for the 2000 and 2002 models is based on the outflow from Lake Ewauna for the corresponding year. This segment was dominated by upstream water quality, therefore the simulated loading time series for phytoplankton, temperature, PO_4, NH_4, NO_2/NO_3, DO, TIC, and Alk from the Lake Ewauna to Keno Dam segment were applied. The four OM constituents predicted by the CE-QUAL-W2 model were combined into one OM constituent and applied to the boundary conditions (as previously discussed).

Downstream Outflow Boundary Conditions: Hydrodynamic downstream boundary condition was set as a stage-discharge relationship, which represents the downstream flow as only outflow; therefore, no concentration boundary condition was needed.

2.3.3.4 Model Segment 4: J.C. Boyle Reservoir

The J.C. Boyle Reservoir extends from the J.C. Boyle headwaters (Keno Reach to J.C Boyle Reservoir) to the J.C. Boyle Dam. There were four types of boundary conditions included in this portion of the model. They are upstream inflow boundary conditions, tributary boundary conditions, downstream outflow boundary conditions, and surface boundary conditions.

Upstream Inflow Boundary Conditions: Klamath River inflow for the 2000 and 2002 models to J.C. Boyle dam is represented by discharge from the Keno Reach during the corresponding year. The upstream boundary conditions for water quality constituents were based on the model results at the downstream node of the Keno Reach portion of the model for the corresponding year. PO_4, NH_4, NO_2/NO_3, DO, phytoplankton, temperature, TIC, and Alk were directly transferred from the RMA-11 model results for Keno Reach to the CE-QUAL-W2 input data file for J.C. Boyle Reservoir. Output for OM from the Keno Reach model was applied to the J.C. Boyle Reservoir (see Section 2.2.1) and was partitioned into four components: LDOM, RDOM, LPOM, and RPOM. The aforementioned dynamic partitioning scheme was applied. This scheme uses the LDOM, RDOM, LPOM, and RPOM fractions derived from model results from the last segment of Keno Reservoir to partition the OM into the four components.

Tributary Boundary Conditions: There is one tributary to J.C. Boyle Reservoir, Spencer Creek. Spencer Creek has very limited inflow information. Therefore, it is not configured as a separate tributary in this model. The minor contribution of flow from Spencer Creek is lumped into the upstream headwater in the original PacifiCorp Model, and directly adopted in the TMDL model. The net reservoir accretion/depletion was calculated through a flow balance process aiming to reproduce the observed surface water elevation in the reservoir. This accretion/depletion was configured as a distributed tributary boundary condition in the model. The concentration of the tributary inflow was set to be the same as in the upstream boundary condition.

Downstream Outflow Boundary Conditions: The outflow from the reservoir was calculated as the sum of all recorded releases to the four outlets in the reservoir (powerhouse canal, dam spillway, bypass releases, and fish ladder releases).

The downstream boundary condition was set to be outflow; therefore, no concentration boundary condition was needed.

2.3.3.5 Model Segment 5: Bypass/Full Flow Reach

The Bypass/Full Flow Reach extends from the J.C. Boyle Dam to the headwaters of Copco Reservoir. There were four types of boundary conditions included in this portion of the model: upstream inflow boundary conditions, tributary boundary conditions, downstream outflow boundary conditions, and surface boundary conditions.

Upstream Inflow Boundary Conditions: There are two inflows to the Bypass/Full Flow Reach. They are releases from J.C. Boyle Dam directly to the Klamath River and the J.C. Boyle Powerhouse tailrace. Measured releases from the dam for 2000 and 2002 were obtained from PacifiCorp and used to represent both inflows for the model for the corresponding years.

For the upstream water quality constituent concentration boundary conditions, the simulated loading time series for phytoplankton, temperature, PO_4, NH_4, NO_2/NO_3, and DO from the J.C. Boyle Reservoir were applied. The four OM constituents predicted by the CE-QUAL-W2 model were combined into one OM constituent as applied in the Keno Reach boundary condition.

Tributary Boundary Conditions: There are no major tributaries, but there are three springs represented by a constant flow of 75 cfs each. The flow rate, temperature, DO, and phytoplankton boundary conditions for the springs were the same as in the original PacifiCorp Model, while the concentrations for the major nutrients (i.e., PO_4, NH_4, and NO_2/NO_3) were derived through model calibration. After several iterations, the concentrations for NH_4, NO_2/NO_3, and PO_4 were determined to be 0.029 mg/L, 0.25 mg/L, and 0.066 mg/L, respectively. OM concentrations were assumed to be a small value of 0.5 mg/L considering the springs are mainly groundwater. These concentrations were applied to both the 2000 and 2002 models for this reach.

Downstream Outflow Boundary Conditions: The downstream boundary condition for the Bypass/Full Flow Reach was configured as a stage-discharge relationship. No concentration boundary condition was needed for the downstream boundary conditions because only outflow exists there.

2.3.3.6 Model Segment 6: Copco Reservoir

The Copco Reservoir model segment extends from Copco Reservoir's headwaters to Copco Dam. Four types of boundary conditions were included in the portion of the model for Copco Reservoir. They are upstream inflow boundary conditions, tributary boundary conditions, downstream outflow boundary conditions, and surface boundary conditions.

Upstream Inflow Boundary Conditions: The inflow for Copco Reservoir was represented as the sum of the inflow into the reservoir and the estimated accretion/depletion for the reservoir. The flows from Bypass/Full Flow Reach were used as inflow to the Copco Reservoir because there are no flow data available at the headwaters of Copco Reservoir. The daily accretion/depletion was the sum of the daily change in storage in the Copco reservoir and the daily average outflow from the reservoir (minus the daily average inflows from Bypass/Full Flow Reach) as derived in the original PacifiCorp Model.

The upstream water quality constituent concentration boundary conditions were based on the model results at the downstream node of the Bypass/Full Flow Reach portion of the model. PO_4, NH_4, NO_2/NO_3, DO, phytoplankton, and temperature were directly transferred from the RMA-11 model results for Bypass/Full Flow Reach to the CE-QUAL-W2 input data file for Copco Reservoir. Output for OM from the Bypass/Full Flow Reach portion of the model was applied to Copco Reservoir (see Section 2.2.1) and is partitioned into four components: LDOM, RDOM, LPOM, and RPOM using the dynamic-partitioning approach as described above.

Tributary Boundary Conditions: The concentrations of the distributed tributary boundary conditions were set to be the same as the upstream concentration boundary condition in the same manner as in the original model.

Downstream Outflow Boundary Conditions: The two main outlets for the Copco Dam are a spillway and two waterway intakes at the Copco powerhouse (treated as a single outlet). Hourly outflow data for the powerhouse and the spillway were available from PacifiCorp and used as reservoir outflow flows.

The downstream boundary condition was set to be outflow; therefore, no concentration boundary condition was needed.

2.3.3.7 Model Segment 7: Iron Gate Reservoir

The Iron Gate Reservoir model segment extends from the headwaters of the Iron Gate Reservoir to Iron Gate Dam. Five types of boundary conditions were included in the portion of the model for Iron Gate Reservoir. They are upstream inflow boundary conditions, tributary boundary conditions, withdrawal boundary conditions, downstream outflow boundary conditions, and surface boundary conditions.

Upstream Inflow Boundary Conditions: There is no gage to measure inflow to Iron Gate Reservoir; therefore, the flows from the Copco Reservoir were used to represent inflow.

Simulated water quality outflow values from Copco Reservoir were applied as the Iron Gate Reservoir inflow water quality constituent concentration boundary conditions, and they were the same configuration as for Lake Ewauna.

Tributary Boundary Conditions: There are three tributaries to the Iron Gate Reservoir. They are Camp Creek, Jenny Creek, and Fall Creek. Limited flow information was available for these creeks. The hourly accretion/depletion for the reservoir was calculated as the sum of the daily inflow, outflow, and change in storage in Iron Gate Reservoir. Jenny Creek was represented by this accretion/depletion, as in the original PacifiCorp Model. Neither Camp Creek nor Fall Creek were explicitly configured with contributions in the model. Tributary boundary conditions were not changed from the original PacifiCorp Model. Since Jenny Creek is represented as an accretion/depletion flow, its water quality is represented using the upstream inflow concentrations. This follows the same assumptions as for the upstream reservoirs.

Withdrawal Boundary Conditions: The dam's spillway was modeled as a withdrawal because it draws water to the side of the dam, not over or through the dam. Representing the spillway as a withdrawal more accurately represents the system. If the spillway were represented as a spillway in W2, water would flow to the end of the reservoir instead of the side, and this can affect the hydrodynamic simulation.

Downstream Outflow Boundary Conditions: The Iron Gate dam has four primary outlets: a spillway, penstock, and two fish hatchery intakes. Outflow from the reservoir was based on the outflow in the original PacifiCorp Model. Outflow was determined from PacifiCorp daily flow records for the Powerhouse release and spill and estimates of fish hatchery releases (50 cfs for lower hatchery release and 0 cfs for upper hatchery release).

The downstream boundary condition was set to be outflow; therefore, no concentration boundary condition was needed.

2.3.3.8 Model Segment 8: Iron Gate Dam to Turwar

Four types of boundary conditions were included in the portion of the model for Iron Gate Dam to Turwar. They are upstream inflow boundary conditions, tributary boundary conditions, downstream outflow boundary conditions, and surface boundary conditions.

Upstream Inflow Boundary Conditions: The upstream inflow boundary conditions for Iron Gate Dam to Turwar were based on PacifiCorp's original model, which used PacifiCorp's measured releases from Iron Gate Dam during 2000.

Upstream water quality constituent boundary conditions were the simulated outflow values from the Iron Gate reservoir.

Tributary Boundary Conditions: There are 23 tributaries to this segment of the Klamath River, including four major tributaries (Shasta, Scott, Salmon, and Trinity rivers). Five tributaries to this reach are actively gauged, including the Shasta, Scott, Salmon, and Trinity rivers, and Indian Creek. Inflows for minor tributaries were defined and quantified as daily accretion/depletions, as in the original PacifiCorp Model.

The Scott and Trinity rivers were assigned by summing USGS-gaged flows and daily accretion/depletions. The daily accretion/depletions were determined on the basis of a USGS methodology. Monthly average values were used to determine accretions and depletions for each river segment on the basis of differences in gage readings, and these accretions and depletions were then assigned to individual tributaries according to the estimated basin area. Appendix D presents the USGS methodology for estimating these flows for tributaries (PacifiCorp 2004). Model node and element numbers and type of flow record employed for each tributary are summarized in Table 2-2.

Table 2-2. Element flow information for the Iron Gate to Turwar simulation

Location	Node	Element	Flow Type
Bogus Creek	7	4	7 day average
Willow Creek	55	28	7 day average
Cottonwood Creek	86	43	7 day average
Shasta River	144	72	Daily measured
Humbug Creek	204	102	7 day average
Beaver Creek	319	160	7 day average
Horse Creek	468	234	7 day average
Scott River	513	257	Daily measured + A/D Ft. Jones to Klamath
Grider Creek	656	328	7 day average (A/D Scott to Seiad)
Thompson Creek	735	368	7 day average
Indian Creek	906	453	Daily measured
Elk Creek	925	463	7 day average
Clear Creek	1000	500	7 day average
Ukonom Creek	1098	549	7 day average
Dillon Creek	1162	581	7 day average
Salmon River	1357	679	Daily measured
Camp Creek	1466	733	7 day average
Red Cap Creek	1511	756	7 day average
Bluff Creek	1547	774	7 day average
Trinity River	1609	805	Daily measured + A/D Hoopa to Klamath
Pine Creek	1644	822	7 day average
Tectah Creek	1850	925	7 day average
Blue Creek	1908	954	7 day average

Shasta River daily flows were taken from USGS Gage 11517500 (Shasta River near Yreka). Scott River daily flows were calculated from USGS Gage 11519500 (Scott River near Ft Jones) and accretion/depletions. Daily Indian Creek flows were taken from USGS Gage 11521500 (Indian Creek near Happy Camp). Salmon River daily flows were from USGS Gage 11522500 (Salmon River at Somes Bar). Trinity River daily flows were calculated from USGS Gage 11530000 (Trinity River at Hoopa) and accretion/depletions.

Water quality constituent concentrations in the tributaries for all parameters except DO were based on U.S. Fish and Wildlife Service (USFWS), USBR, EPA, USGS, California Department of Water Resources (CDWR), NCRWQCB Surface Water Ambient Monitoring Program, and Yurok Tribe Environmental Program (YTEP) data.

Temperature data for the tributaries were very limited, therefore the temperature boundary conditions for all the tributaries were configured on the basis of USGS-estimated temperature for 2002 (Flint, L.E. and Flint, A. L. 2008). It was found that by directly using the USGS-estimated temperatures in these tributaries, the model reproduced observe temperatures in the Klamath River quite well. This is not surprising since the USGS study did show that there is no significant inter-year variation in the predicted in-stream temperature.

There were very little to no water quality data available for most tributaries. The only tributaries with sufficient data to represent seasonal variations for 2000 were the Shasta and Scott Rivers (USBR 2003 data). For the other two major rivers, Salmon and Trinity, NCRWQCB derived representative data to approximate the boundary conditions for 2000, based on statistical analysis of historical tributary data. Several historical datasets (1960s to 1980s) with water quality data from CDWR, STORET, USBR, and USGS were supplemented with more recent data (2000 to 2006) from USFWS, USBR, EPA, USGS, CDWR, NCRWQCB, and YTEP. The data were split into two seasonal periods – Wet (November – April) and Dry (May – October), and years which had similar hydrologic conditions to the year 2000 were selected based on statistical measures. The median water quality values for the two seasonal periods were used for boundary conditions.

In addition to the USBR data, the NCRWQCB compiled nutrient data for several minor tributaries including Beaver Creek, Bluff Creek, Clear Creek, Dillon Creek, Elk Creek, Red Cap Creek, Indian Creek, and Bogus Creek for the period from 2001 to 2006. These data were divided into two categories. The first was data for Bogus Creek that were used to derive the boundary condition for Bogus Creek. Bogus Creek exhibits significantly higher nutrient concentrations than the other tributaries. The second was data for all other minor tributaries, which were combined to derive values representing all the minor tributaries. Because of a lack of sufficient data to characterize temporal variability, it was deemed appropriate to use an annual average value to represent the boundary conditions from the minor tributaries.

DO in all minor tributaries was estimated using 90 percent saturated conditions, except for the Shasta and Scott rivers, where DO data were available. DO saturation concentrations were based on the temperature data and atmospheric pressure corrected for elevation. A detailed description of the boundary conditions for each of the tributaries is provided in Table 2-3.

Table 2-3. Description of Boundary Conditions for Tributaries within the Irongate to Turwar Segment

Tributary name	Temperature	Nutrients	DO	TIC/ALK
Bogus Creek	Based on USGS estimated data	Based on NCRWQCB data	90 % saturation value	Based on the data in the Scott River
Willow Creek	Based on USGS estimated data	Based on NCRWQCB estimated data	90% saturation value	Based on the data in the Scott River
Cottonwood Creek	Based on USGS estimated data	Based on NCRWQCB estimated data	90% saturation value	Based on the data in the Scott River

Tributary name	Temperature	Nutrients	DO	TIC/ALK
Shasta River	Based on 2000 data	Nutrients were set based on USFWS data at the mouth of the Shasta River	DO was based on observed data, except for the period without monitoring data, which was set to be 90% of the saturation value.	Based on the data at the Shasta River mouth
Humbug Creek	Based on USGS estimated data	Based on NCRWQCB estimated data	90% saturation value	Based on the data in the Scott River
Beaver Creek	Based on USGS estimated data	Based on NCRWQCB data	90% saturation value	Based on the data in the Scott River, except for August and September, when limited data were available for 2006. For August and September, the data were used directly.
Horse Creek	Based on USGS estimated data	Based on NCRWQCB estimated data	90% saturation value	Set to be the same as in the Beaver Creek boundary condition
Scott River	Based on 2000 data	Based on USFWS data at the mouth of the Scott River	Based on USFWS data at the mouth of the Scott River. Periods without data were set at 90% saturation value	Based on USFWS data at the mouth of the Scott River
Grider Creek	Based on USGS estimated data	Based on NCRWQCB estimated data	90% saturation value	Set based on the observed data at the mouth of Salmon River
Thompson Creek	Based on USGS estimated data	Based on NCRWQCB estimated data	90% saturation value	Set based on the observed data at the mouth of Salmon River
Indian Creek	Based on USGS estimated data	Based on NCRWQCB data	90% saturation value	Based on the observed data at the mouth of the Salmon River, except for August and September, when 2006 data were available at Indian Creek. For this period, the data were used directly.
Elk Creek	Based on USGS estimated data	Based on NCRWQCB data	90% saturation value	Based on the observed data at the mouth of the Salmon River except for August and September, when 2006 data were available at Elk Creek.

Tributary name	Temperature	Nutrients	DO	TIC/ALK
				For this period, the data were used directly.
Clear Creek	Based on USGS estimated data	Based on NCRWQCB data	90% saturation value	Based on the observed data at the mouth of the Salmon River, except for August and September, when 2006 data were available at Clear Creek. For this period, the data were used directly.
Ukonom Creek	Based on USGS estimated data	Based on NCRWQCB estimated data	90% saturation value	Based on the observed data at the mouth of the Salmon River
Dillon Creek	Based on USGS estimated data	Based on NCRWQCB data	90% saturation value	Based on the observed data at the mouth of the Salmon River, except for August and September, when 2006 data were available at Dillon Creek. For this period, the data were used directly.
Salmon River	Based on 2000 data	Based on USFWS data	90% saturation value	Based on the observed data at the mouth of the Salmon River
Camp Creek	Based on USGS estimated data	Based on NCRWQCB estimated data	90% saturation value	Based on the observed data at the mouth of the Trinity River
Red Cap Creek	Based on USGS estimated data	Based on NCRWQCB data	90% saturation value	Based on the observed data at the mouth of the Trinity River, except for August and September, when 2006 data were available. For this period, the data were used directly.
Bluff Creek	Based on USGS estimated data	Based on NCRWQCB data	90% saturation value	Based on the observed data at the mouth of the Trinity River, except for August and September, when 2006 data were available. For this

Tributary name	Temperature	Nutrients	DO	TIC/ALK
				period, the data were used directly.
Trinity River	Based on 2000 data	Based on USFWS data	90% saturation value	Based on the observed data in the Trinity River
Pine Creek	Based on USGS estimated data	Based on NCRWQCB estimated data	90% saturation value	Based on the observed data at the mouth of the Trinity River
Tectah Creek	Based on USGS estimated data	Based on NCRWQCB estimated data	90% saturation value	Based on the observed data at the mouth of the Trinity River
Blue Creek	Based on USGS estimated data	Based on NCRWQCB estimated data	90% saturation value	Based on the observed data at the mouth of the Trinity River

Downstream Outflow Boundary Conditions: The downstream boundary condition for this section is a stage-discharge condition. No water quality boundary condition is needed because only outflow is represented at the downstream.

2.3.3.9 Model Segment 9: Klamath Estuary (Turwar to the Pacific Ocean)

The estuarine portion of the Klamath River (Turwar to the Pacific Ocean) was modeled using EFDC and was not included in the original PacifiCorp Model. This model segment was ultimately calibrated using data from the year 2004 because it had the most available data for all parameters. Insufficient data were available to calibrate for the year 2000 in the estuarine portion of the Klamath River. Boundary conditions were thus prepared using monitoring data at Turwar. Three types of boundary conditions were included in the Klamath Estuary portion of the model. They are upstream inflow boundary conditions, downstream open boundary conditions, and surface boundary conditions.

Upstream Inflow Boundary Conditions: The portion of the Klamath River represented by EFDC was delineated from the USGS 11530500 streamflow gage at Klamath to the Klamath River's intersection with the Pacific Ocean (Appendix C). Streamflow data from the Klamath River at Klamath USGS gage (11530500) were used as the upstream inflow boundary for model calibration (described in Section 3.0). Model results from the Iron Gate Dam to Turwar portion of the model are used as input for the modeling scenarios.

The upstream boundary condition for water quality was configured using the USFWS/Yurok's 2004 water quality monitoring data at Turwar (for model calibration). The USFWS station was sampled five times from June to September 2004. A time series was generated for water quality using linear interpolation of the five available data points. The following constituents were configured as state variables in the upstream boundary water quality input file using the Turwar data:

1. Phytoplankton
2. LPOC

3. LDOC
4. LPOP
5. LDOP
6. PO_4
7. LPON
8. LDON
9. NH_4
10. NO_3/NO_2
11. DO

Not all data were available to be directly used in the EFDC water quality input file. The following assumptions were made to derive parameters to create the water quality input file:

- The particulate to dissolved OM ratio was assumed to be 0.8:0.2. This ratio was also used to derive the particulate and dissolved components of phosphorus, nitrogen and carbon. It maintains consistency with upstream segments.
- Due to a lack of data to further partition OM between labile and refractory components, labile and refractory components were not considered separately.
- Organic phosphorous was derived by subtracting PO_4 from total phosphorous.
- The ON:OM and OP:OM ratios were assumed to be the same as in upstream reaches, which are ON:OM=0.07, and OP:OM=0.0055. These ratios were used to derive ON from OP data.
- The algae biomass to chlorophyll ratio was assumed to be 0.067 mg algae/ug Chla, which is the same as those in the upstream reaches.

Diel DO and temperature data were not readily available at the Turwar gage for 2004 when this model was developed. Thus, daily average values were computed on the basis of the diel data for the Upper Estuary monitoring site (at Hwy 101) and specified as the upstream boundary condition at Turwar. The model can be updated to reflect additional monitoring data as these data become available.

For modeling scenarios, model output from the Iron Gate Dam to Turwar segment are used. OM conversion from the RMA model to EFDC is presented in Figure 2-4 of Section 2.3.2.

Two tributaries to the Klamath Estuary, Hunter Creek and Salt Creek, were also initially considered as part of the boundary conditions but were later eliminated. Flow estimates were available for Hunter Creek, based on drainage area for the period May 1 through September 30, and were found to be relatively insignificant (median value of 5.9 cfs in 2004) in comparison to the Klamath River flows. Salt Creek flows were smaller than those for Hunter Creek.

Downstream Open Boundary Conditions: The outlet of the Klamath River at the Pacific Ocean is characterized by a widening of approximately 1,400 meters. Depending on the conditions, the outlet may be largely closed off by a transient sand bar. The opening through this sand bar was set to approximately 200 meters in width for the model, based on measured 2004 bathymetry data. To reduce the influence of boundary reflection, the downstream open boundary of the model was set well into the Pacific Ocean, beyond the physical opening in the sand bar (Appendix C). To allow for flexibility in evaluating the effect of different locations of the sand bar opening, the sand bar is included in the grid system as a column of active cells. It has an

internal barrier that blocks the water from penetrating all cells except those representing the opening.

Tidal data from the National Oceanic and Atmospheric Administration (NOAA) gage at Crescent City (9419750) were used to represent the tidal boundary of the model. Tidal elevation data from the Crescent City gage are referenced to a mean lower low water (MLLW) vertical datum, while bathymetry data obtained from the NCRWQCB use the NAVD88. The difference between the two data at this location is approximately 0.38 feet, or 0.116 meters. Tidal elevation data from the Crescent City gage station were adjusted to correspond to the bathymetry datum obtained for the lower portion of the Klamath River.

Surface Boundary Conditions: The surface boundary conditions are based on meteorological conditions. The meteorological data required by the EFDC model are specified in two separate files (*aser.inp* and *wser.inp*). The *aser.inp* file is used to specify the atmospheric pressure, air temperature, relative humidity, precipitation, evaporation, solar radiation and cloud cover. The *wser.inp* file is used to specify the wind speed and direction. Meteorological data from the Arcata Eureka Airport (WBAN 24283), approximately 35 miles downstream of the estuary along the Pacific coastline, were used. Hourly, unedited local meteorological data (atmospheric pressure, air temperature, relative humidity, precipitation, cloud cover, wind speed and direction) were available from this NOAA-NCDC station and were used in creation of the *aser.inp* and *wser.inp* files for the estuary model. These data provided the most complete data set of required surface airways parameters for the EFDC model meteorological file. Solar radiation data were not available. Clear sky solar radiation was computed on the basis of the latitude and longitude and corrected using cloud cover to generate the solar radiation data.

2.3.4 Initial Conditions

The Klamath River model requires specifying initial conditions in the input files. The initial conditions from the original PacifiCorp Model (Model Segments 1 through 8) were maintained for all segments, except BOD was eliminated from the initial condition setting for Link River, Keno Reach, and Bypass/Full Flow Reach (see Section 2.2.1). Where field data were unavailable, the conditions of the first day of available field data were applied. In general, the impact of the initial conditions was insignificant and lasted for less than 10 days in the winter period. The initial condition for Model Segment 9 was set to values similar in magnitude as observed data. Because of the relatively large flow from the Klamath River, however, the impact of initial conditions is noticeable only for a very short (insignificant) time period.

2.4 Modeling Assumptions, Limitations, and Sources of Uncertainty

2.4.1 Assumptions

The major underlying assumptions associated with Klamath River model development are as follows:

- The initial condition and the boundary conditions set for the winter and early spring period do not have a significant effect on the simulated water quality during the critical summer and early fall periods. This assumption permits assigning the initial conditions and winter/early spring boundary conditions using best professional judgment, without impairing the model performance for the critical period.

- Time series flow data were not available for all tributaries and withdrawals. Reliable time series flow data were also not available for many monitoring locations along the length of the Klamath River. In light of the limitations, it was assumed that tributary flows could be reasonably represented through interpolation on the basis of limited flow measurements.
- One phytoplankton species and one periphyton species were assumed to be sufficient for representing the overall primary production and nutrient interactions in the system given no data is available to support multiple species modeling.
- Alkalinity is conservative (as stated in CE-QUAL-W2 manual). Therefore, no internal sources or sinks were considered.
- All the OM in the water column (and that from other sources) has the same stoichiometric ratio unless data are available to derive site-specific ratio.
- The effect of zooplankton and benthic creatures do not have a significant impact on the algal/periphyton dynamics and nutrient recycling.
- A stage-discharge relationship was applied at the Link River boundary to enable predictive simulation downstream. This adjustment was made on the basis of previous peer review comments for the Klamath River Model. Although this configuration does not explicitly simulate backwater effects, it was deemed suitable for TMDL development scenarios. The magnitude of the Link River flow is significant. And because Link River is fairly steep, flow velocities into Lake Ewauna are relatively high. If backwater flow exists, it would not have a significant effect on the nutrient budget downstream.
- The OM in the boundary conditions is lumped (and thus not partitioned between labile and refractory components) due to lack of sufficient data for accurate OM partitioning.
- Denitrification in the riverine sections is not simulated due to the fact that the majority of the river bed is rocky and DO in the water column is high. Neither of these conditions are favorable for denitrification bacteria and corresponding denitrification processes. This assumption may potentially cause overprediction of NO_2/NO_3 in the riverine sections, however the impact is expected to be minimal.
- The sand bar opening at the mouth of the Klamath Estuary has relatively constant dimensions and physical characteristics for a period of time; thus, a fixed grid configuration can be used for a simulation.
- The impact of sediment transport and siltation on channel geometry is not significant; therefore, the same bathymetric configuration can be used for different scenario simulations. Additionally, insufficient data are available to dynamically simulate the time-dependent effect of sediment transport on bathymetry.

2.4.2 Limitations

Potential limitations that have been identified include the following:

- The model's capabilities are constrained by the limited availability and quality of monitoring data. This is particularly the case for boundary conditions to the model, but it is also the case for in-stream model calibration data. The Klamath River model is not expected to be able to mimic the exact timing and location of all water quality conditions. The model can be used to represent the overall water quality trends in response to external loading and internal system dynamics.

- While the multi-model framework might be efficient for calibration, it is also cumbersome in terms of data management and transfer between models. Additionally, because of differences in algorithms and state parameters for RMA, CE-QUAL-W2, and EFDC (e.g., for organic components), conversion of pollutant loads between models could result in slight inaccuracies.
- The model does not simulate multiple species of phytoplankton and periphyton. Therefore, this model is currently not suitable for evaluating competition among multiple species or evolution of the aquatic algal communities and their interaction with nutrients.
- Because of the lack of a direct linkage between OM loading and SOD and benthic nutrient flux, the model in its present stage cannot fully evaluate the long-term effect of load reductions on SOD.
- Neither zooplankton nor benthic animals are simulated in the model; therefore, there could be some uncertainty in the simulation of algal dynamics and nutrient cycling.
- In the estuarine portion of the model, the sand bar opening is fixed. Although this is a reasonable assumption, it can introduce uncertainty in simulating the dynamic features of the system, particularly over an extended period of time.
- Because of a lack of data and the seasonal variability in sand bar location, it is infeasible to configure a long-term simulation model for the estuary. Therefore, the sediment diagenesis model is not activated in EFDC for predicting the sediment-water interaction.
- Algae are represented as one lumped state variable, thus interspecies differences are not simulated. The nitrogen fixing process was not explicitly represented in the model. In general, nitrogen concentrations are high in the water column. Under these circumstances, N-fixing algae tend to uptake dissolved nitrogen directly from the water column as opposed to the air since nitrogen fixation is a highly energy-demanding process.
- Denitrification is not included in the riverine models. This might result in slight overprediction of nitrogen in the water column.
- Some fine scale nutrient patterns might not be accurately represented due to limitations in model formulations related to nutrient-periphyton interaction. RMA-11, for example, assumes periphyton uptakes only inorganic nitrogen and phosphorus and releases only organic nitrogen and phosphorus through respiration. In reality, both the uptake and release processes may involve both the inorganic and organic forms.
- OM for boundary conditions is not partitioned between labile and refractory forms. Therefore, detailed kinetic variability related to OM decay is not fully represented in the reservoirs.

2.4.3 Sources of Uncertainty

As with virtually every hydrodynamic and water quality model, uncertainty is present with regard to various aspects of the Klamath River Model. These uncertainties were minimized to the extent possible in this effort, and thus the model reproduces general trends in the observed data both temporally and spatially. Further reduction of uncertainty is possible through collection of more systematic and accurate data within and external to the system and a more in-depth scientific understanding of the physical, chemical, and biological processes occurring in this unique system.

Some of the major sources of uncertainty include the following:

- *Uncertainty Associated with Boundary Conditions.* Boundary conditions for the Klamath River Model include time series flow, temperature, water quality, and atmospheric

conditions. They provide the driving force for the hydrodynamic and water quality simulations. Therefore, accurate definition of boundary conditions is critical to reducing uncertainty. In developing the Klamath River Model, boundary conditions were defined using available monitoring data or were derived using different techniques (e.g., interpolation). Unfortunately, data are not available for all boundary conditions, and where data are available, they generally do not represent high temporal resolution (i.e., every point in time). Although techniques such as interpolation are a reasonable way to represent general trends in a system, precise prediction of water quality at every single point in time and every location is not possible.

- *Uncertainty in Spatial Representation.* The governing partial differential equations of hydrodynamic and water quality models are solved using the finite difference method (FDM) in CE-QUAL-W2 and finite element method (FEM) in RMA-2 and RMA-11. For both FDM and FEM, the waterbodies need to be discretized into different computational cells or nodes on the basis of topographical data. The accuracy in representing the true bathymetry of a waterbody has a significant effect on model performance. Thus, any uncertainty associated with the data sets used to discretize the waterbodies in the Klamath River has a direct effect on the model's predictive capabilities. Additionally, all the impoundments are represented using a laterally averaged system. This inherently assumes that lateral variability is insignificant, though this might not be the case. Also, all rivers are represented in a single, longitudinal dimension.
- *Uncertainty in Process Representation.* Water quality prediction for the Klamath River involves representing numerous dynamic interactions (including many physical, chemical, and biological processes). Mathematical models offer a simplified representation of these processes. Although the current state of knowledge with respect to fully understanding all the detailed interactions in the Klamath River is somewhat limited, the Klamath River modeling effort takes full advantage of all information amassed and understood to date. Major simplifications associated with the Klamath River Model that introduce uncertainty include representing the entire phytoplankton community as a single algae group, representing the entire periphyton community as a single periphyton group, representing SOD using a zero-order formulation, and representing OM with only four components based on solubility and degradability.
- *Uncertainty in Kinetic Structures.* Both CE-QUAL-W2 and RMA-11 represent major water quality decay and transformation with first-order kinetics. These kinetics are widely tested and accepted with regard to reasonably representing the dynamic interaction between water quality constituents. There is, however, uncertainty introduced in using these formulations because these processes are of higher order in reality.

3.0 Model Testing

Once the Klamath River model was configured, a calibration was performed at multiple locations throughout the system. Calibration refers to the adjustment or fine-tuning of modeling parameters to produce an adequate fit of the simulated output to the field observations. The sequence of calibration for the Klamath River model involved calibrating flow and water surface elevation first and then calibrating water quality using available monitoring data. Since the original PacifiCorp Model was already calibrated for hydrodynamics (see Section 3.2), this section of the report mainly focuses on the hydrodynamic calibration of the EFDC portion of the model and the water quality calibration of the entire model.

The upper Klamath River model (Model Segments 1 through 8) was calibrated using data from the year 2000. This year was selected for calibration because relatively good boundary condition data and in-stream data were available in the upper portion of the system (particularly for Lake Ewauna). Data were available, but not to the same extent, for the lower portion of the system (particularly downstream of Iron Gate Dam). Selection of this year was deemed appropriate because water quality conditions in the upper portion of the system drive the response downstream. To improve confidence in model predictions, the model was also corroborated (validated) using data from the year 2002 for Model Segments 1 through 5. Again, considerably more data were available for the upper portion of the system in 2002 than for other years. The estuarine portion (Model Segment 9) was calibrated using data from the year 2004, because bathymetric data and data for key water quality parameters were available. Water quality data were collected as part of an intensive monitoring effort. Insufficient data were available to calibrate for the year 2000 or 2002 in the estuarine portion of the Klamath River.

Hydrodynamic and water quality model calibration is typically guided by visual comparison between simulated and observed data and/or error statistics. Klamath River Model calibration was primarily guided by the former approach. Comparing time series plots of modeled versus observed data provides more insight into the nature of the system and is more useful, particularly for water quality calibration, than a statistical comparison. Trends in the observed data and cause-effect relationships between various parameters can be replicated with a model, although precise values at each and every point in time may not be. As long as the trends, relationships, and magnitudes are well-represented, and thus the underlying physics and kinetics are also being represented, a model can be confidently applied to scenario analysis, such as for TMDL development. Previous studies, such as Arhonditsis and Brett (2004), have indicated a reliance on visual comparison as opposed to error statistics for aquatic bio-chemical modeling. In the 153 papers surveyed by Arhonditsis and Brett during the 1992 to 2002 period, only 30% quantified error statistics while the majority (70%) relied only on visual comparison to evaluate model performance.

Although error statistics are often used in evaluating model calibration, they are not recommended for evaluating Klamath River Model reliability due to the following reasons: (1) Due to data gaps associated with configuring the modeling framework, it's unrealistic to assume that the model will be able to precisely predict each and every condition. (2) Most of the available data for calibration were not continuous. Point data only permits comparison during a snapshot in time, and this snapshot is representative of only a single condition. Although multiple water quality data are available, they are not necessarily representative of all conditions (which are, in fact, simulated by the model because it is continuous). (3) Making a "point-by-point" comparison (i.e. a comparison of a water quality observation for a given date and time versus the modeled value for the same date and time) may result in poor statistical results, because the precise timing of all physical, chemical, and biological phenomenon are likely not

perfect in a model. Although calibration was guided by visual analysis, error statistics were calculated. Mean Error (ME) and Absolute Mean Error (AME) were computed for several locations characterized by a relative abundance of monitoring data. These statistics are presented in Appendix E for Miller Island and Hwy 66, and Appendix H for Shovel Creek and Stateline.

Theoretically, model reliability can be improved by modeling a longer period of time. This is one reason the model was calibrated and corroborated for separate years (2000 and 2002, respectively). The ability to readily expand the time period modeled using the Klamath River model is severely limited by a number of factors. Boundary conditions for the Klamath River are quite variable over time, and insufficient monitoring data are available to fully characterize this variability. Additionally, the Klamath River is characterized by a very short retention time. As such, signals from major inflows have a significant impact on the in-stream water quality. Modeling multiple years therefore largely involves estimating/deriving/refining boundary conditions rather than adjusting internal model parameter values. Discrepancies between model predictions and observations may be due solely or primarily due to inaccurate boundary conditions as opposed to model settings. Model reliability was deemed sufficient based on the ability to represent the water quality trends and magnitudes for both the calibration and corroboration periods.

3.1 Monitoring Locations

The water quality monitoring stations with relevant data used for the 2000 model calibration are presented in Table 3-1, Figure 3-1, and Appendix C.

Table 3-1. Monitoring stations used for Klamath River model calibration (2000)

Station/Location	Site ID	Source
Klamath River at Miller Island boat ramp	KR24589/ KR24594	City of Klamath Falls/ODEQ/ USBR/PacifiCorp
Klamath River at Keno Bridge (Hwy 66)	KR23490	USBR/PacifiCorp/ODEQ
J.C. Boyle Reservoir at deepest point	KR22505	USBR/STORET/ODEQ/ BEAK
Klamath River u/s Shovel Creek	KR20642	NCRWQCB
Copco Lake near Copco	KR19874	USBR/STORET
Iron Gate Reservoir	KR19021	USBR/STORET
Klamath River below Iron Gate Dam	KR18952	USBR/STORET/SWAM/ KRIS/USGS
Klamath River above Shasta River	KR17608	USBR
Klamath River above Scott River	KR14260	USBR/USFWS
Klamath River near Seiad Valley	KR12858	USBR/STORET
Klamath River at Youngs Bar	KR04036	USBR
Upper Estuary	UE	NCRWQCB/Yurok Tribe
Middle Estuary	ME	NCRWQCB/Yurok Tribe
Lower Estuary	LE	NCRWQCB/Yurok Tribe

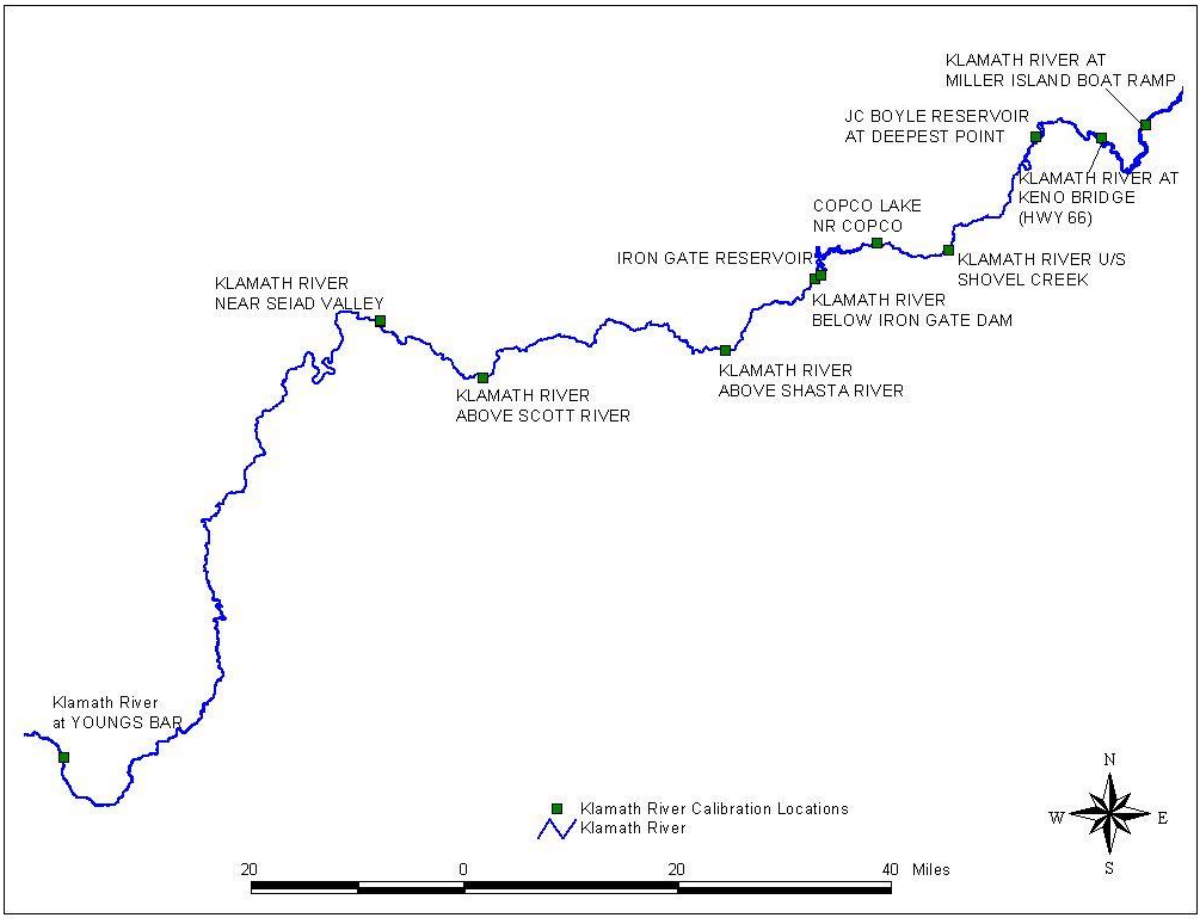

Figure 3-1. Calibration locations for Klamath River modeling (above the Klamath Estuary)

In 2002 data were collected at several additional stations in the upper portion of the river. Model results were therefore also evaluated at these stations (Table 3-2). Figure 3-2 shows the locations of the additional stations in the Lake Ewauna to Keno Dam modeling segment. Figure 3-3 shows the locations of the additional stations in the Keno Dam to J.C. Boyle modeling segment.

Table 3-2. Additional monitoring stations used for Klamath River model calibration (2002)

Station/Location	Site ID	Source
Lake Ewauna at Railroad Bridgespan	KR25173	City of Klamath Falls
Klamath River at South-Side Bypass Bridge	KR25079	City of Klamath Falls/ ODEQ/USBR/PacifiCorp
Lost River Diversion	LK	City of Klamath Falls/PacifiCorp
Klamath River at HWY 97 BR NE	KR24901	City of Klamath Falls
Klamath River below Boyle Dam	KR22129/KR22460	PacifiCorp
Klamath River u/s of Boyle Powerhouse Tailrace	KR22128	USFWS
Klamath River d/s of Boyle Powerhouse Tailrace	KR22127	ODEQ
J.C. Boyle Powerhouse Tailrace	BTR	USFWS
Klamath River near Stateline	KR20932	PacifiCorp/SWAMP

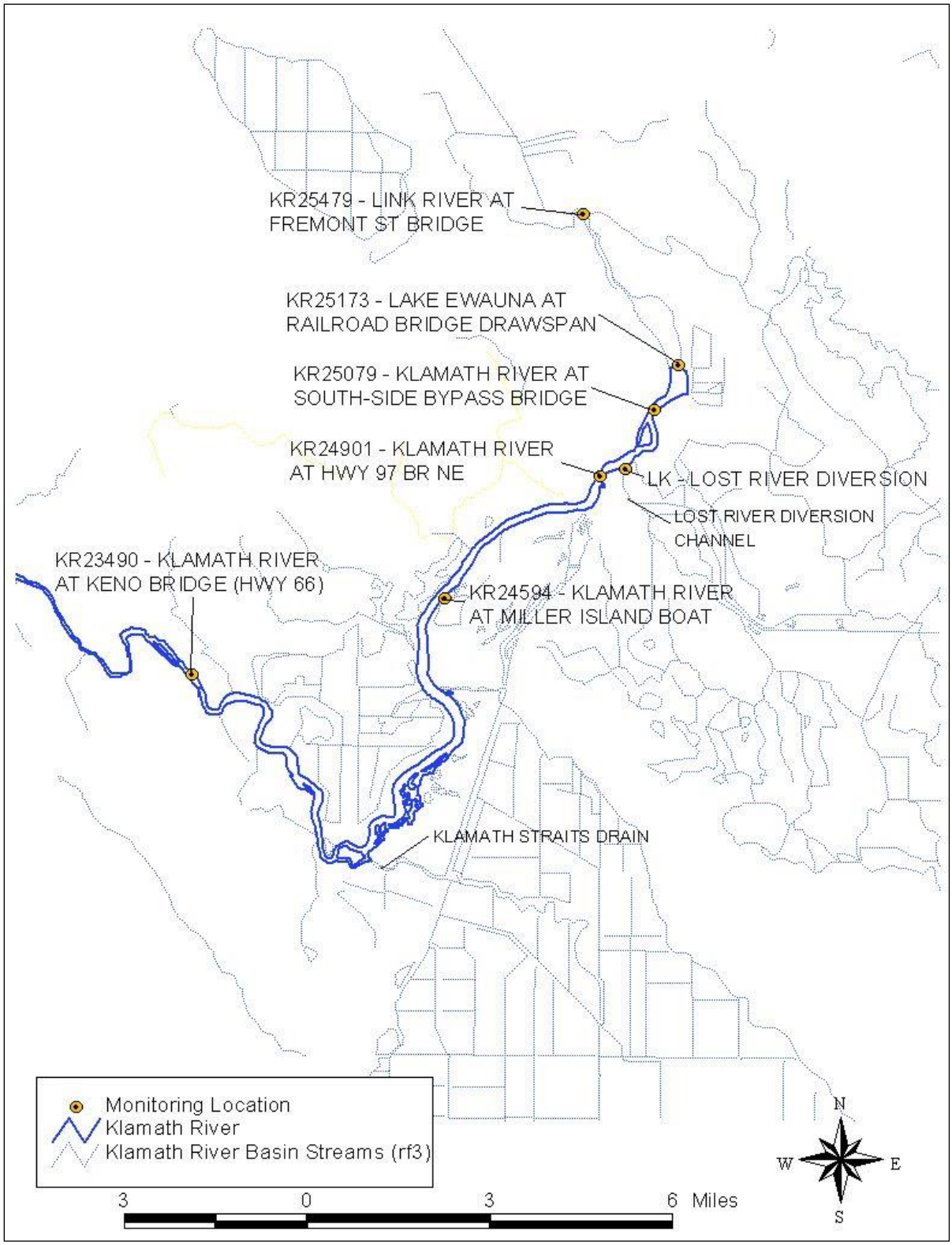

Figure 3-2. Additional calibration locations for Klamath River modeling—Lake Ewauna to Keno Dam modeling segment (2002)

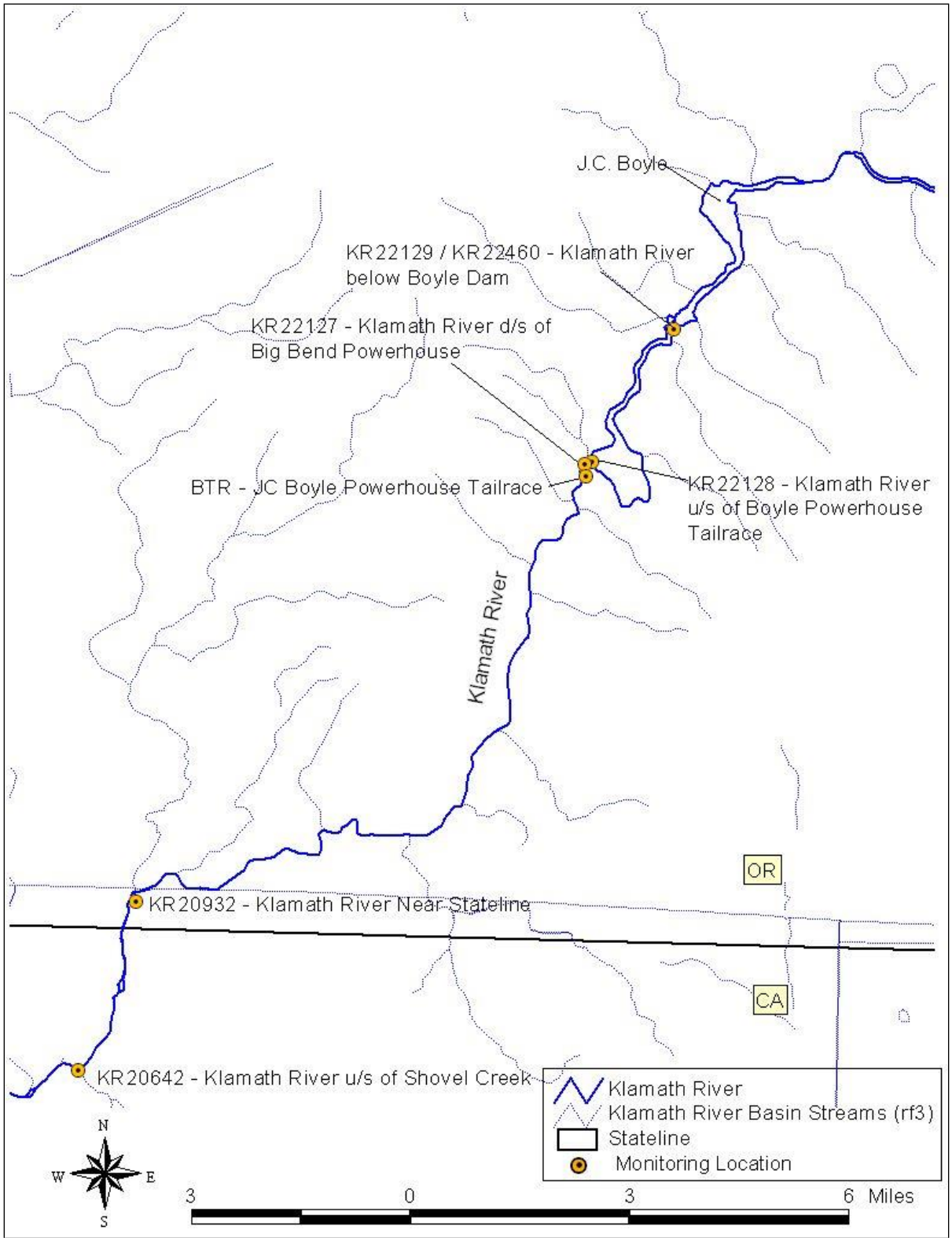

Figure 3-3. Additional calibration locations for Klamath River modeling—Keno Dam to J.C. Boyle modeling segment (2002)

3.2 Hydrodynamic Calibration

It was not necessary to perform additional hydrodynamic calibration for Klamath River Model Segments 1 through 8. The grid layout and hydrodynamic configuration and calibrations for the PacifiCorp Model were found to be reasonable, and no better information is available to further refine this component of the model. Therefore, there has been no additional effort to further refine the hydrodynamic model. Hydrodynamic calibration results (for temperature) are presented in Appendices E through K for Lake Ewauna through Turwar.

Hydrodynamic results for temperature and salinity in the estuarine portion of the Klamath River (Model Segment 9) are presented in Appendix L (Figures L-1 through L-6). Temperature and salinity sonde data collected at the surface and bottom were compared to model output for three separate locations. In general, the temperature calibration followed the observed data trend fairly well with the model underpredicting slightly at the Upper Estuary site. The model was able to simulate lower temperatures at the bottom and higher temperatures at the surface in the lower estuary where salinity and temperature stratification exist. It was able to capture the magnitude of peaks and trends and the spatial variability of salinity fairly well (i.e., high salinity at the Lower Estuary site and low salinity at the Upper Estuary site). Also, the model predicted high salinity at the bottom and lower salinity at the surface, which matches the observed salinity profile. The model also predicts significant temporal variability of salinity as a result of the complex interactions between upstream freshwater inflows and downstream tidal impact. Some disparity does exist between the simulated and observed salinity, and this can be explained by uncertainty in physical representation. For example, the exact dimensions of the sand bar opening for the simulated period are not known. Also, representation of downstream tidal characteristics is limited by available data. Overall, the model predicts the observed temperature and salinity trends and thus reasonably represents physical circulation and transport in the estuary.

3.3 Water Quality Calibration

The Klamath River modeling system was developed in a piecewise manner, where models for different sections of the river were linked by routing flow and constituent mass from upstream to downstream. The water quality calibration process involved first calibrating the upstream waterbodies and then using the resulting flow and predicted concentration time series (together with the watershed and other tributary inputs) to drive the downstream waterbody simulations.

Calibration of the water quality model was implemented by fine-tuning major kinetic parameters such as algal growth rate, death rate, nitrification/denitrification rates, OM decay rates, and SOD rates. The calibration process started with the existing PacifiCorp Model and continued with fine-tuning of parameter values after the major boundary conditions were set. This entailed comparison of model predictions to monitoring data and iterative adjustment of parameter values. The overall goal was to most accurately match observed data while maintaining consistency among all the waterbodies. In the following sections, the water quality calibration results at each station and in each modeled segment are presented. The major calibrated parameters in the CE-QUAL-W2 models are presented in Tables 3-3 and 3-4, and those for the RMA-11 models are presented in Table 3-5. Because the water quality parameters in all the riverine sections are the same, they are not listed by modeling segment.

It should be noted that while most CE-QUAL-W2 parameters were consistent from one model segment to the next, those associated with algae dynamics and OM dynamics differed somewhat. The algae parameters include growth rate, respiration rate, and death rate and are used to characterize the algae communities in each lake. In different waterbodies, algae communities can consist of different algae species, and each of these species exhibits different characteristics.

Additionally, a single algae species can exhibit different characteristics in different waterbodies because of a variety of factors. Since the model represents a single, lumped algae species and represents only the impacts of temperature, light, and nutrients on algae, algae-related parameters differ from one waterbody to the next. Although these parameter values differ, they are all within the range of literature values.

The OM parameters differ among model segments in that the decay rates for labile particulate and dissolved OM are higher in the upstream modeling segments than in the lower segments. This is because all the OM from the boundary conditions is lumped together and represented using the labile OM slots. An average decay rate is used to reflect the characteristics of the OM. Because an average value is used, it can be taken to mean that a combination of both extremely labile OM and refractory OM are considered. The decay rate of the OM decreases in a downstream manner since the more labile OM fraction is lost faster than the less labile fraction

Table 3-3. Nutrient input parameters used in the CE-QUAL-W2 Models

Parameter	Description	Units	Lake Ewauna-Keno Dam (Model Segment 2)	J.C. Boyle Reservoir (Model Segment 4)	Copco Reservoir (Model Segment 6)	Iron Gate Reservoir (Model Segment 7)	Typical literature values[a]
PO4R	Sediment release rate of phosphorus	fraction of SOD	0.01	0.01	0.01	0.01	0.001 to 0.03
ORGP	Fraction of phosphorus in OM	--	0.0055	0.0055	0.0055	0.0055	0.005 to 0.011
ORGN	Fraction of nitrogen in OM	--	0.07	0.07	0.07	0.07	0.08
NO3DK	Nitrate decay rate	day^{-1}	0.1	0.1	0.1	0.1	0.05 to 0.15
NO3T1	Lower temperature for nitrate decay	^oC	5	5	5	5	5
NO3T2	Upper temperature for nitrate decay	^oC	25	25	25	25	25
NO3K1	Lower temperature rate multiplier for nitrate decay	--	0.1	0.1	0.1	0.1	0.1
NO3K2	Upper temperature rate multiplier for nitrate decay	--	0.99	0.99	0.99	0.99	0.99
NH4DK	Ammonium decay rate	day^{-1}	0.10	0.1	0.1	0.1	0.00 to 0.80
NH4R	Sediment release rate of ammonium	fraction of SOD	0.05	0.05	0.05	0.05	0.00 to 0.40
NH4T1	Lower temperature for ammonium decay	^oC	5	5	5	5	5
NH4T2	Upper temperature for ammonium decay	^oC	25	25	25	25	25
NH4K1	Lower temperature rate multiplier for ammonium decay	--	0.1	0.1	0.1	0.1	0.1
NH4K2	Upper temperature rate multiplier for ammonium decay	--	0.99	0.99	0.99	0.99	0.99

Parameter	Description	Units	Lake Ewauna-Keno Dam (Model Segment 2)	J.C. Boyle Reservoir (Model Segment 4)	Copco Reservoir (Model Segment 6)	Iron Gate Reservoir (Model Segment 7)	Typical literature values[a]
LDOMDK	LDOM decay rate	day^{-1}	0.20	0.15	0.10	0.05	0.01 to 0.63
RDOMDK	RDOM decay rate	day^{-1}	0.001	0.001	0.001	0.001	0.001
LPOMDK	LPOM decay rate	day^{-1}	0.20	0.15	0.10	0.05	0.001 to 0.11
RPOMDK	RPOM decay rate	day^{-1}	0.001	0.001	0.001	0.001	0.001
SOD	Sediment oxygen demand	gram $O_2/m^2/day$	3.0	1.4	1.4	1.1	0.1 to 5.8

[a] Literature values are from the CE-QUAL-W2 Users Manual which compiled data from a range of sources. The only exception is the stoichiometric coefficient, which was derived from Chapra 1997.

Table 3-4. Phytoplankton input parameters used in the CE-QUAL-W2 Models

Parameter	Description	Units	Lake Ewauna-Keno Dam (Model Segment 2)	J.C. Boyle Reservoir (Model Segment 4)	Copco Reservoir (Model Segment 6)	Iron Gate Reservoir (Model Segment 7)	Typical literature values[a]
AG	Growth rate	day^{-1}	2.3	1.2	1.2	1.2	0.2 to 9.0
AR	Dark respiration rate	day^{-1}	0.18	0.1	0.1	0.1	0.01 to 0.92
AE	Excretion rate	day^{-1}	0.05	0.05	0.02	0.02	0.01 to 0.044
AM	Mortality rate	day^{-1}	0.15	0.06	0.06	0.07	0.03 to 0.30
AS	Settling rate	day^{-1}	0.3	0.3	0.3	0.3	0.001 to 13.20
AHSP	Phosphorous half-saturation coefficient	$g.m^{-3}$	0.003	0.003	0.003	0.003	0.001 to 1.520
AHSN	Nitrogen half-saturation coefficient	$g.m^{-3}$	0.014	0.014	0.014	0.014	0.01 to 4.32
ASAT	Light saturation	$W.m^{-3}$	75	75	75	100	10 to 150
AT1	Lower temperature for minimum algal rates	^oC	5	5	5	5	N/A
AT2	Lower temperature for maximum algal rates	^oC	17	17	17	14	N/A
AT3	Upper temperature for minimum algal rates	^oC	35	35	35	35	N/A
AT4	Upper temperature for maximum algal rates	^oC	45	45	45	45	N/A
AK1	Lower temperature rate multiplier for minimum algal rates	--	0.1	0.1	0.1	0.1	N/A
AK2	Lower temperature rate multiplier for maximum algal rates	--	0.99	0.99	0.99	0.99	N/A
AK3	Upper temperature rate multiplier for minimum algal rates	--	0.99	0.99	0.99	0.99	N/A

Parameter	Description	Units	Lake Ewauna-Keno Dam (Model Segment 2)	J.C. Boyle Reservoir (Model Segment 4)	Copco Reservoir (Model Segment 6)	Iron Gate Reservoir (Model Segment 7)	Typical literature values[a]
AK4	Upper temperature rate multiplier for maximum algal rates	--	0.1	0.1	0.1	0.1	N/A
ALGP	Phosphorus to biomass ratio	--	0.0055	0.0055	0.0055	0.0055	0.005 to 0.08
ALGN	Nitrogen to biomass ratio	--	0.07	0.07	0.07	0.07	0.08
ALGC	Carbon to biomass ratio	--	0.45	0.45	0.45	0.45	0.45

[a] Literature values are from the CE-QUAL-W2 Users Manual Cole and Wells (2003); which compiled data from a range of sources. The only exception is the stoichiometric coefficient, which includes information derived from Chapra 1997.

Table 3-5. Parameters used in the RMA-11 Models

Variable	Description, units	Value	Typical literature values
ALP0	Chl a to algal biomass conversion factor, phytoplankton, mg Chl_a to mg-A	67	22 to 220
ALP1	Fraction of algal biomass that is nitrogen, phytoplankton, mg-N/mg A	0.07	0.08
ALP2	Fraction of algal biomass that is phosphorous, phytoplankton, mg-P/mg A	0.0055	0.005 to 0.08
MUMAX	Maximum specific growth rate, phytoplankton, 1/d	1.00	0.2 to 9.0
RESP	Local respiration algae, phytoplankton, 1/d	0.18	0.01 to 0.92
MORT	Local mortality rate of algae, phytoplankton, 1/d	0.05	0.03 to 0.30
KLIGHT	Half saturation coefficient for light, phytoplankton, KJ m-2 s-1	0.10	N/A
PREFN	Preference factor for NH3-N, phytoplankton	0.60	N/A
ABLP0	Chl a to algal biomass conversion factor, bed algae, mg Chl_a to mg-A	67	22 to 220
BMUMAX	Maximum specific growth rate, bed algae, 1/d	1.15	0.45 to 2.0
BRESP	Local respiration rate of algae, bed algae, 1/d	0.20	N/A
BMORT	Local mortality rate of algae, bed algae, 1/d	0.20	N/A
KBLIGHT	Half-saturation coefficient for light, bed algae, KJ m-2 s-1	0.05	N/a
PBREFN	Preference factor for NH3-N, bed algae	0.75	N/A
BET1	Rate constant: biological oxidation NH3-N, 1/d	0.30	0.0 to 0.8
BET2	Rate constant: biological oxidation NO2-N, 1/d	0.50	N/A
BET3	Rate constant: hydrolysis OM to NH3-N, 1/d	0.20	0.001 to 0.63
KNITR	Michaelis-Menton half saturation constant: nitrogen, phytoplankton, mg/l	0.014	0.01 to 4.32
KPHOS	Michaelis-Menton half saturation constant: phosphorous, phytoplankton, mg/l	0.003	0.001 to 1.52

Variable	Description, units	Value	Typical literature values
KBNITR	Half-saturation coefficient for nitrogen, bed algae, mg/lFraction of algal biomass that is phosphorus, bed algae, mg/l	0.014	N/A
KBPHOS	Half-saturation coefficient for phosphorus, bed algae, mg/lHalf-saturation coefficient for nitrogen, bed algae, mg/l	0.003	N/A
ALP3	Rate O2 production per unit of algal photosynthesis, phytoplankton, mg-O/mg-AHalf-saturation coefficient for phosphorus, bed algae, mg/l	1.40	1.40
ALP4	Rate O2 uptake per unit of algae respired, phytoplankton, mg-O/mg-ARate O2 production per unit of algal photosynthesis, phytoplankton, mg-O/mg-A	1.4	1.4
ALP5	Rate O2 uptake per unit NH3-N oxidation, mg-O/mg-NRate O2 uptake per unit of algae respired, bed algae, mg-O/mg-A	3.43	3.43

3.3.1 Link River (Model Segment 1)

Link River is a short, 1.31 mile segment that is characterized by a steep slope and rapid flow. With an average flow velocity at the end of Link River equivalent to approximately 0.9 m/s, it takes less than an hour for water to flow from Link Dam to Lake Ewauna (the next downstream segment). In this short time frame, significant water quality variation is not expected to occur. Model simulation results demonstrate this characteristic and show that the segment's outflow water quality is nearly the same as the inflow conditions.

The Link River model was developed on the basis of the RMA-11 modeling framework. In the original PacifiCorp Model, nine water column constituents and one benthic constituent were simulated. The nine water column constituents include an arbitrary constituent, BOD, DO, OM, NH_4, NO_2/NO_3, PO_4, phytoplankton, and temperature. The benthic constituent is used to simulate benthic algae such as periphyton. In this system configuration, the simultaneous representation of the BOD and OM provide some redundancy because BOD essentially is a surrogate for OM. Therefore, BOD and OM were combined into one constituent (see Section 2.2.1).

The model was run for the period from January 1, 2000, to December 31, 2000 for the 2000 calibration run. I It was also run from January 1, 2002 to December 31, 2002 for the corroboration run. No data were available to calibrate the model for the reach.

3.3.2 Lake Ewauna-Keno Dam (Model Segment 2)

The Lake Ewauna segment was developed on the basis of the CE-QUAL-W2 modeling framework. In the original PacifiCorp Model, 18 water column constituents were simulated, which included four OM components and one BOD component. In the present study, BOD was eliminated from the active constituent list in the model input data file (see Section 2.2.1).

In the calibration run, the model was run for the period from January 1, 2000, to December 31, 2000. The model output was compared to observations at two water quality stations in Lake Ewauna: Klamath River at Miller Island boat ramp and Klamath River at Keno bridge (Hwy 66). As shown in Figures E-1 through E-16 in Appendix E, the model reproduced the observed water

quality pattern reasonably well. The final calibrated parameters for Lake Ewauna are presented in Tables 3-3 and 3-4.

The model reproduces the supersaturation of DO in June well, as well as the extended anoxic period in July. The DO data show strong diurnal fluctuation and supersaturation conditions during May, however, it seems to contradict the phytoplankton data. Phytoplankton data exhibit low chlorophyll *a* concentrations during this period, and these concentrations are insufficient to generate the supersaturated DO concentrations observed in the water column. Since the May chlorophyll *a* data correspond with algae levels in UKL, it was assumed that the DO concentrations in May are not entirely reliable. Therefore, no attempt was made to reproduce the supersaturation in May. The model also was able to reproduce DO recovery in early August and the subsequent dip in late August and through September. It is worth noting that the data show low DO in late fall and winter while the model simulates relatively high DO concentrations. During this period, water temperature dropped rapidly, and algae and OM loading from UKL decreased. One would expect that these monitored phenomena would result in DO recovery from the summer anoxic conditions (as predicted by the model). Lake Ewauna, however, is a unique system that is highly dynamic and subject to tremendous OM loading from UKL. The lake also experiences an extended period of summer hypoxic/anoxic conditions which result in quick removal of algae and generation of extra OM. Therefore, it is highly likely that the lake's late fall and winter DO concentrations do not respond similarly to most other impoundments.

One possible cause might be that the extremely high organic loading from both UKL and algae death during the summer result in a tremendous amount of OM being settled into the sediment layer during the summer (forming a highly enriched bed). During late fall and winter, even though OM and algae loadings cease, this highly enriched bed may provide significant oxygen consumption potential (preventing high DO concentrations). This could be the ultimate cause of the observed low DO during the late fall and winter. Without a predictive sediment diagenesis module, however, the existing CE-QUAL-W2 model is not capable of fully representing the dynamic interaction and feedback between the sediment and water column. This limitation is not expected to impact TMDL determination, because the critical, anoxic period occurs during the summer.

The predicted phytoplankton biomass matches the observed trends very well, especially the decline during the summer anoxic period and the difference in magnitude between Miller Island and Hwy 66. The model does overpredict chlorophyll *a* during the month of June at both Miller Island and Hwy 66 due to the lack of temporally variable data in UKL to set the boundary condition. The boundary condition data for UKL shows a chlorophyll *a* peak during June, and this is transported quickly downstream, resulting in the peak in June at Miller Island and Hwy 66. In general, the model also predicts nutrients well, except for timing in some situations. This is likely because of limitations surrounding the definition of boundary conditions (i.e., the use of limited data to derive the boundaries). The model was able to predict relatively high NH_4 and PO_4 concentrations during the anoxic period likely due to a combination of multiple water quality processes including upstream and tributary loading, OM decay, algae die-off, and release from sediment.

It should be noted that simulated NO_2/NO_3 is relatively low compared with the observed values. The accuracy of these data, however, is unknown. Measurements made by different agencies during this time period were found to be significantly different (approximately an order of magnitude). It is suspected that the high NO_2/NO_3 measurements are incorrect. During the summer anoxic period, nitrification, which is the source of NO_2/NO_3, is inhibited by the low DO concentration. NO_2/NO_3 levels are expected to be high only if an external source is supplying a

significant amount. This, however, is not supported by currently available data. The model predicts the trends exhibited by the lower level NO_2/NO_3 measurements. The model results also show good agreement between the simulated and observed pH at the two locations, indicating a reasonable representation of the fate and transport of pH related constituents and their interactions.

The Lake Ewauna to Keno Dam model segment was further tested using monitoring data in 2002. In 2002 the city of Klamath Falls collected a significant amount of data in this reach. Data were collected at six monitoring stations, including Lake Ewauna at Railroad Bridge Drawspan (LERBD), Klamath River at South Side Bypass Bridge (KRSSBB), Klamath River at Hwy 97 (KR97), Klamath River at Lost River Diversion Channel (KRLRDC), Klamath River at Miller Island (KRMI), and Klamath River at Hwy 66 (KR66). The simulated temperature, nutrients, DO, and algae biomass are plotted against the observed data at these locations in Figures E-17 to E-57. The model reproduces the observed water quality conditions and trends well. A disparity between observed and modeled DO does exist between March and June. During this period, the model tends to underpredict DO. This suggests that the estimated OM boundary condition at Link River might be too high for this period and results in excessive deoxygenation potential in the water column. More representative monitoring data characterizing this boundary would improve the model predictions. Fortunately this time period is outside the critical summer months of July and August. Another observation is that the model tends to overpredict chlorophyll *a* during the month of June. This might be due to uncertainty in the upstream boundary condition as well as possible inter-year variability in water column kinetic characteristics that cannot be accounted for by using the same parameter values as in the 2000 calibration model. Despite this minor disparity between model results and data, the 2002 model represents the chlorophyll *a* trends well.

Model results from 2000 can also be used to determine the significance of nutrient limiting effects on algae growth. Figure E-62 presents the simulated nutrient limiting condition at Hwy66 in 2000. Due to the high incoming nutrient loading from UKL, as well as significant contributions from LRDC and KSD, nutrient limiting factors for both nitrogen and phosphorus are very high (>0.9). This indicates that algae growth is not limited by nutrient availability. If either nutrient group (i.e., phosphorus or nitrogen) showed a significant divergence from a value of 1.0, nutrient availability would be limiting algae growth. In the spring, it appears that nitrogen might be slightly more limiting than phosphorus.

3.3.3 Keno Dam to J.C. Boyle Reservoir (Model Segment 3)

The portion of the water quality model for Keno Reach was developed using the RMA-11 modeling framework. In the original PacifiCorp Model, nine water column constituents and one benthic constituent were simulated as in the Link River model. In this river segment, BOD and OM were combined to form a unified constituent as was done for the Link River model segment.

The model was run for the period from January 1, 2000, to December 31, 2000. No data were available to calibrate the model for the year 2000. Data were available for the year 2002 at a location downstream of Keno Dam. Figures F-1 through F-7 in Appendix F show the calibration results for the year 2002. The model reproduces the observed nutrients and pH well. The model results for DO also match the observed magnitudes and trends well. It does, however, predict a lower DO than the data show during the summer (Figure F-2). One reason might be that the model is not representing sufficient reaeration downstream of the dam. This would result in slower recovery from the low DO conditions seen upstream of the dam. It should also be noted

that only one monitoring point is available during this extended time period. A single DO sample is insufficient to reflect the likely range of DO levels that would occur over a day and throughout this critical time period.

3.3.4 J.C. Boyle Reservoir (Model Segment 4)

The J.C. Boyle Reservoir segment was developed using the CE-QUAL-W2 modeling framework. The model was run for the period from January 1, 2000, to December 21, 2000. The constituent configuration in this river segment is the same as the Lake Ewauna segment (Section 3.3.2).

For calibration, the model was run for the period from January 1, 2000, to December 31, 2000, and the simulated water quality is compared with observed profiles in the reservoir at water quality monitoring station J.C. Boyle Reservoir (at deepest point). Major parameters adjusted during the calibration process included algae growth rate, algae respiration rate, algae death rate, particulate OM settling velocity, OM decay rate, and suspended solids settling velocity. As shown in Figures G-1 through G-7 in Appendix G, the model reproduced the observed pattern reasonably well.

Although the model overpredicts NH_4 and NO_3 concentrations on some dates and underpredicts them on other dates, it predicts concentrations within the range of observed data. These differences are caused by uncertainty in boundary conditions. To more accurately represent such fine-scale variability (both temporally and on a depth basis), higher resolution data (i.e., temporally and spatially) are necessary to configure boundary conditions representing major tributaries and inflows. The final calibrated parameters for J.C. Boyle Reservoir are presented in Tables 3-3 and 3-4.

The J.C. Boyle model was further tested using the 2002 data. Only three constituents are available for 2002: temperature, pH, and DO. Model predictions for these constituents follow the overall trends well and suggest a reasonable calibration (Figures G-8 through G-10 in Appendix G).

3.3.5 Bypass/Full Flow Reach (Model Segment 5)

The Bypass/Full Flow Reach segment was developed using the RMA-11 modeling framework. In the original PacifiCorp Model, nine water column constituents and one benthic constituent were simulated as in the Link River model. In this study, BOD and OM are combined to form a unified constituent as was done for Link River model (see Section 2.2.1).

For calibration, the model was run for the period from January 1, 2000, to December 31, 2000. Data for temperature, nutrients, DO, Alkalinity, and pH were available to calibrate the model. Figures H-26 through H-33 in Appendix H show the comparison of model results versus observed data for the Klamath River upstream of Shovel Creek. The results indicate reasonable agreement between predictions and monitoring data. The overprediction of chlorophyll *a* during June is due to uncertainty in the UKL boundary condition. Similarly, the overprediction of NH4 during summer and fall can also be attributed to uncertainty in the upstream boundary conditions in Lake Ewauna. The model was further tested using data collected in 2002 and was run from January 1, 2002, through December 31, 2002. Figures H-34 through H-40 in Appendix H show the comparison of model results versus observed data for the Klamath River upstream of Shovel Creek.

In 2002 data were collected at more locations, including at the Klamath River downstream of J.C. Boyle Dam (KRJCB) (but upstream of the J.C. Boyle Powerhouse), Klamath River upstream of J.C. Boyle Powerhouse Tailrace (KRUPT), Klamath River downstream of Big Bend Powerhouse (KRBP), Klamath River at J.C. Boyle Powerhouse Tailrace (KRPT), and Klamath River near Stateline (KRS). The sampled constituents include temperature, DO, pH, and nutrients. The predicted results are plotted against the data in Appendix H (Figures H-1 to H-25).

As shown, the model accurately reproduces the general trends and magnitudes observed in the data. There are, however, some discrepancies between model results and data at various locations and times. For example, Figure H-1 shows that although the model has reproduced the seasonal variability and peaks of temperature downstream of J.C. Boyle, it underpredicts the diurnal fluctuation. This discrepancy may be due to local conditions not entirely captured by the model. Data collection could have occurred in a shallow region that exhibits a wider range of temperature variability while the model segment represents laterally and vertically averaged. This particular location is almost immediately downstream of J.C. Boyle, and thus a significant amount of water is always discharged from the dam (greater than 100 cfs). Under these conditions, the average temperature in this segment should be primarily controlled by the discharge temperature from the dam. The model reflects this condition while the data could actually represent a highly localized condition. The discrepancy between model results and DO data in Figure H-2 is likely also caused by this same condition. Figures H-7 and H-10 show that the model slightly overpredicts and underpredicts, respectively, the observed temperatures. This is likely due to differences between the modeled spring water flow and temperature and actual conditions in these portions of the river data. For example, the model represents the spring discharge in this area as three discrete tributaries with constant flow rates and temperatures. In reality, the spring discharge can be variable in quantity as well as temperature. The model's overprediction of chlorophyll *a* in Figure H-17 is likely caused by the overprediction of chlorophyll *a* in Lake Ewauna during the early summer, which propagate to this location in the system.

Neither nitrogen nor phosphorus appears to significantly limit algae growth in this portion of the river. Figure H-41 presents the simulated nutrient limiting factors on periphyton growth for both nutrient classes during 2000, at Stateline. Neither nutrient class diverges significantly from a value of 1.0. As with the Hwy66 location, nitrogen appears to be slightly more limiting than phosphorus in the spring.

3.3.6 Copco Reservoir (Model Segment 6)

The water quality model for Copco Reservoir was developed on the basis of the CE-QUAL-W2 modeling framework. The water quality constituent configuration in this segment is the same as for the Lake Ewauna segment.

The model was run for the period from January 1, 2000, to December 31, 2000. The simulated water quality output was compared with the observed profile data in the reservoir at water quality station Copco Lake near Copco. Key parameters that were changed through this calibration process include algae growth rate (AG), particulate organic matter settling velocity (POMS), labile dissolved organic matter decay rate (LDOMDK), and labile particulate organic matter decay rate (LPOMDK).

The final calibrated parameters for Copco Reservoir are presented in Tables 3-3 and 3-4. The model results are plotted against observed data at water quality station Copco Lake near Copco in

Figures I-1 through I-7 in Appendix I. The model matched the monitoring data reasonably well. It overpredicts NH_4 and NO_3 concentrations on some dates and underpredicts them on other dates for Copco Reservoir. In general, however, it predicts concentrations within the range of observed data. Differences are likely caused by uncertainty in boundary conditions from limited data availability.

3.3.7 Iron Gate Reservoir (Model Segment 7)

The model was run for the period from January 1, 2000, to December 21, 2000. The simulated water quality output was compared with the observed profile data in the reservoir at the water quality station in Iron Gate Reservoir (Figures J-1 through J-7 in Appendix J).

The Iron Gate Reservoir portion of the model was updated using the new parameter values from Copco Reservoir. It was found that by changing the values of several kinetic parameters, including SOD, AG, LDOMDK, and LPOMDK (as shown in Table 3-3 and 3-4), the model was able to predict a reasonable water quality response for DO, phytoplankton, and nutrients. Additional parameters that were fine-tuned include sediment NH_4 release rate in proportion to SOD (NH4R), sediment PO_4 release rate in proportion to SOD (PO4R), algae death rate (AM). The detailed parameter values are listed in Tables 3-3 and 3-4. The model achieves a reasonable agreement with the data, indicating that the water quality dynamics in the reservoir are reasonably represented.

3.3.8 Iron Gate Dam to Turwar (Model Segment 8)

The water quality model for this segment was developed using the RMA-11 modeling framework, and the water quality constituent configuration is the same as for the upstream riverine RMA models.

The model was run for the period from January 1, 2000, to December 31, 2000. Data for only temperature and DO were available at five stations along this reach to calibrate the model. The five stations are the Klamath River downstream of Iron Gate Dam, Klamath River above Shasta River, Klamath River above Scott River, Klamath River above Seiad Valley, and Klamath River at Youngs Bar. Model results are plotted against observed data in Appendix K. The model reproduces the observed temperature very well at these locations.

The model also reproduces DO concentrations. As noted earlier in this report, a scaling factor was introduced into the RMA-11 model to better represent reaeration just downstream of Iron Gate Dam. The scaling factor was determined through an inverse modeling process which involved estimating reaeration based on upstream and downstream DO concentrations. DO predictions further downstream generally also replicate monitoring data. The Klamath River is steep and is generally characterized by a large flow. This results in significant reaeration along the length of the river. Modeling results for this segment show that DO in the river increases to approximately saturation because of this reaeration effect. At monitoring locations farther downstream, e.g., above Seiad Valley and at Youngs Bar, data however do not show this expected trend. In fact, the model tends to overpredict DO. Observed DO can reach very low levels, e.g., 2.5 to 4.0 mg/L; however, the model tends to predict concentrations around 8.0 mg/L (close to saturation).

This disparity in results was investigated through a number of sensitivity analyses. The following adjustments to the model were made to determine their potential effect on in-stream DO concentrations:

- Tributary DO boundary conditions were reduced to 0.0 mg/L (for all incoming tributaries where monitoring data are available, except major rivers such as Shasta and Scott).
- SOD was increased to an extremely high value along the length of the river (to 5.0 g/m2/day). This represents a highly enriched substrate, although this is uncharacteristic of this region of the Klamath River.
- A very high OM concentration was set for all boundary conditions. The value used is equivalent to roughly 45.0 mg/L of CBOD.
- A series of different reaeration equations were used.

None of these adjustments was able to sufficiently lower the DO concentrations to the monitoring levels. It should also be noted that the low DO does not appear to be caused by biological activity (e.g., periphyton), based on the minimal observed diel DO fluctuation range. After running these sensitivity analyses, the quality of the DO monitoring data were further explored.

Upon further review, DO data for this time period were found to be inaccurate. The Klamath River Water Quality 2000 Monitoring Program—Project Report (Watercourse Engineering, Inc. 2003) indicated that biofouling of the DO membrane was an issue at nearly all monitoring locations (including the locations identified in this section for model calibration). Biofouling refers to the impact of biological activity on instrumentation, and it results in inaccurate DO measurements. It typically occurred within 24 to 96 hours of probe deployment and resulted in degradation (i.e., reduction) of DO concentrations. The extent of degradation in measurements is apparent from the DO monitoring data plotted in Appendix K. Sudden step increases of 2 to 3 mg/L occur multiple times over the course of the summer (e.g., beginning of August and September at the Youngs Bar station). These increases occur when a probe is removed, cleaned, and re-deployed. Subsequent to these increases, the DO concentrations again decline. Because of these inaccuracies, the model predictions should not (and do not) closely match the measured DO levels. The model predictions do tend to follow the trend in maximum DO concentrations measured for this period (where biofouling is not an issue).

In this stretch of the river, nutrient limitation is a more significant factor than at upstream locations. Figure K-26 suggests that nitrogen becomes a factor that can limit periphyton growth at Turwar during the late spring and summer. The limiting factor value for nitrogen falls to 0.4 while that for phosphorus remains close to 1.0. This significant divergence from 1.0 for nitrogen is more pronounced at this location than at Hwy66 or Stateline.

3.3.9 Klamath Estuary - Turwar to the Pacific Ocean (Model Segment 9)

EFDC was used to model this portion of the Klamath River. The simulated water quality output was compared with grab sample data and measured DO sonde data at three water quality stations in the lower, middle, and upper estuary for the year 2004 (Figures L-7 through L-9 in Appendix L).

Calibration data were available for 2004 because of an intensive monitoring effort conducted by the NCRWQCB and Yurok Tribe in June, July, August, and September. Data were collected as grab samples at the surface and bottom of the estuary for a suite of nutrients along with algae measurements and sonde data measurements for temperature, DO, and salinity. Continuous sonde data were collected each month for 4–5 days at the surface and bottom.

The water quality constituents evaluated for calibration include chlorophyll *a*, DO (surface and bottom), PO_4, NH_4, and NO_2/NO_3 at each of the three locations in the estuary. Although the grab sampling data provided a variety of data for calibration, all except one data point for PO_4, NH_4 and NO_2/NO_3 were reported as non-detects. It was noted that these samples were diluted, and that the reporting limit was raised on the basis of different dilutions (e.g., 5x, 10x and 20x) for different sampling days (because of matrix interference, possibly chloride). To consider this uncertainty in the data, error bars were provided in the calibration figures in Appendix L. These bars show the potential range of the laboratory measurements. The lower bound was estimated as half of the lowest report limit.

The water quality predictions follow the overall trends and magnitudes at the calibration locations fairly well. DO concentrations at the surface and bottom locations are replicated, and the model is able to predict low DO conditions during the summer period. The model also reproduces the observed diel fluctuation of DO in both the surface and bottom water. Since the model and observed data both show very low algae concentrations in the estuary, significant diel fluctuations of DO do not occur as a result of phytoplankton. Periphyton biomass, however, is predicted at high levels in the shallow regions of the estuary. This is likely a key contributor to diel DO fluctuation. Periphyton also influences diel fluctuation of nutrients. Table 3-6 presents the calibration parameter values for the EFDC model.

Table 3-6. Calibrated parameter values for the Klamath Estuary

Parameter	Description	Value
PMc	Algae growth rate (1/day)	1.8
BMRc	Algae respiration rate (1/day)	0.1
PRRc	Algae mortality rate (1/day)	0.05
WSc	Algae settling velocity (m/day)	0.2
TMc1	Lower optimal temperature for algae growth (^oC)	20
TMc2	Upper optimal temperature for algae growth (^oC)	25
rNitM	Nitrification rate (1/day)	0.06
KLN	Minimum hydrolysis rate for LPON (1/day)	0.07
KDN	Minimum hydrolysis rate for LDON (1/day)	0.1
KLP	Minimum hydrolysis rate for LPOP (1/day)	0.07
KDP	Minimum hydrolysis rate for LDOP (1/day)	0.1
KLC	Minimum hydrolysis rate for LPOC (1/day)	0.07
KDC	Minimum hydrolysis rate for LDOC (1/day)	0.1
SOD	Sediment oxygen demand (g O_2/m^2/day)	2.0
FPO4	Benthic flux rate of PO4 (g/ m^2/day)	0.002
FNH4	Benthic flux rate of NH4 (g/m^2/day)	0.01
PMM	Periphyton growth rate (1/day)	1.5
BMRM	Periphyton respiration rate (1/day)	0.1
PRRM	Periphyton mortality rate (1/day)	0.05
TMM1	Lower optimal temperature for periphyton growth (^oC)	20
TMM2	Upper optimal temperature for periphyton growth (^oC)	25

References

Arhonditsis, G.B. and M.T. Brett. 2004. Evaluation of the current state of mechanistic aquatic biogeochemical modeling. *Marine Ecology Progress Series* 271: 13-26.

Baric, A., B. Grbec, G. Kuspilic, I. Marasovic, Z. Nincevic, and I. Grubelic. 2003. Mass Mortality Event in a Small Saline Lake (Lake Rogoznica) caused by Unusual Holomictic Conditions. *Scientia Marina* 67(2):129–141.

Cole, T.M. and S.A. Wells. 2003. *CE-QUAL-W2: A two-dimensional, laterally averaged, Hydrodynamic and Water Quality Model, Version 3.1*, Instruction Report EL-03-1, US Army Engineering and Research Development Center, Vicksburg, MS.

Chapra, S.C. 1997. *Surface Water-Quality Modeling*. McGraw-Hill, Inc., New York.

Deas, M. 2000. *Application of numerical water quality model in ecological assessment*. Ph.D. dissertation. University of California, Davis.

Flint, L.E. and Flint, A.L., 2008. A Basin-Scale Approach to Estimating Stream Temperatures of Tributaries to the Lower Klamath River, California. J Environ Qual 37:57-68.

McGlashan, H.D. and H.J. Dean. 1913. *Surface Water Supply of the United States 1913, Part XI, Pacific Slope Basins in California.* USGS Water Supply Paper 300. Washington: Government Printing Office.

National Research Council. 2004. *Endangered and Threatened Fishes in the Klamath Basin*. Committee on Endangered and Threatened Fishes in the Klamath River Basin, The National Academies Press, Washington, DC.

NCRWQCB. 2008. *Analysis of Klamath Tributary Data*. North Coast Regional Water Quality Control Board. July 2, 2008.

PacifiCorp. 2005. *Klamath River Water Quality Model Implementation, Calibration, and Validation.* Klamath Hydroelectric Project (FERC Project No. 2082) - Response to November 10, 2005, FERC AIR GN-2. December 16, 2005, FERC filing.

Park, K., A.Y. Kuo, J. Shen, and J.M. Hamrick. 1995. *A three-dimensional hydrodynamic-eutrophication model (HEM-3D): description of water quality and sediment process submodels*. Special Report in Applied Marine Science and Ocean Engineering No. 327. School of Marine Science Virginia Institute of Marine Science, College of William and Mary, January 1995.

Tetra Tech, Inc. 2004. *Data Review and Modeling Approach – Klamath and Lost Rivers TMDL Development*. Prepared for U.S. Environmental Protection Agency Region 10, U.S. Environmental Agency Region 9, Oregon Department of Environmental Quality, and North Coast Regional Water Quality Control Board.

Watercourse Engineering, Inc. 2003. *Klamath River Water Quality 2000 Monitoring Program - Project Report*. Prepared for U.S. Bureau of Reclamation with support from PacifiCorp. (January, 25, 2003).

Watercourse Engineering, Inc. 2004. *Klamath River Modeling Framework to Support the PacifiCorp Federal Energy Regulatory Commission Hydropower Relicensing Application* [DRAFT] Prepared for PacifiCorp (March 9, 2004).

Appendix A

pH Simulation Module Equations - From Chapra, 1997

In natural waters, much of the buffering capacity for modulating pH is provided by dissolved inorganic carbon species, including CO_2, HCO_3^-, and CO_3^{2-} that satisfy the chemical equilibrium equation:

$$H_2CO_3^* <=> HCO_3^- + H^+$$

where $H_2CO_3^*$ is approximately equal to the concentration of CO_2.

The first dissociation constant of carbonic carbon is thus:

$$K_1 = [H^+][HCO_3^-] / [H_2CO_3^*]$$

which can be calculated using equation:

$$pK_1=3404.71 / T_a + 0.032786\ T_a – 14.8435$$

where T_a = water temperature (in Kelvin)

The bicarbonate ion, HCO_3^-, further dissociates to produce CO_3^{2-} and H^+:

$$HCO_3^{-1} <=> CO_3^{2-} + H^+$$

The equilibrium coefficient, i.e., the second dissociation constant of carbonic acid, is thus:

$$K_2 = [H^+][CO_3^{2-}] / [HCO_3^-]$$

which can be calculated as:

$$pK_2=2902.39 / T_a +0.02379\ T_a – 6.498$$

TIC is defined as the summation of all the carbonic species:

$$TIC = [H_2CO_3^*] + [HCO_3^-] + [CO_3^{2-}]$$

And Alk is defined as the acid-neutralizing capacity of the system, and is formulated as:

$$Alk = [HCO_3^-] + 2[CO_3^{2-}] + [OH^-]+ [H^+]$$

Three intermediate ratios are defined as:

$$a = K_1 \times [H^+] / ([H^+]^2 + K_1 \times [H^+] + K_1 \times K_2)$$
$$b = K_1 \times K_2 / ([H^+]^2 + K_1 \times [H^+] + K_1 \times K_2)$$

Then, a nonlinear equation can be derived to solve for the $[H^+]$:

$$a \times TIC + 2 \times b \times TIC + Kw / [H^+] - [H^+] - Alk = 0$$

where K_w is the dissociation coefficient of water.

While Alk is generally assumed to be conservative in water quality models, this assumption does not apply to TIC because the carbonic system is under constant impact from multiple environmental factors, including biological activities, atmospheric impact, organic decay, and benthic impact. The interaction between TIC and the major impacting factors can be represented using the following differential equation:

$$\frac{dc_{TIC}}{dt} = W_{bio} + W_{atm} + W_{om} + W_{ben}$$

where c_{TIC} is the concentration of TIC (mg/L), W_{bio} is the biological contribution term (mg/L/day); W_{atm} is the atomospheric exchange term (mg/L/day); W_{om} is the organic matter contribution term (mg/L/day); and W_{ben} is the benthic contribution term (mg/L/day). The biological term represents the consumption of CO_2 through the photosynthesis process and the production of CO_2 through the respiration process, which can be represented as:

$$W_{bio} = R - P$$

where R is the CO_2 production rate by respiration (mg/L/day), and P is the CO_2 consumption rate by photosynthesis (mg/L/day).

The atmospheric exchange can be represented as:

$$W_{atm} = Kc \times ([H_2CO_3^*]s - [H_2CO_3^*])$$

where, Kc is the water-air surface exchange coefficient for CO_2 (d^{-1}) and $[H_2CO_3^*]s$ is equivalent to the saturation concentration of CO_2 (mg/L)

The organic matter decay term can be represented as:

$$W_{om} = k \times C_{om}$$

where k is organic matter decay rate (d^{-1}) and C_{om} is the concentration of organic matter as carbon (mg/L).

The benthic contribution term is formulated following the general idea in CE-QUAL-W2:

$$W_{ben} = Cc \times SOD / H$$

where Cc is a dimensionless conversion factor; SOD is the local sediment oxygen demand (g/m2/day); and H is the water depth (m).

Appendix B

System Geometry - Excerpt from the PacifiCorp, 2005 Report

Link River Reach

The Link River reach starts at Link dam (RM 254) and terminates 1.3 miles downstream at Lake Ewauna (RM 253). The Link River reach is simulated with two junctions, representing separate powerhouse discharges into the reach and no element side flows. This reach is modeled with the RMA-2 and RMA-11 models.

Link River Reach Geometry Summary

Node spacing	75 meters
Number of nodes	29 nodes in length; 37 nodes total including junctions
Length	1.31 miles from RM 252.57-253.88
Elevations	Range: 1245-1259 meters
Widths	Constant widths: 5 meters mainstem; 20 meters junction elements
Side slopes	20:1 mainstem; 1:1 junctions
Data sources	UTM coordinates from CH2M HILL; Elevations estimated from USGS topographic maps
Notes	2 junctions: East side, West side; Nodes 30-33 at East side; 34-37 at West side

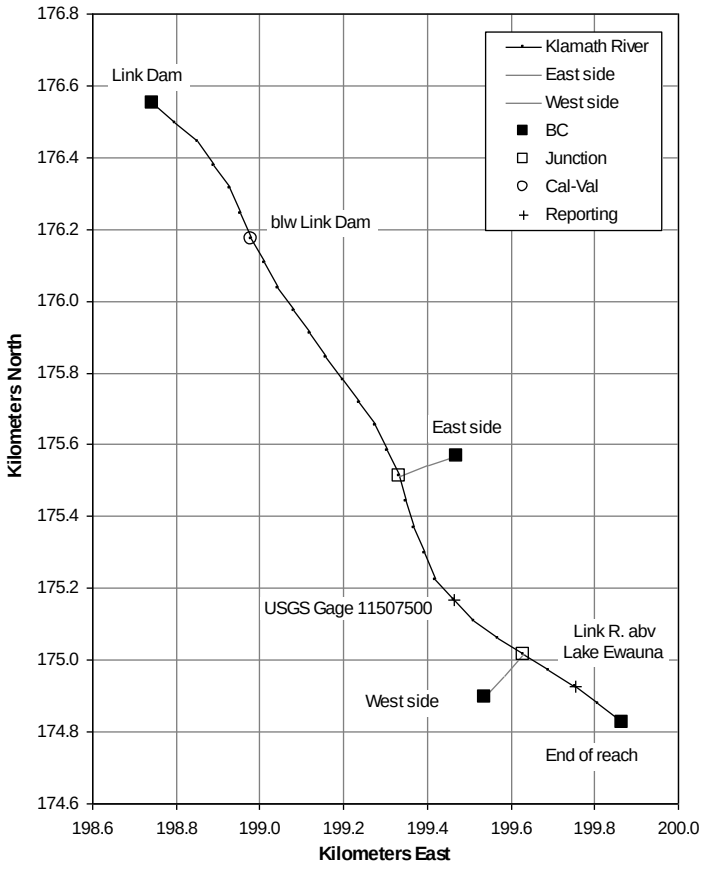

Map of Link River Representation

Geometry Information for Link River

Location	Node	Element	x-coord	y-coord	Site type
Link Dam	1	1	198.8	176.6	BC
East Side	17	9	199.9	174.8	BC
West Side	25	13	199.5	175.6	BC
End Link R reach	29	14	199.5	174.9	BC
East Side	30	15	199.3	175.5	Junction, inflow
West Side	34	16	199.6	175.0	Junction, inflow
USGS Gage 11507500	22	--	199.5	175.2	Reporting Point
Link River above Lake Ewauna	27	--	199.8	174.9	Reporting Point

Bed Elevations/Slope

Bed slope for the Link River reach was estimated from USGS topographic maps and assumed Lake Ewauna elevations. Elevations were estimated from topographic contours to preserve the general slope of the river. Upstream reach elevation was set at 4131 ft (1259 m) MSL and downstream reach elevation was set at 4085 ft (1245 m) MSL.

Cross-sections

Link River widths were obtained from 1:7,500-scale aerial photos taken July 21, 1988. Daily average flow for that day was 920 cfs. For numerical stability in this short and steep reach, bottom width of the mainstem was set to a constant 5 meters. These widths were assumed to represent bottom widths of trapezoidal cross-sections with twenty-to-one side slopes on the mainstem and one-to-one side slopes in tributaries.

Lake Ewauna-Keno Reservoir

The Lake Ewauna to Keno dam reach extends from the headwaters of Lake Ewauna (RM 253) 20 miles downstream to Keno dam (RM 233). The impoundment (i.e., Keno reservoir) is generally a broad, shallow body of water. Widths range from several hundred to over 1,000 feet (a range of about 90 to 300 meters), and depths range to a maximum of roughly 20 feet (approximately 6 meters). A total of 18 discharges and 7 withdrawals were represented in the model. This reach is modeled with CE-QUAL-W2.

Keno Dam Features

The Keno dam spillway, with an invert elevation of 4,070 feet, contains six Taintor gates. Three additional outlets include a sluice conduit, the fish attraction outlet, and a fish ladder.

Keno Dam Outlet Features

Outlet	Invert Elevation	Dimension	Operation
Sluice Conduit	4,073.0 ft	36 inch diameter	Manual gate
Fish Attraction Outlet	4,075.0 ft	30 inch diameter	Manual gate
Fish Ladder	4,078.5 ft	60 inch width	Stop logs
Spillway	4,070.0 ft	6 gates @ 40 ft width each	Remote control on three gates

Sources: PacifiCorp (2002), PacifiCorp (2000)

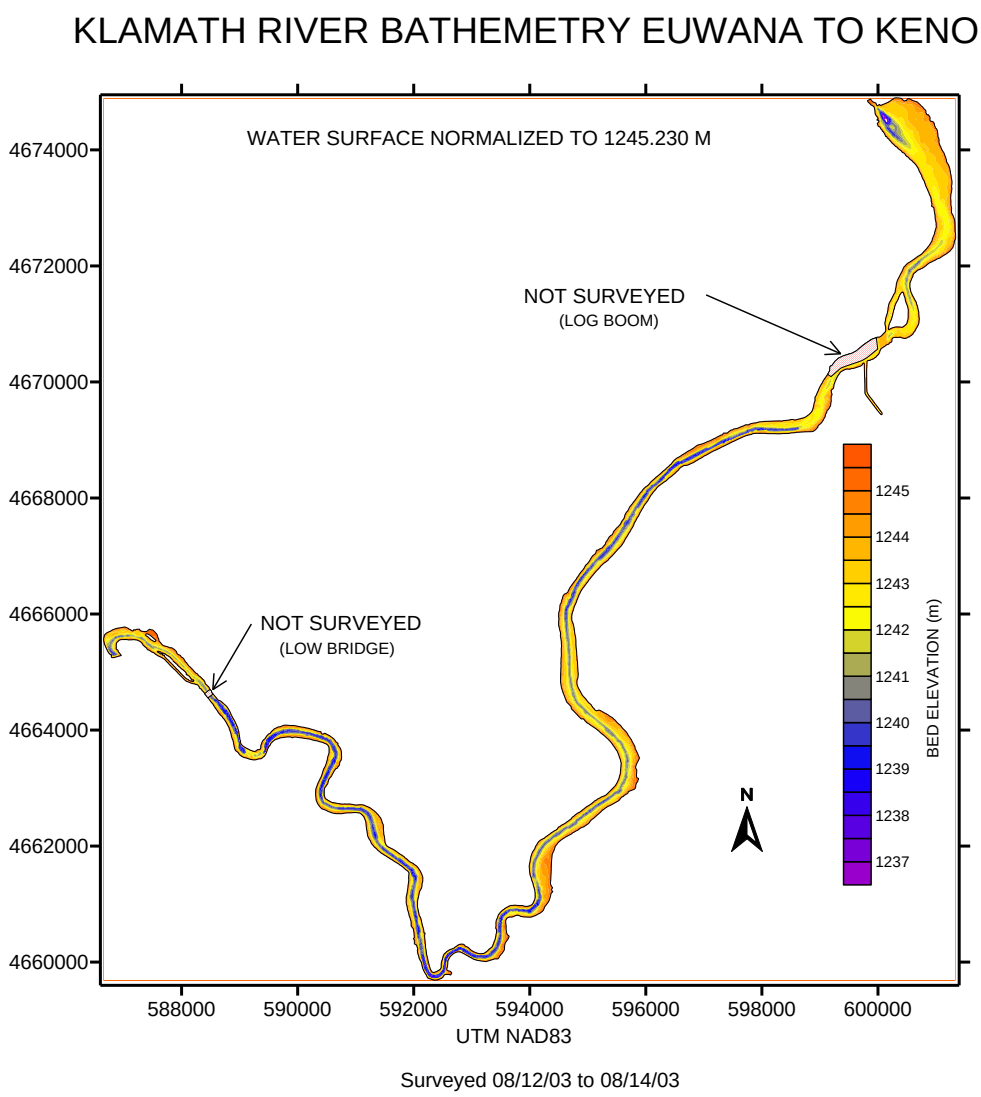

Keno Reservoir Bathymetry (PacifiCorp, 2004a)

Reservoir Bathymetry

The Lake Ewauna to Keno dam model was originally implemented with bathymetry derived from an earlier model of this reach created by Wells (ODEQ, 1995). This original representation was replaced with data from a recent bathymetric survey of the entire reservoir (PacifiCorp, 2004a).

The number of segments, number of layers, segment lengths, layer widths per segment and water surface elevation were largely retained from the previous CE-QUAL-W2 modeling of the reach by ODEQ (1995), but were supplemented with new segment orientations calculated from x-y coordinates obtained from digitized versions of 1:24,000 USGS topographic quadrangles. River segment orientations were updated because the original orientations (ODEQ 1995) contained discrepancies when applied to the newer versions of CE-QUAL-W2 used in this study.

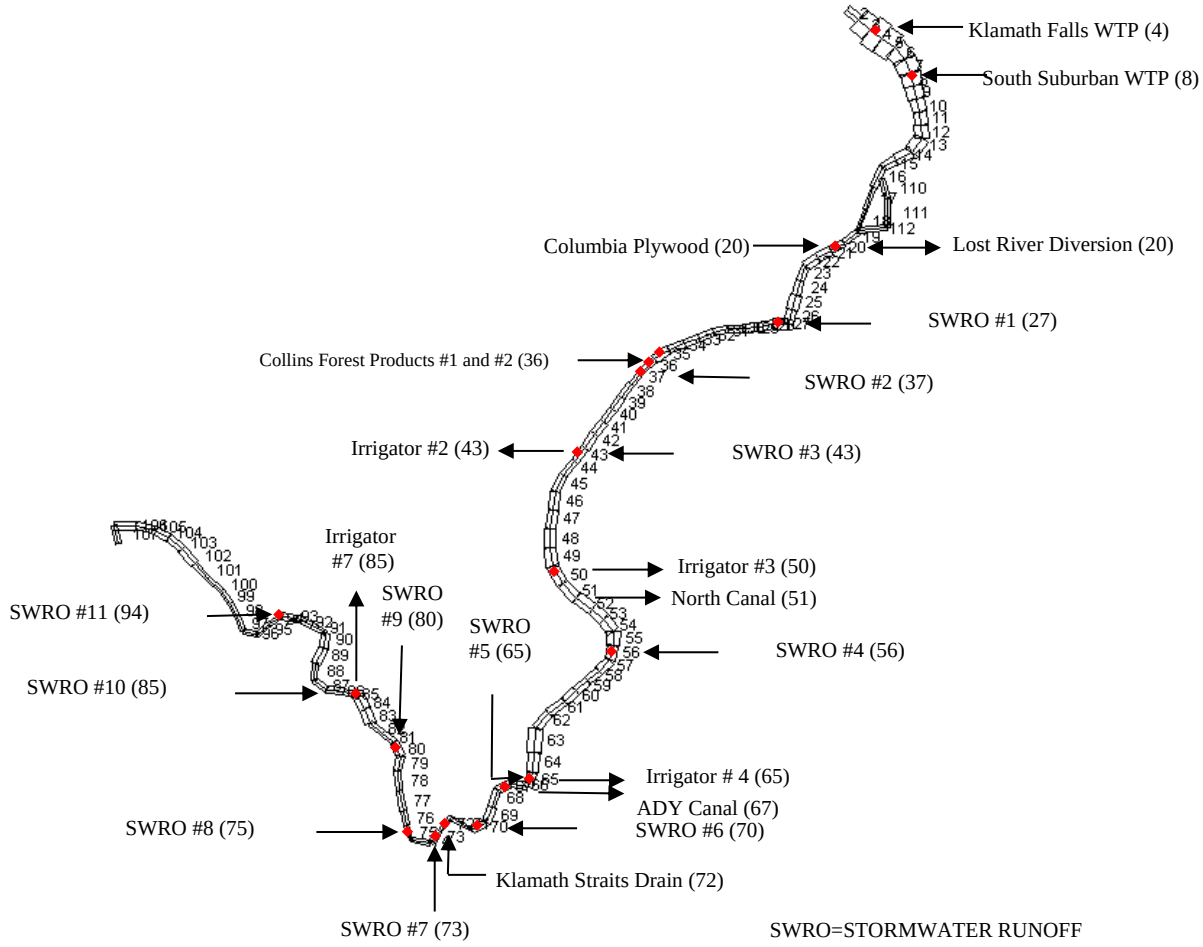

Map of Lake Ewauna to Keno Dam CE-QUAL-W2 Representation, Identifying Inputs and Withdrawals

The CE-QUAL-W2 representation of Lake Ewauna to Keno dam reach consists of two connected reservoir sections, or branches. The main branch, Branch 1, spans the entire length of the reach and is comprised of 106 active segments, all 1,000 to 2,000 ft (304.8 m) in length. A second, smaller branch, Branch 2, provides an alternate flow path from segment 14 to segment 18 of Branch 1. Branch 2 has no external inflows or outflow and is comprised of three active segments, each 800 ft (243.8 m) in length. A total of 18 discharges and 7 withdrawals were represented in the model. The 15 active layers of this reach are all 2.00 ft (0.61 m) thick. Total volume generated by this model representation was consistent with volume calculated from reservoir bathymetry available from PacifiCorp.

Modeled Inflows and Outflows in the Lake Ewauna to Keno Dam Reach

Name	Type	River Bank [a]	Approximate RM [b]	Model Segment
Klamath Falls Wastewater Treatment Plant	Inflow	Left	253	4
South Suburban Sanitation District	Inflow	Left	252	8
Columbia Plywood	Inflow	Right	250	20
Lost River Diversion	Inflow/Outflow	Left	250	20
Collins Forest Products #1	Inflow	Right	247	36
Collins Forest Products #2	Inflow	Right	247	36
Klamath Straits Drain	Inflow	Left	240	72
Stormwater Runoff #1	Inflow	NA	249	27
Stormwater Runoff #2	Inflow	NA	247	37
Stormwater Runoff #3	Inflow	NA	246	43
Stormwater Runoff #4	Inflow	NA	243	56
Stormwater Runoff #5	Inflow	NA	242	65
Stormwater Runoff #6	Inflow	NA	241	70
Stormwater Runoff #7	Inflow	NA	240	73
Stormwater Runoff #8	Inflow	NA	240	75
Stormwater Runoff #9	Inflow	NA	239	80
Stormwater Runoff #10	Inflow	NA	238	85
Stormwater Runoff #11	Inflow	NA	236	94
North Canal	Outflow	Left	247	35
ADY Canal	Outflow	Left	241	67
Irrigator #2 [c]	Inflow/Outflow	NA	246	43
Irrigator #3 [c]	Inflow/Outflow	NA	244	50
Irrigator #4 [c]	Inflow/Outflow	NA	242	65
Irrigator #7 [c]	Inflow/Outflow	NA	238	85

[a] River bank is given for reference only. The model does not discriminate between banks when simulating flows.

[b] River miles are approximate as each model segment is 1000 ft in length.

[c] Nomenclature after Wells (ODEQ, 1995)

Placement of stormwater runoff and irrigator flows is as per ODEQ (1995).

Klamath River from Keno Dam to J.C. Boyle Reservoir Reach

The Keno reach extends 5.4 miles from Keno dam (RM 233) downstream to the headwaters of J.C. Boyle reservoir (RM 227). No appreciable tributary inflows occur in this reach. This reach is modeled with the RMA models.

Klamath River, Keno Reach Geometry Information for the RMA-2 and RMA-11 Models

Location	Node	Element	x-coord	y-coord	Site type
Keno Dam	1	1	186.8	165.4	BC, upper
End Keno R reach	117	58	181.0	166.9	BC, lower
A/D Keno reach	73	37	183.7	167.0	A/D
1/4 mi abv J.C. Boyle	110	56	181.4	166.9	Cal/Val and Reporting

BC – boundary condition (flow, constituent concentration, stage)

A/D – accretion/depletion location

Reporting – model output location

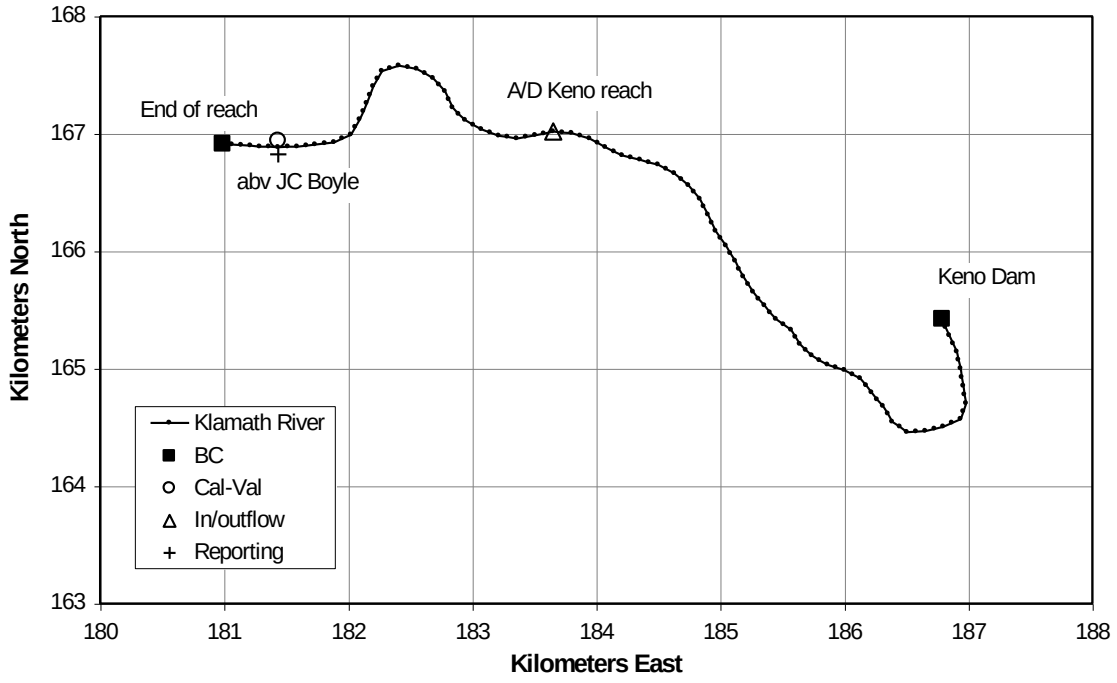

Klamath River, Keno Reach Representation

Bed Elevation/Slope

Bed slope for the Keno reach was estimated from USGS topographic maps, known elevations at Keno Dam, and estimated water surface elevations downstream in J.C.

Boyle reservoir. Estimated reach elevations range from approximately 3796 ft (1158 m) MSL to 4019 ft (1225 m) MSL.

Cross-sections

Keno reach widths were obtained from habitat surveys conducted by Thomas R. Payne and Associates (TRPA) (PacifiCorp, 2004b). Measurements were completed at roughly eight locations per mile. Because measurement locations did not always coincide with the x-y coordinates of the model, field data were linearly interpolated to determine widths for model cross sections. Extreme variations in measured widths were smoothed with a seven-times running average to produce estimates of bottom width. Using these estimates of bottom width, trapezoidal river cross-sections were constructed for each node of the reach at evenly spaced intervals of 75 meters, assuming 1:1 side slopes.

Klamath River, Keno Reach Geometry Summary

Node spacing	75 meters
Number of nodes	117 nodes in length
Length	5.37 miles from RM 228.69-234.06
Elevations	Range: 1158-1225 meters
Widths	Range: 28-78 meters
Side slopes	1:1
Data sources	UTM coordinates from CH2M HILL; Elevations estimated from USGS topographic maps
Notes	n/a

J.C. Boyle Reservoir

The J.C. Boyle reservoir reach extends 3.3 miles from the headwaters of J.C. Boyle reservoir (RM 228) to J.C. Boyle dam (RM 224). This reservoir primarily serves to regulate flows for the J.C. Boyle powerhouse located downstream at RM 220. The one significant tributary to this reach, Spencer Creek, is represented in the model as inflow added to Klamath River inflows at the headwater of the reservoir.

J.C. Boyle Dam Features

J.C. Boyle dam has four primary outlets: a spillway, a fish ladder, and two outlets into the waterway intake (a fish screen bypass and a waterway pipeline). This reach is modeled with CE-QUAL-W2.

J.C. Boyle Dam Outlet Features

Outlet	Invert Elevation	Dimension	Operation
Fish ladder	3780.0 ft	24 inch diameter	Manual
Fish Screen Bypass	3757.0 ft	24 inch diameter	Manual
Waterway pipeline	3775.0 ft	14 foot diameter	**
Spillway	3782.0 ft	3 radial gates @ 35 ft width each	Remote control on one gate

Sources: PacifiCorp (2002), PacifiCorp (2000), PacifiCorp drawing: Exhibit L-4

Reservoir Bathymetry

Unlike the Lake Ewauna to Keno dam reach, J.C. Boyle reservoir has never been modeled with CE-QUAL-W2. Reservoir geometry was derived from bathymetric data (PacifiCorp, 2004a). Segment length, segment orientation, layer thickness and width were required for the reservoir model. Based on the variation in the reservoir morphology and widths, the reservoir was divided into 20 active segments 887 ft (270m) in length. Segments were chosen to capture both the general shape of J.C. Boyle reservoir and pertinent features.

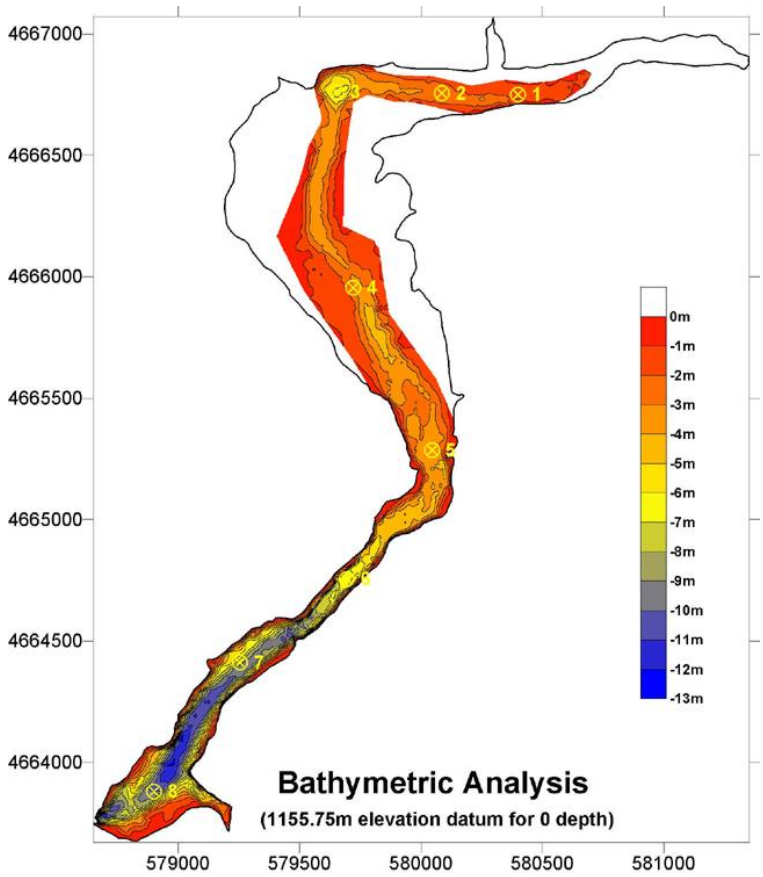

J.C. Boyle Reservoir Bathymetry (PacifiCorp, 2004a)

Layer thickness was set to 3.28 feet (1.0 meter). Layer widths were determined from cross-sectional information taken at the middle of each segment. Twelve active layers of varying widths were determined for each segment from this method. Although a representation using finer resolution (i.e., smaller layer thickness less than 1 meter) was attempted, models using these refined cross-sections took an uncommonly long time (on the order of a day) to run for each one-year simulation period). The model was continually adding and subtracting both layers and segments to account for the dynamic water surface elevations imposed by hydropower operations. A layer thickness of 1 meter produced reasonable results, and one-year simulation times were appreciably reduced to approximately 10 minutes.

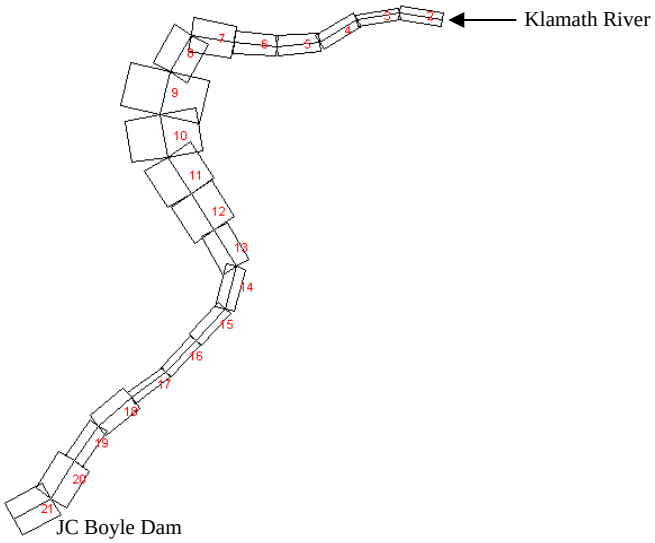

Representation of J.C. Boyle Reservoir in CE-QUAL-W2

J.C. Boyle Bypass and Peaking Reaches

The J.C. Boyle bypass and peaking reaches extend 20.8 miles from J.C. Boyle dam (RM 224) to the headwaters of Copco reservoir (RM 204). Noteworthy features of the reaches include diversion of mainstem flows at J.C. Boyle dam for hydropower production, the powerhouse penstock return marking the beginning of the peaking reach roughly 4 miles downstream from J.C. Boyle dam (RM 220), a large springs complex in the bypass reach, and hydropower peaking operations downstream of the powerhouse. A few small streams enter the reach, the most significant of which is Shovel Creek. Important locations within the bypass and peaking reaches are presented in the table below. These reaches are modeled with the RMA models.

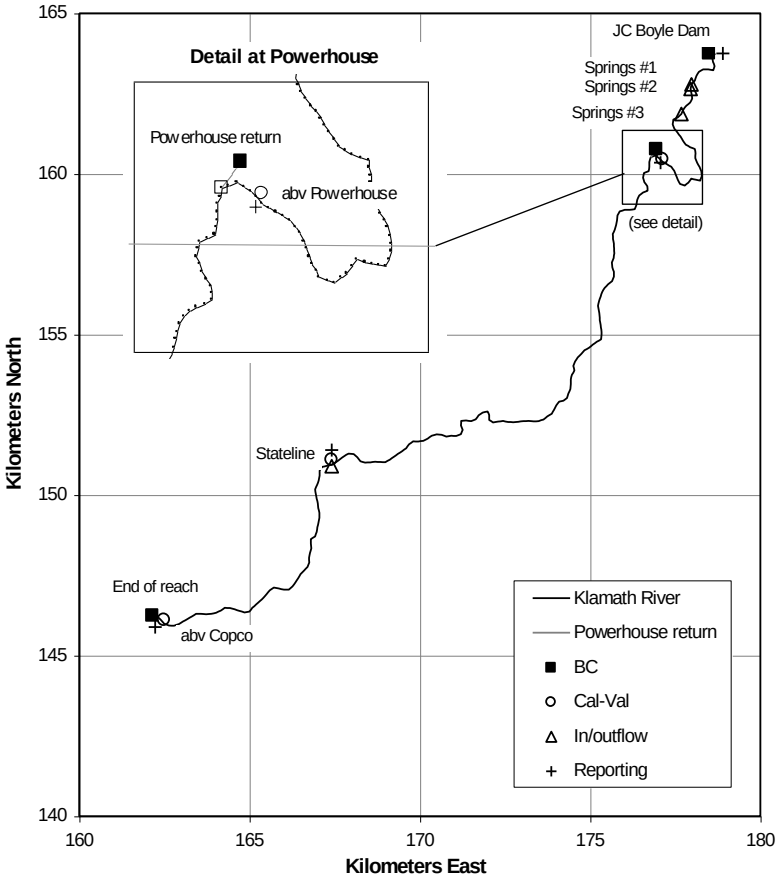

J.C. Boyle Bypass and Peaking Reach Representation

Geometry Information for J.C. Boyle Bypass and Peaking Reach EC Simulation

Location	Node	Element	x-coord	y-coord	Site type
J.C. Boyle Dam	1	1	178.7	163.7	BC, upper
End Peaking reach	453	226	162.2	146.2	BC, lower
J.C. Boyle Powerhouse	95	48	176.9	160.8	BC
Simulated Powerhouse Return	97	49	176.8	160.5	Junction, inflow
1/4 mi abv Powerhouse	91	46	177.1	160.4	Cal-Val
1/4 mi abv Shovel Cr	389	195	166.3	147.2	Cal-Val
1/4 mi abv Copco	447	224	162.5	146.00	Cal-Val
CA-OR Stateline	331	166	167.4	151.1	Cal-Val, A/D
Springs #1	21	11	178.0	162.8	A/D
Springs #2	23	12	178.0	162.6	A/D
Springs #4	35	18	177.7	161.9	A/D

BC – boundary condition

A/D – accretion/depletion location

Cal-Val – calibration and validation location

Bed Elevation/Slope

Bed slope for these reaches was estimated from USGS topographic maps and reported elevations at J.C. Boyle dam and Copco reservoir water surface elevations. Reach elevations range from approximately 2592 ft (790 m) MSL to 3760 ft (1146 m) MSL.

Cross-sections

J.C. Boyle bypass and peaking reach widths were obtained from habitat surveys completed by TRPA (PacifiCorp, 2004b). Measurements were completed at roughly eight locations per mile. Because measurement locations did not always coincide with the 1:24,000 x-y coordinates of the model, field data were linearly interpolated to provide widths for cross-sections of the model. Extreme variations in measured widths were smoothed with a seven-times running average to produce estimates of bottom width. Using these estimates of bottom width, trapezoidal river cross-sections were constructed for each node of the reach at evenly spaced intervals of 75 meters, assuming 1:1 side slopes. Widths and other geometric characteristics of the bypass and peaking reaches are summarized in the table below.

J.C. Boyle Bypass and Peaking Reach Geometry Summary

Node spacing	75 meters
Number of nodes	459 nodes in length
Length	20.81 miles from RM 204.72-225.53
Elevations	Range: 790-1146 meters
Widths	Range: 12-66 meters
Side slopes	1:1
Data sources	UTM coordinates from CH2M HILL; Elevations estimated from USGS topographic maps
Notes	1 junction: J.C.B Powerhouse; Nodes 97, 458, 459

Copco Reservoir

The Copco reservoir reach extends 5.0 miles from Copco reservoir headwaters (RM 204) downstream to Copco dam (RM 199). No tributaries are represented in this section of the model. Physical data for the Copco reservoir model are outlined below. This reach is modeled with CE-QUAL-W2.

Copco Dam Features

Copco dam has three primary outlets: a spillway and two penstocks that provide flows to the Copco No. 1 powerhouse. The two penstocks, fed by three intakes, are treated as a single outlet with an average centerline elevation of 2,581 feet. Because of the close proximity and similar invert elevations, the outlet works were represented in the reservoir as a single withdrawal with a midline elevation of 2,581 ft (786.6 m).

Copco Dam Outlet Features

Outlet	Invert Elevation	Dimension	Operation
Penstock Intake (Unit 1)	2575 ft	Two intakes @ 10-foot diameter each	Remote Operation
Penstock Intake (Unit 2)	2575 ft	14 foot diameter	Remote Operation
Spillway	2594 ft	3 radial gates @ 35 ft width each	Remote control on one gate, others by motorized hoist

Sources: PacifiCorp (2002), PacifiCorp (2000)

Reservoir Bathymetry

Copco reservoir geometry was derived from bathymetric data of Copco reservoir (PacifiCorp, 2004a). Segment length, segment orientation, layer thickness and width were required for the reservoir model. Segments were identified based on changes in reservoir morphology and widths. The reservoir was divided into 17 active segments 1,329 ft (405.4 m) in length. Segments were chosen to capture both the general shape of Copco reservoir and pertinent features, such as the submerged features near the dam. Due to the large bedrock outcrop in the vicinity of the Copco dam, a submerged weir was implemented in the model from layer 20 to 32.

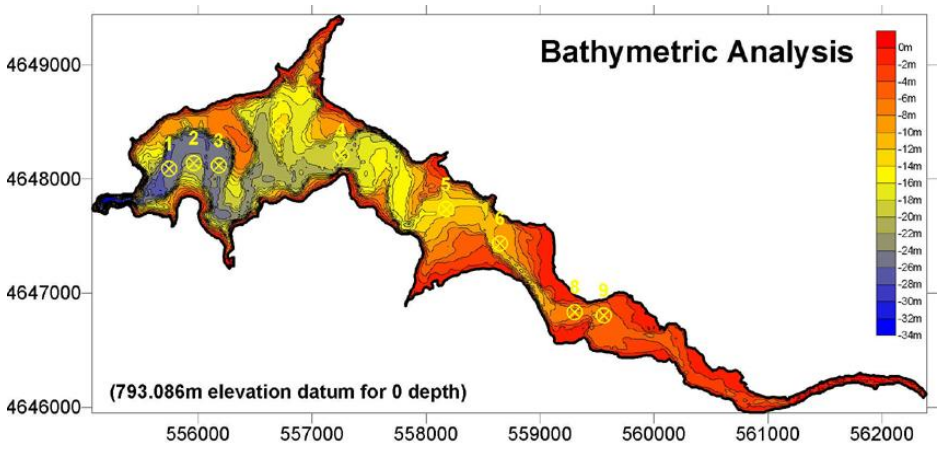

Copco Reservoir Bathymetry (PacifiCorp, 2004a)

Layer thickness was set to 3.28 ft (1.0 m). Layer widths were determined from cross-sectional information taken at the middle of each segment. Thirty-two active layers of varying widths were determined for each segment from this method. The 3.28 ft (1.0 m) layer thickness produced reasonable results and resulted in reasonable execution times. One-year simulation times were approximately 15 minutes. Final CE-QUAL-W2 representation of Copco reservoir is shown in the Figure below.

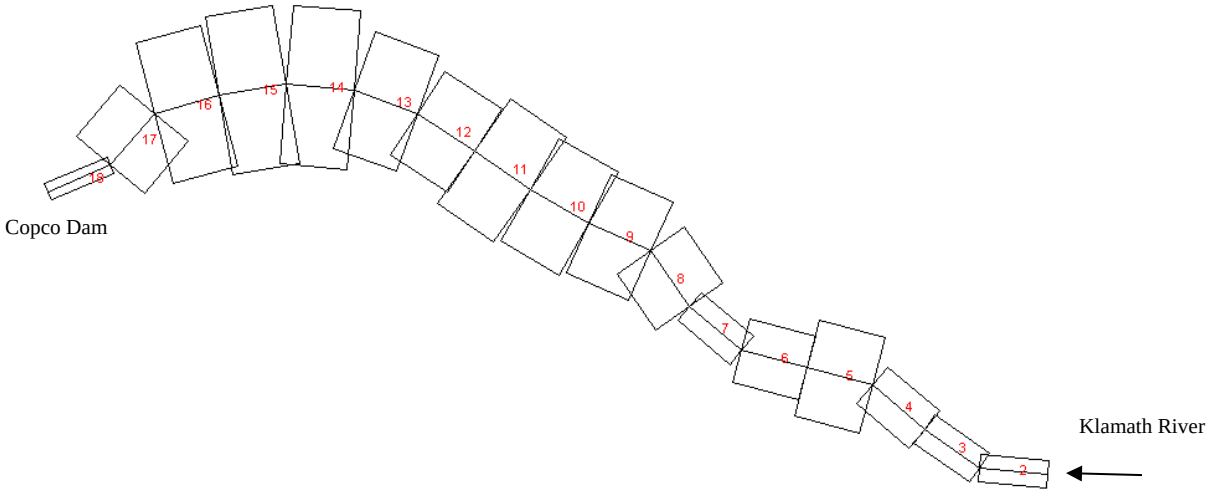

Representation of Copco Reservoir in CE-QUAL-W2

Iron Gate Reservoir

Iron Gate reservoir extends 6.4 miles from the headwaters of Iron Gate reservoir (RM 197) to Iron Gate dam (RM 190). Except in "Without Project" scenarios, the small Copco #2 Reservoir and short river reach between Copco and Iron Gate reservoirs are not represented in the model. Instead, Copco reservoir runs directly into Iron Gate reservoir. Three tributaries to Iron Gate reservoir are represented in this CE-QUAL-W2 model: Camp Creek, Jenny Creek, and Fall Creek. The spillway for the dam is modeled as a withdrawal in the last active segment because the spillway structure draws water to the side of the dam, not over or through the dam itself. Due to its dendritic shape, Iron Gate reservoir is represented by two branches, including a main branch that receives water released from Copco Reservoir and a Camp Creek branch that represents a sizeable arm of the reservoir running up to Camp Creek. Geometry of the reservoir is outlined below.

Iron Gate Dam Features

Iron Gate dam has four primary outlets: a spillway, a penstock, and two outlets that supply fish hatchery intakes. The details of these outlets are summarized in the table below.

Iron Gate Dam Outlet Features

Outlet	Invert Elevation	Dimension	Operation
Upper Fish Hatchery	2293 ft	24 inch diameter	Manual
Penstock Intake	2309 ft	12 foot diameter	Remote operation
Lower Fish Hatchery	2253 ft	24 inch diameter	Manual
Spillway	2328 ft	Side channel (727 feet in length)	Overflow

Sources: PacifiCorp (2002), PacifiCorp (2000)

Reservoir Bathymetry

Reservoir geometry was derived from bathymetric data of Iron Gate reservoir (PacifiCorp, 2004a). Segments were laid out on the basis of changes in reservoir orientation and width. The main branch, Branch 1, has 30 active segments and the Camp Creek Branch, Branch 2, has five active segments. Segment lengths were 1,204 ft (367 m), with the exception of the narrows near the upper end of the reservoir, where half element lengths were used. Branch 2 has an external upstream boundary (Camp Creek) and connects with Branch 1, Segment 23.

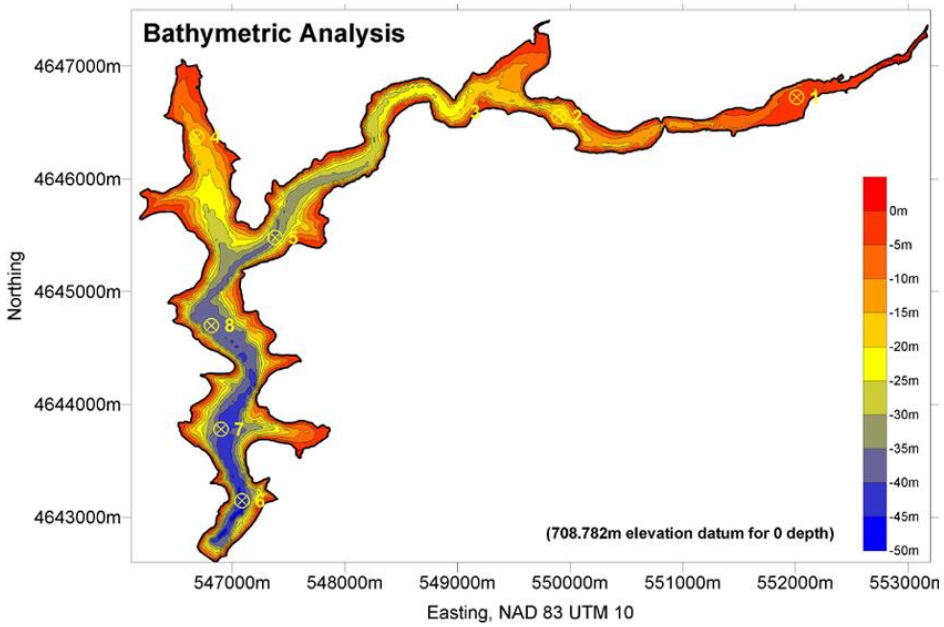

Iron Gate Bathymetry (PacifiCorp, 2004a)

Based on cross-sectional information from the mid-point of each segment, Iron Gate Reservoir is represented by 50 active layers, each 3.28 ft (1 m) in thickness.

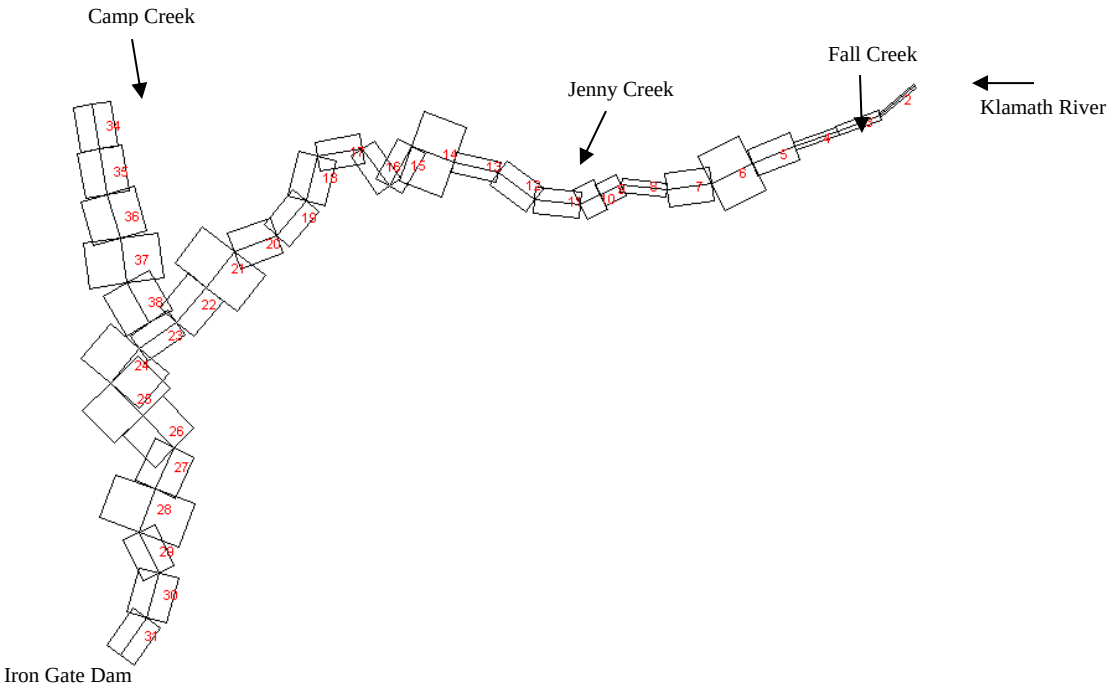

Representation of Iron Gate Reservoir for CE-QUAL-W2

Iron Gate to Turwar Reach

The Iron Gate dam to Turwar reach extends 185 miles from Iron Gate dam (RM 190) to Turwar near the mouth of the Klamath River (RM 5). Several main tributaries flow into the reach: Shasta River, Scott River, Salmon River, and Trinity River. Many smaller creeks contribute significant flow to the river along this reach and these creeks are also included in the simulation. Geometry of this reach is outlined below.

Map Coordinates

X-Y coordinates describing the course of the river were taken from a digitized version of the 1:24,000 USGS topographic quadrangles. This information was translated into a series of nodes and elements for use by the numerical model. The model network is shown with simulated tributaries in the figure below. Important locations within the reach, including tributaries and output locations, are presented in the Table below. Nodal spacing for the numerical grid was roughly 490 feet (150 meters). Sensitivity analyses showed model results to be relatively insensitive to a reduction in grid spacing.

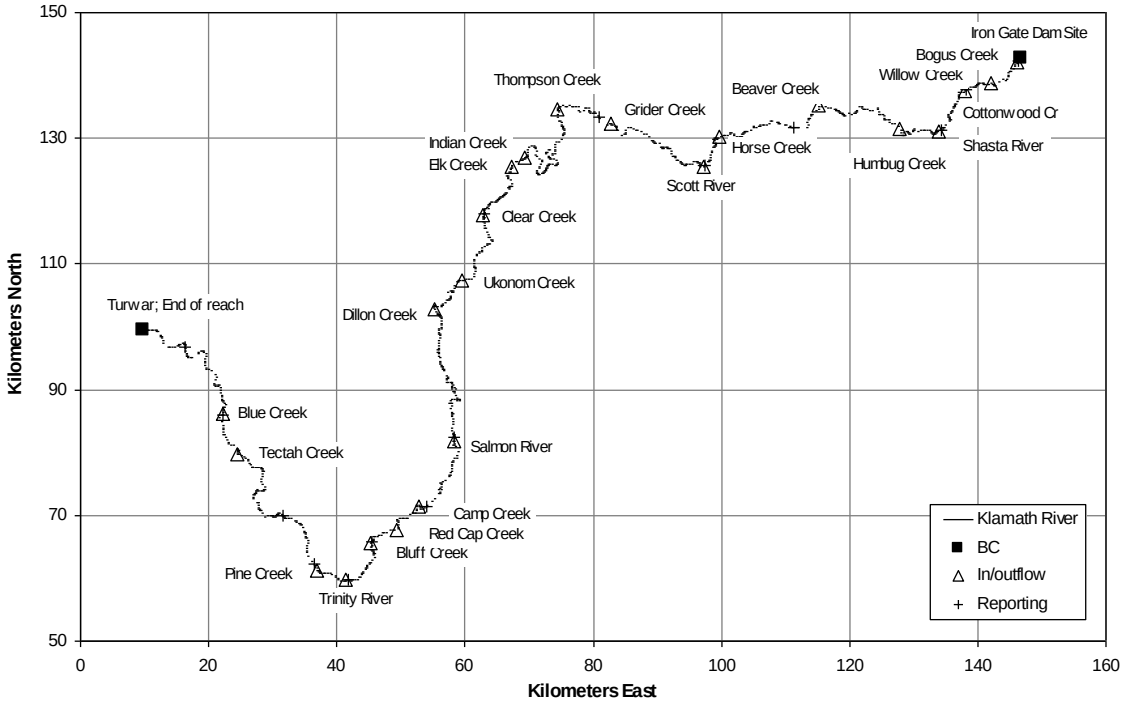

Iron Gate Dam to Turwar Reach Representation Showing Tributary Names

Geometry Information for the IG-Turwar reach (150-meter grid)

Location	Node	Element	x-coord	y-coord	Site Type
Iron Gate Dam	1	1	146.747	142.634	BC, upper
End IG-Turwar reach	2081	1040	9.821	99.506	BC, lower
Bogus Creek	7	4	146.141	142.022	A/D
Willow Creek	55	28	142.035	138.739	A/D
Cottonwood Creek	86	43	137.904	137.535	A/D
Shasta River	144	72	133.963	131.178	A/D
Humbug Creek	204	102	127.848	131.402	A/D
Beaver Creek	319	160	115.190	135.232	A/D
Horse Creek	468	234	99.597	130.180	A/D
Scott River	513	257	97.299	125.428	A/D
Grider Creek (A/D Scott to Seiad)	656	328	82.714	132.246	A/D
Thompson Creek	735	368	74.440	134.626	A/D
Indian Creek	906	453	69.371	126.831	A/D
Elk Creek	925	463	67.209	125.507	A/D
Clear Creek	1000	500	62.733	117.818	A/D
Ukonom Creek	1098	549	59.559	107.347	A/D
Dillon Creek	1162	581	55.209	102.905	A/D
Salmon River	1357	679	58.333	81.788	A/D
Camp Creek	1466	733	52.865	71.474	A/D
Red Cap Creek	1511	756	49.403	67.773	A/D
Bluff Creek	1547	774	45.339	65.584	A/D
Trinity River	1609	805	41.415	59.672	A/D
Pine Creek	1644	822	36.954	61.269	A/D
Tectah Creek	1850	925	24.557	79.833	A/D
Blue Creek	1908	954	22.306	86.220	A/D
1/4 mi bl Iron Gate	4	2	146.419	142.345	reporting
1/4 mi ab Cottonwood	84	42	138.117	137.743	reporting
1/4 mi ab Shasta	142	71	134.262	131.198	reporting
Walker Bridge	369	185	111.329	131.759	reporting
1/4 mi ab Scott	511	256	97.348	125.720	reporting
USGS Gage at Seiad Valley	672	336	80.887	133.289	reporting
1/4 mi ab Clear Cr.	998	499	62.908	118.058	reporting
1/2 mi ab Salmon (Ishi Pishi)	1352	676	58.231	82.372	reporting
USGS Gage at Orleans	1454	727	54.016	71.457	reporting
1/4 mi ab Bluff Cr.	1545	773	45.357	65.876	reporting
1/4 mi ab Trinity	1607	804	41.692	59.692	reporting
Martin's Ferry	1651	826	36.505	62.187	reporting
Young's Bar	1722	861	31.541	69.894	reporting
1/4 mi ab Blue Cr.	1906	953	22.177	85.992	reporting
USGS Gage nr Turwar	2024	1012	16.341	96.868	reporting

River Bed Elevation

Bottom elevations along the reach were estimated from USGS topographic maps and reported elevations at Iron Gate dam. These elevations determined bed slope. Reach elevations range from approximately sea level to roughly 2200 ft (671 m) MSL.

Cross-sections

Klamath River widths for the Iron Gate dam to Turwar reach were estimated from meso-habitat surveys compiled by US Fish and Wildlife Service (1997). This dataset included a reach-by-reach description of 1,741 units, or sections of the river, by habitat type, width, and maximum depth. Measurements were not uniformly spaced. Because measurement locations did not always coincide with the 1:24,000 x-y coordinates, field data were linearly interpolated to produce widths for model cross-sections. Large variations in river width were smoothed with a seven-point running average to provide estimates of bottom width for the model. From these estimated bottom widths, trapezoidal cross-sections were constructed at each node assuming 1:1 side slopes. Widths and other geometric characteristics for the Iron Gate to Turwar reach are summarized in the table below.

Klamath River, Iron Gate Dam to Turwar Reach Geometry Summary

Node spacing	150 meters
Number of nodes	2082 nodes in length
Length	190.54 miles from RM 0.00-190.54
Elevations	Range: 0-671 meters
Widths	Range: 17-340 meters
Side slopes	1:1
Data sources	UTM coordinates from CH2M HILL; Elevations estimated from USGS topographic maps
Notes	n/a

Appendix C

Klamath Estuary EFDC Grid

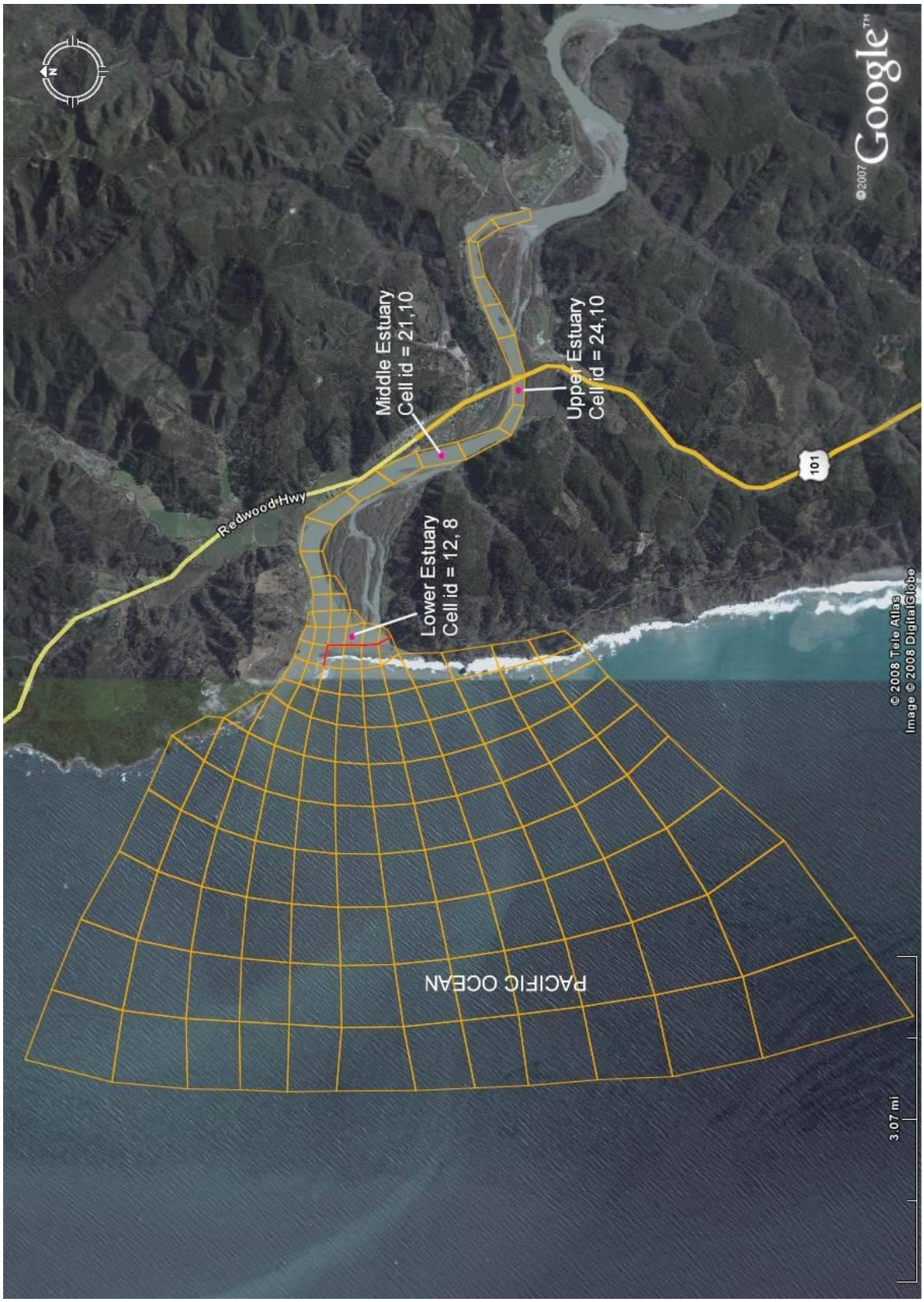

Source of Image: Google

Appendix D

Determination of Accretions for Tributaries from Iron Gate Dam to Turwar - Excerpt from the PacifiCorp, 2004 Report

Determination of Flow for Tributaries from Iron Gate Dam to Turwar using USGS Methodology

Accretions from Iron Gate Dam to Turwar were defined and quantified according to the methodology identified by USGS (1995, 1997). In sum, the river was divided into multiple segments (reaches) based on available gages with full coverage between 1961 and 1922. USGS used monthly averages to determine accretions and depletions for each reach based on the differences in gage readings. These accretions and depletions were then assigned to individual tributaries based on estimated basin area (individual sub-basin contributions were obtained from personal communication with Mr. M. Flug). Not all tributaries to the Klamath River were included.

For this exercise, 7-day average values were used to identify accretions and depletions for identified tributaries. The same tributaries identified by USGS (1997) were used herein.

The methodology is outlined below.

Total Accretion from Iron Gate Dam to Seiad Valley.
Accretion value is equal to the flow at gage 11520500 (Klamath River nr. Seiad Valley) minus the sum of the flows at gages 11516530 (KR below Iron Gate Dam), 11517500 (Shasta River nr. Yreka), 11519500 (Scott River nr Fort Jones). This reach accretion is further subdivided into shorter sub-reaches by according to the following criteria.

Klamath River from Iron Gate Dam to the confluence of the Shasta River.
Accretion equals 24.2% of the total area accretion. This accretion is distributed between the following creeks as determined by watershed area:

Bogus Creek – 41%
Willow Creek – 22%
Cottonwood Creek – 37%

Klamath River from the confluence of the Shasta River to the confluence of the Scott River.
Accretion equals 38.2% of the total area accretion. This accretion is distributed between the following creeks as determined by watershed area:
Humbug Creek – 28%
Beaver Creek – 32%
Horse Creek – 40%

Scott River from Ft. Jones to the confluence of the Klamath River.
Accretion equals 29.0% of the total area accretion.

Klamath River from the confluence of the Scott River to Seiad valley.
Accretion equals 8.6% of the total area accretion. This accretion is applied at Grider Creek.

Total Accretion from Klamath River from Seiad Valley to Orleans.
Accretion equals the flow at gage 11523000 (Klamath River at Orleans) minus the sum of the flows at gages 11520500 (Klamath River nr Seiad Valley), 11522500 (Salmon River at Somes Bar, Ca), and 11521500 (Indian Cr nr Happy Camp).
This accretion is distributed between the following creeks as determined by watershed area:

Thompson Creek – 16.6%
Elk Creek – 16.6%
Clear Creek – 21.4%
Ukonom Creek – 12.9%
Dillon Creek – 32.5%

Total Accretion from Klamath River from Orleans to the Mouth.
Accretion equals gage 15530500 (KR nr Klamath (Turwar), CA) minus gage 15523000 (KR at
Orleans) and 11530000 (Trinity River at Hoopa).

Klamath River from Orleans to the confluence of the Trinity River.
Accretion equals 29.3% of the total area accretion. This accretion is distributed between the following creeks as determined by watershed area:

Camp Creek – 33.3%
Red Cap Creek – 33.3%
Bluff Creek – 33.3%

Trinity River from Hoopa to the confluence with the Klamath River.
Accretion equals 12.3% of the total area accretion.

Klamath River from the confluence of the Trinity River to the mouth.
Accretion equals 58.4% of total area accretion. This accretion is distributed between the following creeks as determined by watershed area:

Pine Creek – 33.3%
Tectah Creek – 33.3%
Blue Creek – 33.3%

Appendix E

Calibration Results for Lake Ewauna to Keno Dam (Modeling Segment 2)

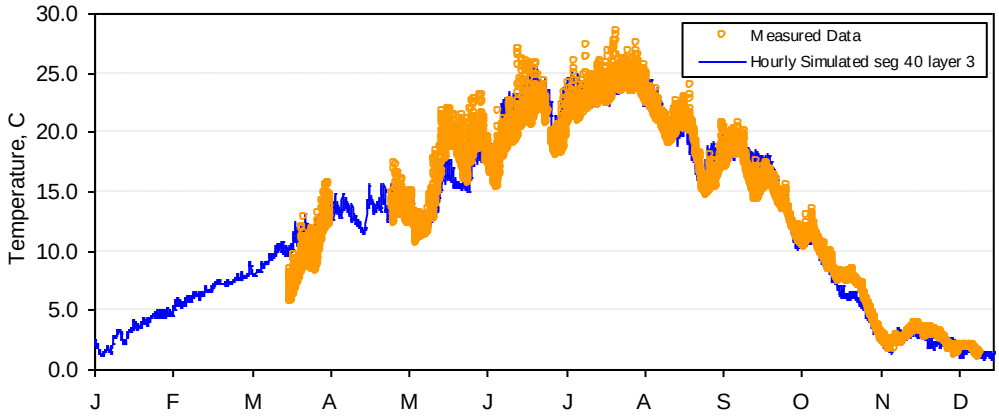

Figure E-1. Temperature calibration results for Lake Ewauna—Keno Dam at Klamath River at Miller Island boat ramp (2000).

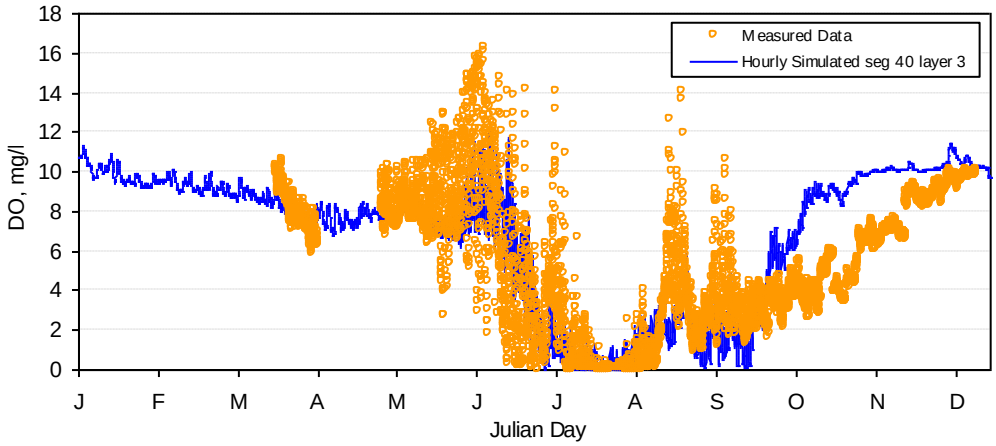

Figure E-2. Dissolved oxygen calibration results for Lake Ewauna—Keno Dam at Klamath River at Miller Island boat ramp (2000).

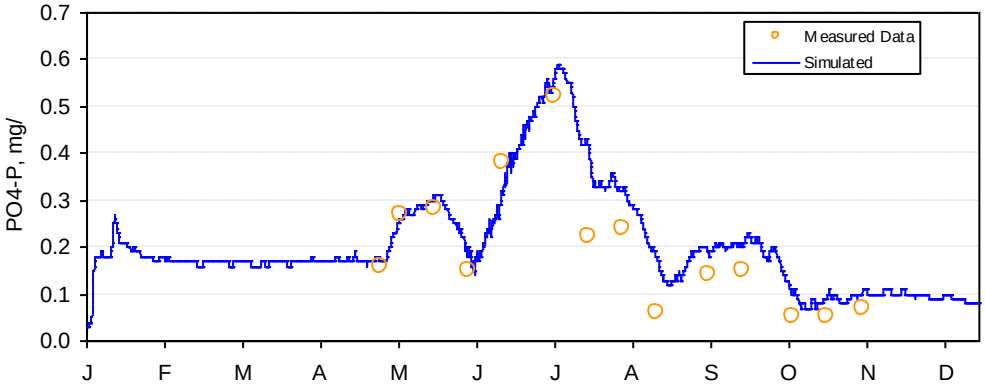

Figure E-3. PO4-P calibration results for Lake Ewauna—Keno Dam at Klamath River at Miller Island

boat ramp (2000).

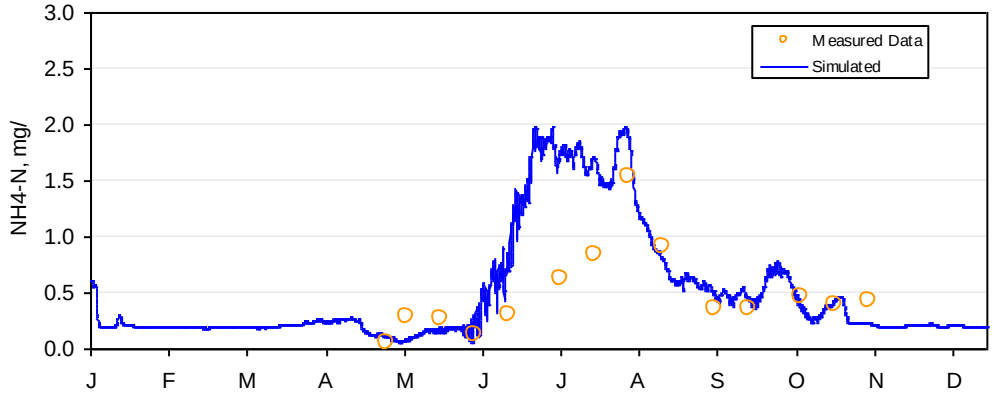

Figure E-4. NH4-N calibration results for Lake Ewauna—Keno Dam at Klamath River at Miller Island boat ramp (2000).

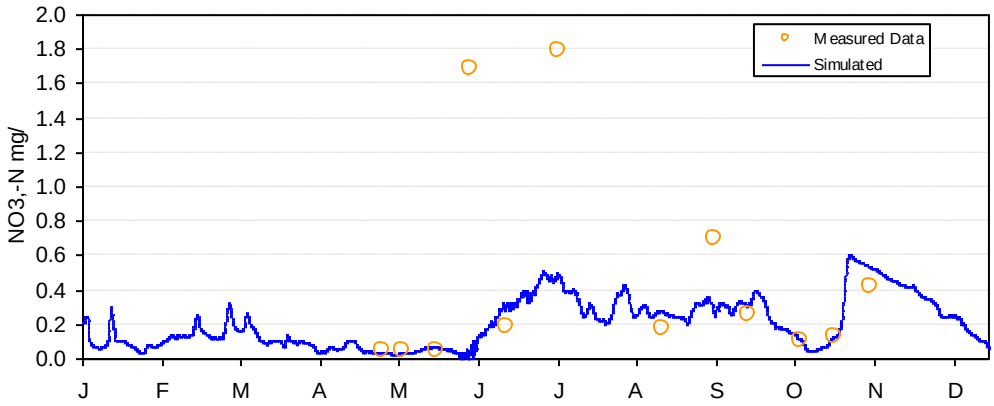

Figure E-5. NO3-N calibration results for Lake Ewauna—Keno Dam at Klamath River at Miller Island boat ramp (2000).

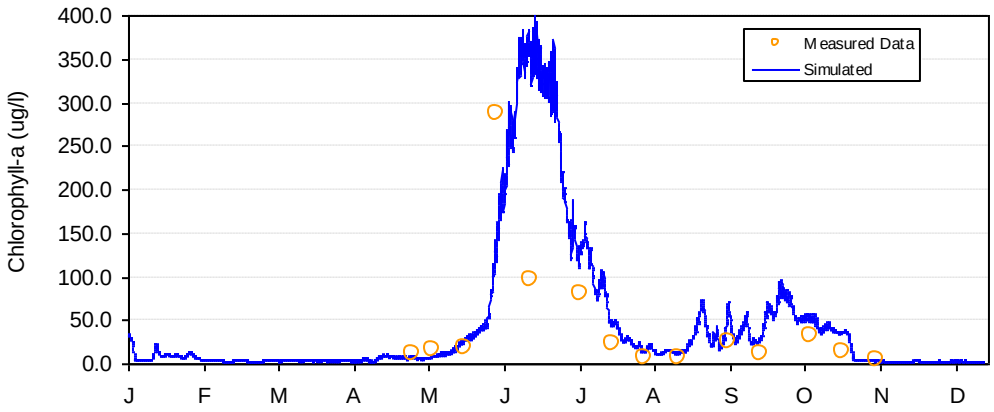

Figure E-6. Chlorophyll-a calibration results for Lake Ewauna—Keno Dam at Klamath River at Miller Island boat ramp (2000).

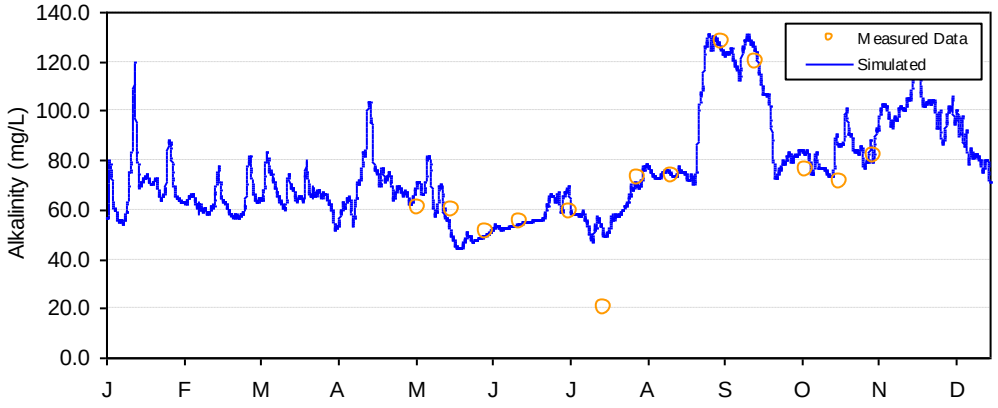

Figure E-7. Alkalinity calibration results for Lake Ewauna—Keno Dam at Klamath River at Miller Island boat ramp (2000).

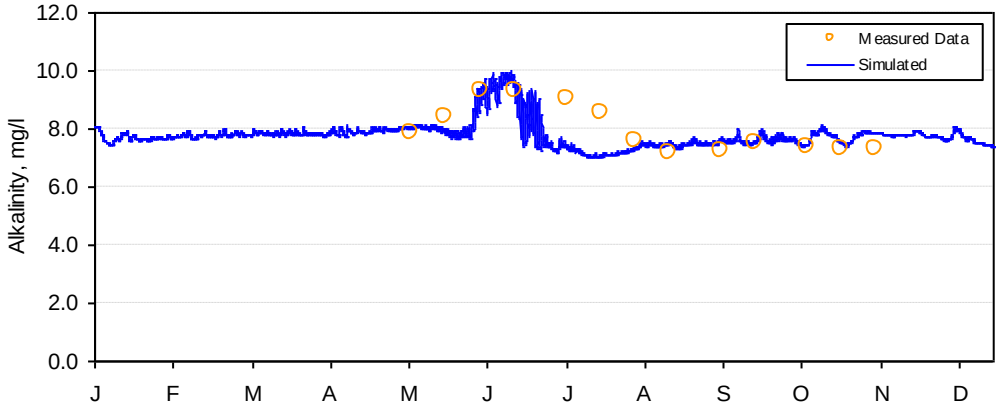

Figure E-8. pH calibration results for Lake Ewauna—Keno Dam at Klamath River at Miller Island boat ramp (2000).

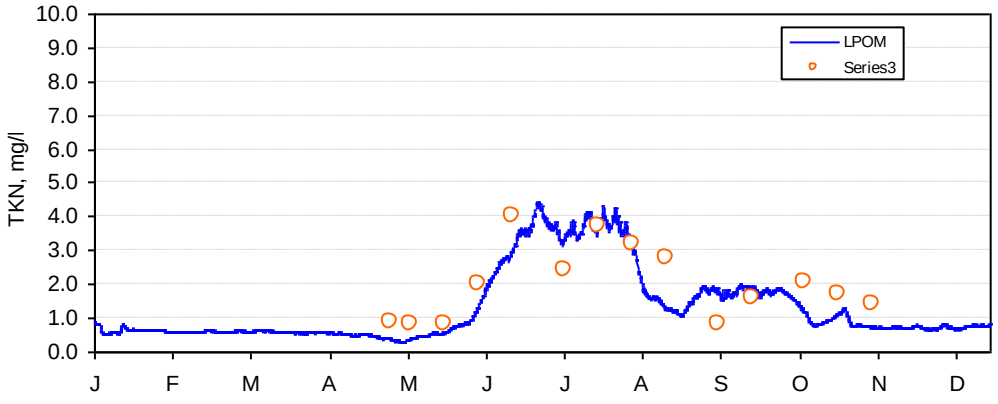

Figure E-9. TKN calibration results for Lake Ewauna—Keno Dam at Klamath River at Miller Island boat ramp (2000).

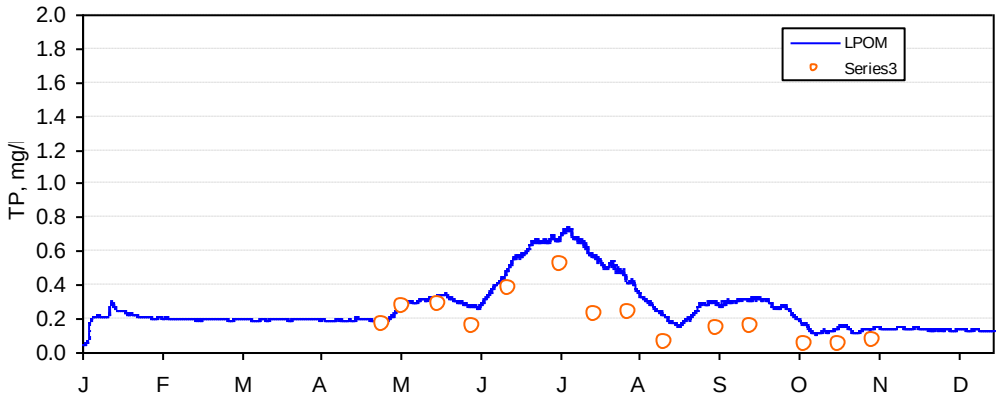

Figure E-10. TP calibration results for Lake Ewauna—Keno Dam at Klamath River at Miller Island boat ramp (2000).

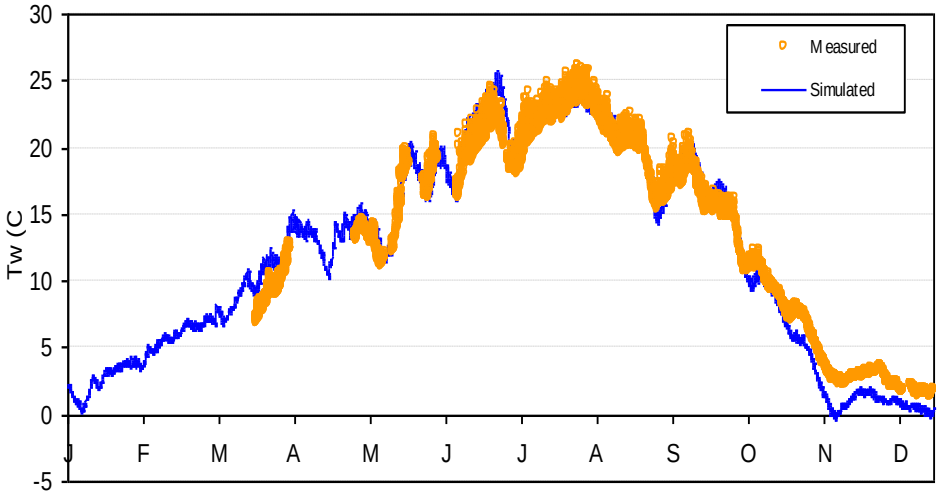

Figure E-11. Temperature calibration results for Lake Ewauna—Keno Dam at Klamath River at Keno Bridge (Hwy 66) (2000).

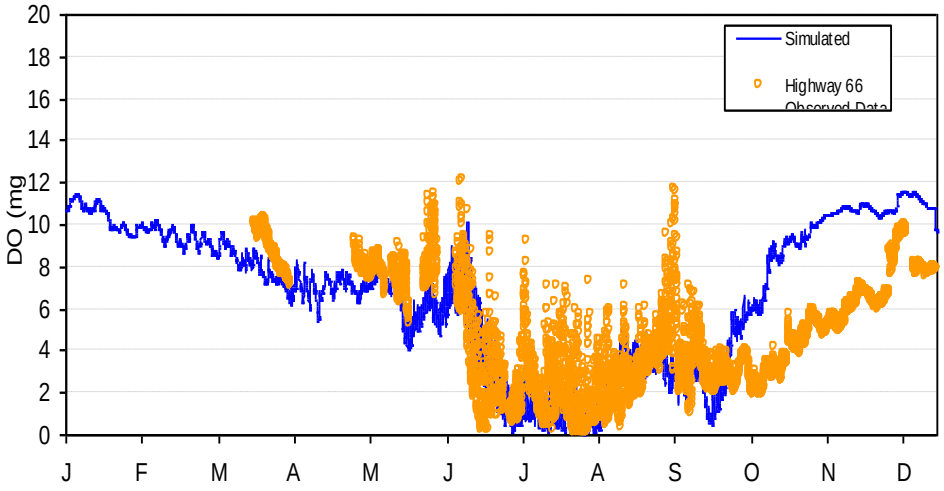

Figure E-12. Dissolved oxygen calibration results for Lake Ewauna—Keno Dam at Klamath River at Keno Bridge (Hwy 66) (2000).

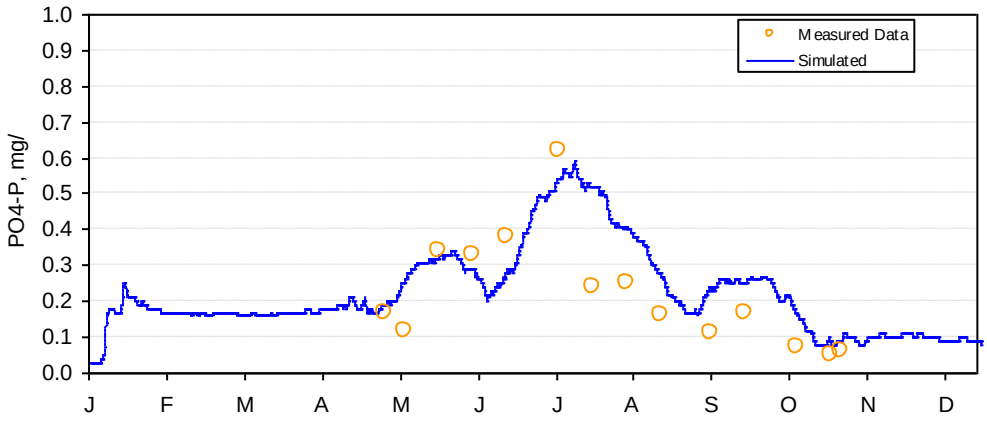

Figure E-13. PO4-P calibration results for Lake Ewauna—Keno Dam at Klamath River at Keno Bridge (Hwy 66) (2000).

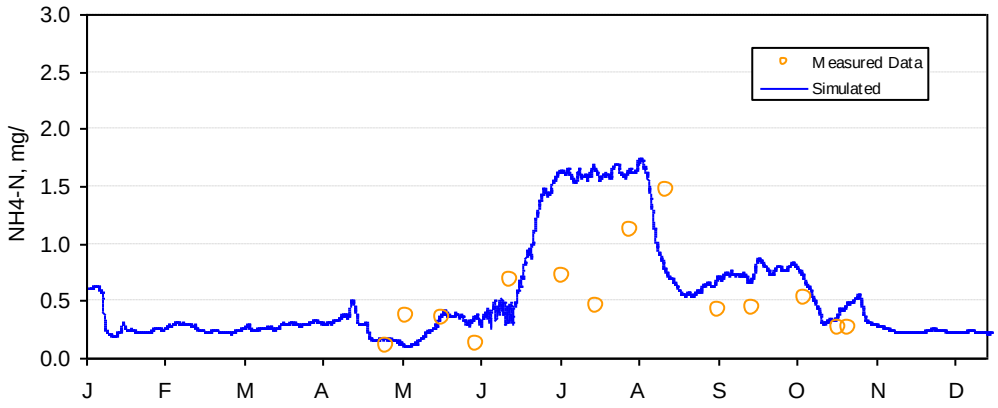

Figure E-14. NH4-N calibration results for Lake Ewauna—Keno Dam at Klamath River at Keno Bridge (Hwy 66) (2000).

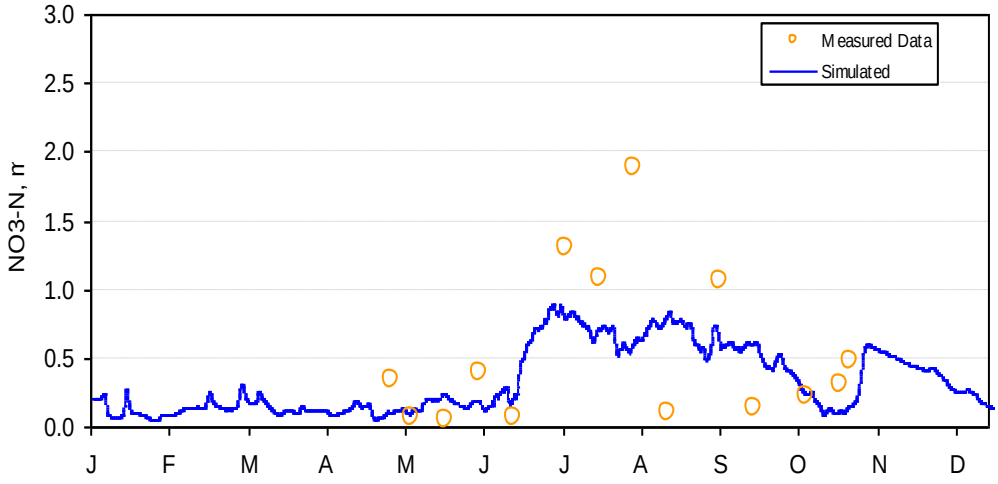

Figure E-15. NO3-N calibration results for Lake Ewauna—Keno Dam at Klamath River at Keno Bridge (Hwy 66) (2000).

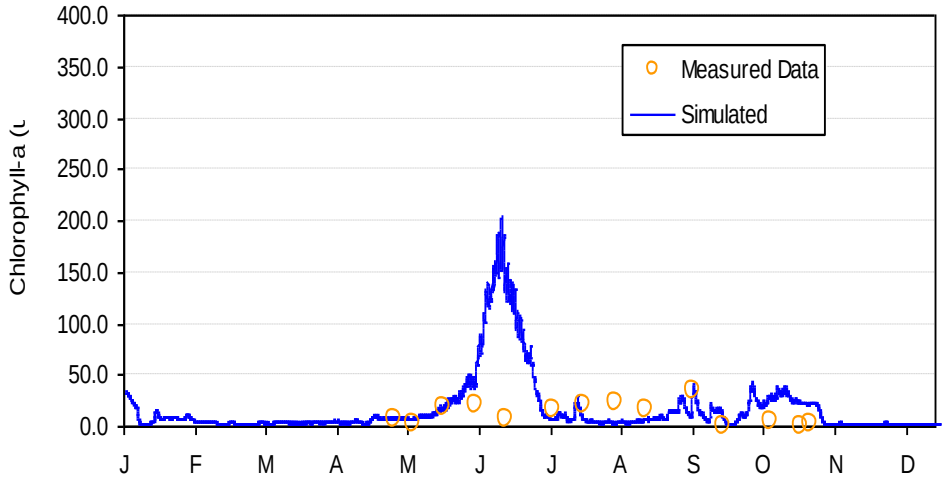

Figure E-16. Chlorophyll-a calibration results for Lake Ewauna—Keno Dam at Klamath River at Keno Bridge (Hwy 66) (2000).

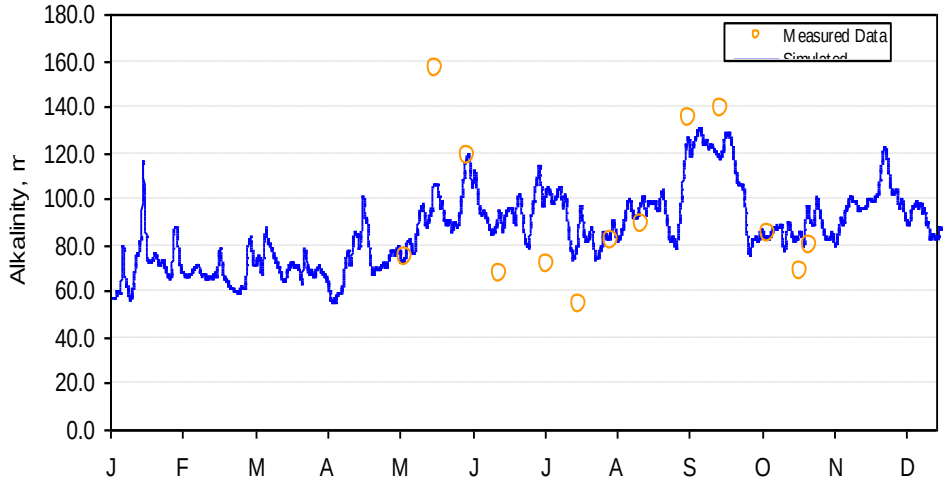

Figure E-17. Alkalinity calibration results for Lake Ewauna—Keno Dam at Klamath River at Keno Bridge (Hwy 66) (2000).

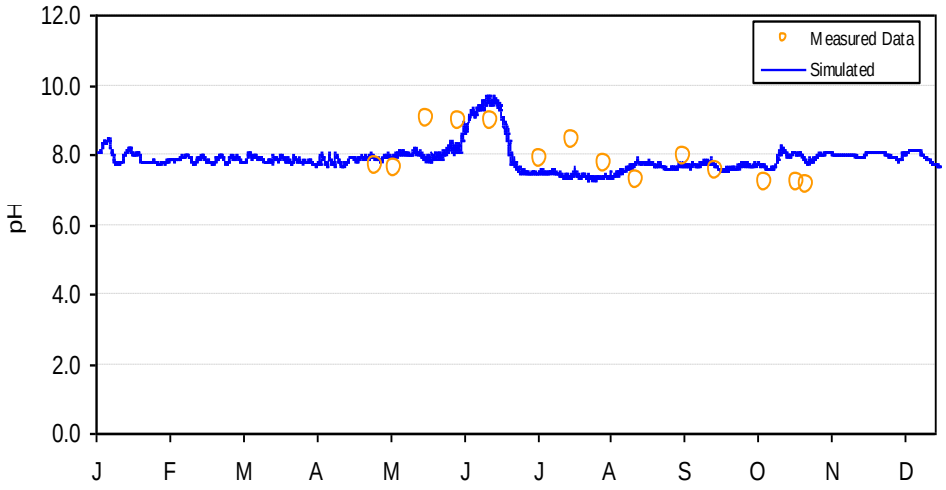

Figure E-18. pH calibration results for Lake Ewauna—Keno Dam at Klamath River at Keno Bridge (Hwy 66) (2000).

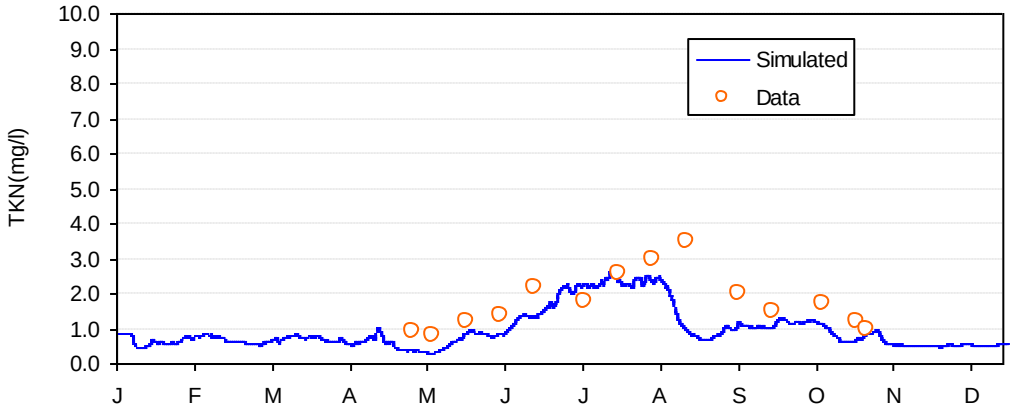

Figure E-19. TKN calibration results for Lake Ewauna—Keno Dam at Klamath River at Keno Bridge (Hwy 66) (2000).

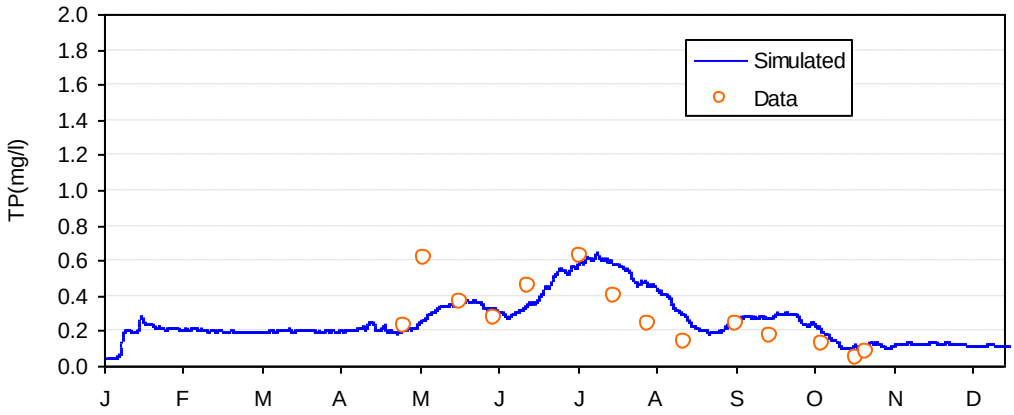

Figure E-20. TP calibration results for Lake Ewauna—Keno Dam at Klamath River at Keno Bridge (Hwy 66) (2000).

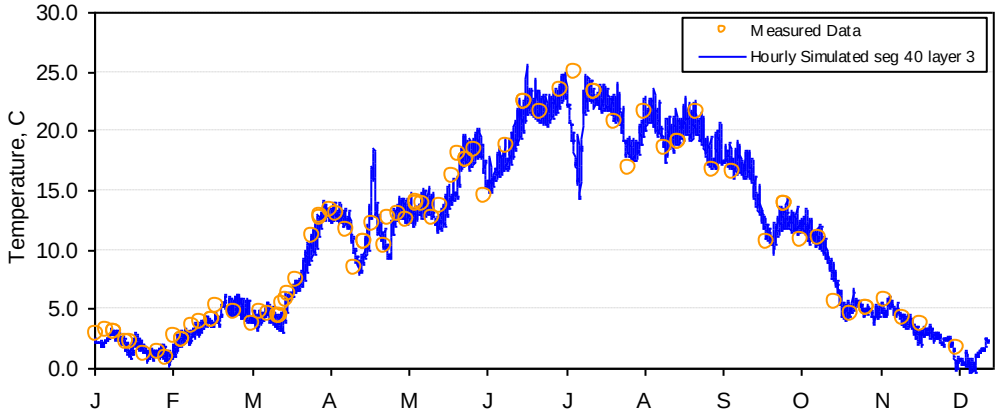

Figure E-21. Temperature calibration results for Lake Ewauna—Railroad Bridge Drawspan (2002).

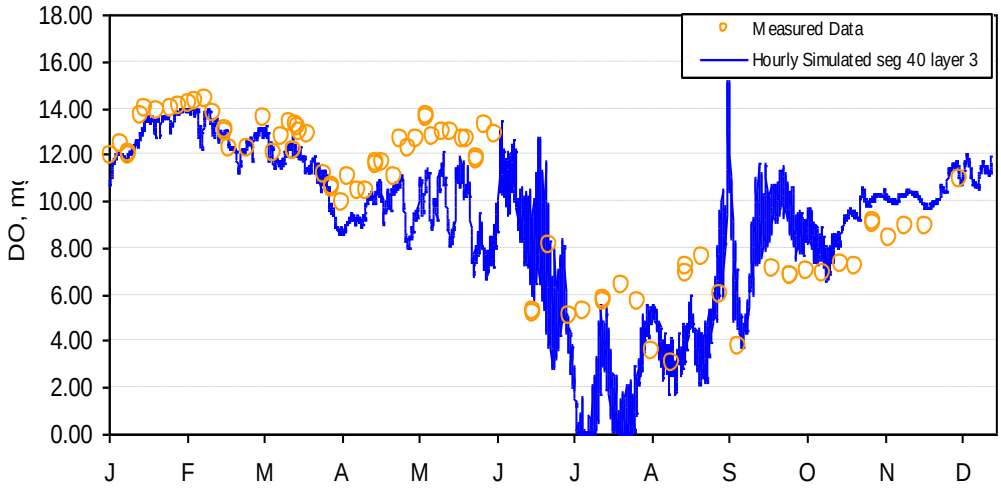

Figure E-22. Dissolved Oxygen calibration results for Lake Ewauna—Railroad Bridge Drawspan (2002).

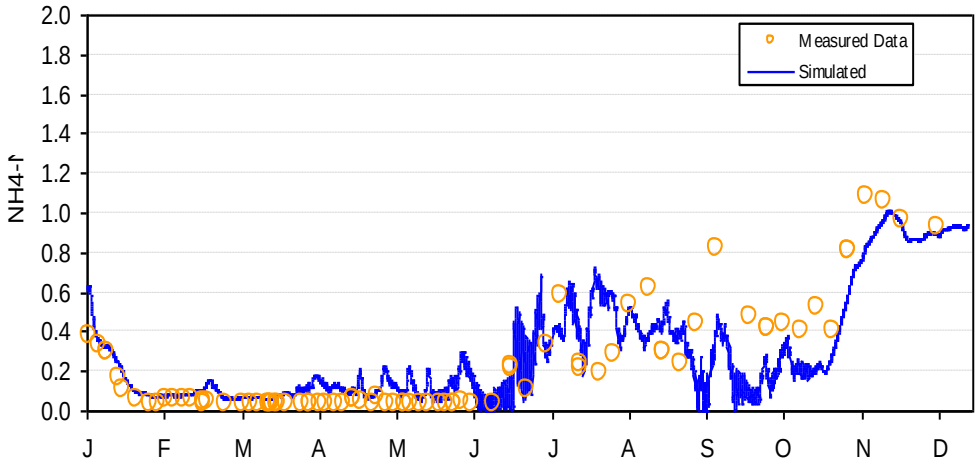

Figure E-23. NH4-N calibration results for Lake Ewauna—Railroad Bridge Drawspan (2002).

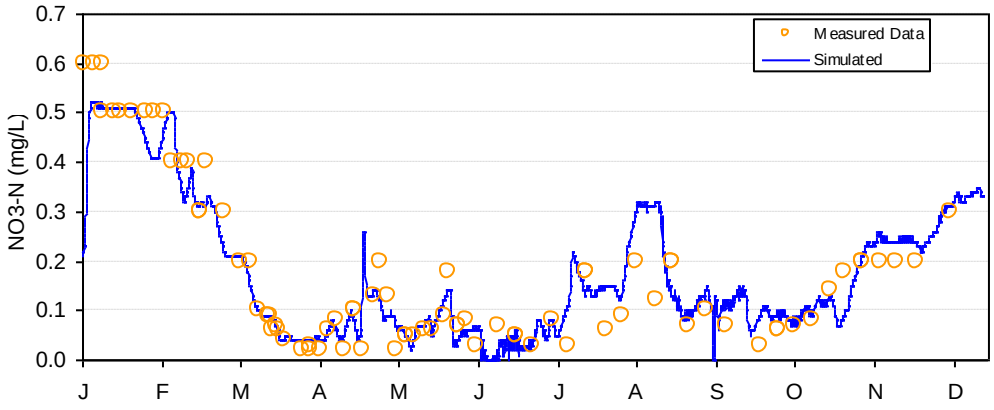

Figure E-24. NO3-N calibration results for Lake Ewauna—Railroad Bridge Drawspan (2002).

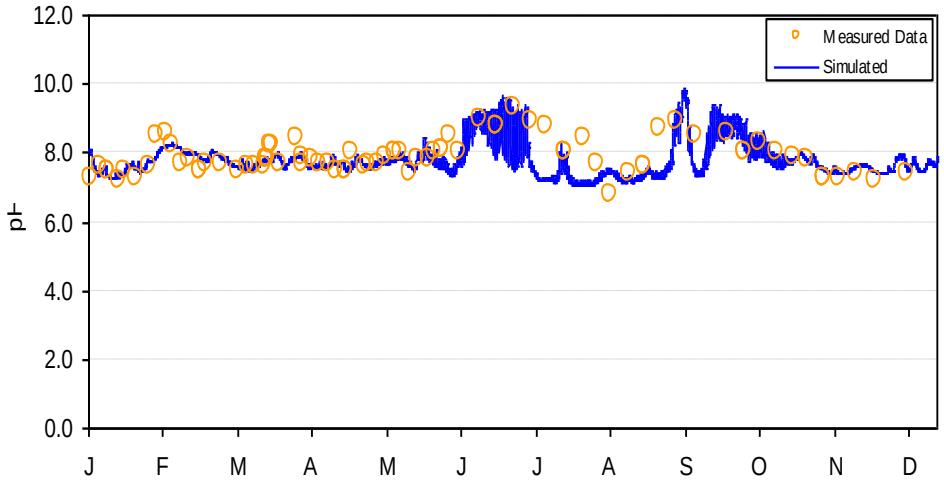

Figure E-25. pH calibration results for Lake Ewauna—Railroad Bridge Drawspan (2002).

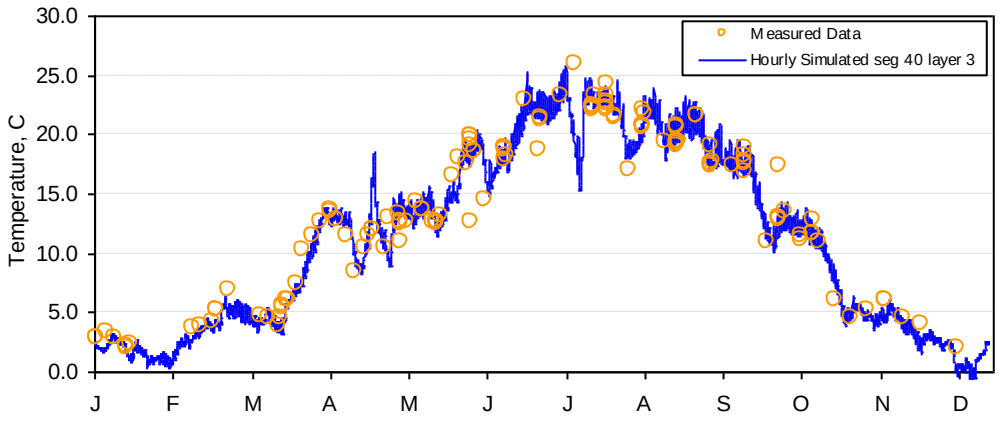

Figure E-26. Temperature calibration results for Lake Ewauna—South Side Bypass Bridge (2002).

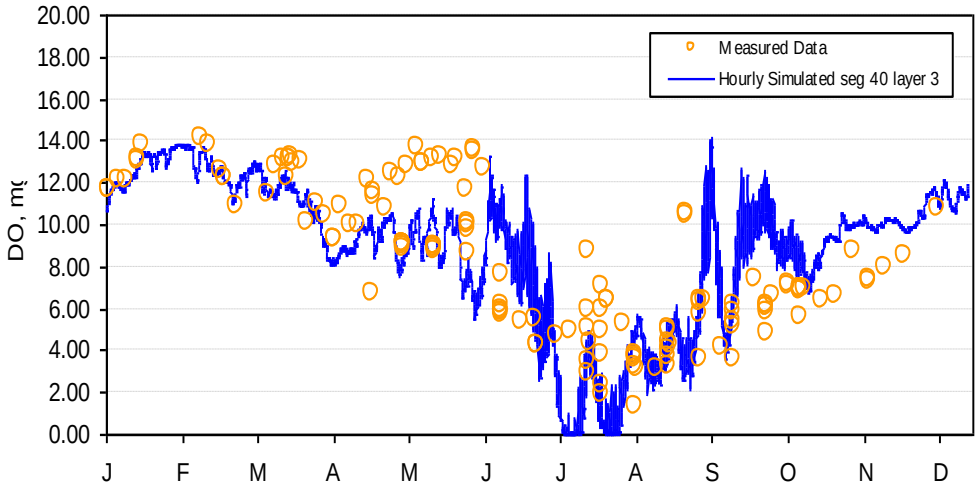

Figure E-27. Dissolved Oxygen calibration results for Lake Ewauna—South Side Bypass Bridge (2002).

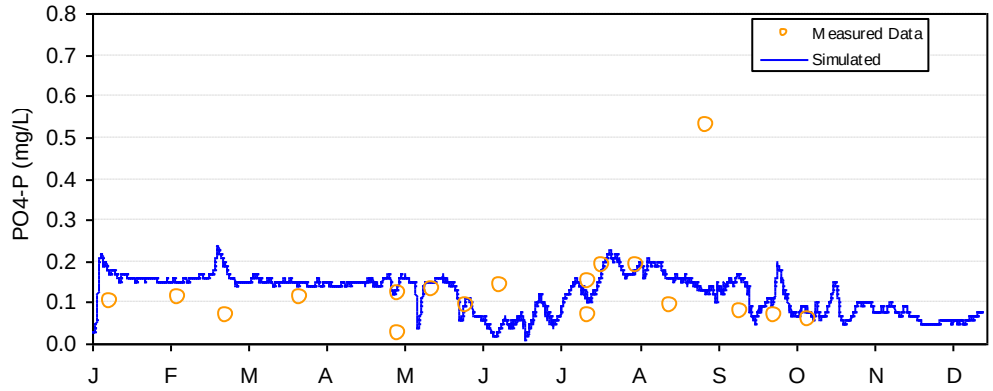

Figure E-28. PO4-P calibration results for Lake Ewauna—South Side Bypass Bridge (2002).

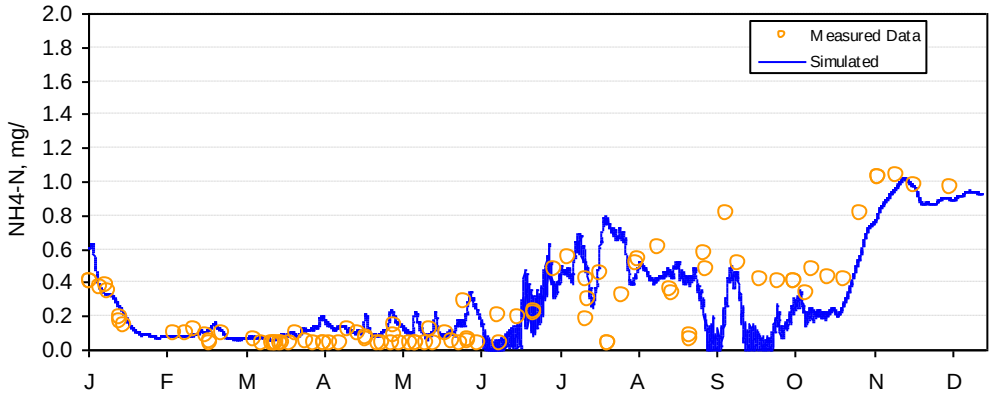

Figure E-29. NH4-N calibration results for Lake Ewauna—South Side Bypass Bridge (2002).

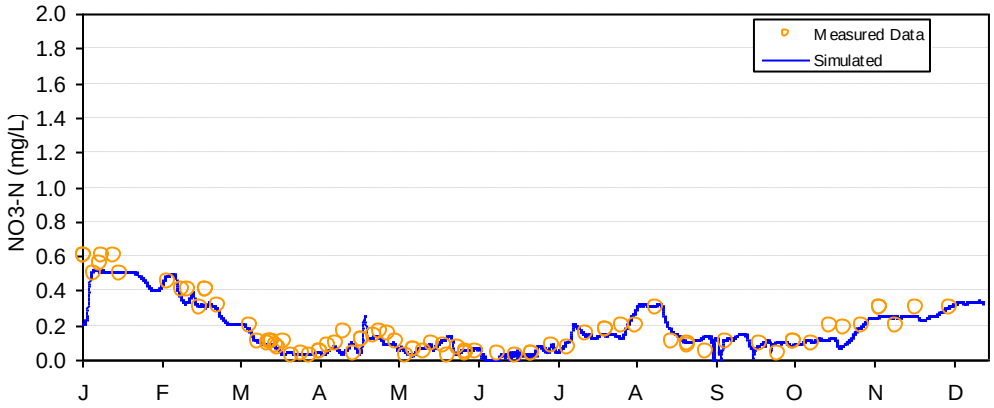

Figure E-30. NO3-N calibration results for Lake Ewauna—South Side Bypass Bridge (2002).

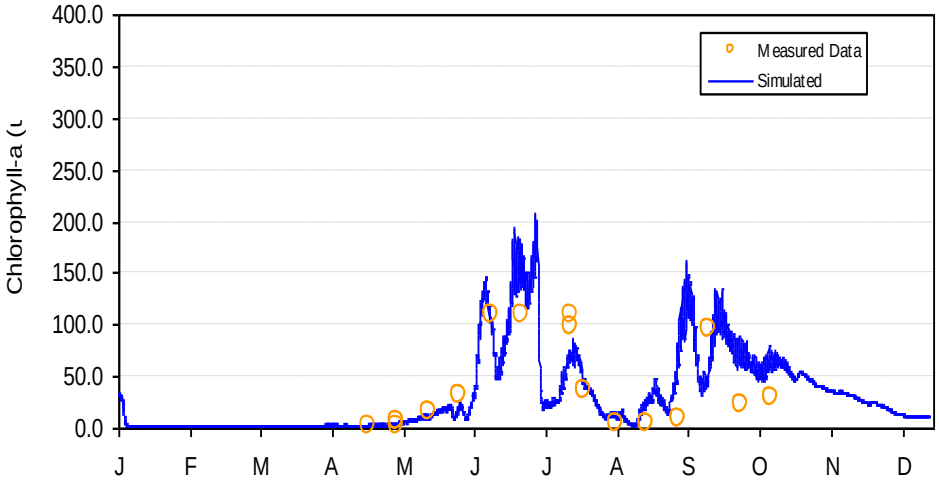

Figure E-31. Chlorophyll-a calibration results for Lake Ewauna—South Side Bypass Bridge (2002).

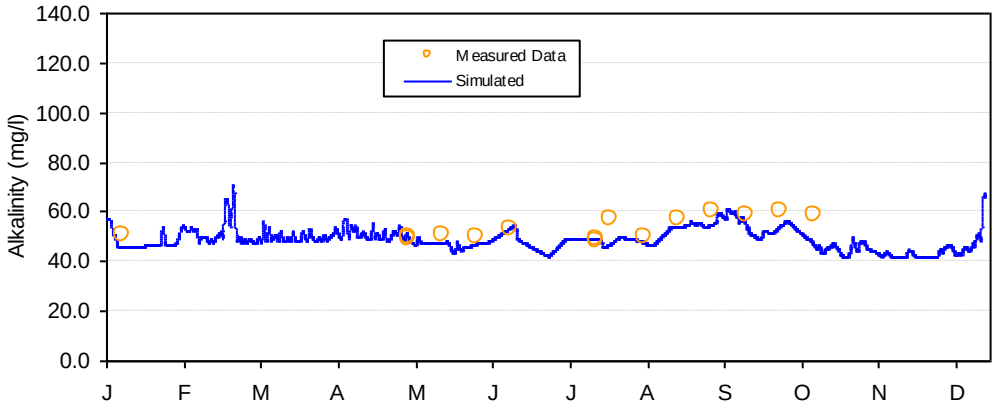

Figure E-32. Alkalinity calibration results for Lake Ewauna—South Side Bypass Bridge (2002).

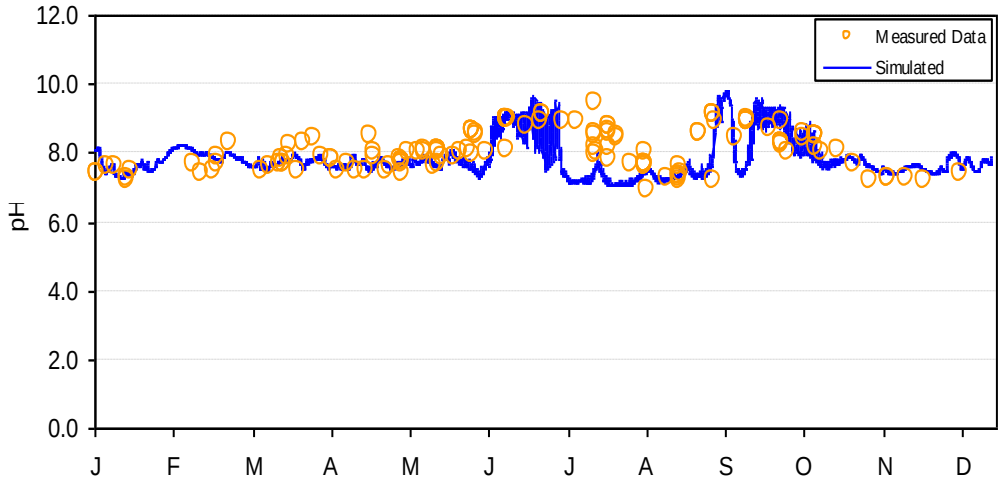

Figure E-33. pH calibration results for Lake Ewauna—South Side Bypass Bridge (2002).

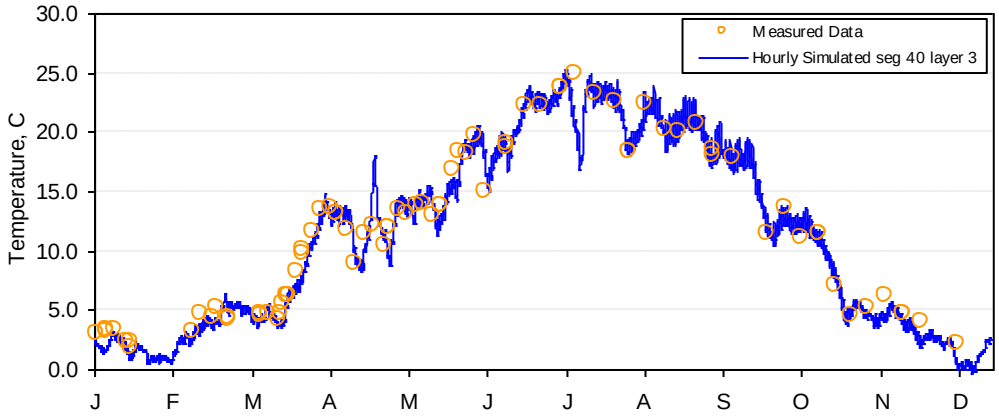

Figure E-34. Temperature calibration results for Lake Ewauna—Klamath River at Hwy 97 (2002).

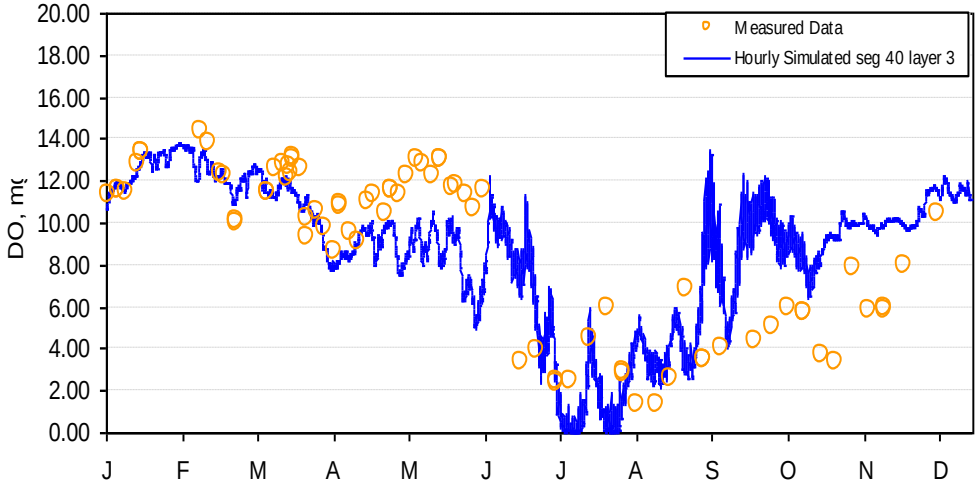

Figure E-35. Dissolved Oxygen calibration results for Lake Ewauna—Klamath River at Hwy 97 (2002).

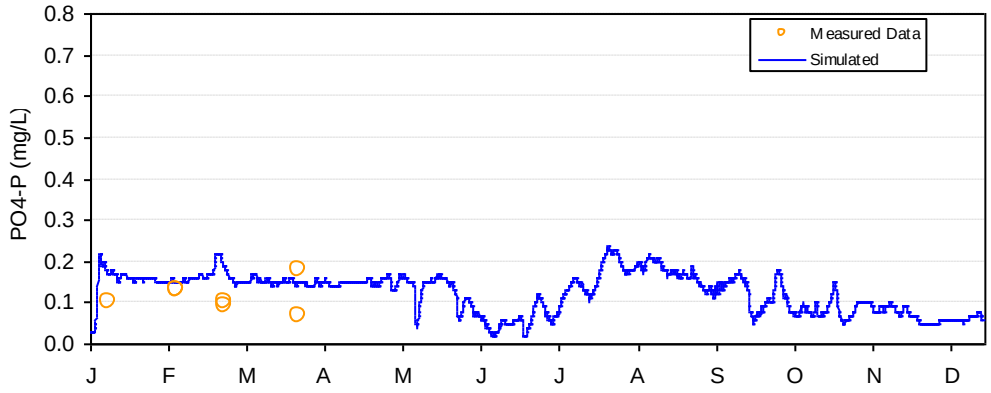

Figure E-36. PO4-P calibration results for Lake Ewauna—Klamath River at Hwy 97 (2002).

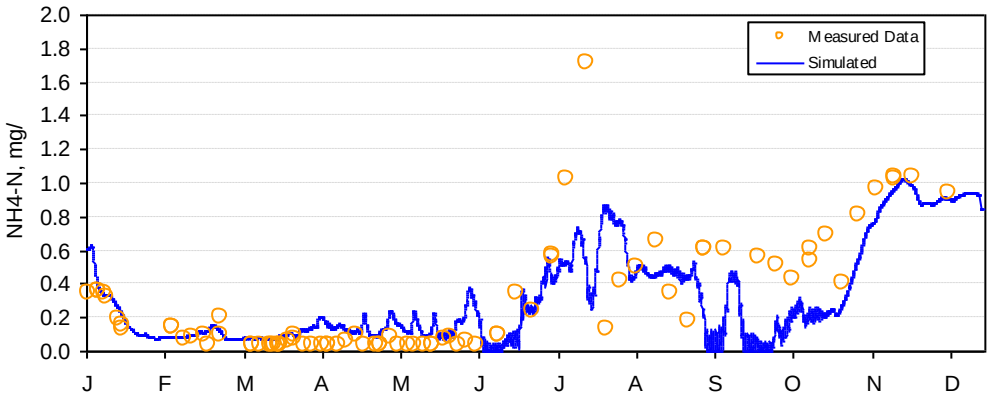

Figure E-37. NH4-N calibration results for Lake Ewauna—Klamath River at Hwy 97 (2002).

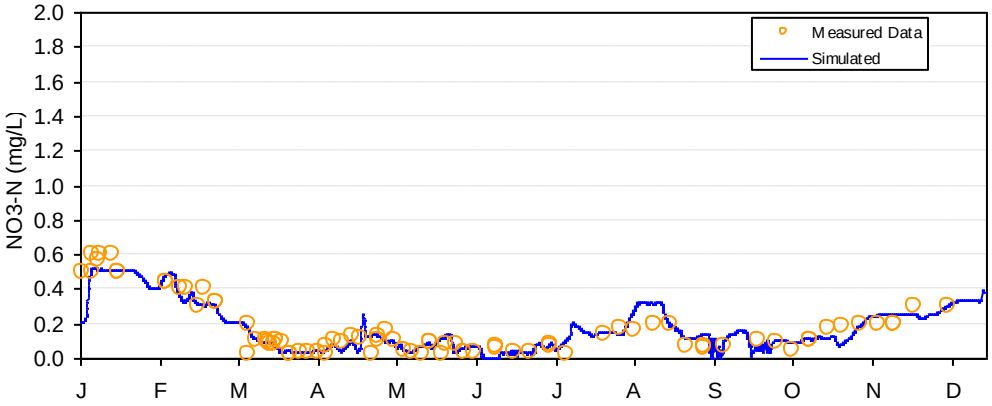

Figure E-38. NO3-N calibration results for Lake Ewauna—Klamath River at Hwy 97 (2002).

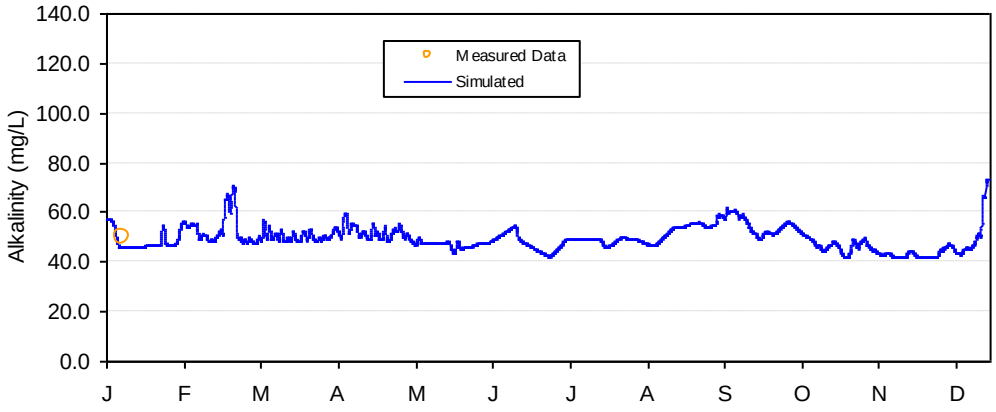

Figure E-39. Alkalinity calibration results for Lake Ewauna—Klamath River at Hwy 97 (2002).

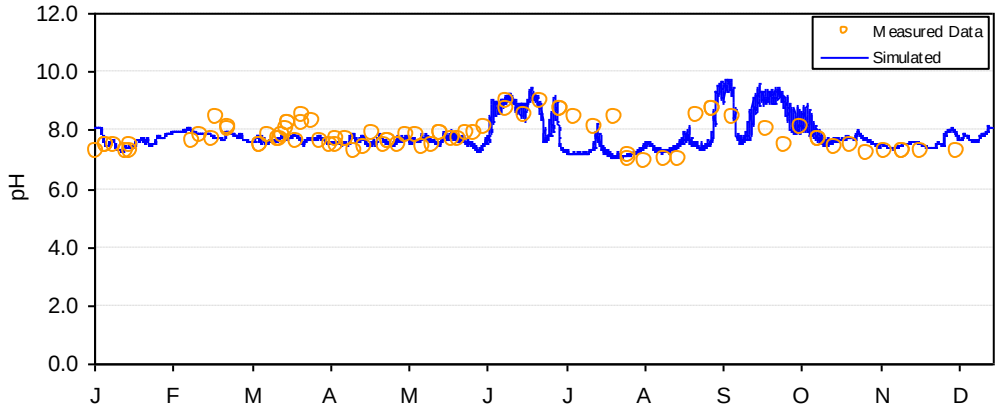

Figure E-40. pH calibration results for Lake Ewauna—Klamath River at Hwy 97 (2002).

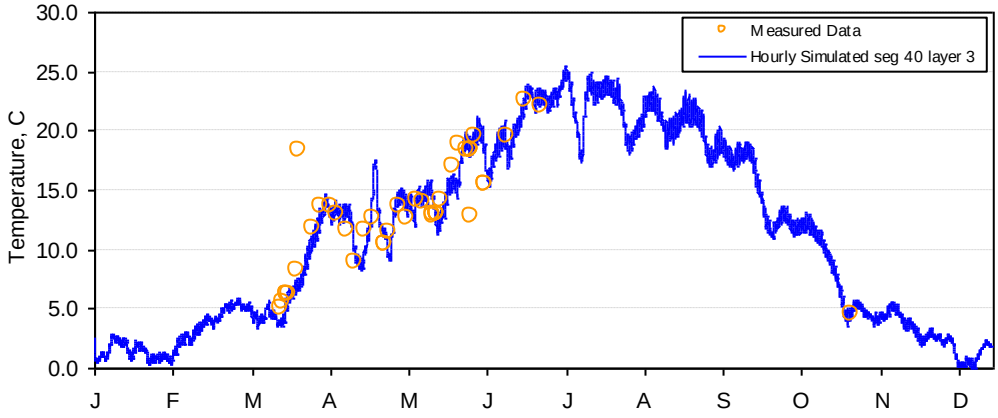

Figure E-41. Temperature calibration results for Lake Ewauna—Lost River Diversion at Klamath River (2002).

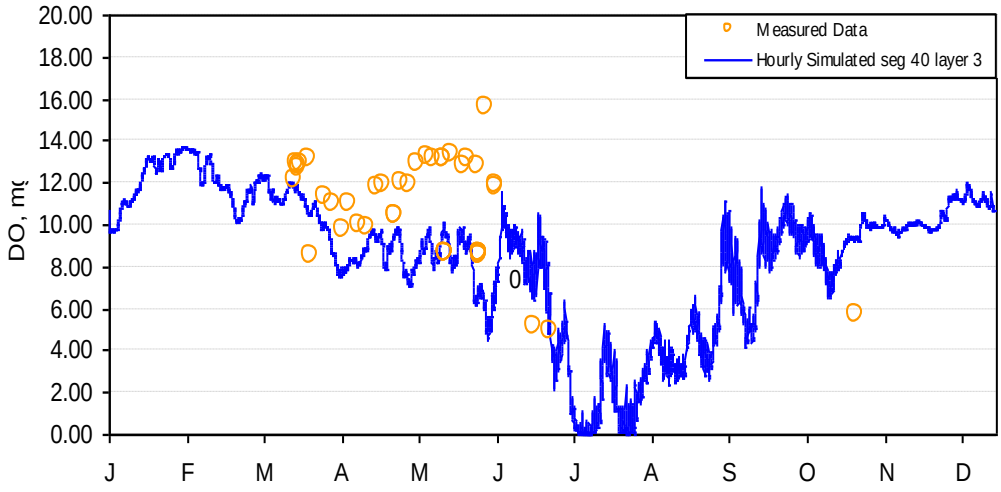

Figure E-42. Dissolved Oxygen calibration results for Lake Ewauna—Lost River Diversion at Klamath River (2002).

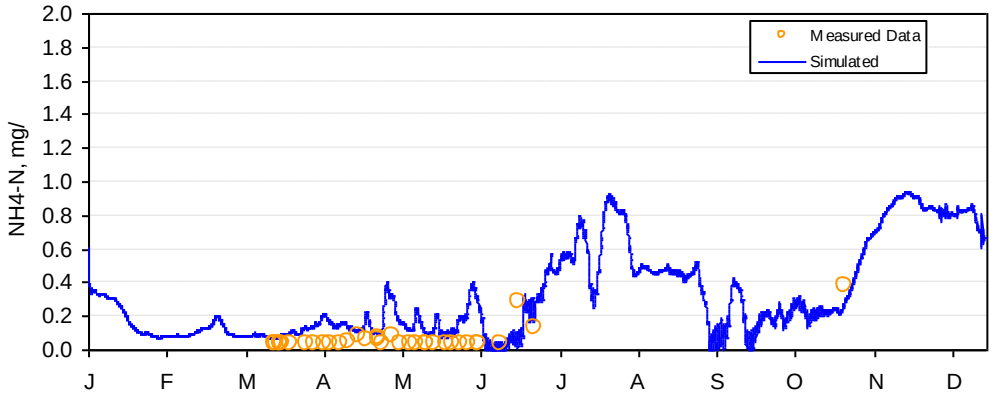

Figure E-43. NH4-N calibration results for Lake Ewauna—Lost River Diversion at Klamath River (2002).

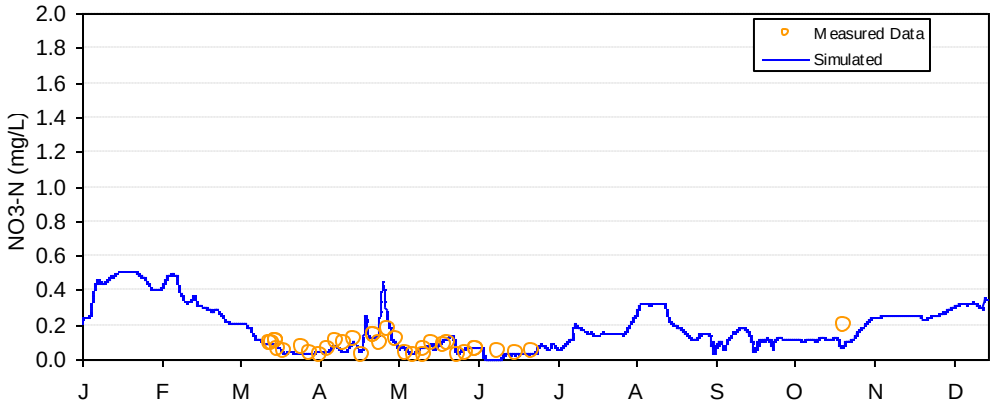

Figure E-44. NO3-N calibration results for Lake Ewauna—Lost River Diversion at Klamath River (2002).

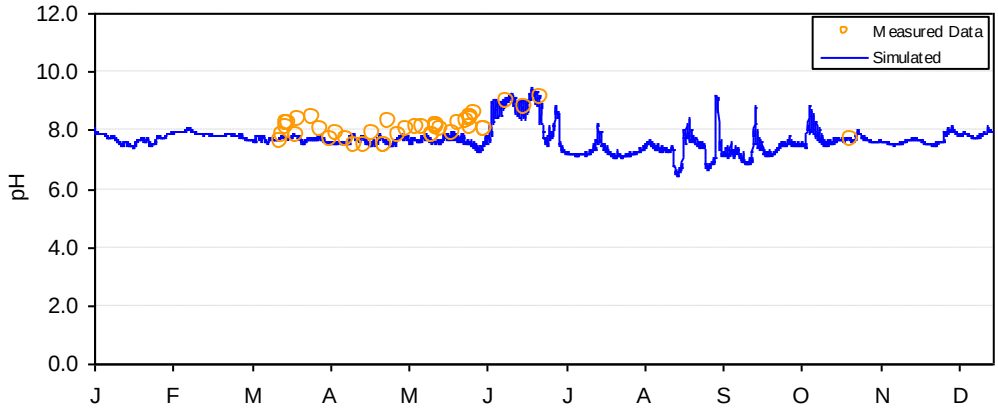

Figure E-45. pH calibration results for Lake Ewauna—Lost River Diversion at Klamath River (2002).

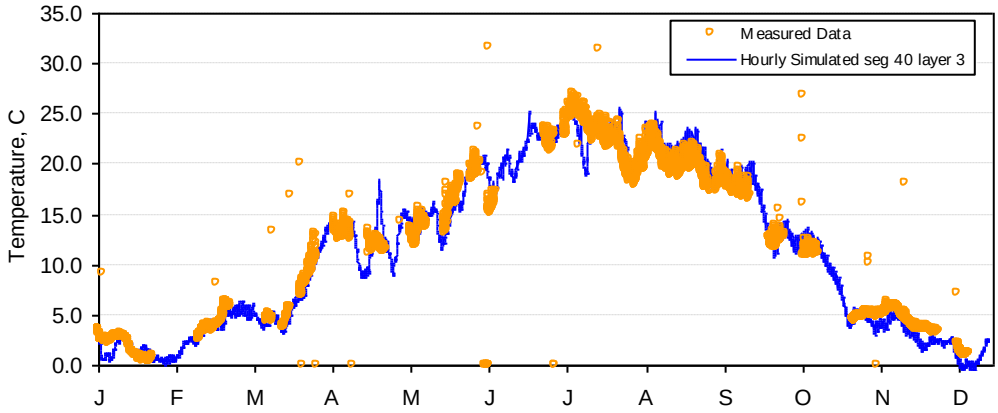

Figure E-46. Temperature calibration results for Lake Ewauna—Klamath River at Miller Island (2002).

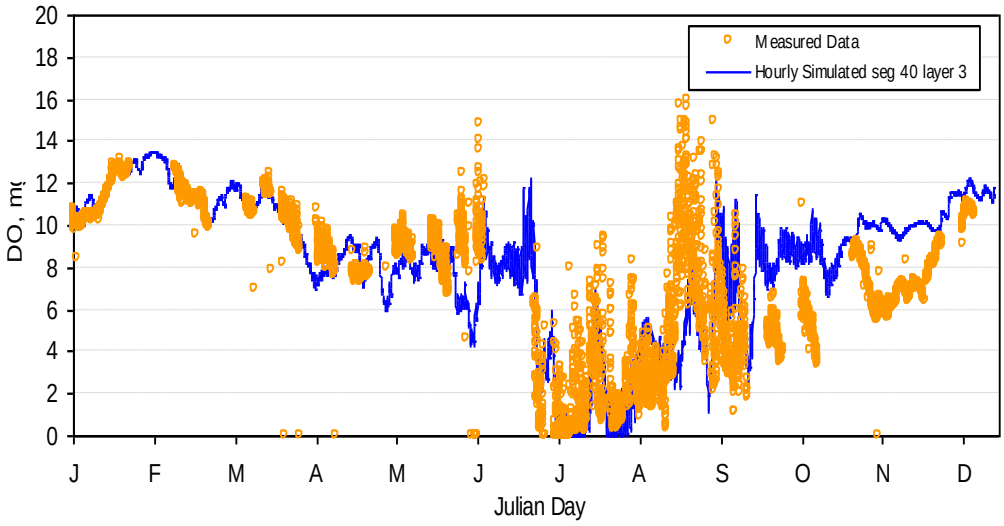

Figure E-47. Dissolved Oxygen calibration results for Lake Ewauna—Klamath River at Miller Island (2002).

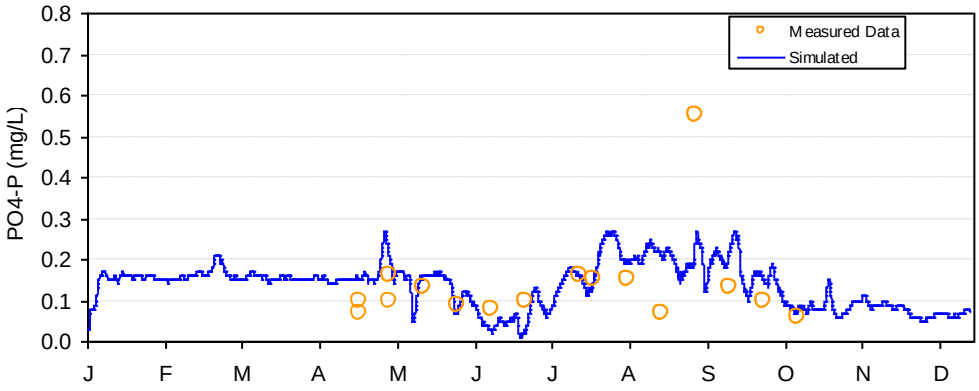

Figure E-48. PO4-P calibration results for Lake Ewauna—Klamath River at Miller Island (2002).

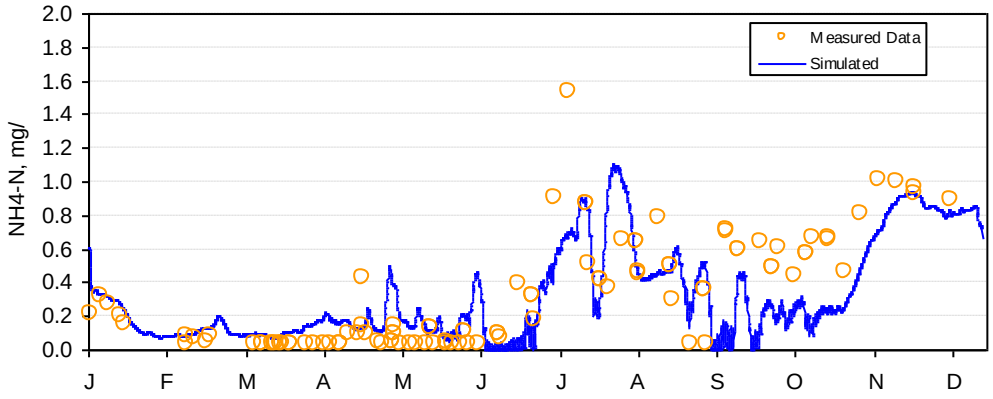

Figure E-49. NH4-N calibration results for Lake Ewauna—Klamath River at Miller Island (2002).

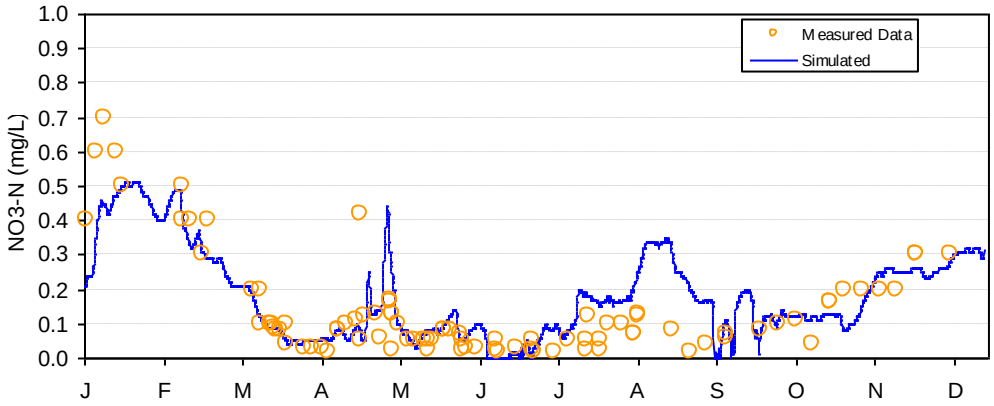

Figure E-50. NO3-N calibration results for Lake Ewauna—Klamath River at Miller Island (2002).

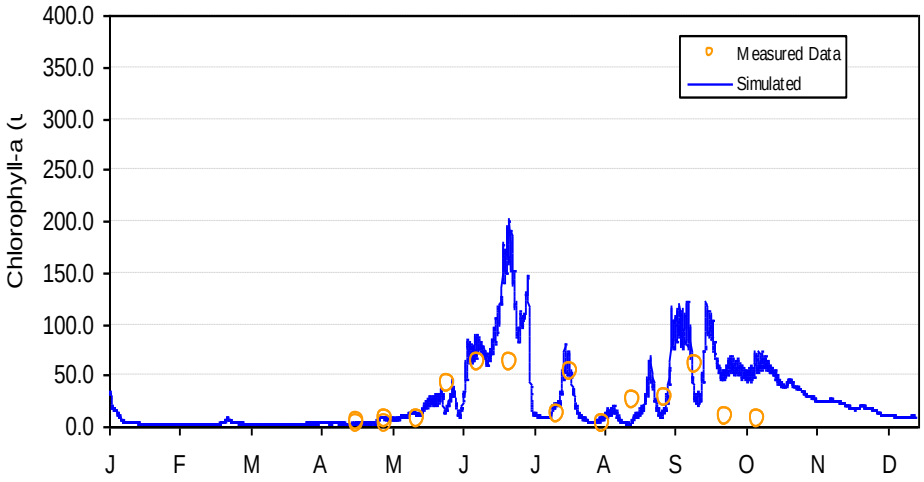

Figure E-51. Chlorophyll-a calibration results for Lake Ewauna—Klamath River at Miller Island (2002).

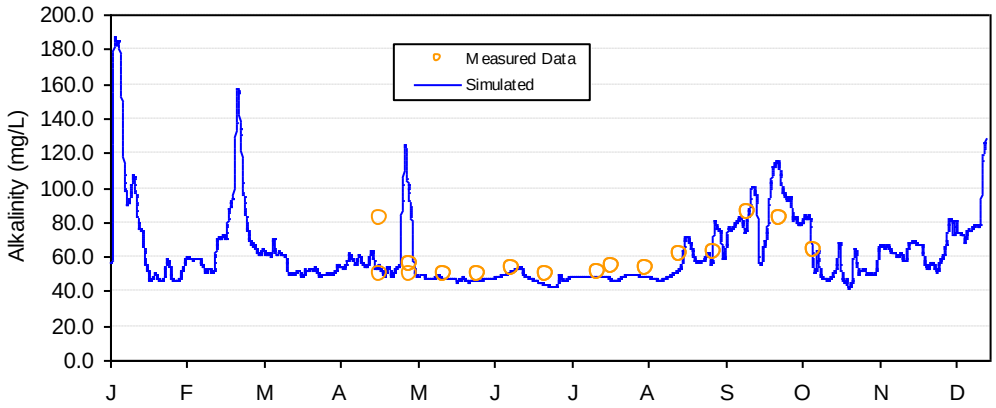

Figure E-52. Alkalinity calibration results for Lake Ewauna—Klamath River at Miller Island (2002).

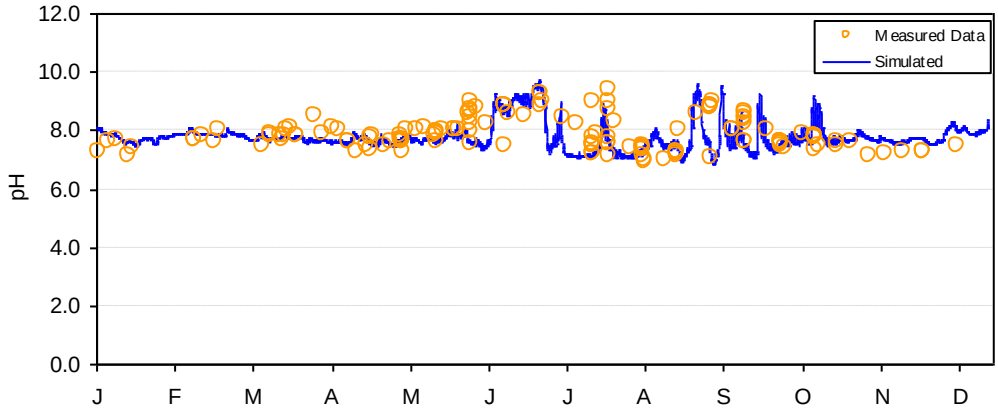

Figure E-53. pH calibration results for Lake Ewauna—Klamath River at Miller Island (2002).

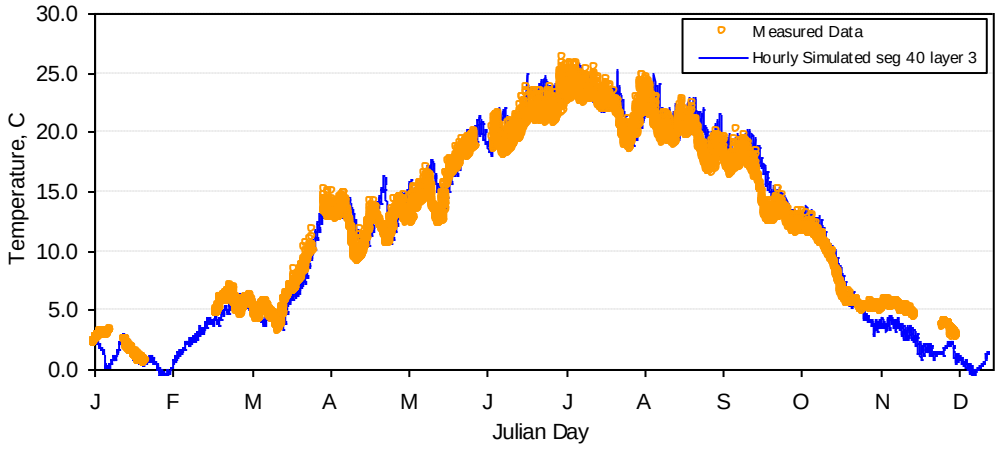

Figure E-54. Temperature calibration results for Lake Ewauna—Klamath River at Keno Bridge (Hwy 66) (2002).

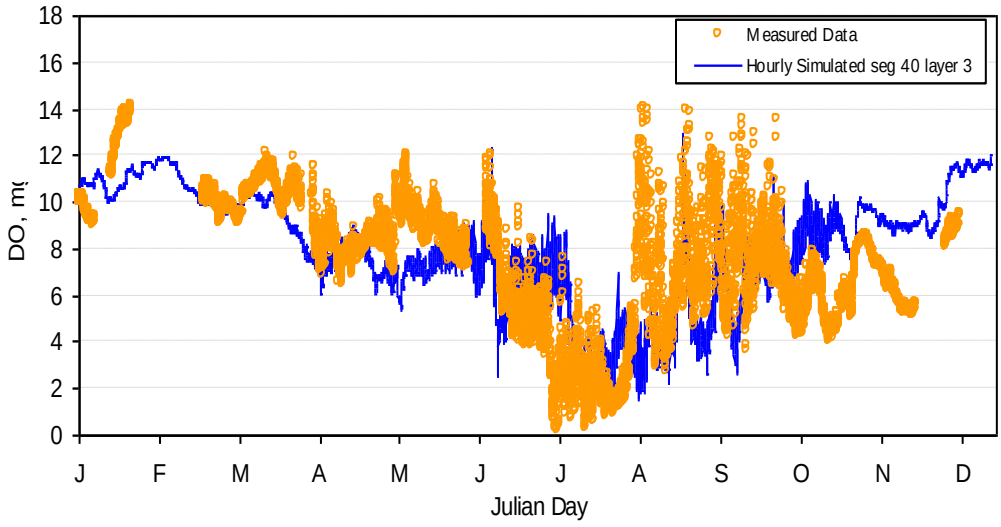

Figure E-55. Dissolved Oxygen calibration results for Lake Ewauna—Klamath River at Keno Bridge (Hwy 66) (2002).

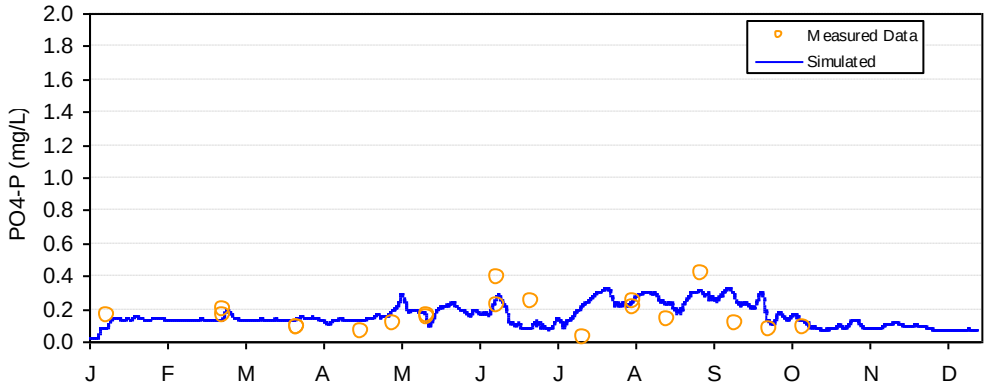

Figure E-56. PO4-P calibration results for Lake Ewauna—Klamath River at Keno Bridge (Hwy 66) (2002).

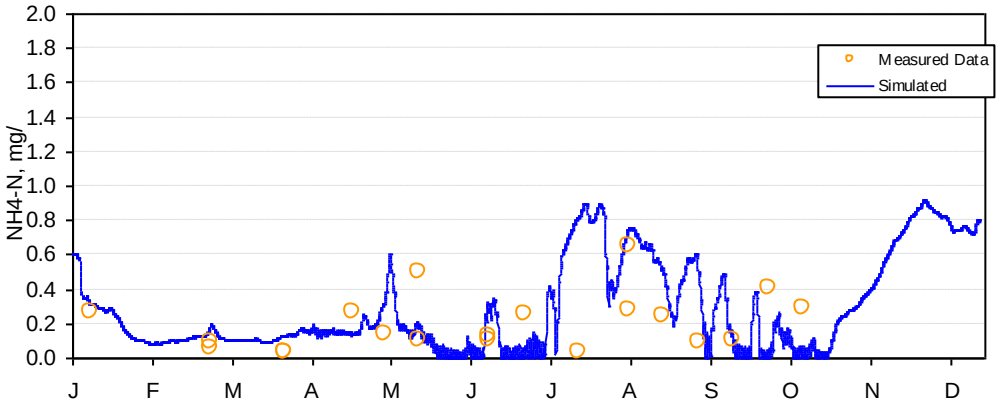

Figure E-57. NH4-N calibration results for Lake Ewauna—Klamath River at Keno Bridge (Hwy 66) (2002).

Figure E-58. NO3-N calibration results for Lake Ewauna—Klamath River at Keno Bridge (Hwy 66)

(2002).

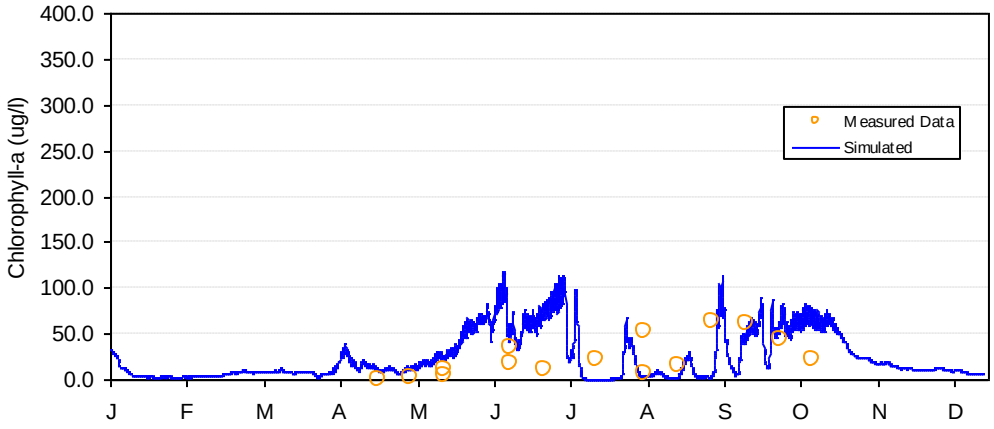

Figure E-59. Chlorophyll-a calibration results for Lake Ewauna—Klamath River at Keno Bridge (Hwy 66) (2002).

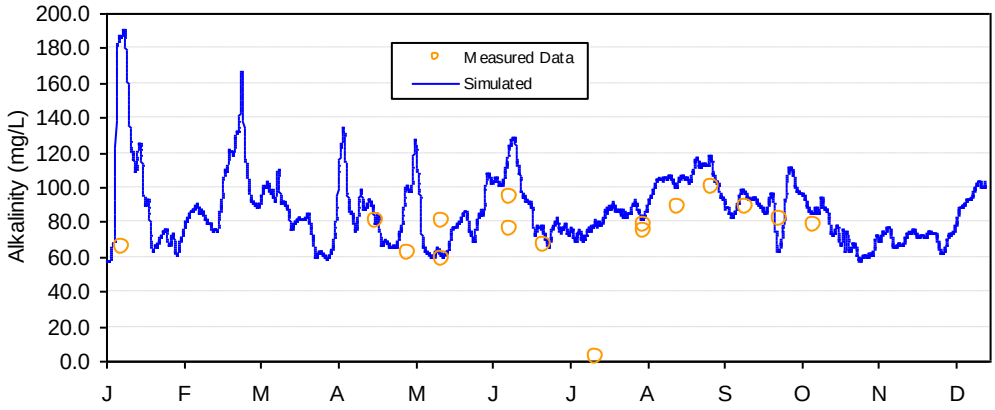

Figure E-60. Alkalinity calibration results for Lake Ewauna—Klamath River at Keno Bridge (Hwy 66) (2002).

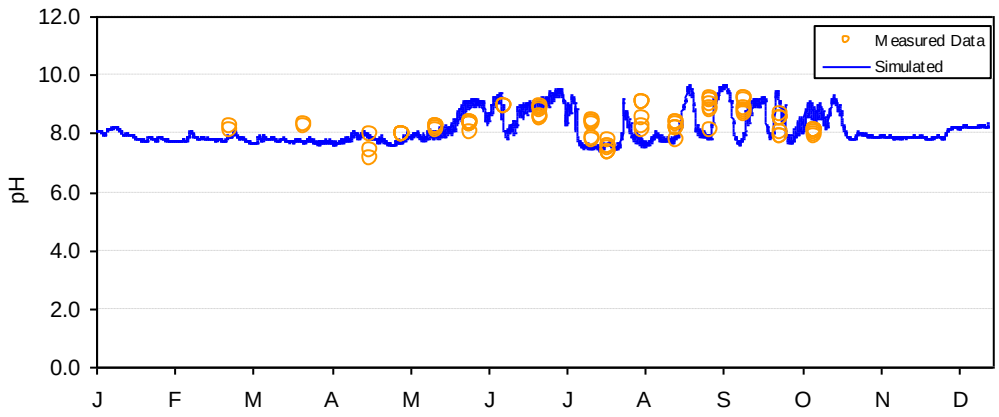

Figure E-61. pH calibration results for Lake Ewauna—Klamath River at Keno Bridge (Hwy 66) 2002).

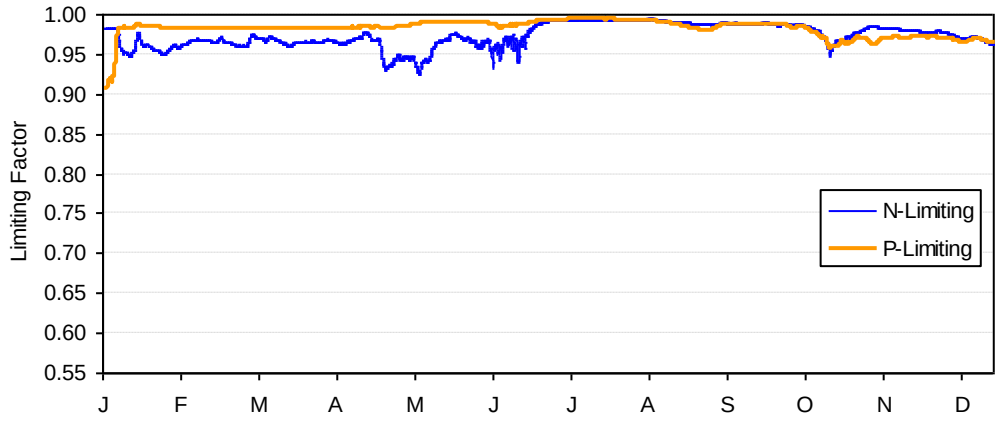

Figure E-62. Simulated Nutrient Limiting Condition—Klamath River at Keno Bridge (Hwy 66) 2000.

Table E-1. Calibration error statistics for Lake Ewauna

Parameter	MES	AME	Data Type	Unit
MILLER ISLAND (2000)				
CHLA	-24.08	43.85	Grab	ug/L
DO	-0.45	1.95	Continuous	mg/L
NH4	-0.09	0.24	Grab	mg/L
NO3	0.50	0.56	Grab	mg/L
pH	-0.11	0.58	Continuous	
pH	-0.47	1.06	Grab	
PO4	-0.04	0.05	Grab	mg/L
Temperature	0.15	1.11	Continuous	deg C
HWY 66 (2000)				

CHLA	-14.85	22.09	Grab	ug/L
DO	-0.83	2.33	Continuous	mg/L
NH4	-0.08	0.33	Grab	mg/L
NO3	0.14	0.37	Grab	mg/L
pH	-0.35	0.60	Continuous	
pH	-0.03	0.54	Grab	
PO4	-0.04	0.09	Grab	mg/L
Temperature	0.15	1.06	Continuous	deg C

Table E-2. Corroboration error statistics for Lake Ewauna

Parameter	MES	AME	Data Type	Unit
MILLER ISLAND (2002)				
CHLA	-13.07	24.12	Grab	ug/L
DO	0.58	1.74	Continuous	mg/L
DO	0.40	2.82	Grab	mg/L
NH4	0.02	0.17	Grab	mg/L
NO3	0.00	0.12	Grab	mg/L
pH	0.09	0.58	Continuous	
PO4	0.00	0.06	Grab	mg/L
Temperature	0.11	0.99	Continuous	deg C
Temperature	-0.14	1.24	Grab	deg C
HWY 66 (2002)				
NH4	-0.08	0.22	Grab	mg/L
NO3	0.08	0.22	Grab	mg/L
PO4	-0.01	0.07	Grab	mg/L
CHLA	-7.07	26.25	Grab	ug/L
DO	0.20	2.59	Grab	mg/L
Temp	-0.90	1.63	Grab	deg C
pH	0.17	0.57	Grab	
Temp	-0.29	0.94	Continuous	deg C
DO	0.65	1.69	Continuous	mg/L

Appendix F

Calibration Results for Keno Dam to J. C. Boyle Reservoir (Modeling Segment 3)

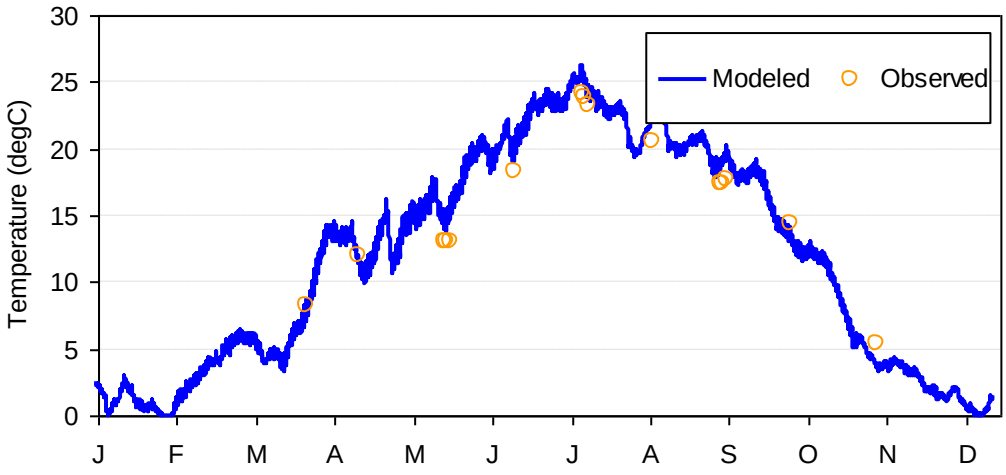

Figure F-1. Temperature calibration results for Klamath River downstream of Keno Dam (2002).

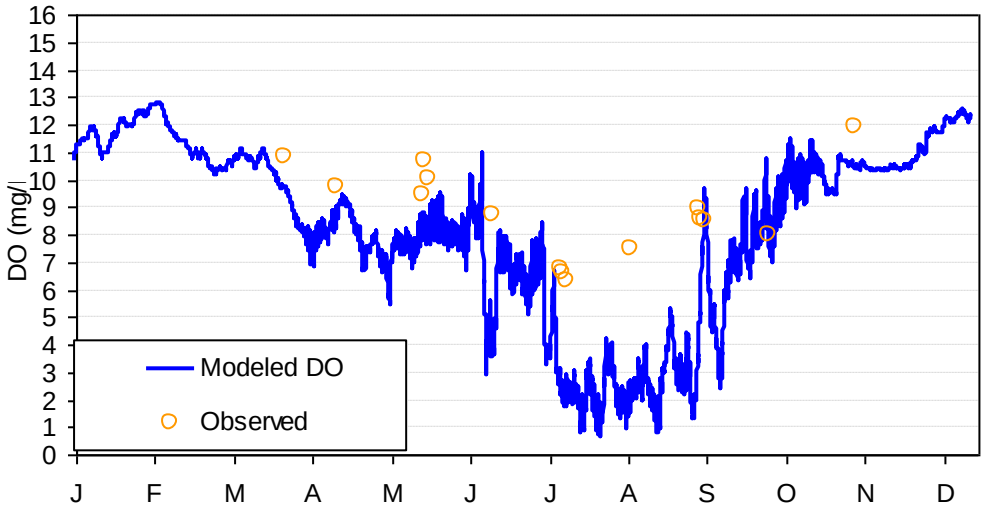

Figure F-2. Dissolved oxygen calibration results for Klamath River downstream of Keno Dam (2002).

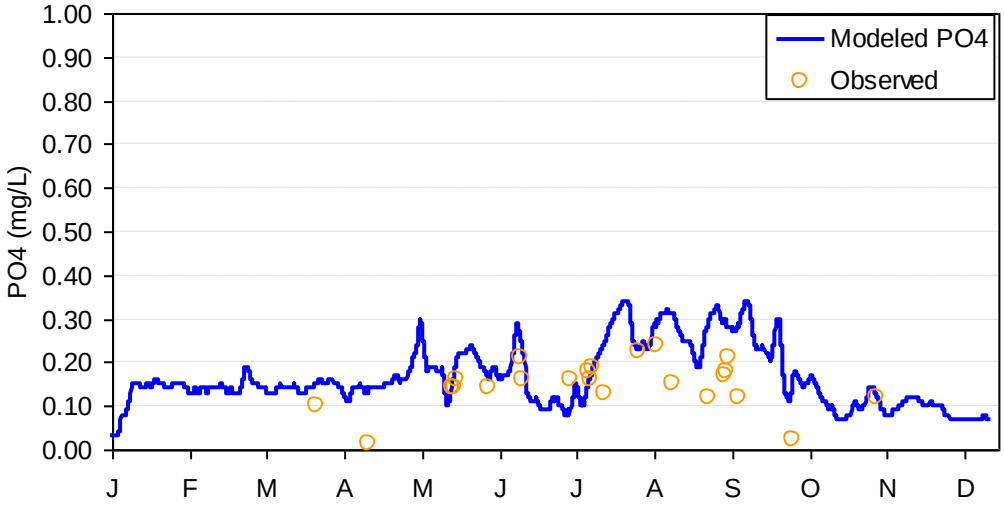

Figure F-3. PO_4 calibration results for Klamath River downstream of Keno Dam (2002).

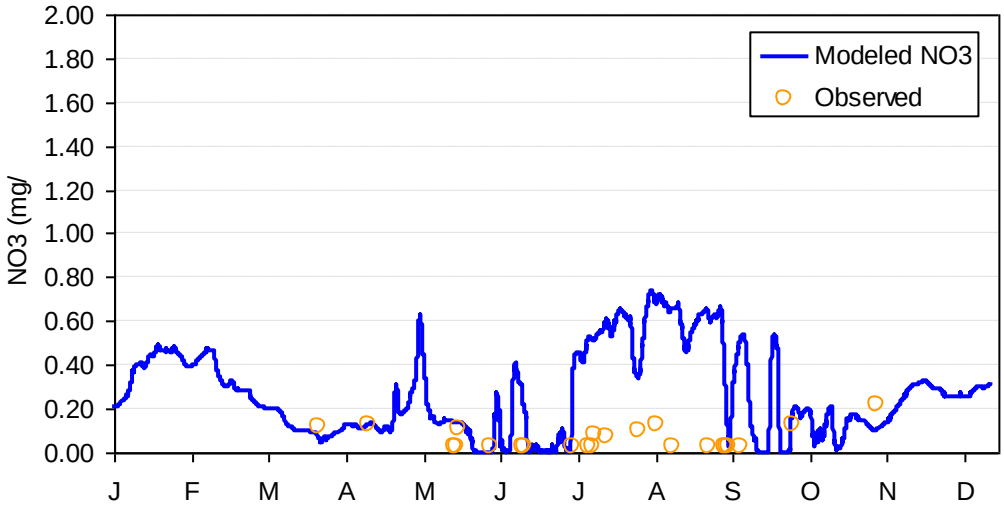

Figure F-4. NO_3 calibration results for Klamath River downstream of Keno Dam (2002).

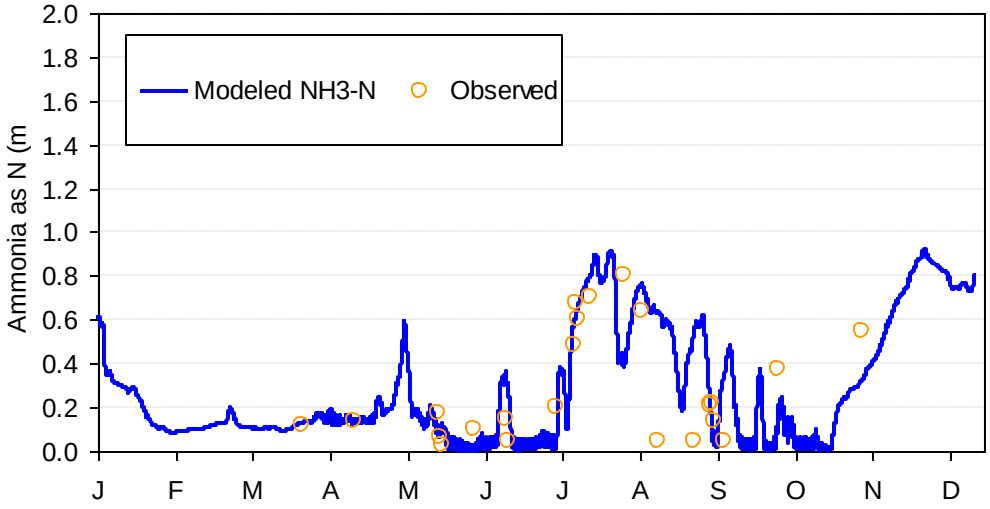

Figure F-5. NH_4-N calibration results for Klamath River downstream of Keno Dam (2002).

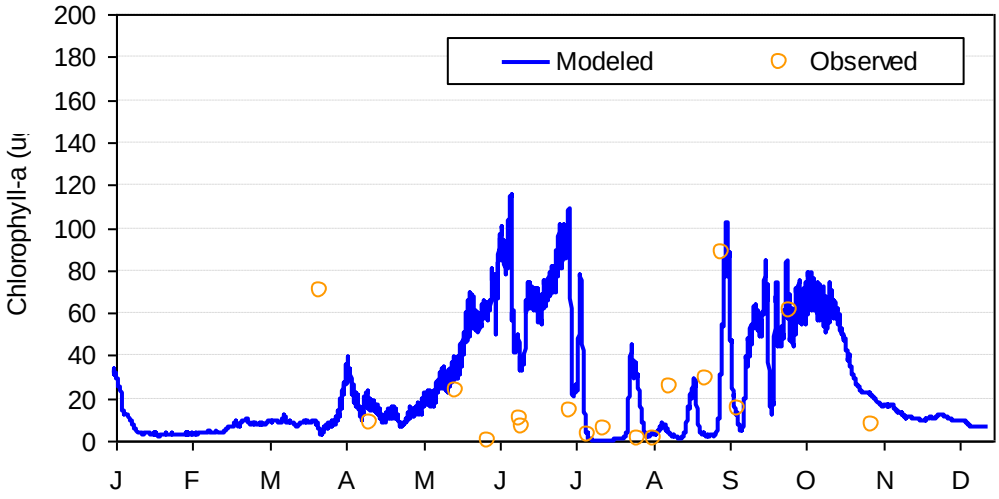

Figure F-6. Chlorophyll *a* calibration results for Klamath River downstream of Keno Dam (2002).

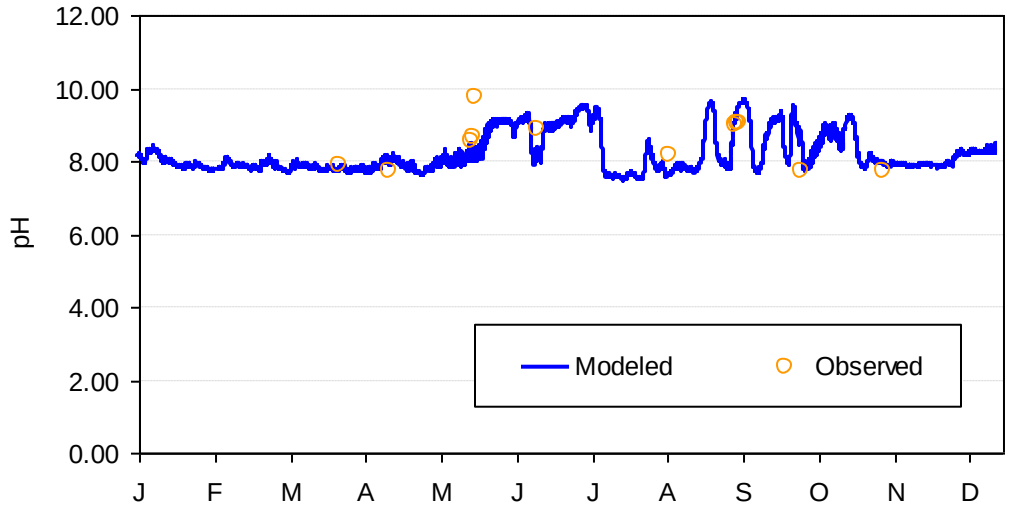

Figure F-7. pH calibration results for Klamath River downstream of Keno Dam (2002).

Appendix G

Calibration Results for J.C. Boyle Reservoir (Modeling Segment 4)

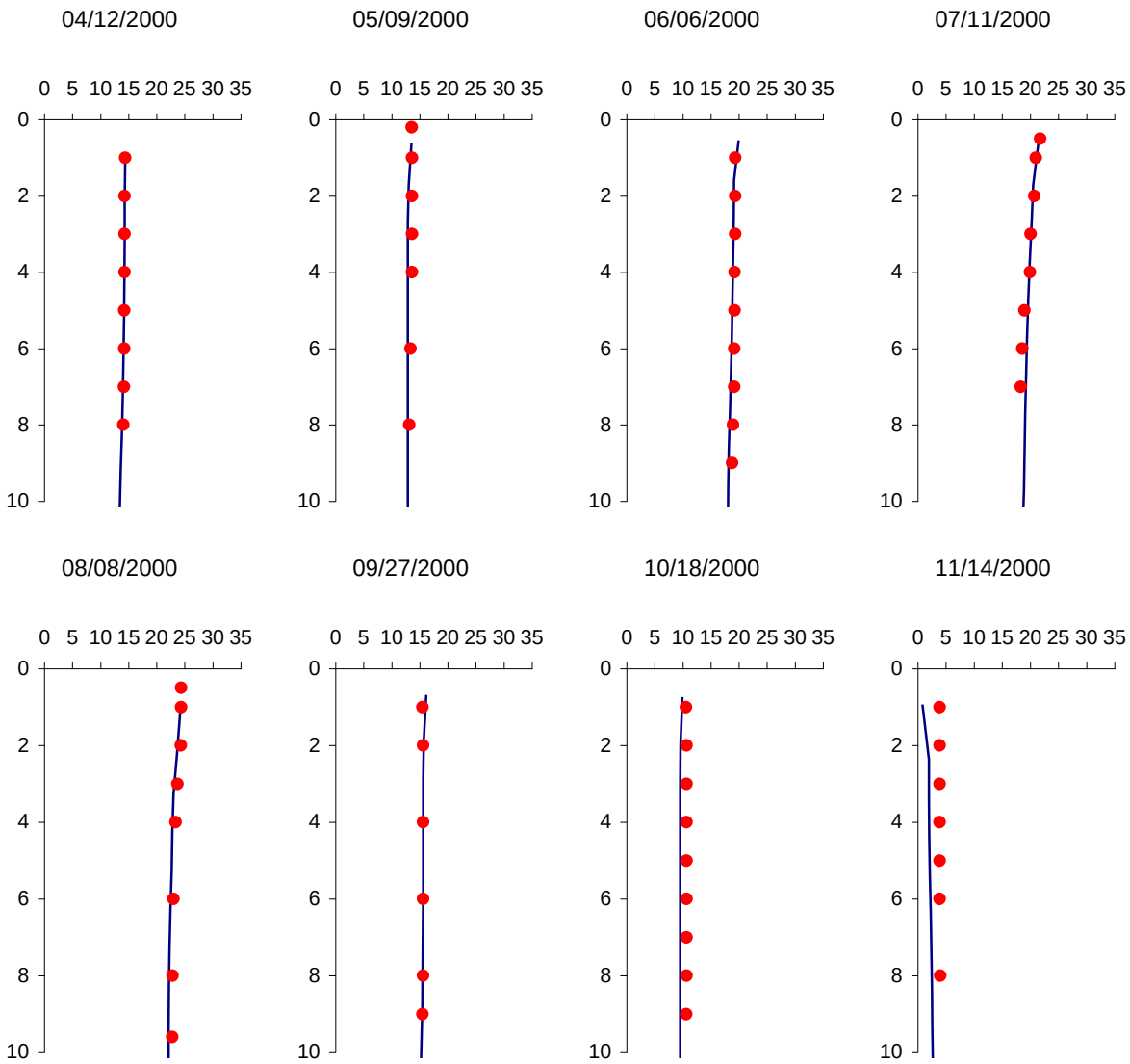

Figure G-1. Temperature profile calibration results at J.C. Boyle Reservoir at deepest point - 2000 [X-axis Temperature (degC) vs. Y-axis Depth (m)].

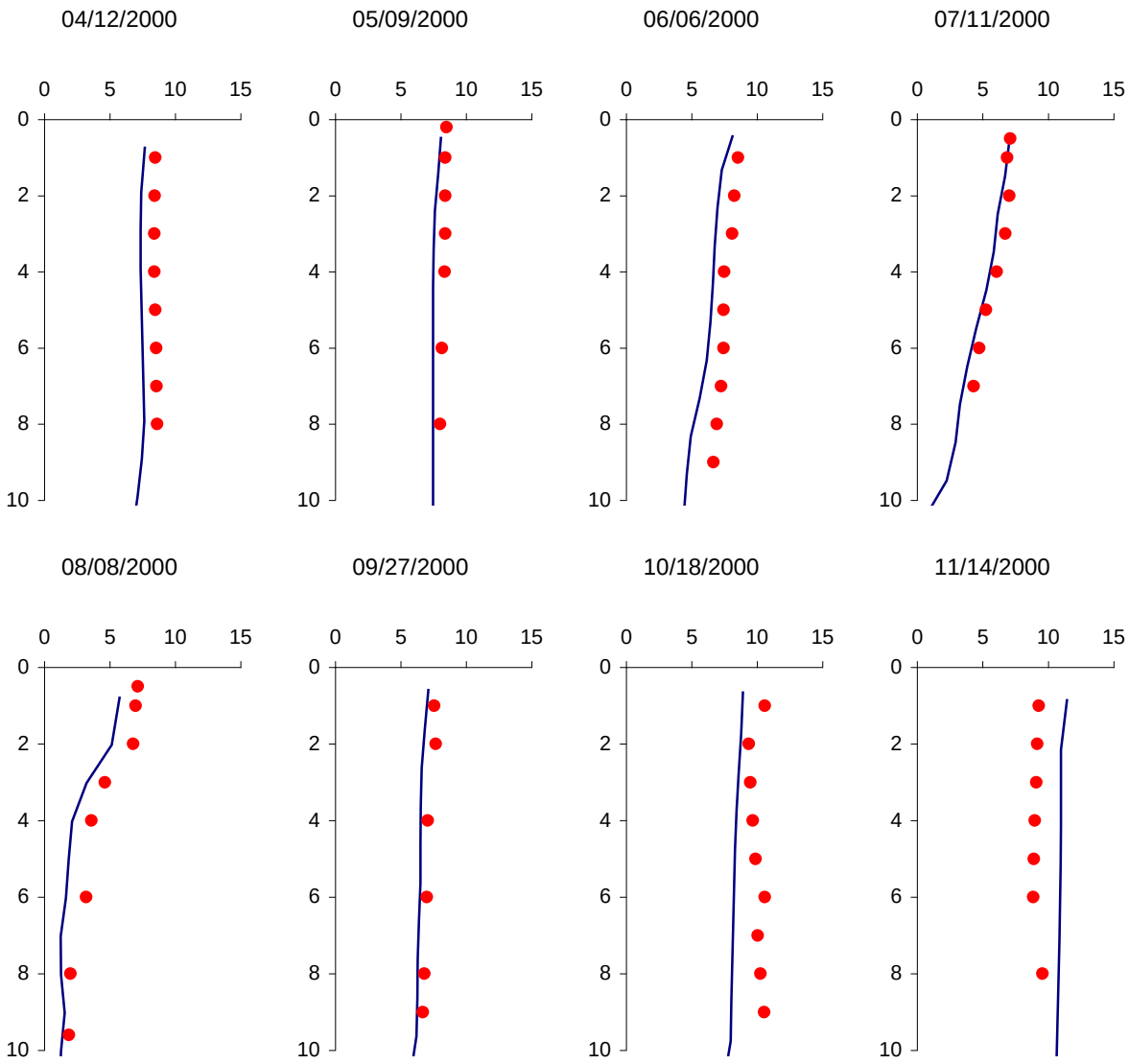

Figure G-2. Dissolved oxygen profile calibration results at J.C. Boyle Reservoir at deepest point - 2000 [(X-axis Dissolved oxygen (mg/L) vs. Y-axis Depth (m)].

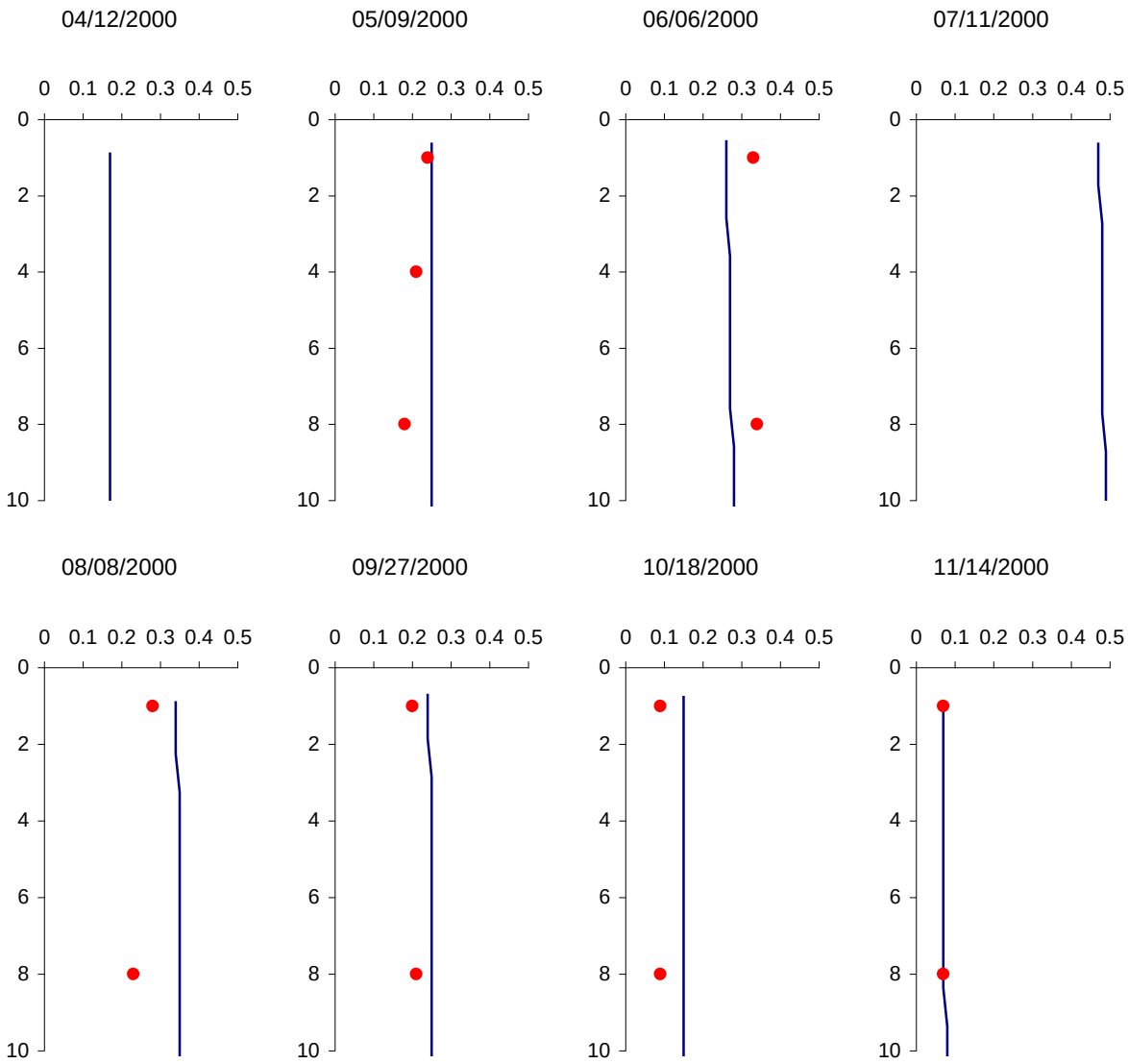

Figure G-3. PO_4 profile calibration results at J.C. Boyle Reservoir at deepest point - 2000 [(X-axis PO_4 (mg/L) vs. Y-axis Depth (m)].

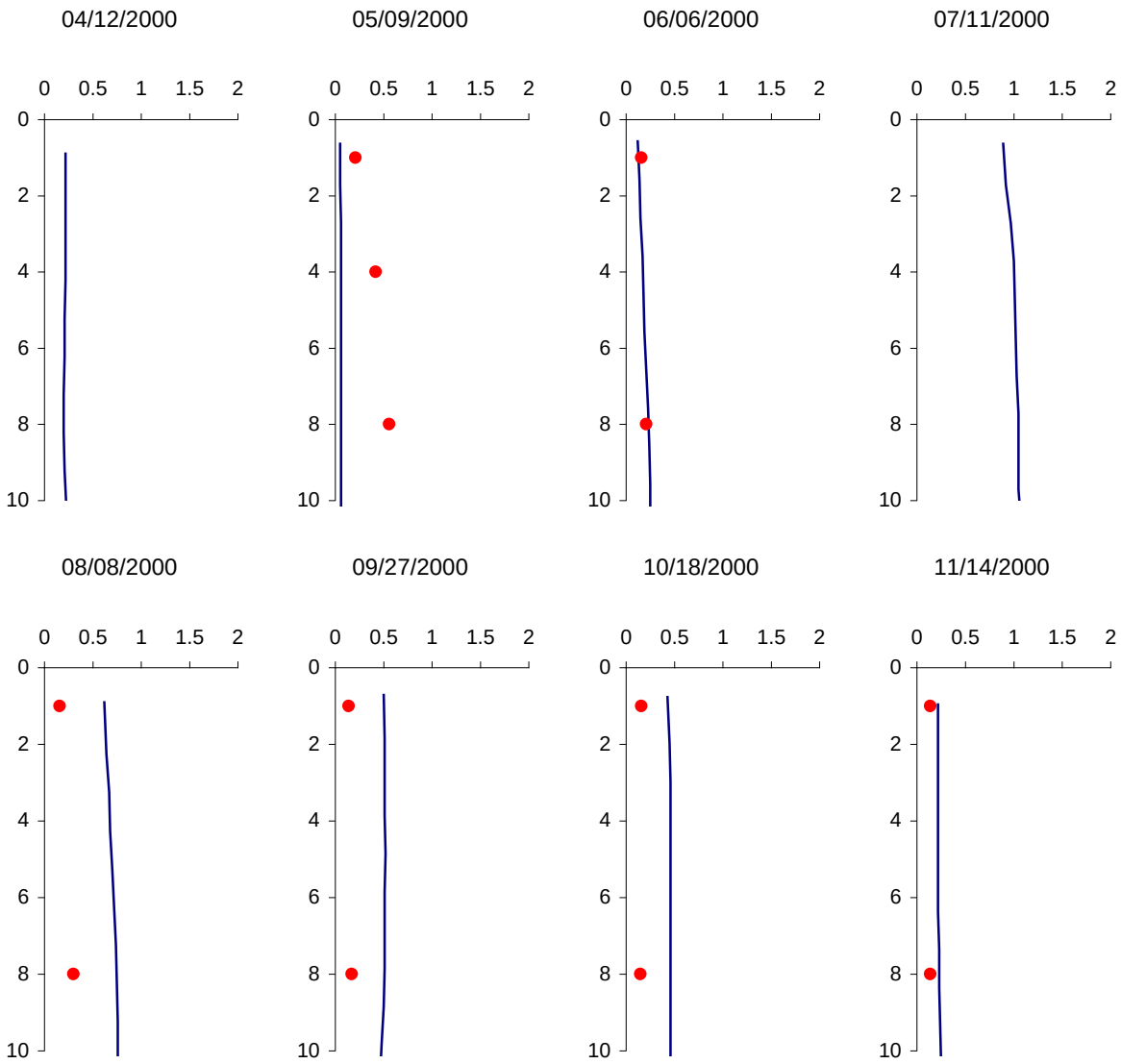

Figure G-4. NH_4 profile calibration results at J.C. Boyle Reservoir at deepest point - 2000 [(X-axis NH_4 (mg/L) vs. Y-axis Depth (m)].

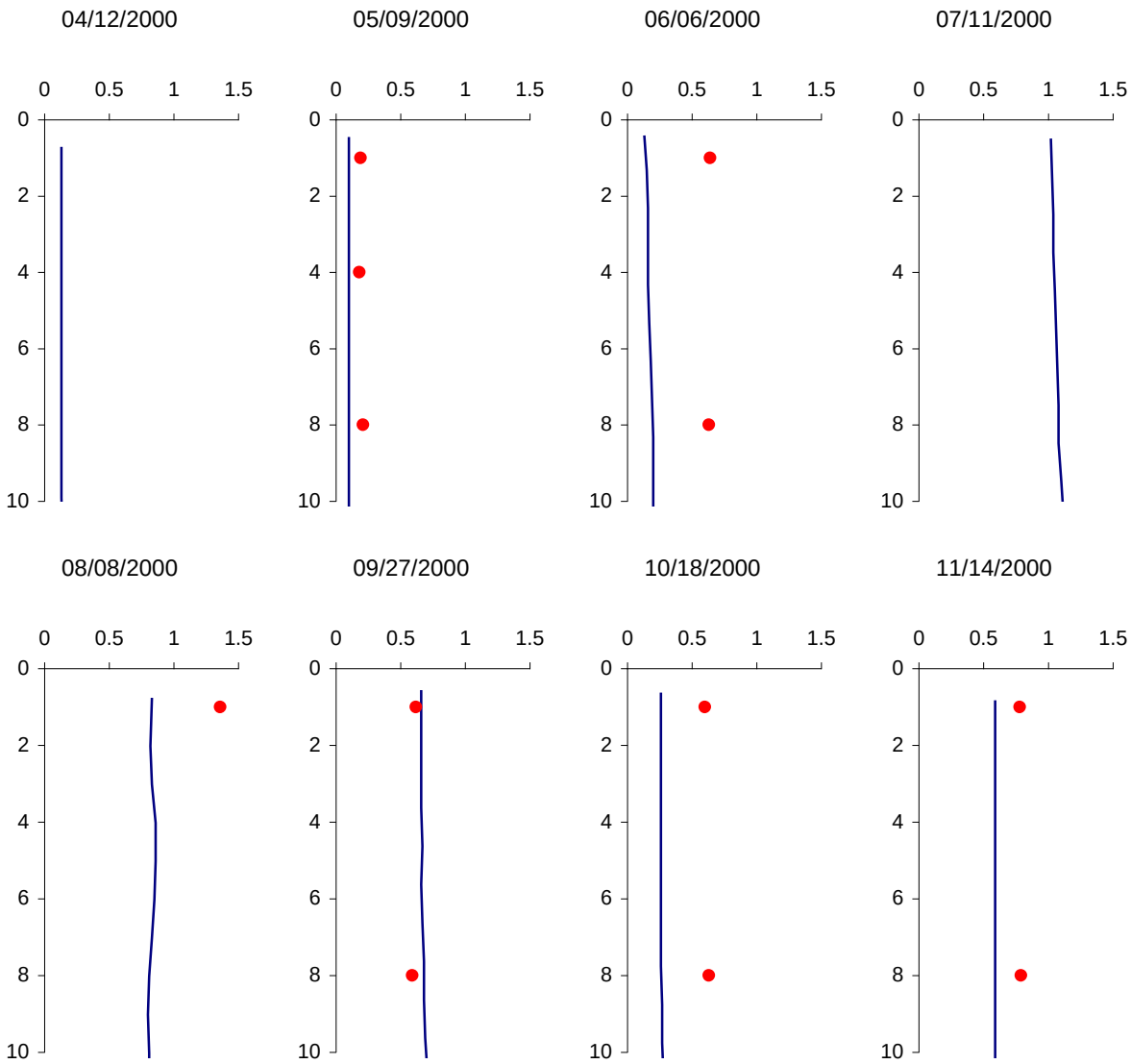

Figure G-5. NO_3 profile calibration results at J.C. Boyle Reservoir at deepest point - 2000 [(X-axis NO_3 (mg/L) vs. Y-axis Depth (m)].

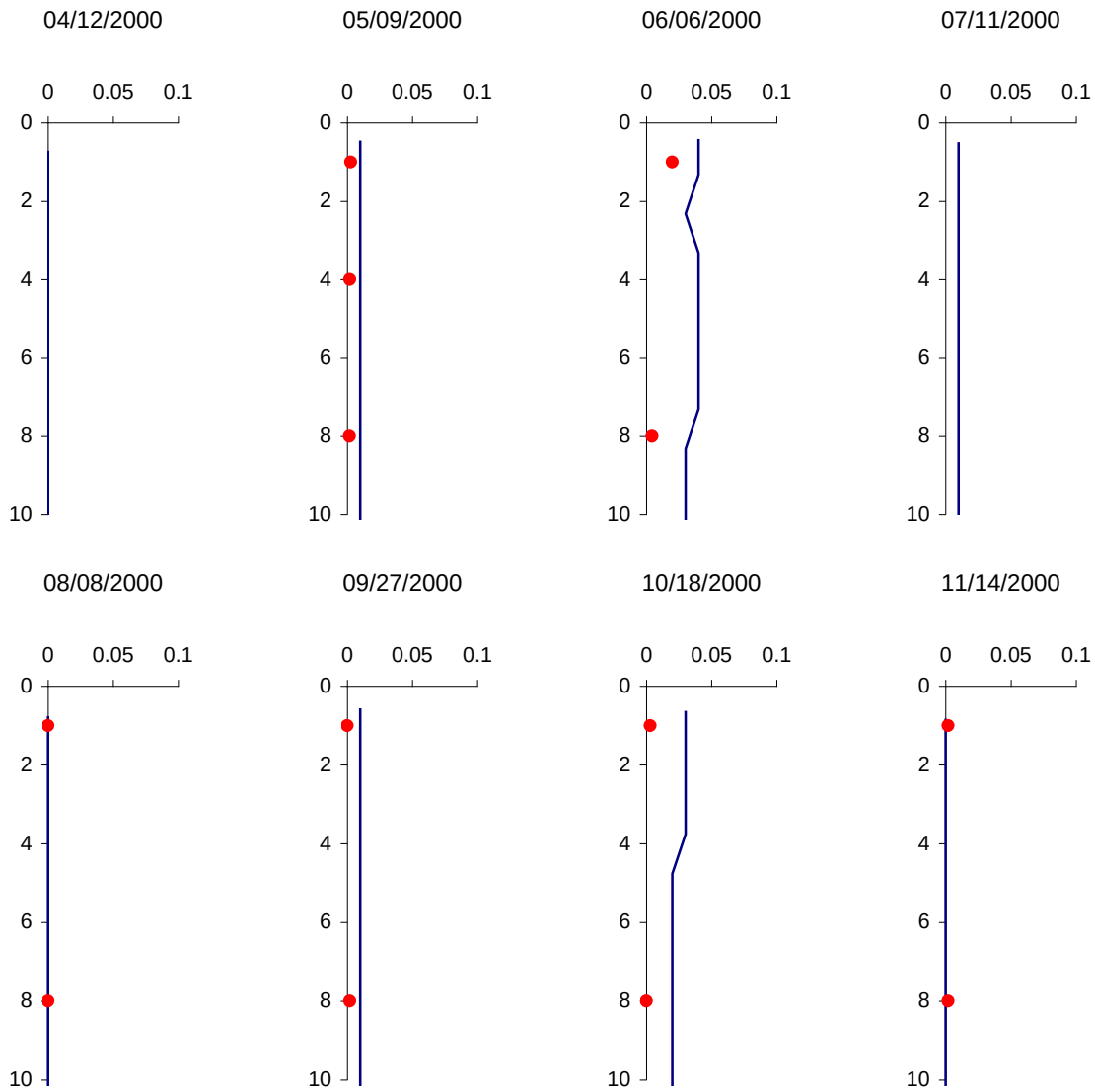

Figure G-6. Chlorophyll-a profile calibration results at J.C. Boyle Reservoir at deepest point - 2000 [(X-axis Chlorophyll-a (mg/L) vs. Y-axis Depth (m)].

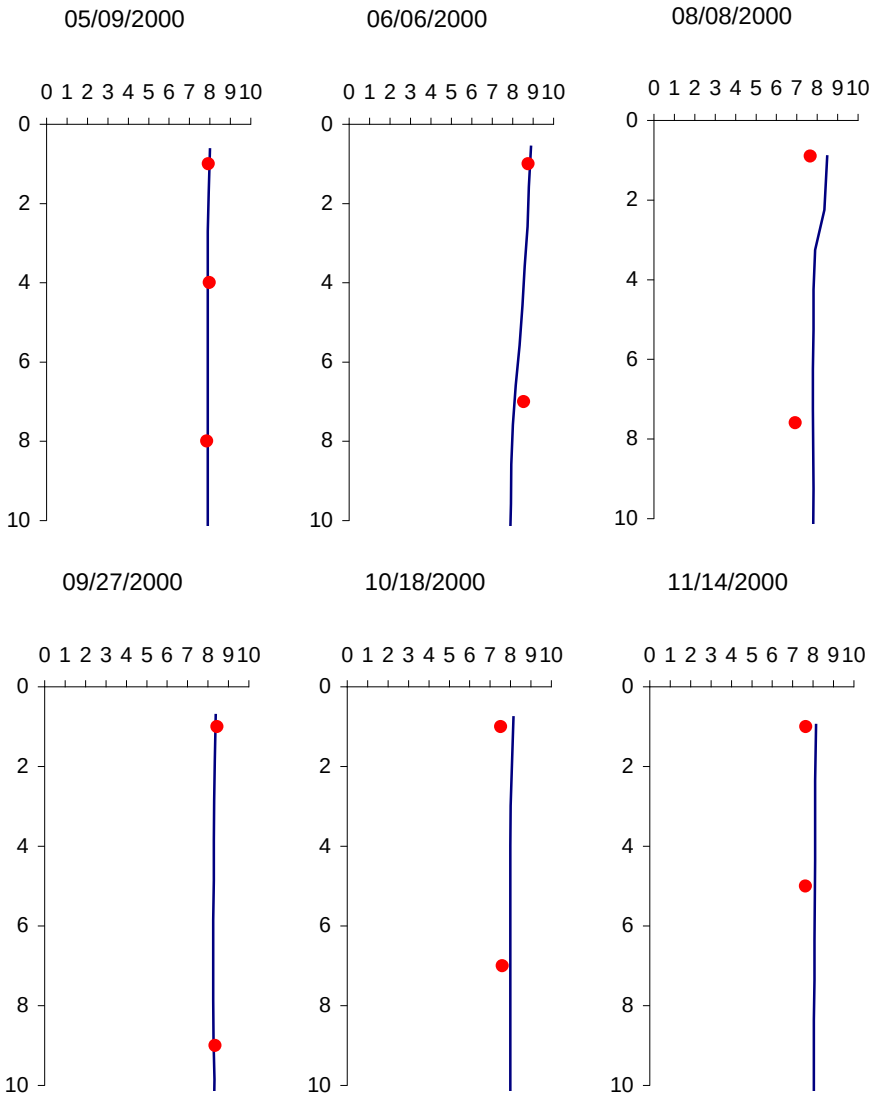

Figure G-7. pH profile calibration results at J.C. Boyle Reservoir at deepest point - 2000 [(X-axis pH vs. Y-axis Depth (m)].

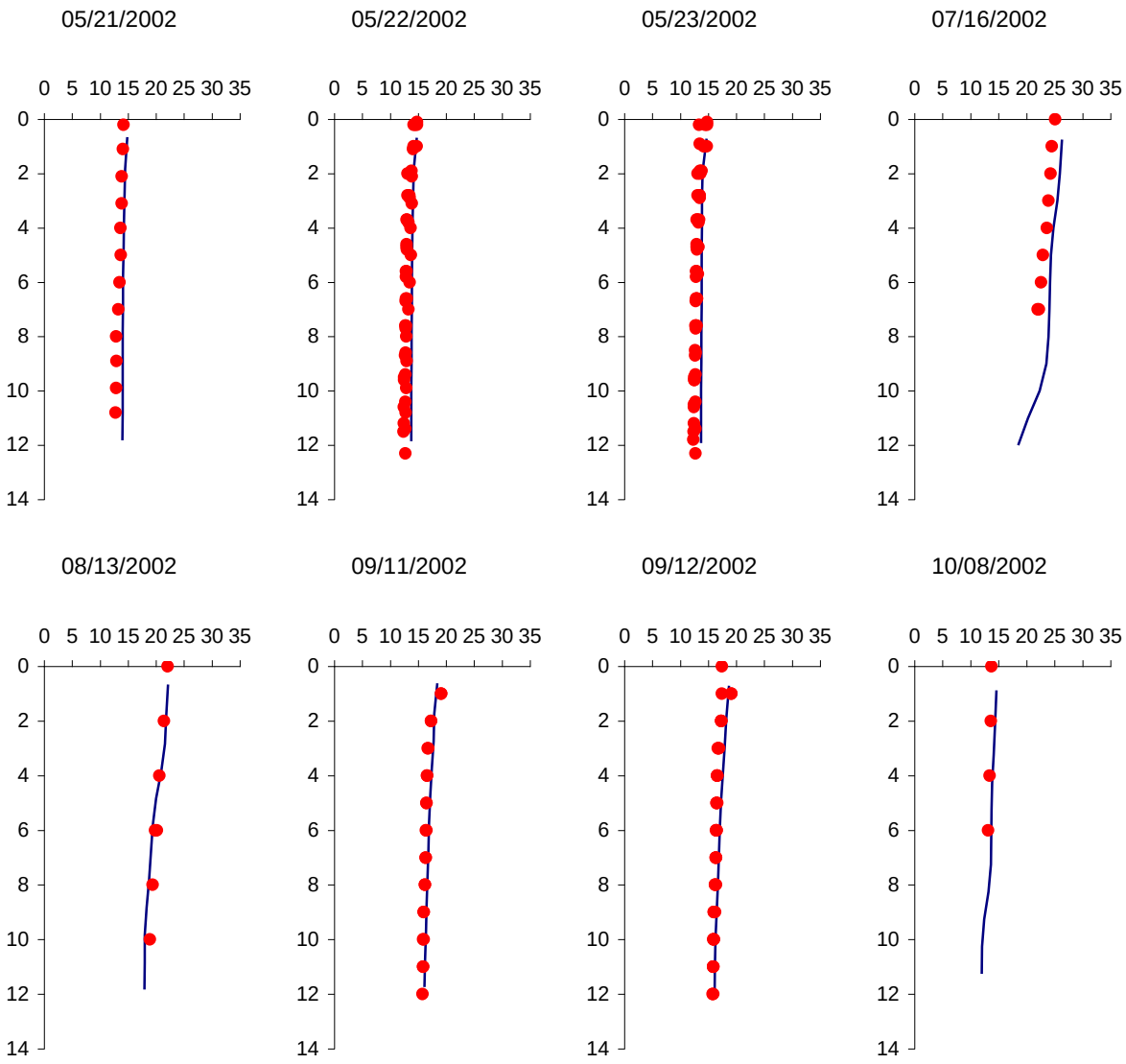

Figure G-8. Temperature profile calibration results at J.C. Boyle Reservoir at deepest point - 2002 [(X-axis Temperature (degC) vs. Y-axis Depth (m)].

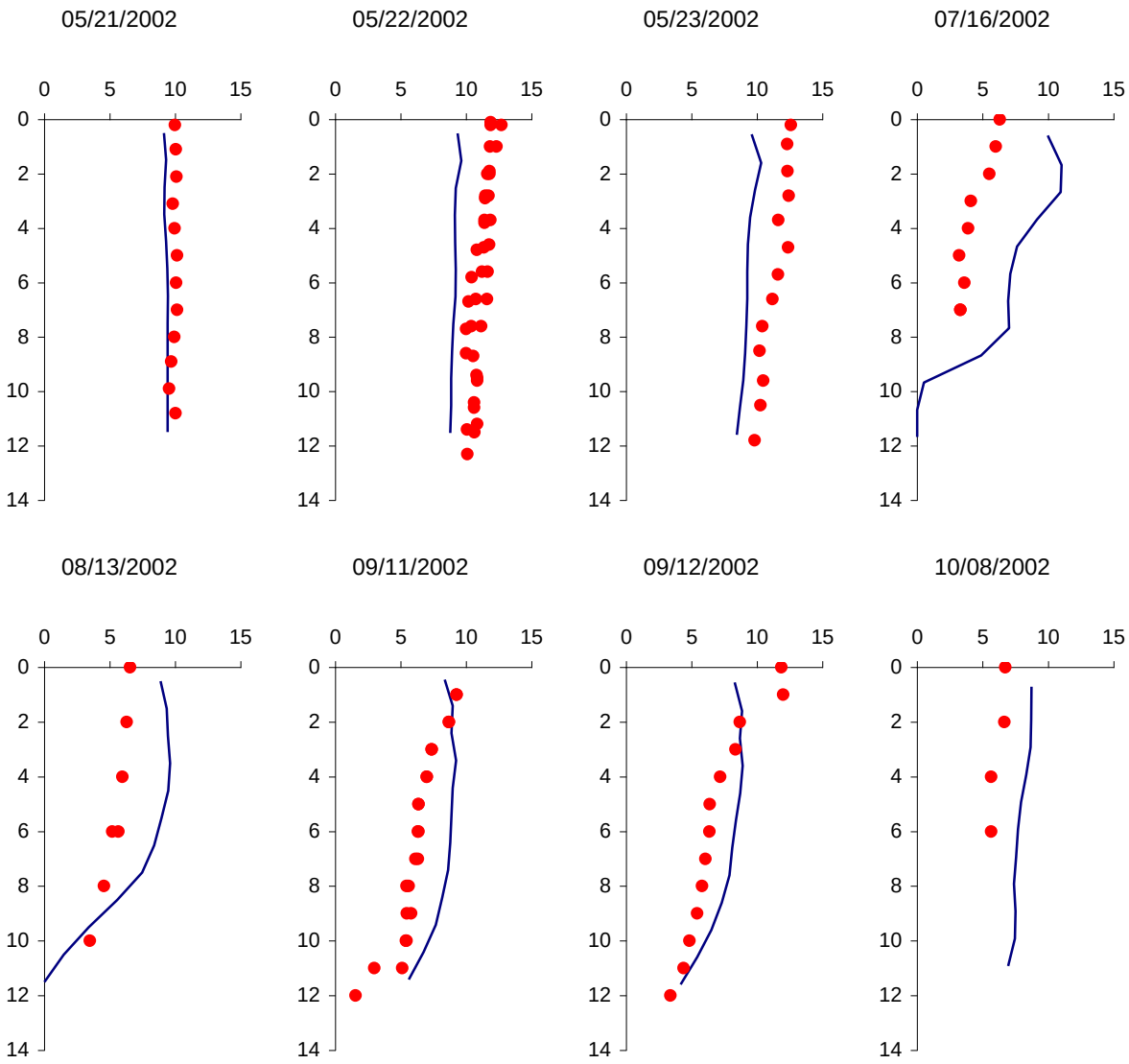

Figure G-9. Dissolved oxygen profile calibration results at J.C. Boyle Reservoir at deepest point - 2002 [(X-axis Dissolved oxygen (mg/L) vs. Y-axis Depth (m)].

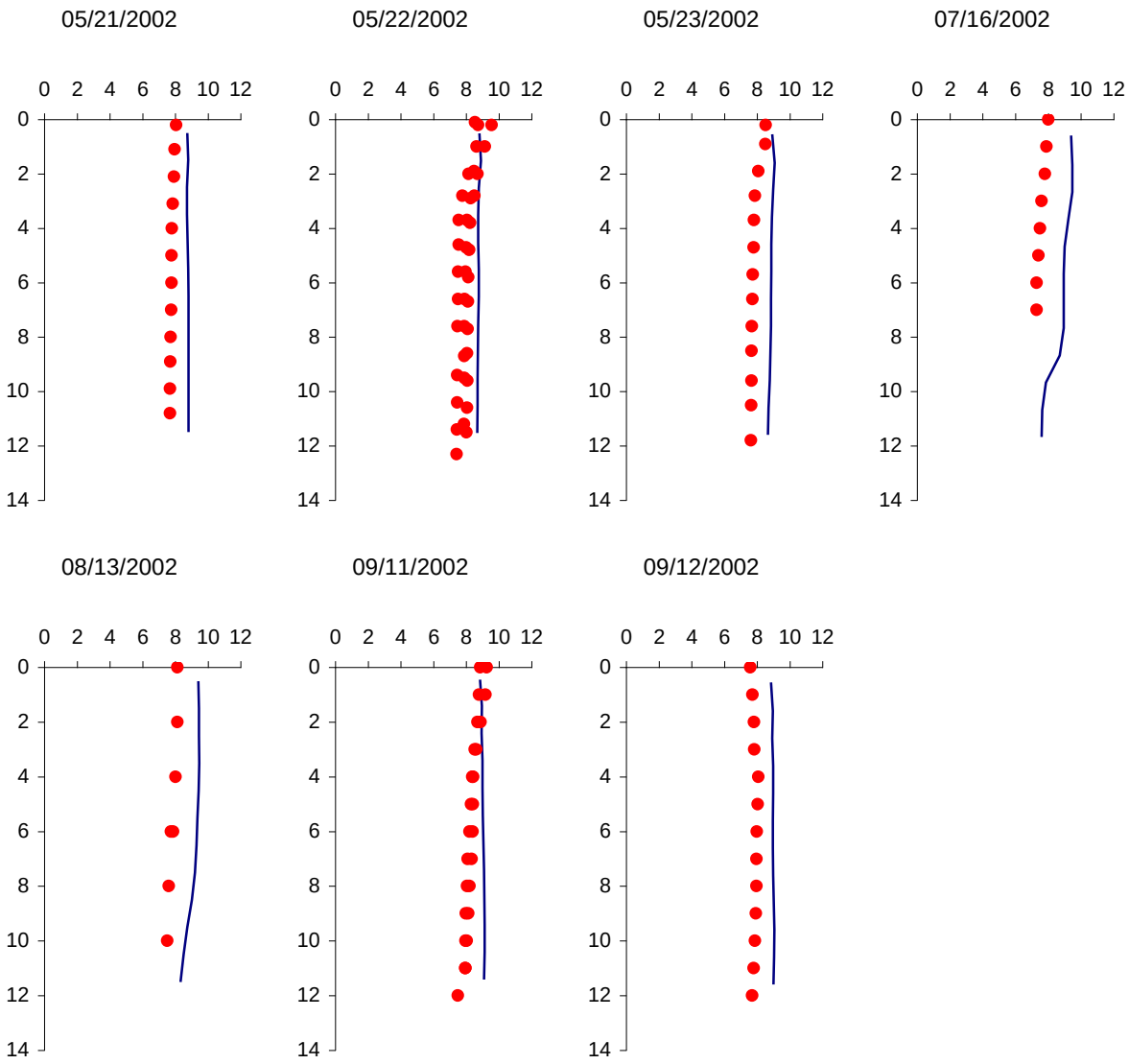

Figure G-10. pH profile calibration results at J.C. Boyle Reservoir at deepest point - 2002 [(X-axis pH vs. Y-axis Depth (m)].

Appendix H

Calibration Results for Bypass/Full Flow Reach (Modeling Segment 5)

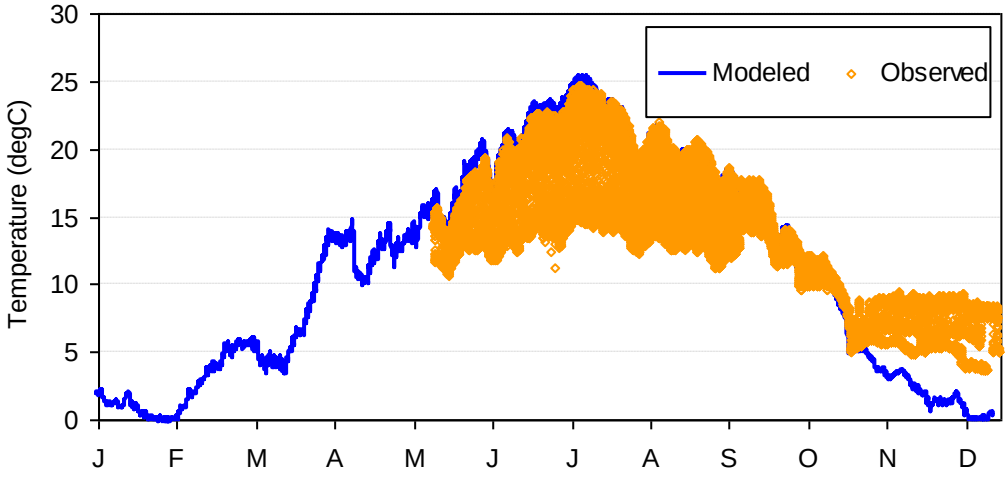

Figure H-1. Temperature calibration results for Klamath River downstream of J. C. Boyle Dam (2002).

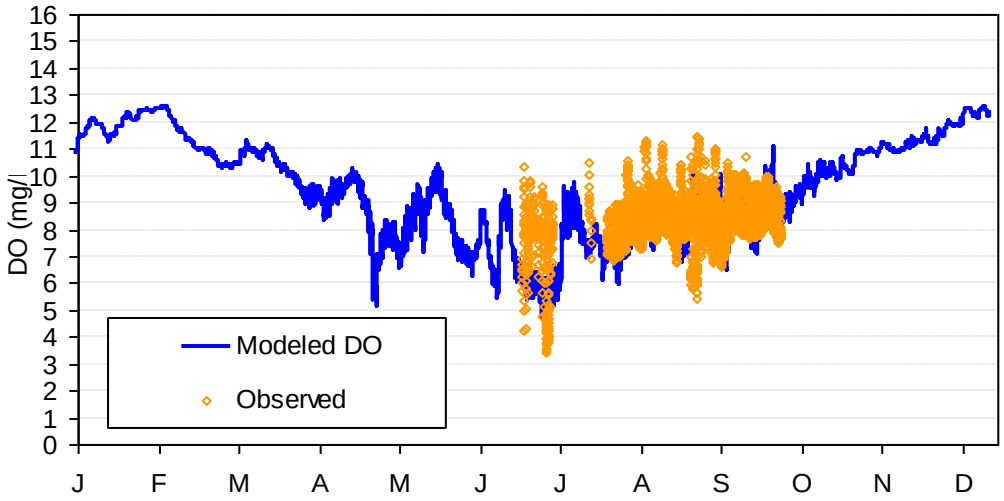

Figure H-2. Dissolved oxygen calibration results for Klamath River downstream of J. C. Boyle Dam (2002).

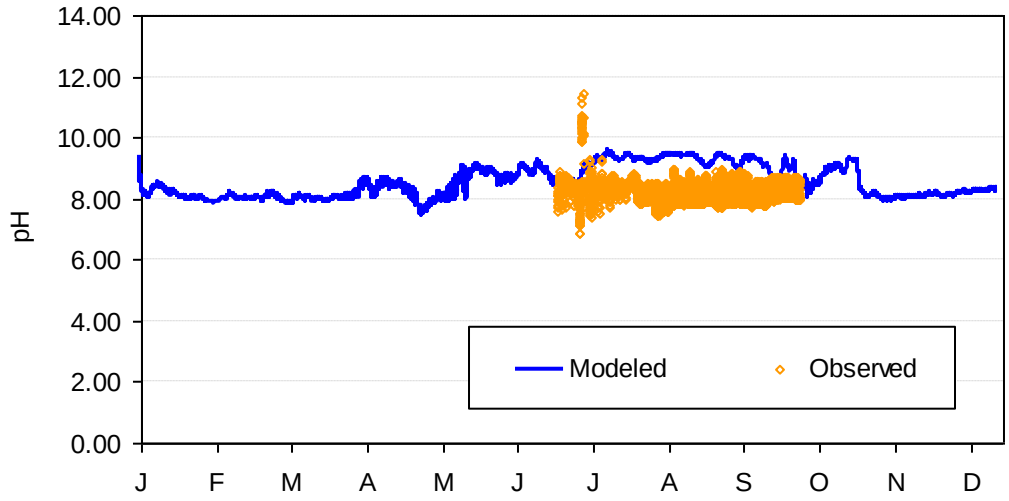

Figure H-3. pH calibration results for Klamath River downstream of J. C. Boyle Dam (2002).

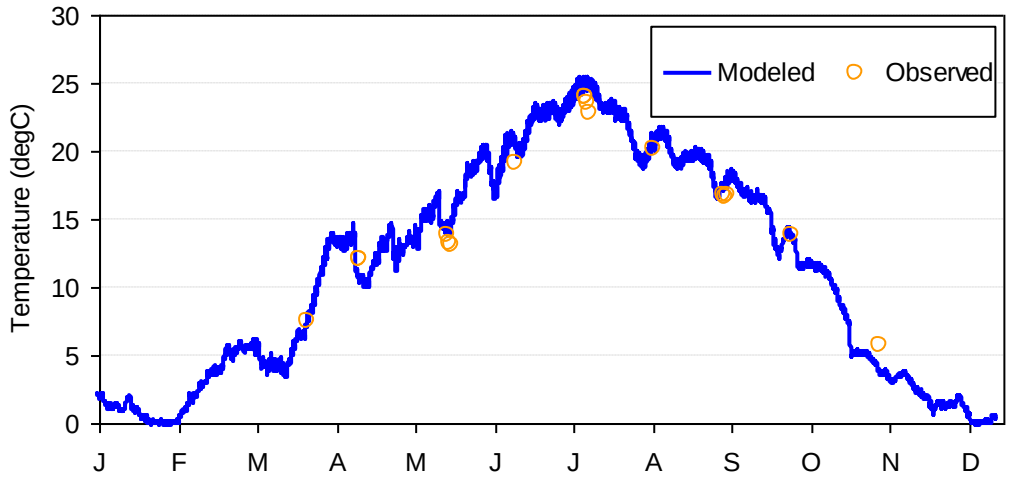

Figure H-4. Temperature calibration results for Klamath River below J. C. Boyle Dam – KR2 (2002).

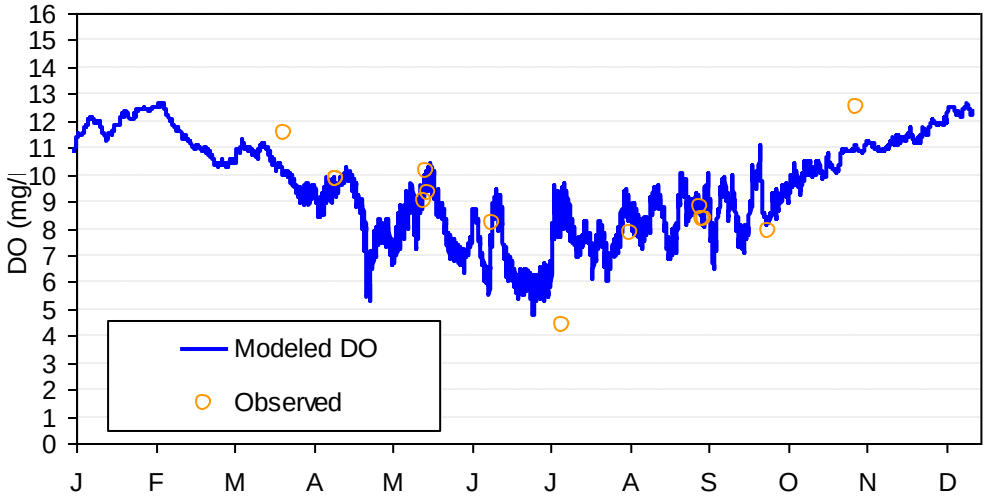

Figure H-5. Dissolved oxygen calibration results for Klamath River below J. C. Boyle Dam – KR2 (2002).

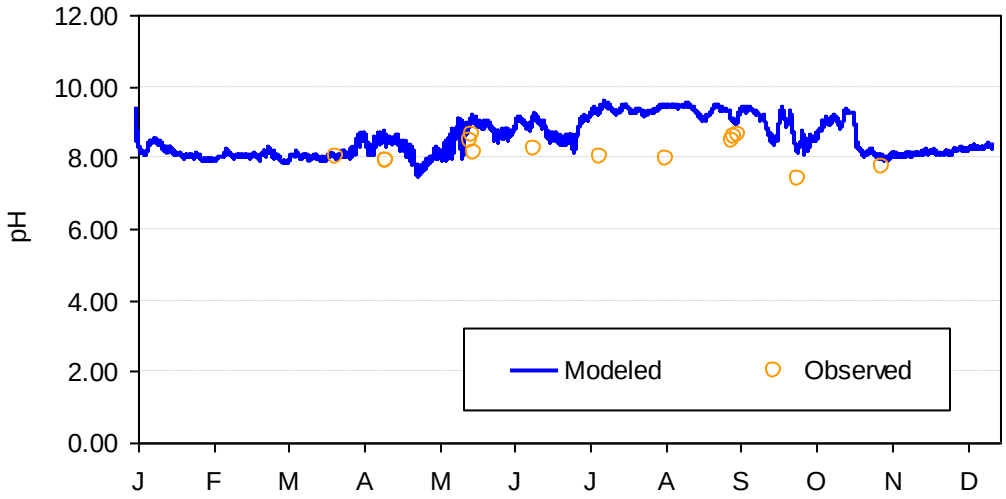

Figure H-6. pH calibration results for Klamath River below J. C. Boyle Dam – KR2 (2002).

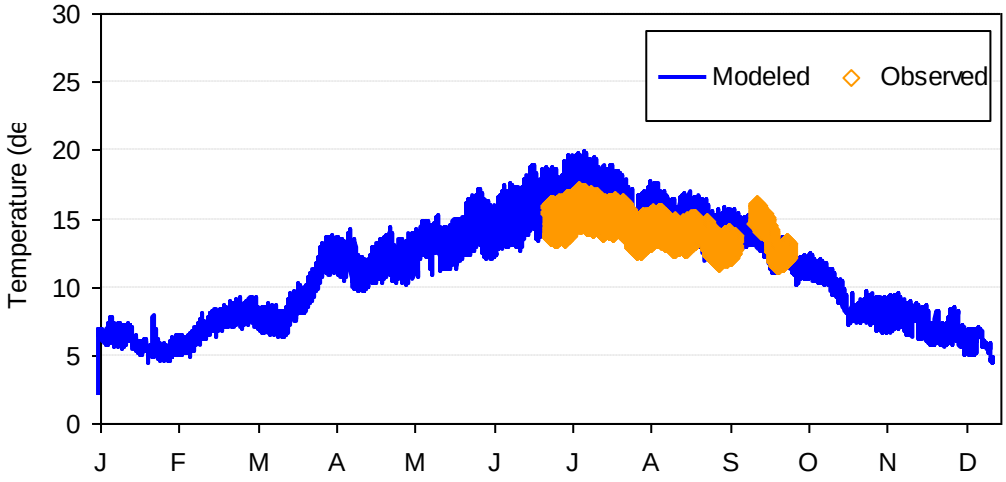

Figure H-7. Temperature calibration results for Klamath River upstream of J. C. Boyle Powerhouse tailrace (2002).

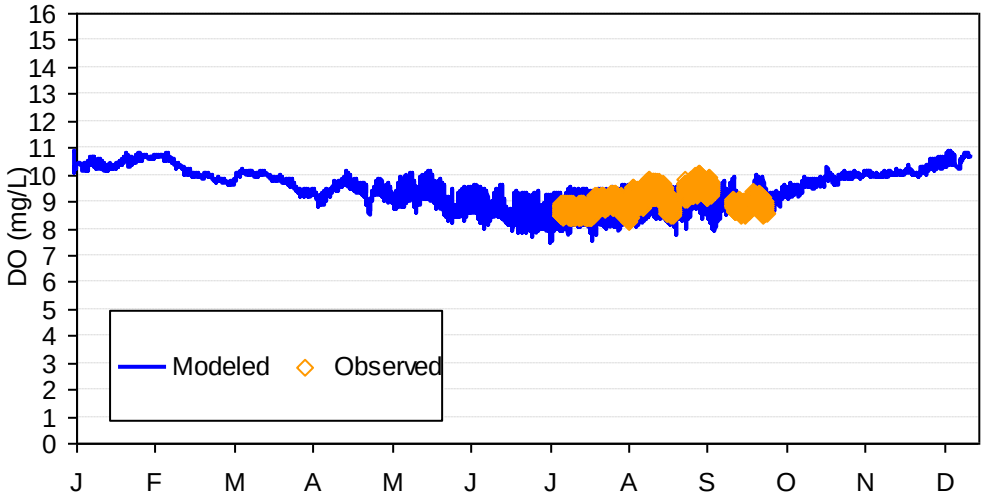

Figure H-8. Dissolved oxygen calibration results for Klamath River upstream of J. C. Boyle Powerhouse tailrace (2002).

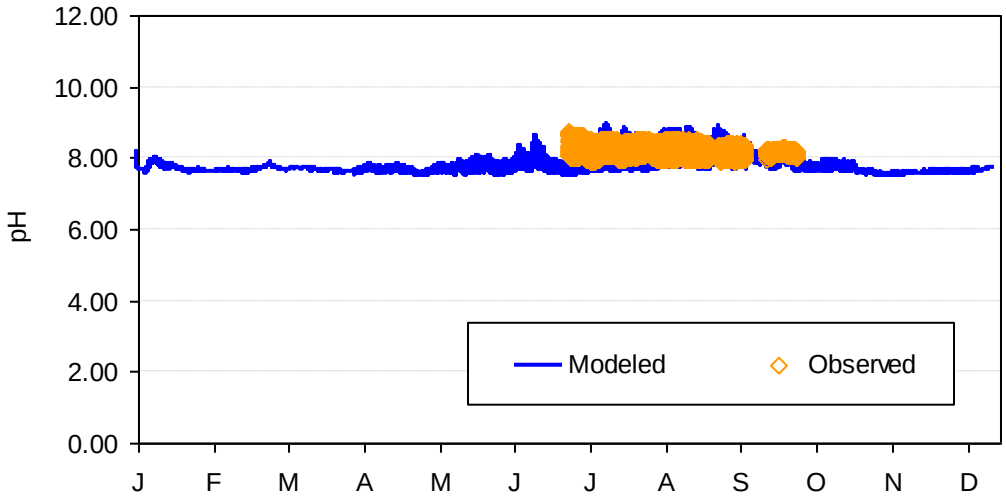

Figure H-9. pH calibration results for Klamath River upstream of J. C. Boyle Powerhouse tailrace (2002).

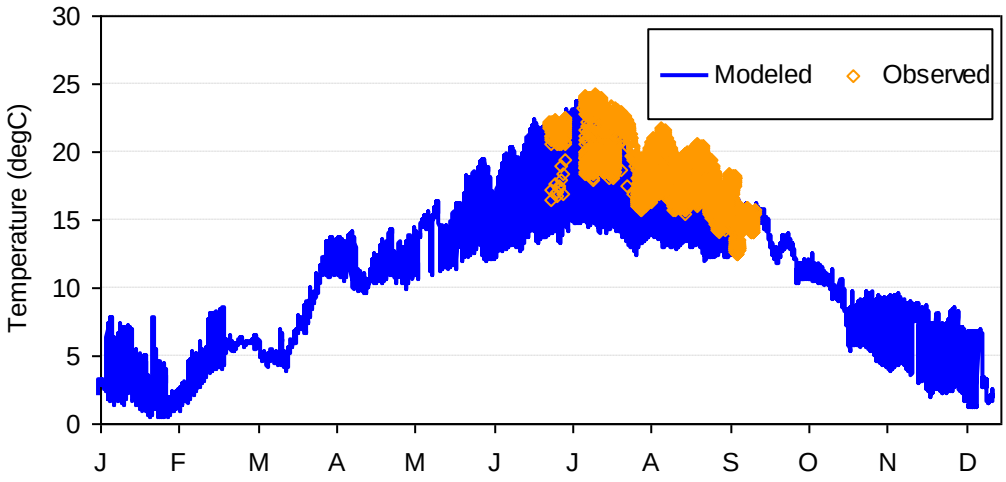

Figure H-10. Temperature calibration results for Klamath River downstream of big bend Powerhouse tailrace (2002).

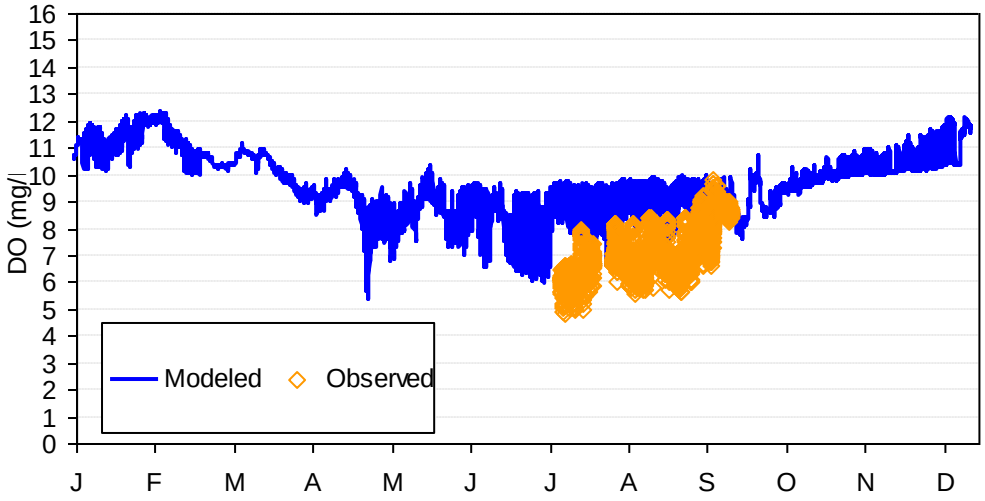

Figure H-11. Dissolved oxygen calibration results for Klamath River downstream of big bend Powerhouse tailrace (2002).

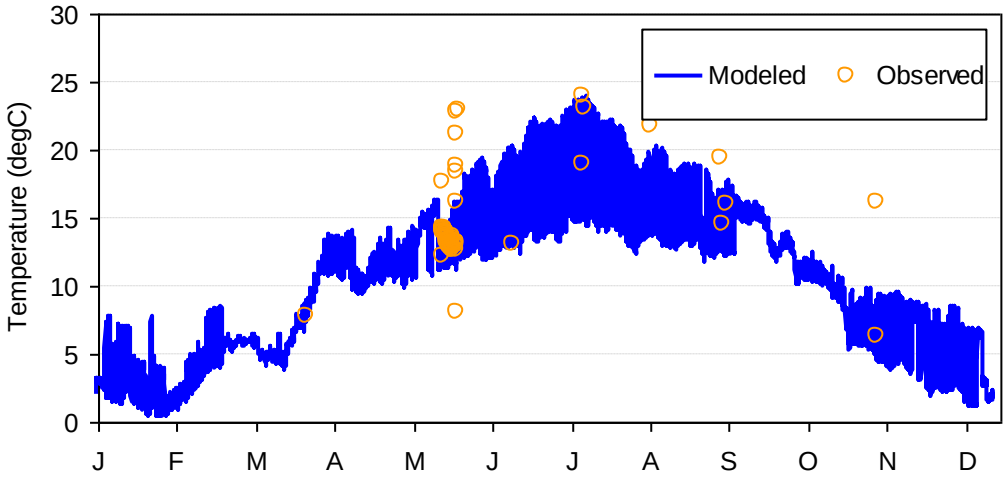

Figure H-12. Temperature calibration results for J. C. Boyle Powerhouse tailrace (2002).

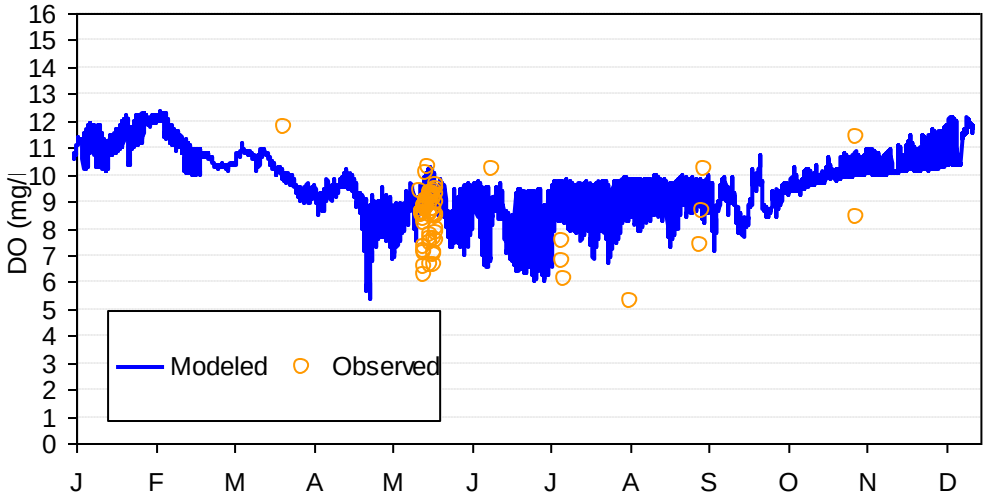

Figure H-13. Dissolved oxygen calibration results for J. C. Boyle Powerhouse tailrace (2002).

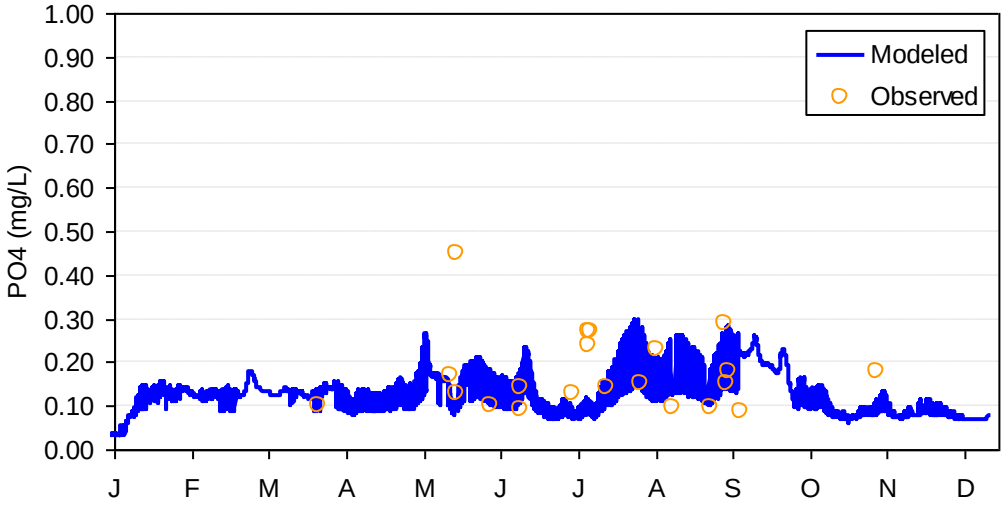

Figure H-14. PO_4 calibration results for J. C. Boyle Powerhouse tailrace (2002).

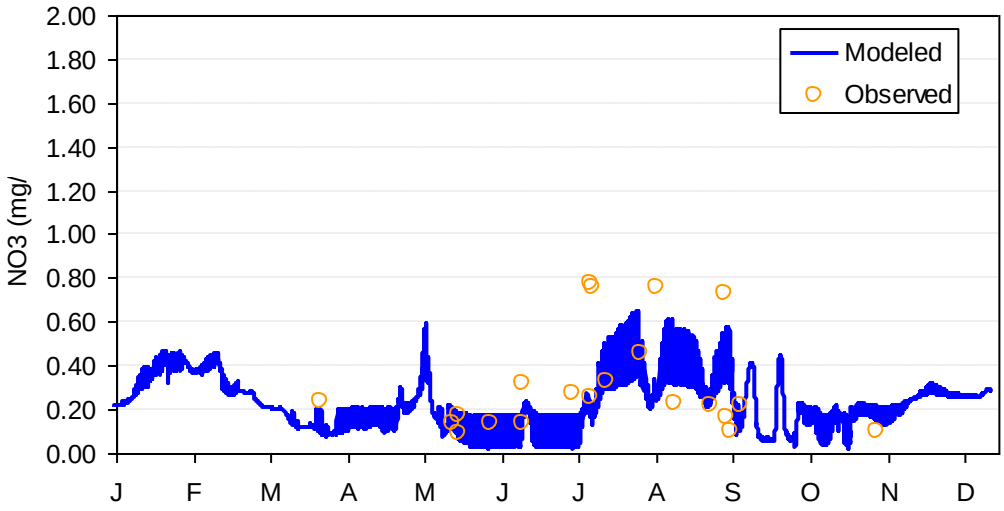

Figure H-15. NO_3 calibration results for J. C. Boyle Powerhouse tailrace (2002).

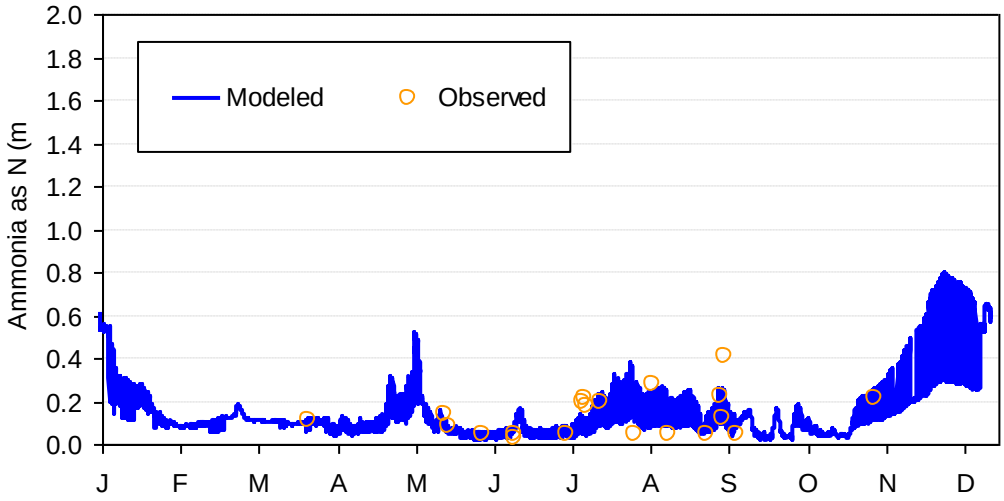

Figure H-16. NH_4-N calibration results for J. C. Boyle Powerhouse tailrace (2002).

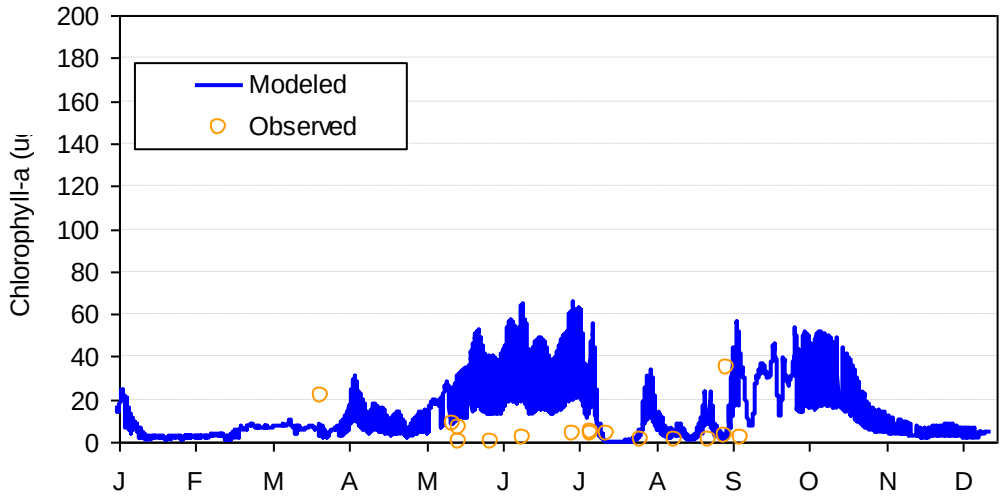

Figure H-17. Chlorophyll *a* calibration results for J. C. Boyle Powerhouse tailrace (2002).

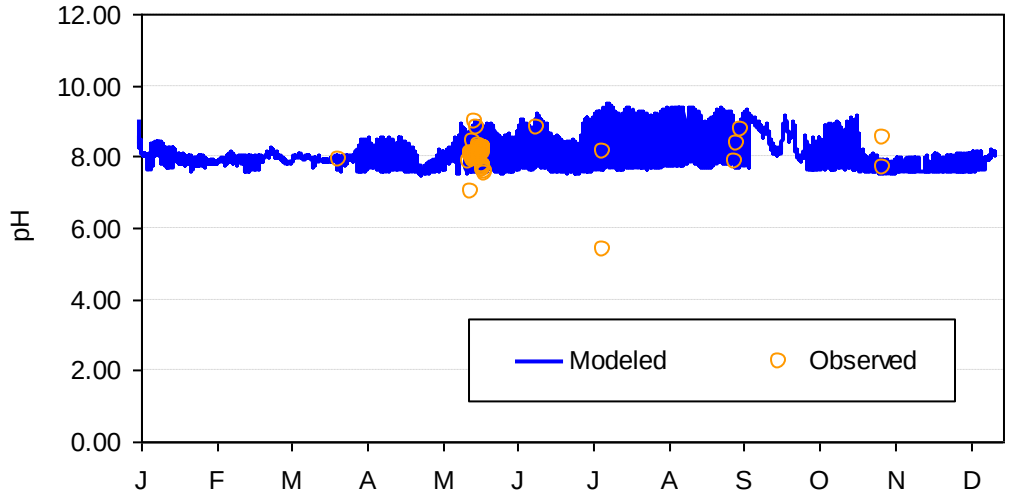

Figure H-18. pH calibration results for J. C. Boyle Powerhouse tailrace (2002).

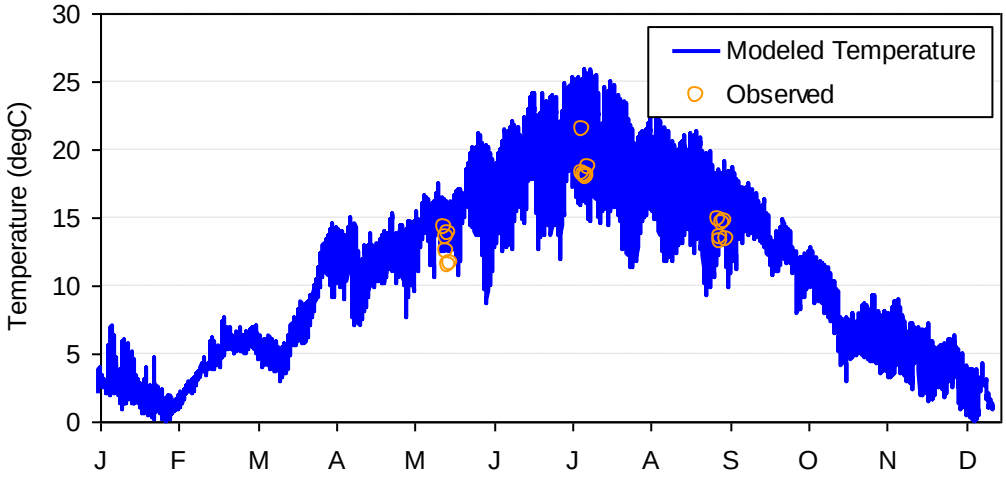

Figure H-19. Temperature calibration results for Klamath River near Stateline—KR4 (2002).

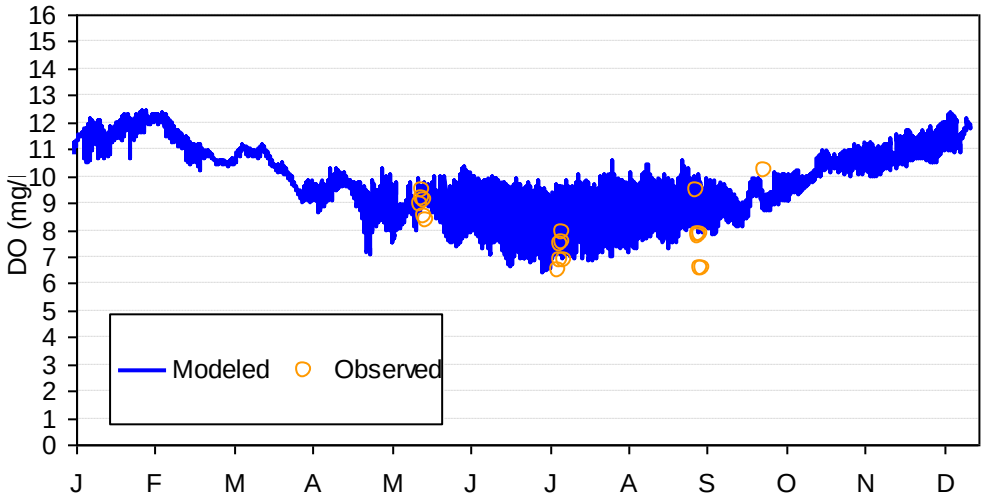

Figure H-20. Dissolved oxygen calibration results for Klamath River near Stateline—KR4 (2002).

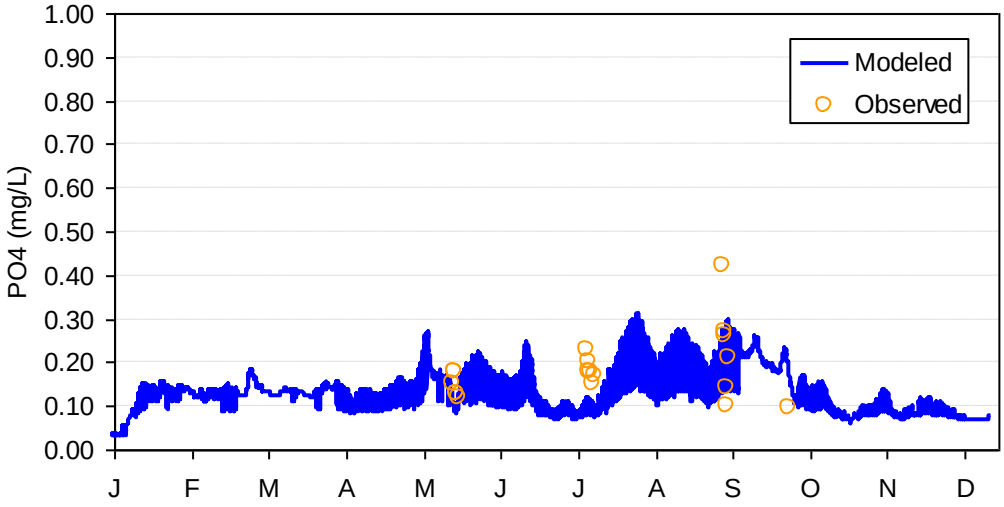

Figure H-21. PO_4 calibration results for Klamath River near Stateline—KR4 (2002).

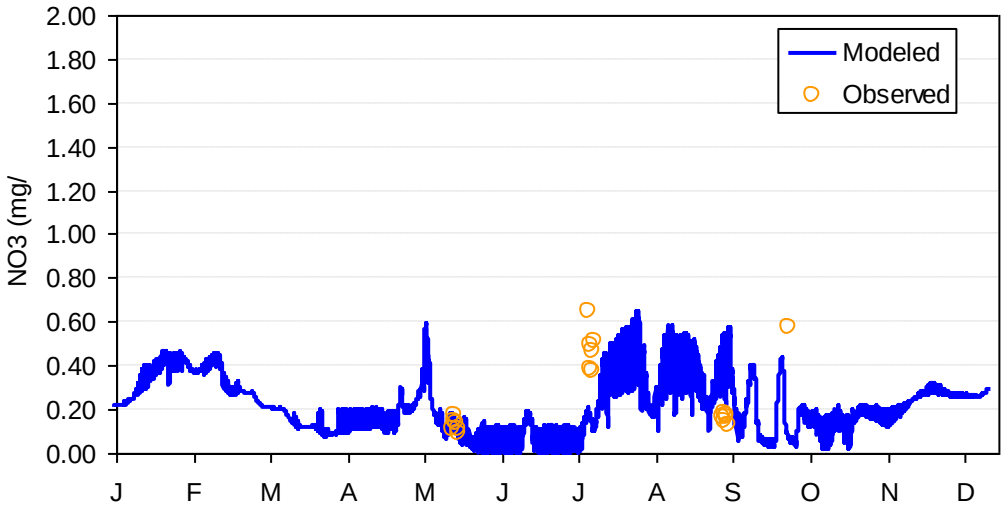

Figure H-22 NO_3 calibration results for Klamath River near Stateline—KR4 (2002).

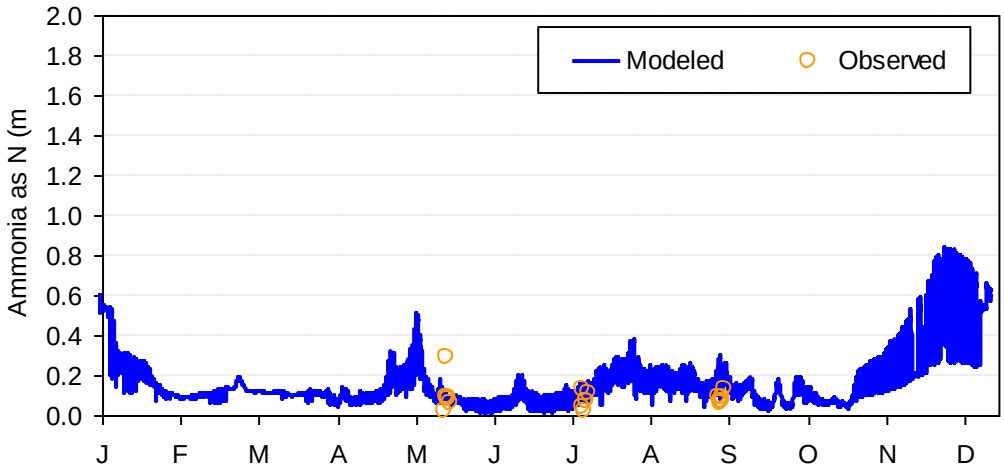

Figure H-23 NH_4-N calibration results for Klamath River near Stateline-KR4 (2002).

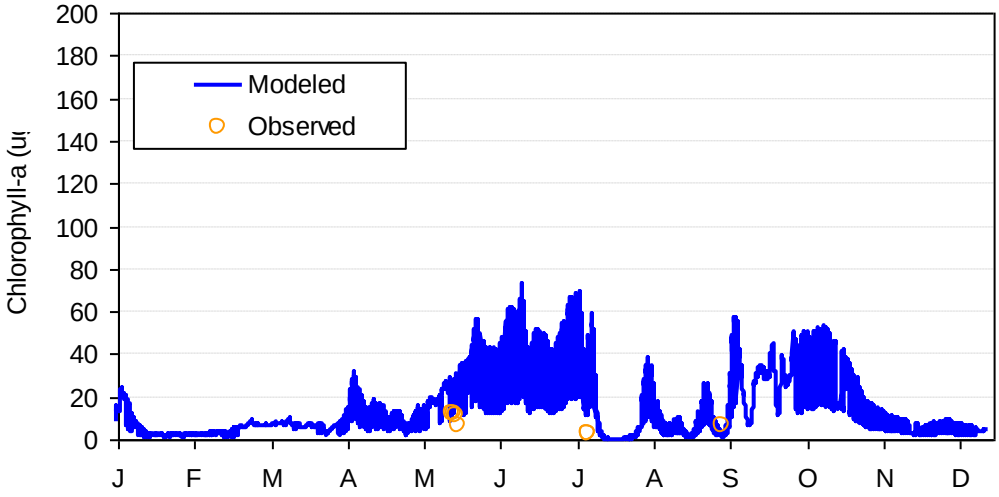

Figure H-24 Chlorophyll *a* calibration results for Klamath River near Stateline—KR4 (2002).

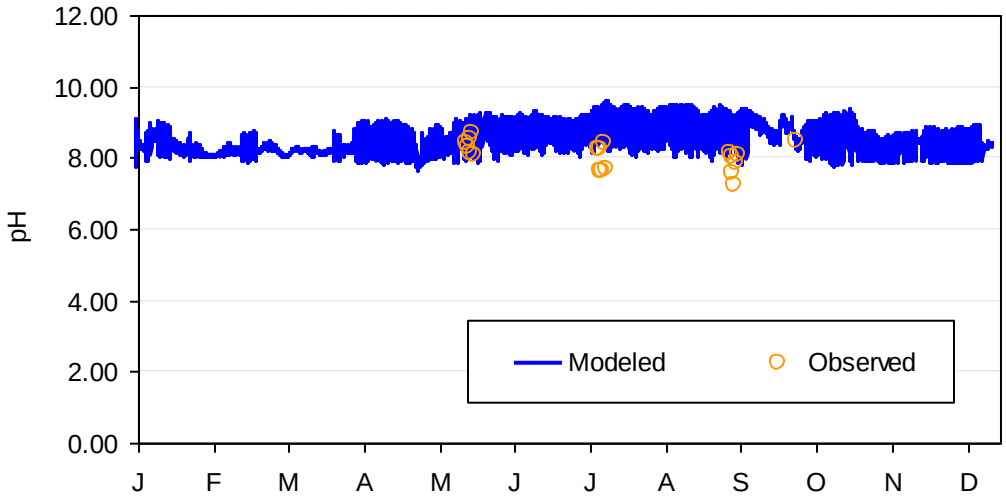

Figure H-25 pH calibration results for Klamath River near Stateline—KR4 (2002).

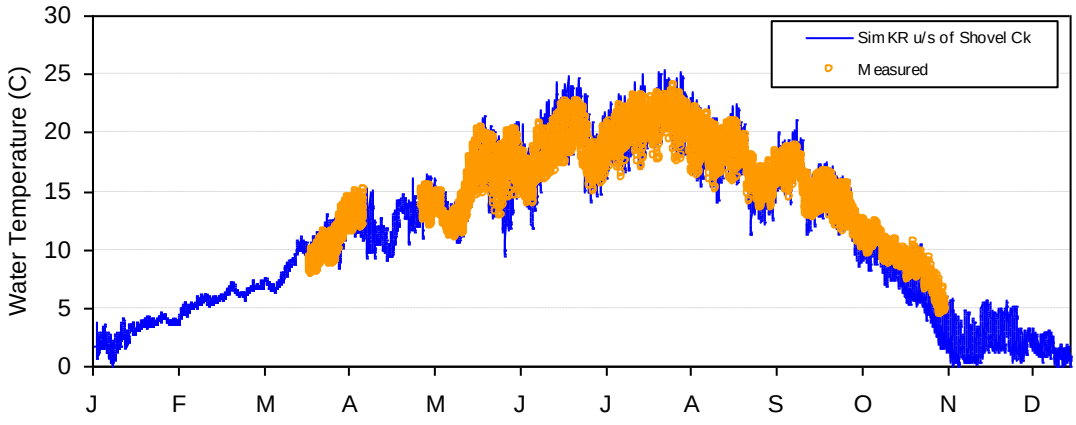

Figure H-26. Temperature calibration results for the Klamath River at Shovel Creek (2000).

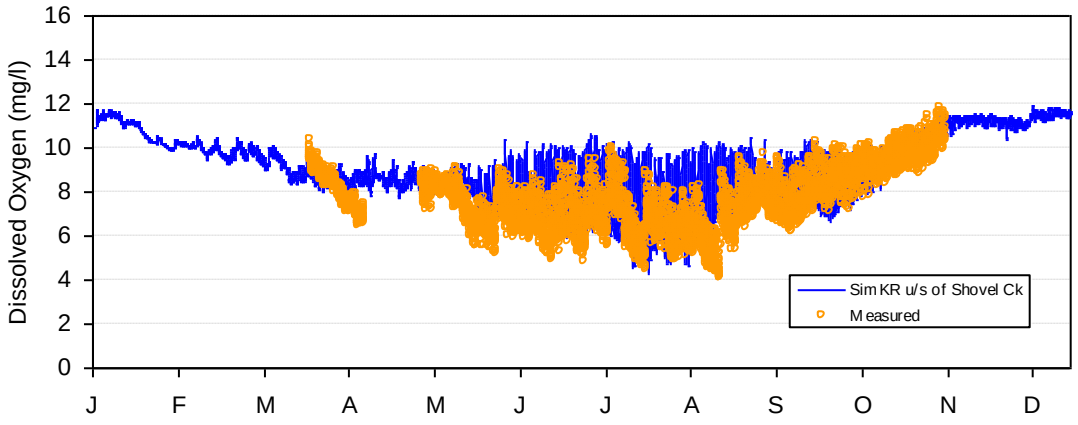

Figure H-27. Dissolved oxygen calibration results for the Klamath River at Shovel Creek (2000).

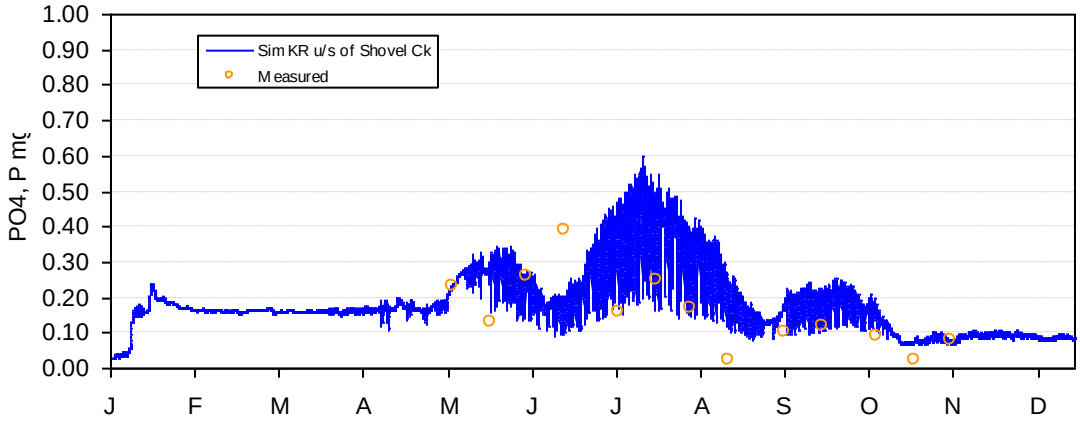

Figure H-28. PO_4-P calibration results for the Klamath River at Shovel Creek (2000).

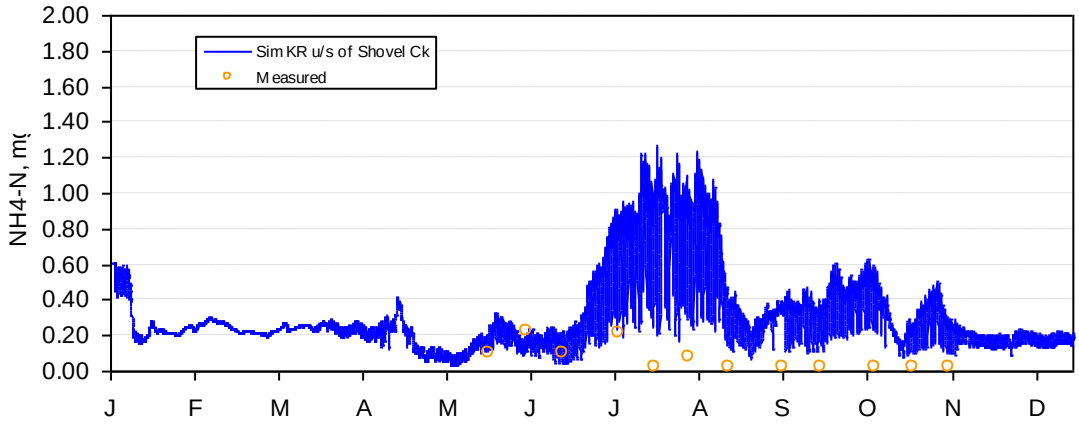

Figure H-29. NH_4-N calibration results for the Klamath River at Shovel Creek (2000).

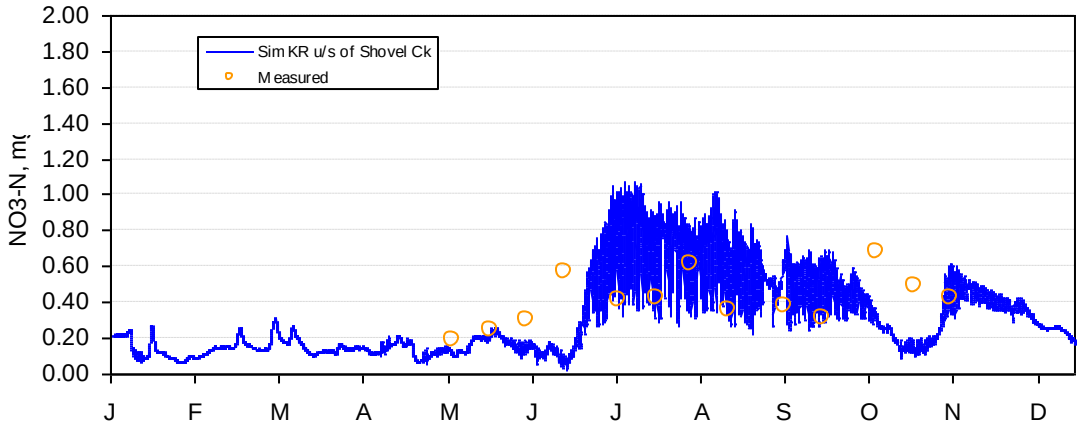

Figure H-30. NO_3-N calibration results for the Klamath River at Shovel Creek (2000).

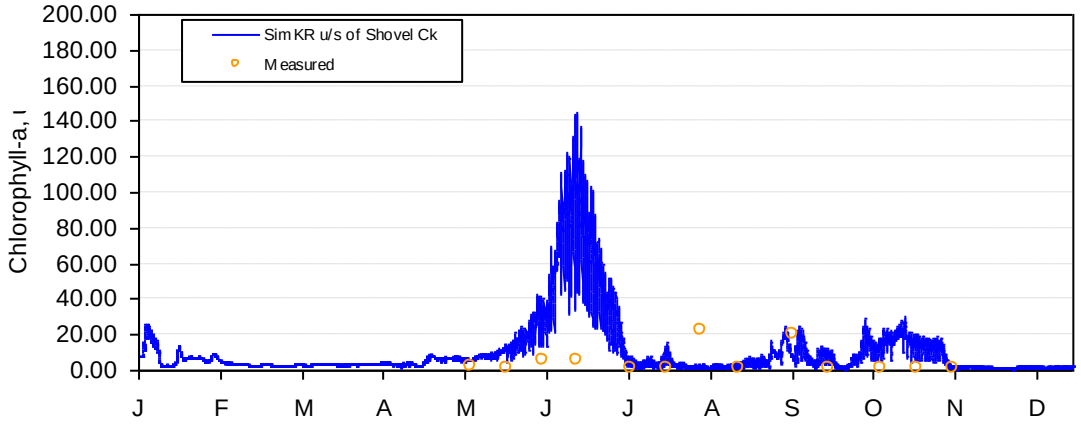

Figure H-31. Chlorophyll *a* calibration results for the Klamath River at Shovel Creek (2000).

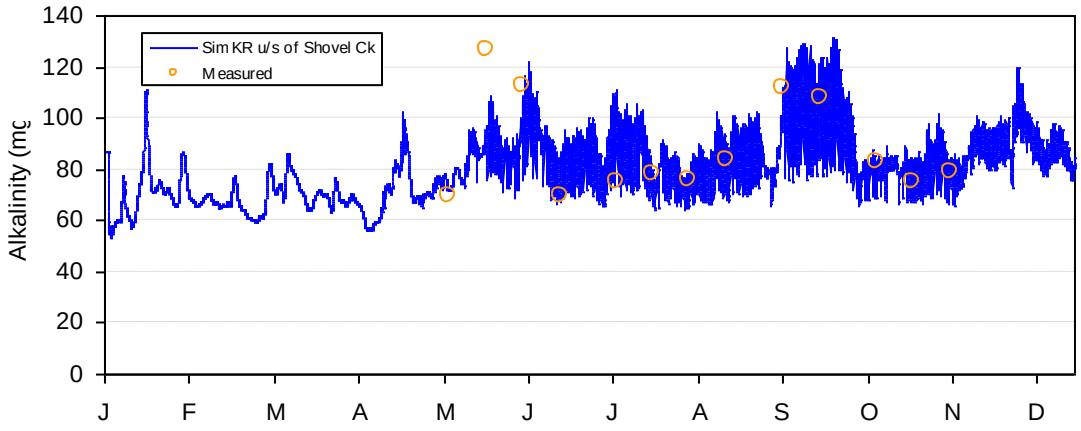

Figure H-32. Alkalinity calibration results for the Klamath River at Shovel Creek (2000).

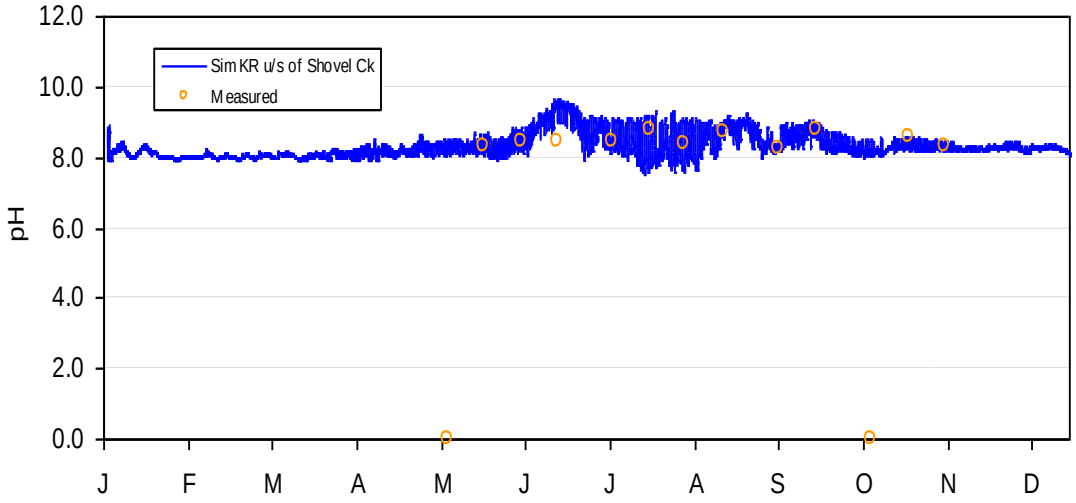

Figure H-33. pH calibration results for the Klamath River at Shovel Creek (2000).

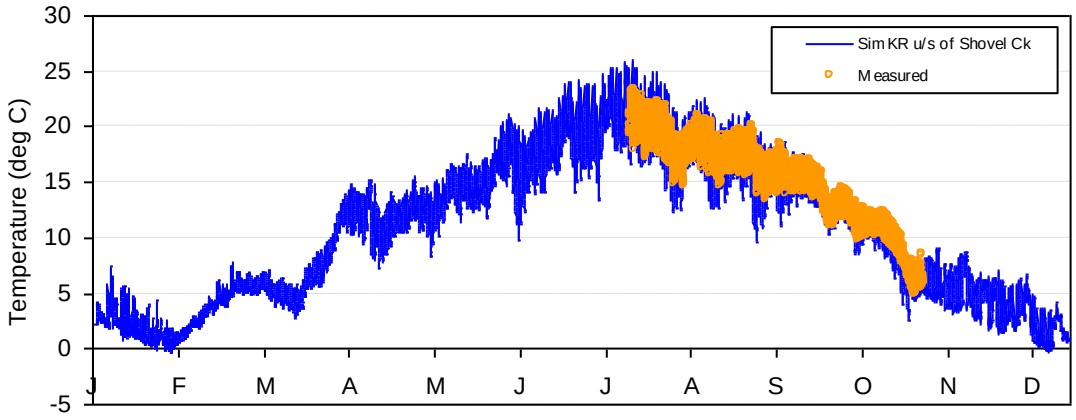

Figure H-34. Temperature calibration results for the Klamath River at Shovel Creek (2002).

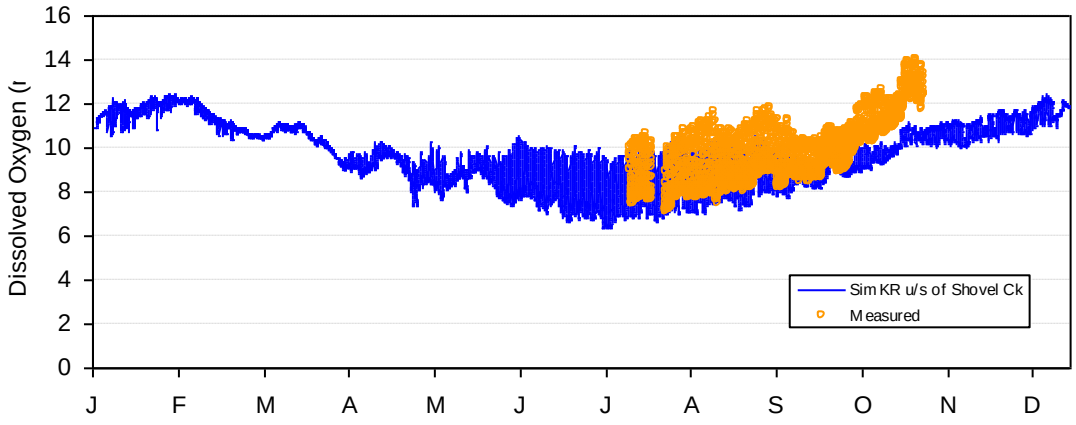

Figure H-35. Dissolved oxygen calibration results for the Klamath River at Shovel Creek (2002).

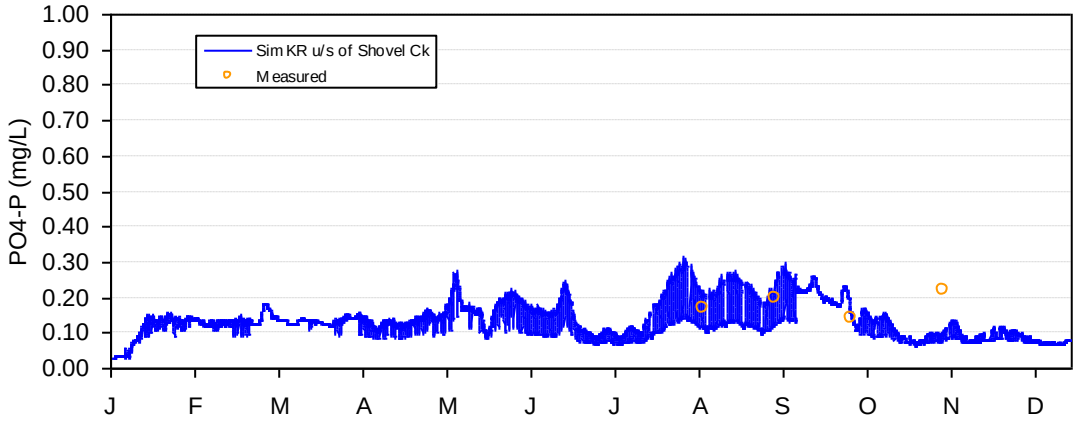

Figure H-36. PO_4-P calibration results for the Klamath River at Shovel Creek (2002).

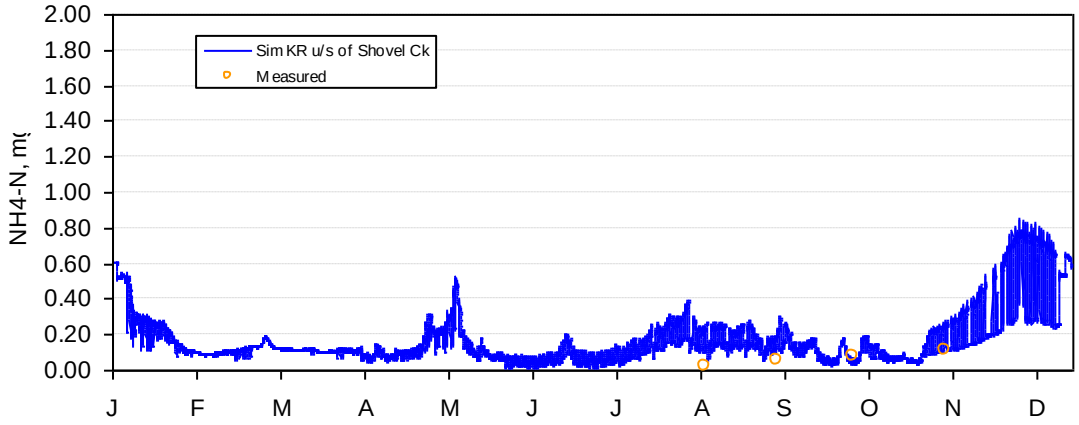

Figure H-37. NH_4-N calibration results for the Klamath River at Shovel Creek (2002).

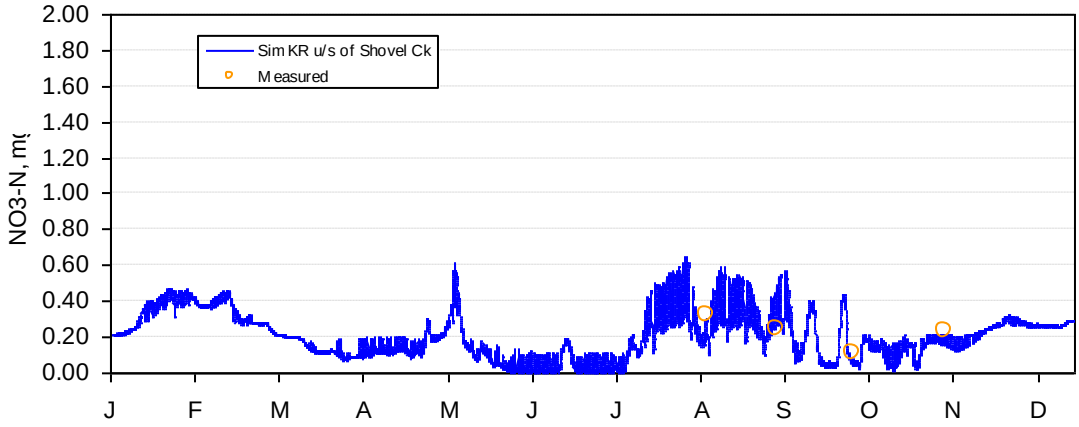

Figure H-38. NO_3-N calibration results for the Klamath River at Shovel Creek (2002).

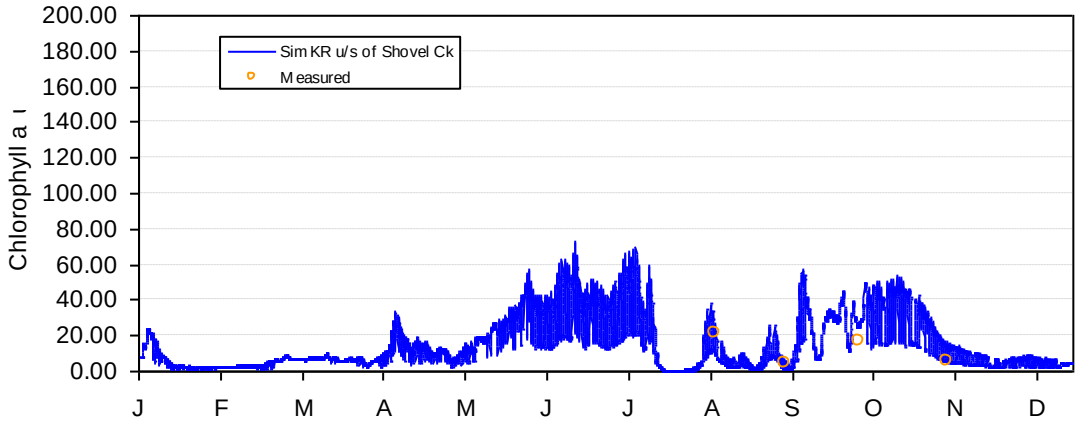

Figure H-39. Chlorophyll a calibration results for the Klamath River at Shovel Creek (2002).

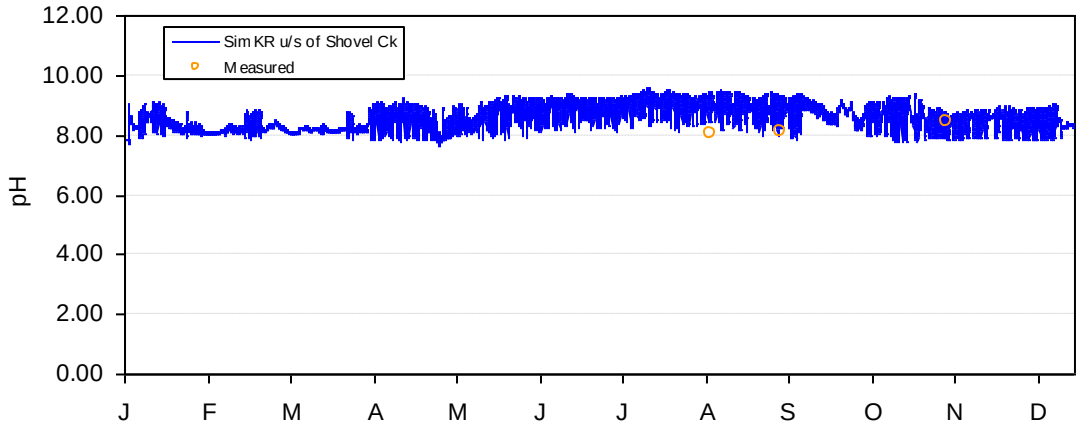

Figure H-40. pH calibration results for the Klamath River at Shovel Creek (2002).

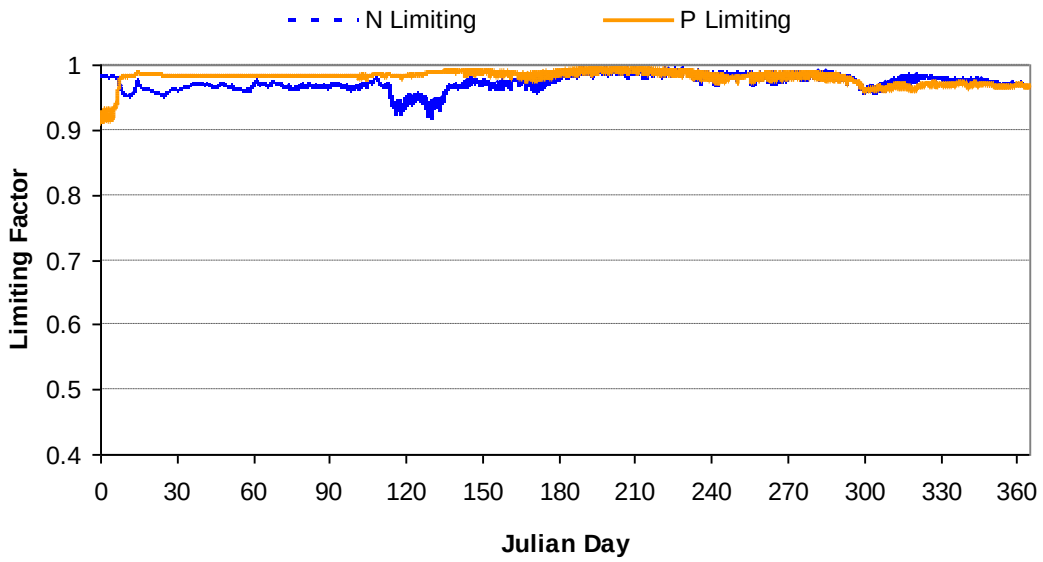

Figure H-41. Simulated Nutrient Limiting Condition for the Klamath River at Stateline (2000).

Table H-1. Calibration error statistics for Bypass/Full Flow Reach

Parameter	MES	AME	Data Type	Unit
SHOVEL CREEK (2000)				
CHLA	-13.59	18.56	Grab	ug/L
DO	-0.77	0.93	Continuous	mg/L
DO	1.81	1.66	Grab	mg/L
NH4	-0.36	0.37	Grab	mg/L
NO3	-0.06	0.29	Grab	mg/L
pH	0.13	0.33	Grab	
PO4	-0.09	0.13	Grab	mg/L
Temperature	0.31	1.09	Continuous	deg C
Temperature	0.04	1.62	Grab	deg C

Table H-2. Corroboration error statistics for Bypass/Full Flow Reach

Parameter	MES	AME	Data Type	Unit
SHOVEL CREEK (2002)				
CHLA	-13.50	17.05	Grab	ug/L
DO	0.84	0.93	Continuous	mg/L
DO	1.09	1.11	Grab	mg/L
NH4	-0.07	0.08	Grab	mg/L
NO3	0.40	0.40	Grab	mg/L
pH	-0.74	0.74	Grab	
PO4	0.03	0.05	Grab	mg/L
Temperature	0.84	1.27	Continuous	deg C
Temperature	-0.89	1.87	Grab	deg C
STATELINE (2002)				
CHLA	-10.56	12.09	Grab	ug/L
DO	-1.23	1.39	Grab	mg/L
NH4	-0.03	0.05	Grab	mg/L
NO3	0.08	0.19	Grab	mg/L
pH	-0.65	0.66	Grab	
Temperature	0.59	2.62	Grab	deg C

Appendix I

Calibration Results for Copco Reservoir (Modeling Segment 6)

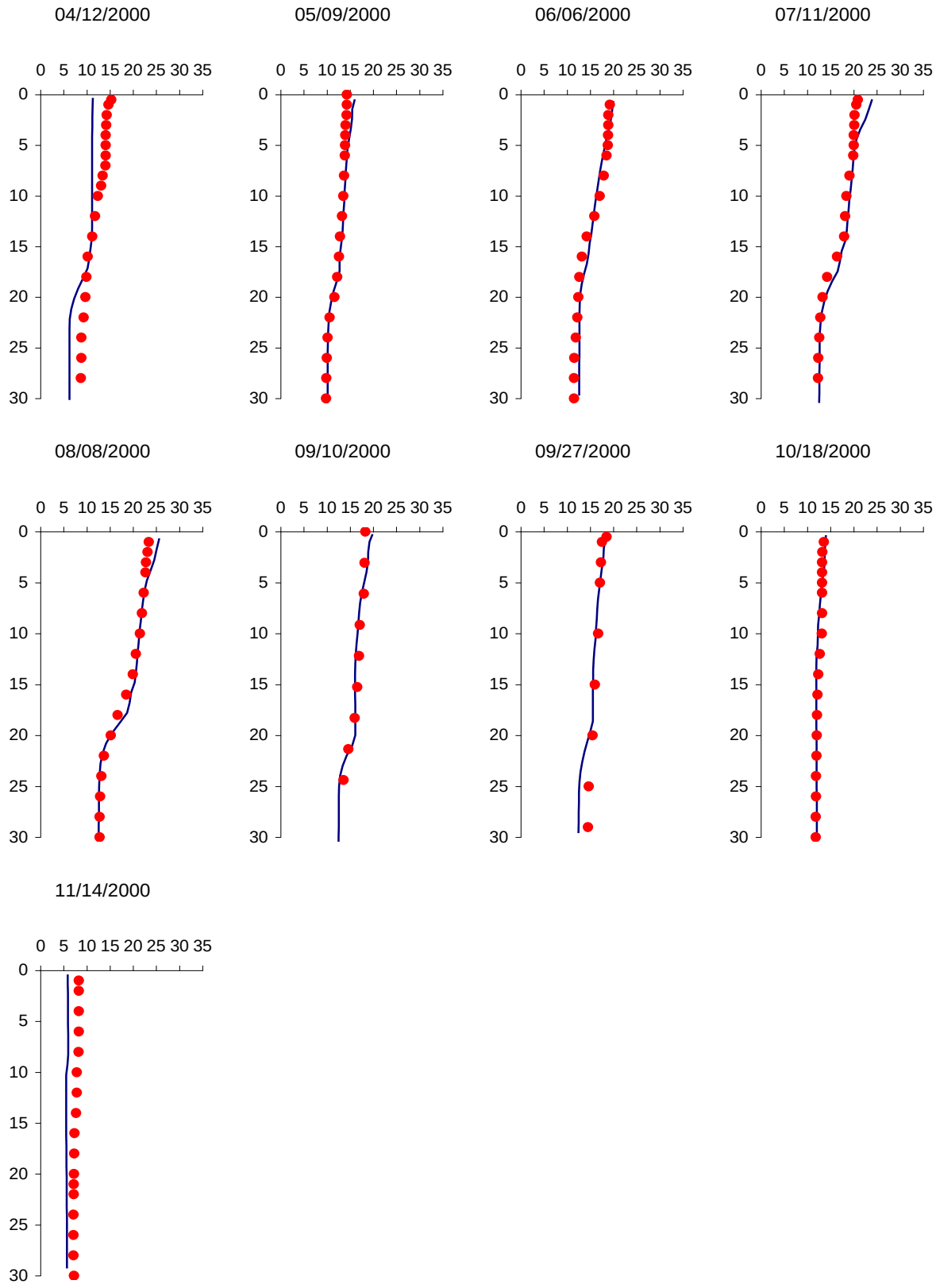

Figure I-1. Temperature profile calibration results for Copco Reservoir at Copco Lake near Copco

(2000) [X-axis Temperature (degC) vs. Y-axis Depth (m)].

04/12/2000

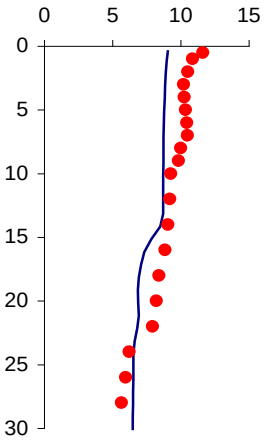

05/09/2000

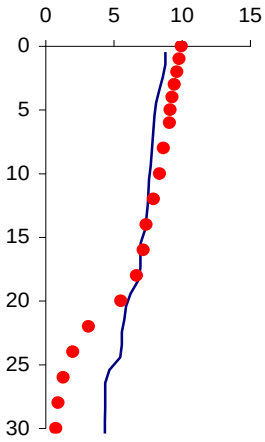

06/06/2000

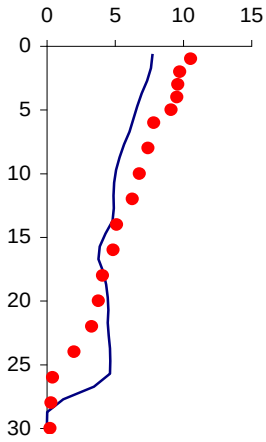

07/11/2000

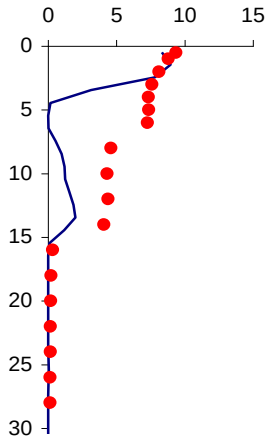

08/08/2000

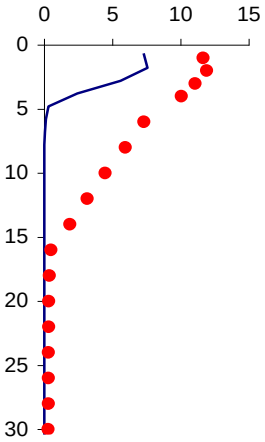

09/10/2000

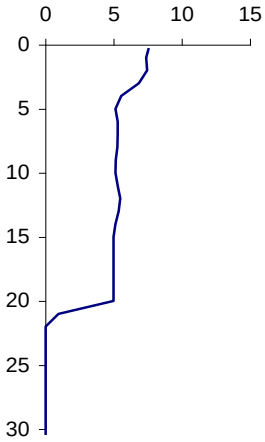

09/27/2000

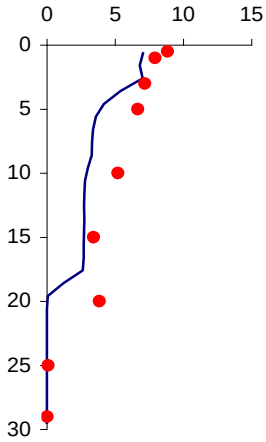

10/18/2000

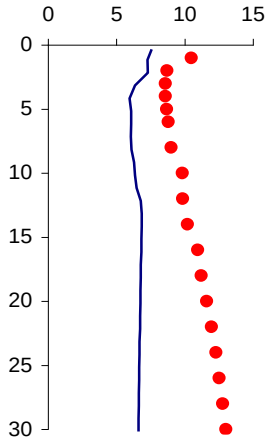

11/14/2000

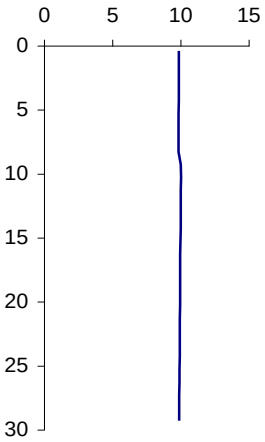

Figure I-2. Dissolved oxygen profile calibration results for Copco Reservoir at Copco Lake near Copco (2000) [X-axis Dissolved oxygen (mg/L) vs. Y-axis Depth (m)].

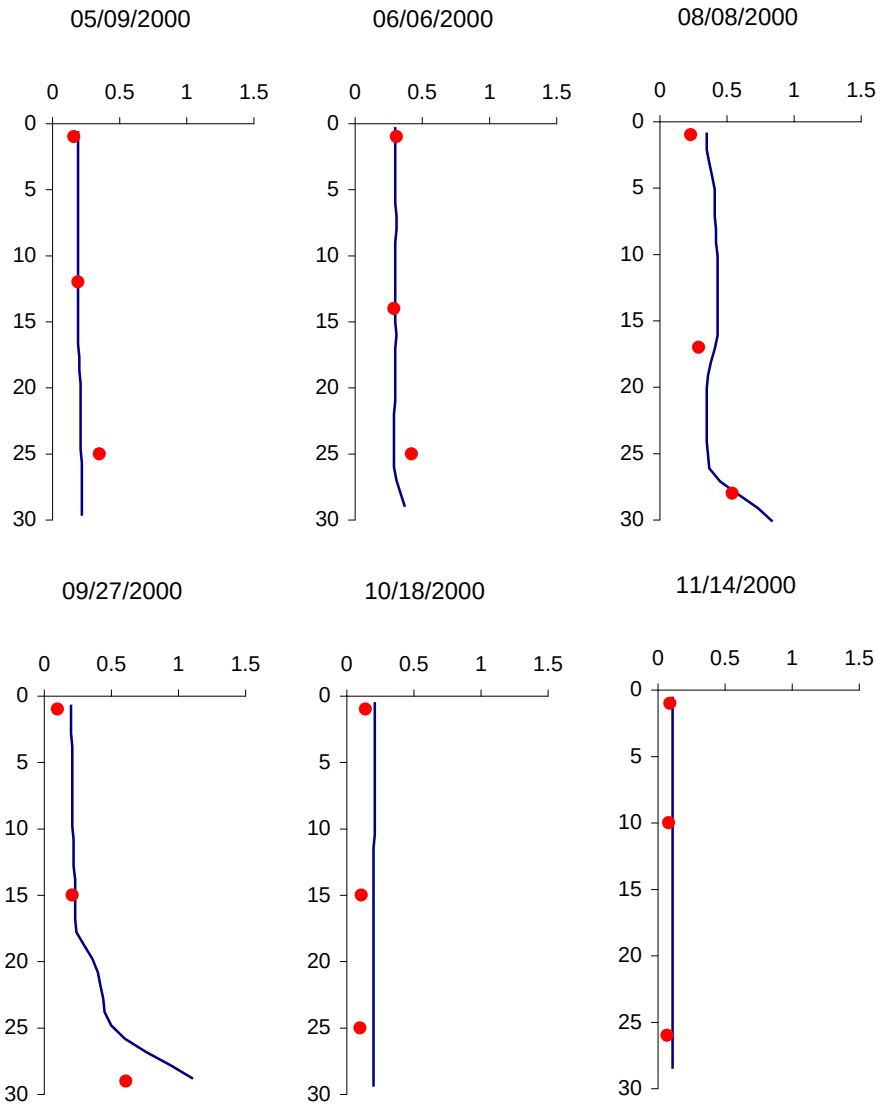

Figure I-3. PO_4 profile calibration results for Copco Reservoir at Copco Lake near Copco (2000) [X-axis PO_4-P (mg/L) vs. Y-axis Depth (m)].

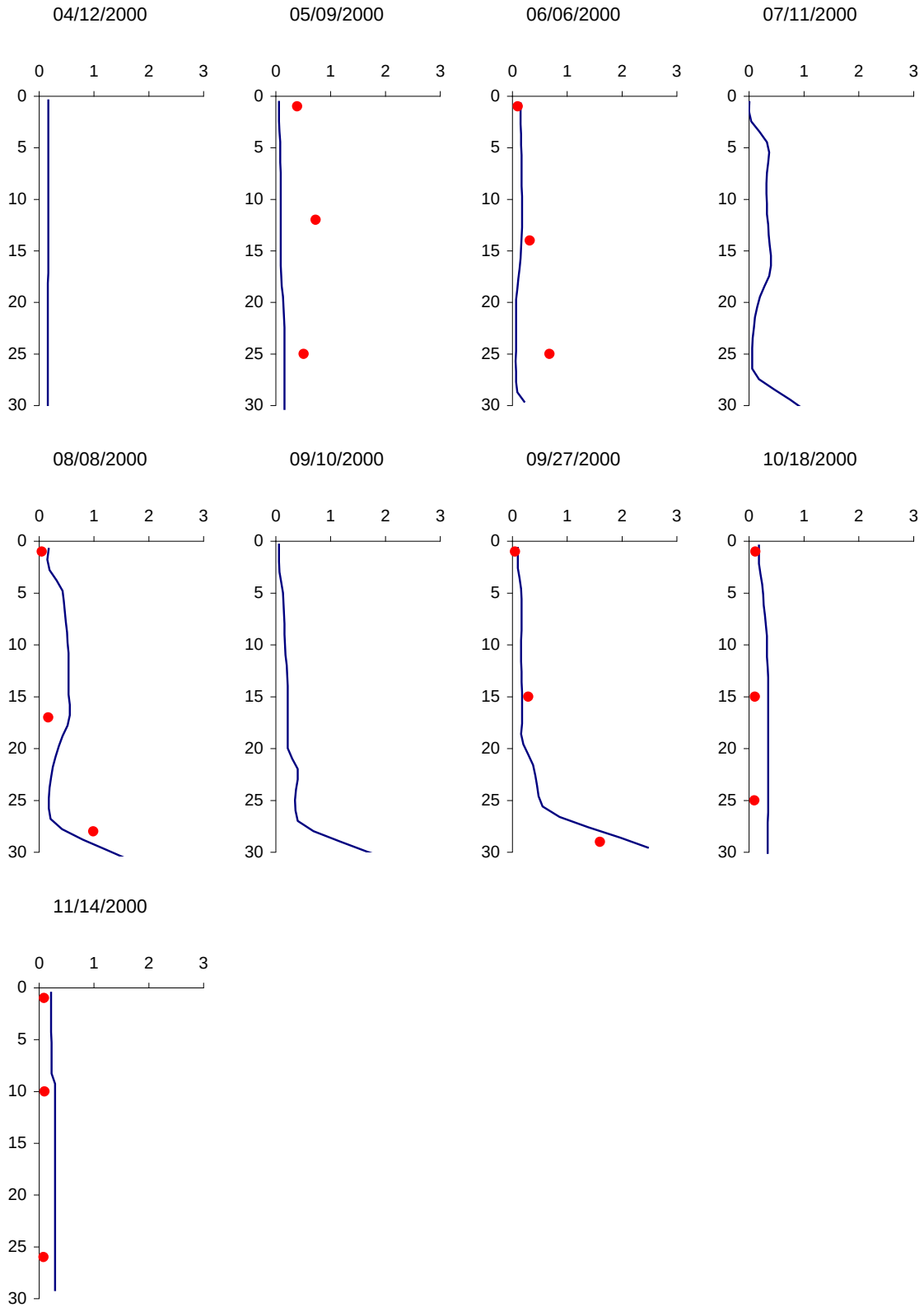

Figure I-4. NH_4 profile calibration results for Copco Reservoir at Copco Lake near Copco (2000) [X-axis NH_4 (mg/L) vs. Y-axis Depth (m)].

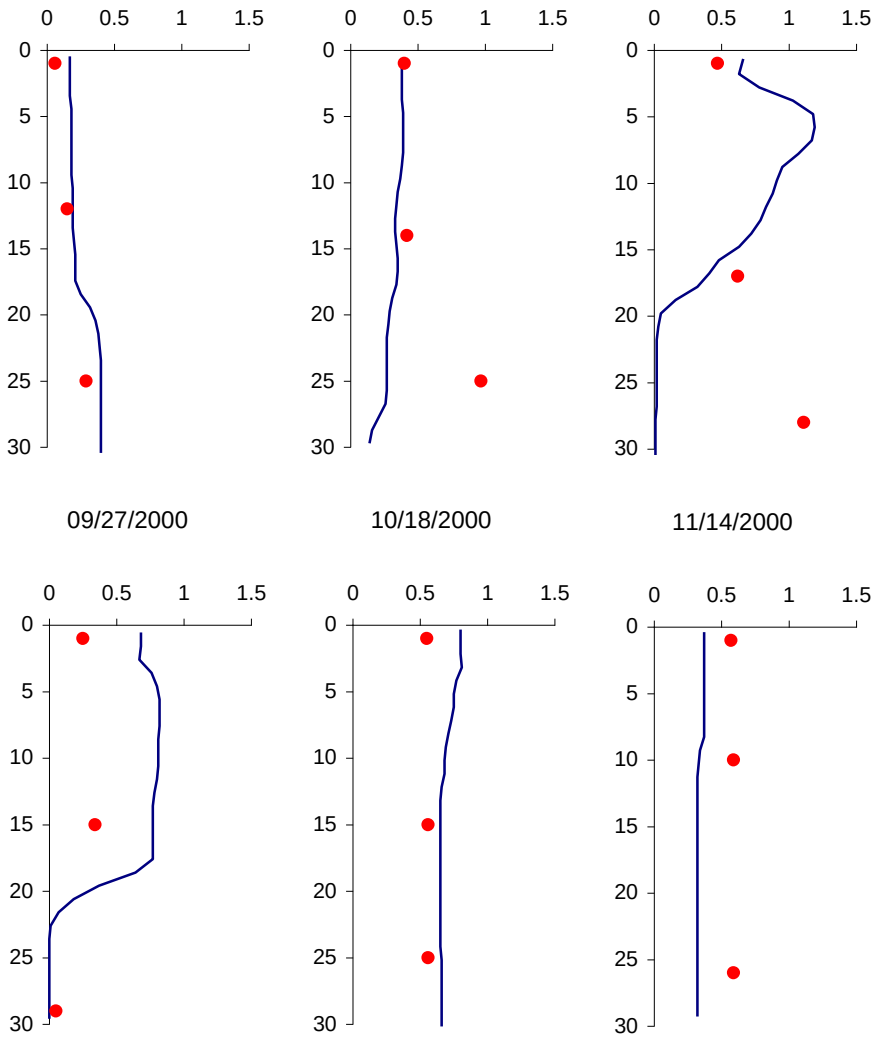

Figure I-5. NO_3 profile calibration results for Copco Reservoir at Copco Lake near Copco (2000) [X-axis NO_3 (mg/L) vs. Y-axis Depth (m)].

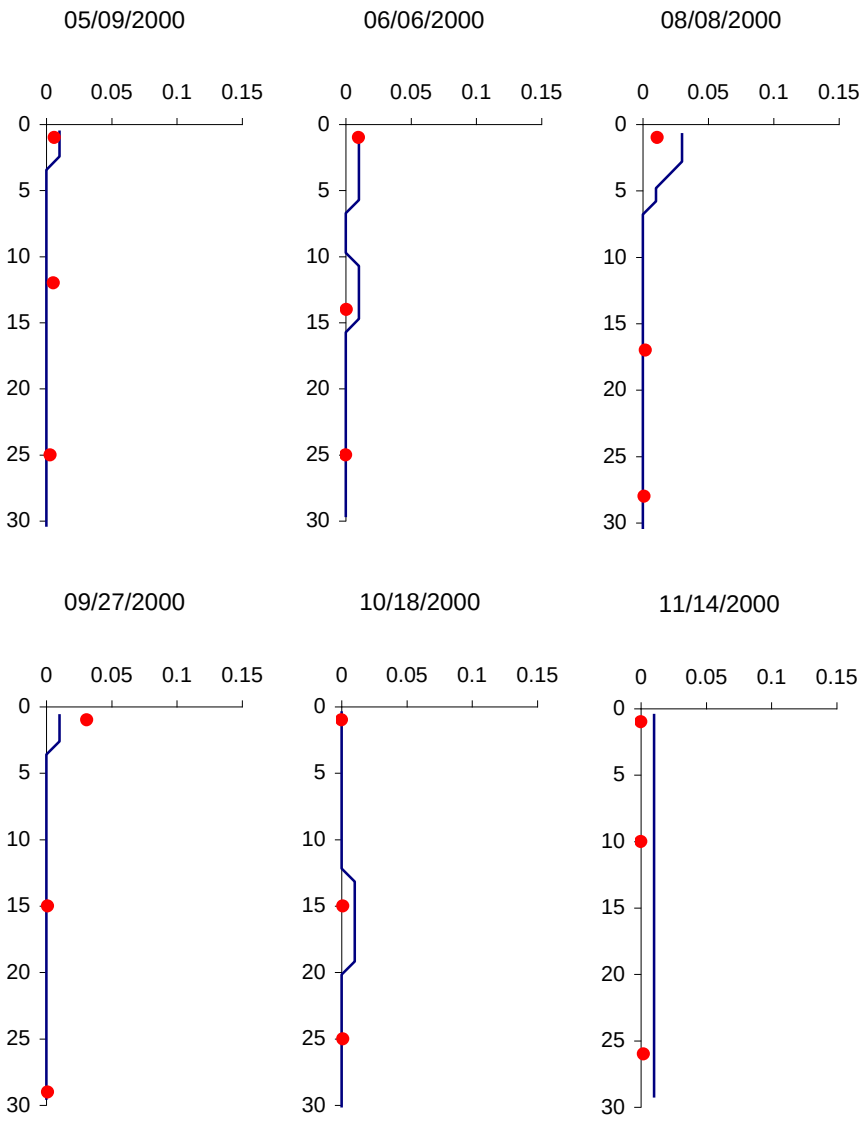

Figure I-6. Chlorophyll *a* profile calibration results for Copco Reservoir at Copco Lake near Copco (2000) [X-axis Chlorophyll *a* (mg/L) vs. Y-axis Depth (m)].

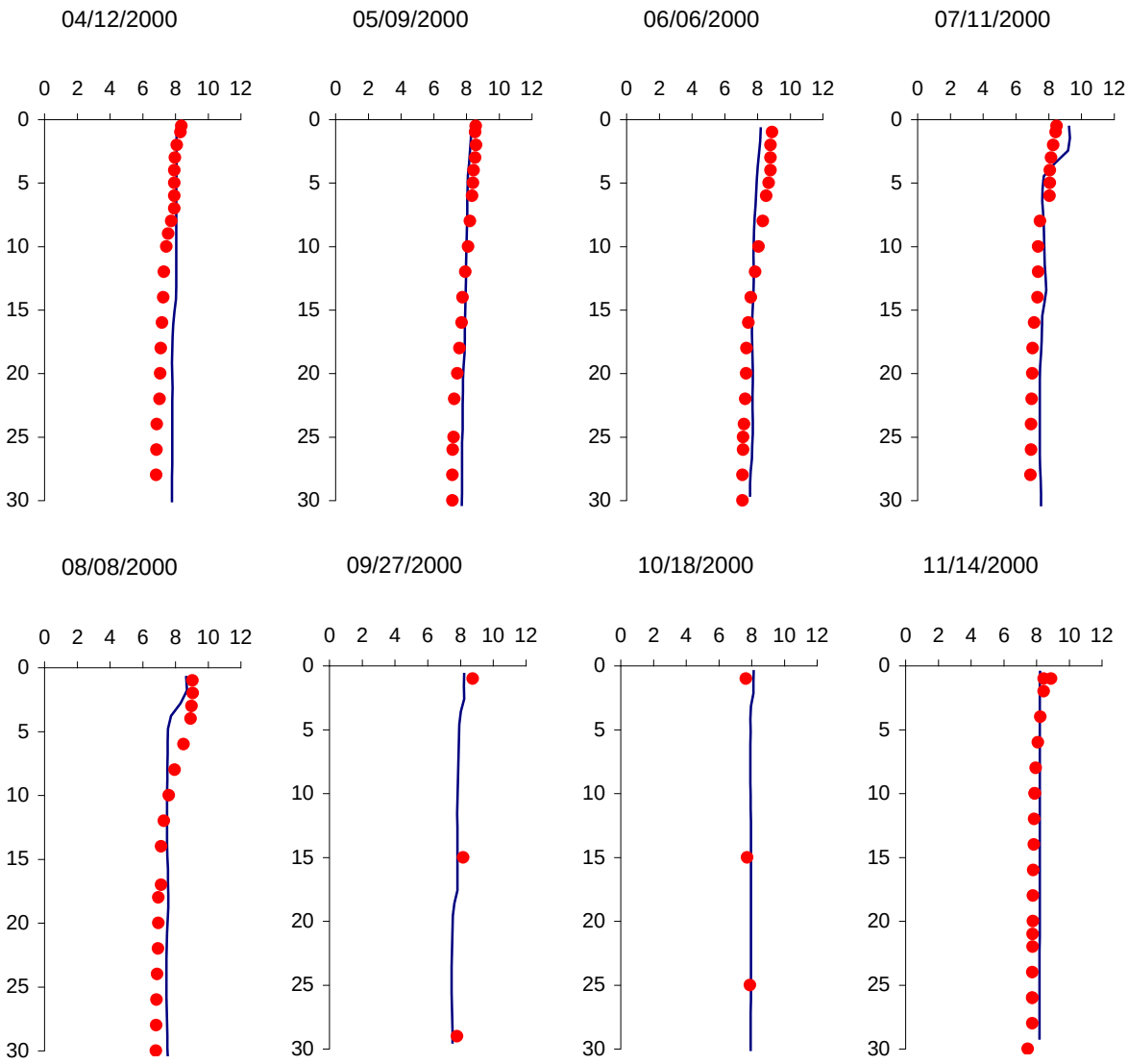

Figure I-7. pH profile calibration results for Copco Reservoir at Copco Lake near Copco (2000) [X-axis pH vs. Y-axis Depth (m)].

Appendix J

Calibration Results for Iron Gate Reservoir (Modeling Segment 7)

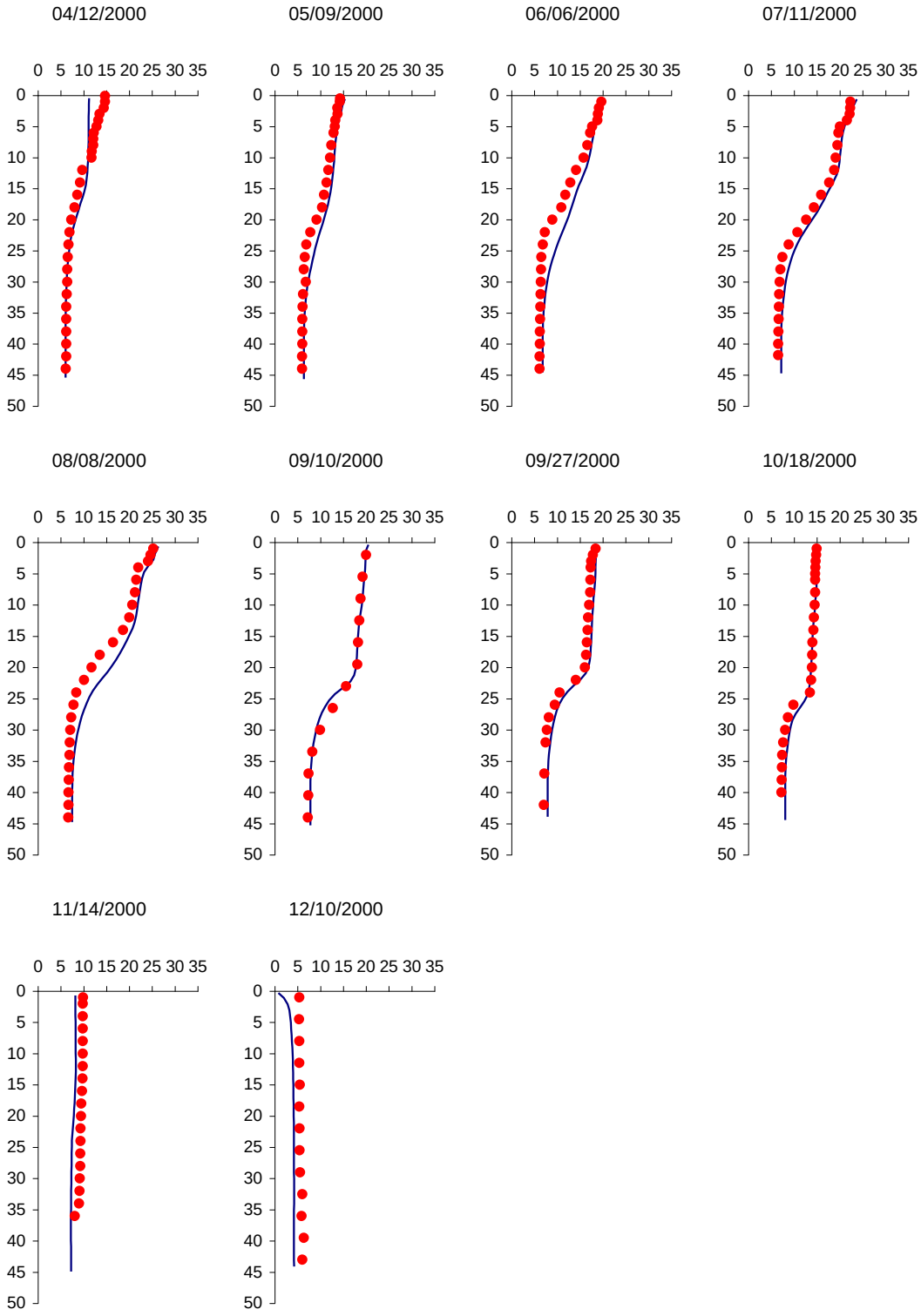

Figure J-1. Temperature profile calibration results at Iron Gate Reservoir (2000) [X-axis Temperature (deg C) vs. Y-axis Depth (m)].

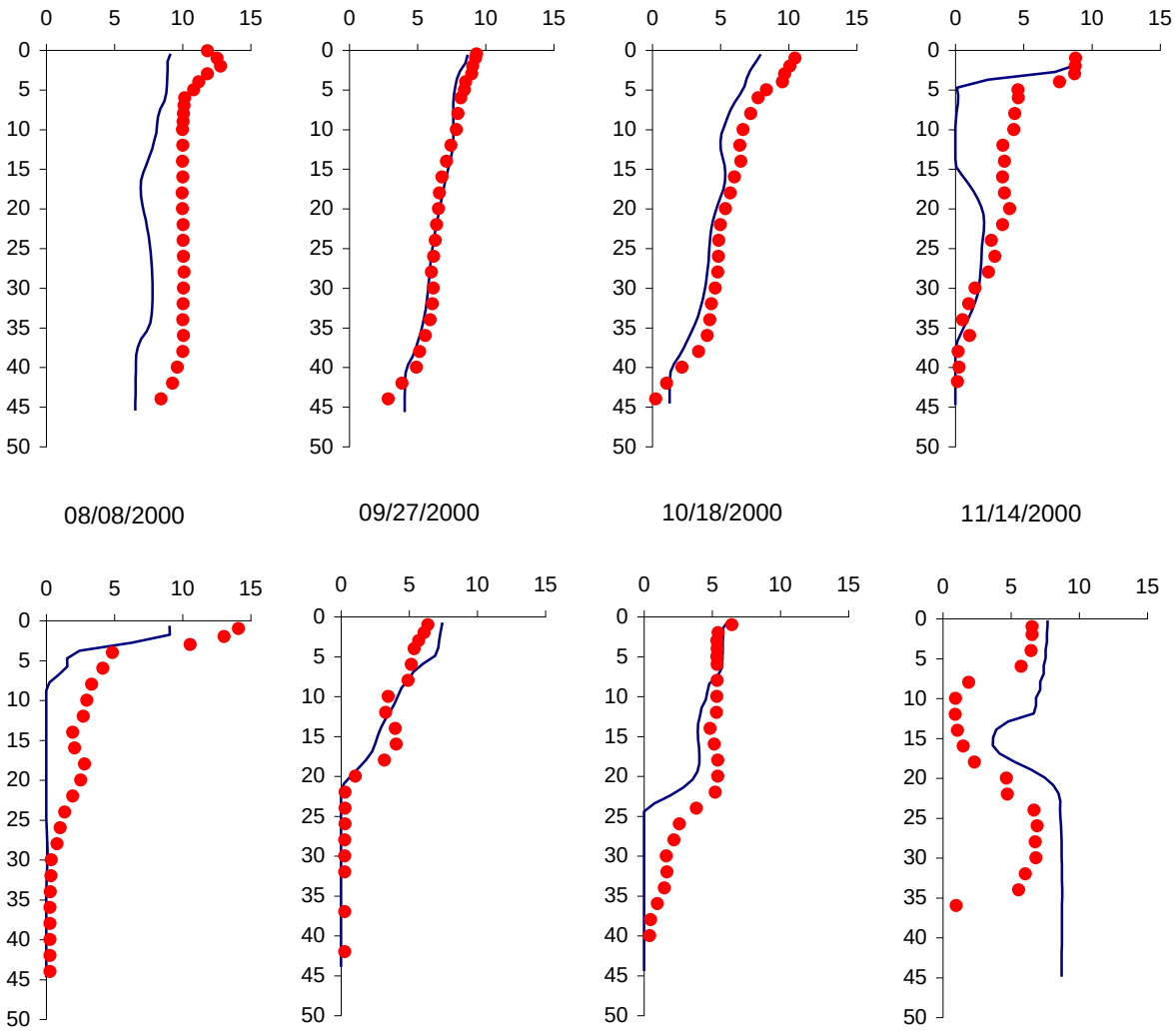

Figure J-2. Dissolved oxygen profile calibration results at Iron Gate Reservoir (2000) [X-axis Dissolved oxygen (mg/L) vs. Y-axis Depth (m)].

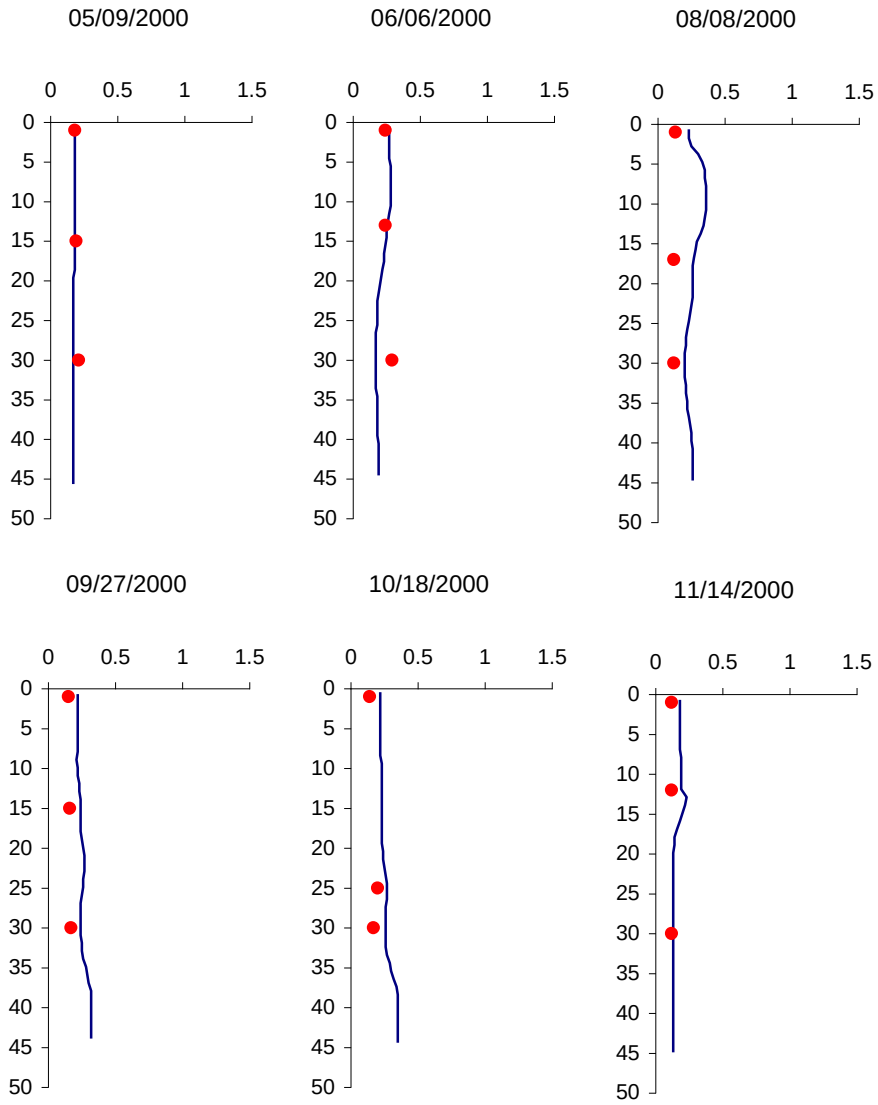

Figure J-3. PO_4 profile calibration results at Iron Gate Reservoir (2000) [X-axis PO_4 (mg/L) vs. Y-axis Depth (m)].

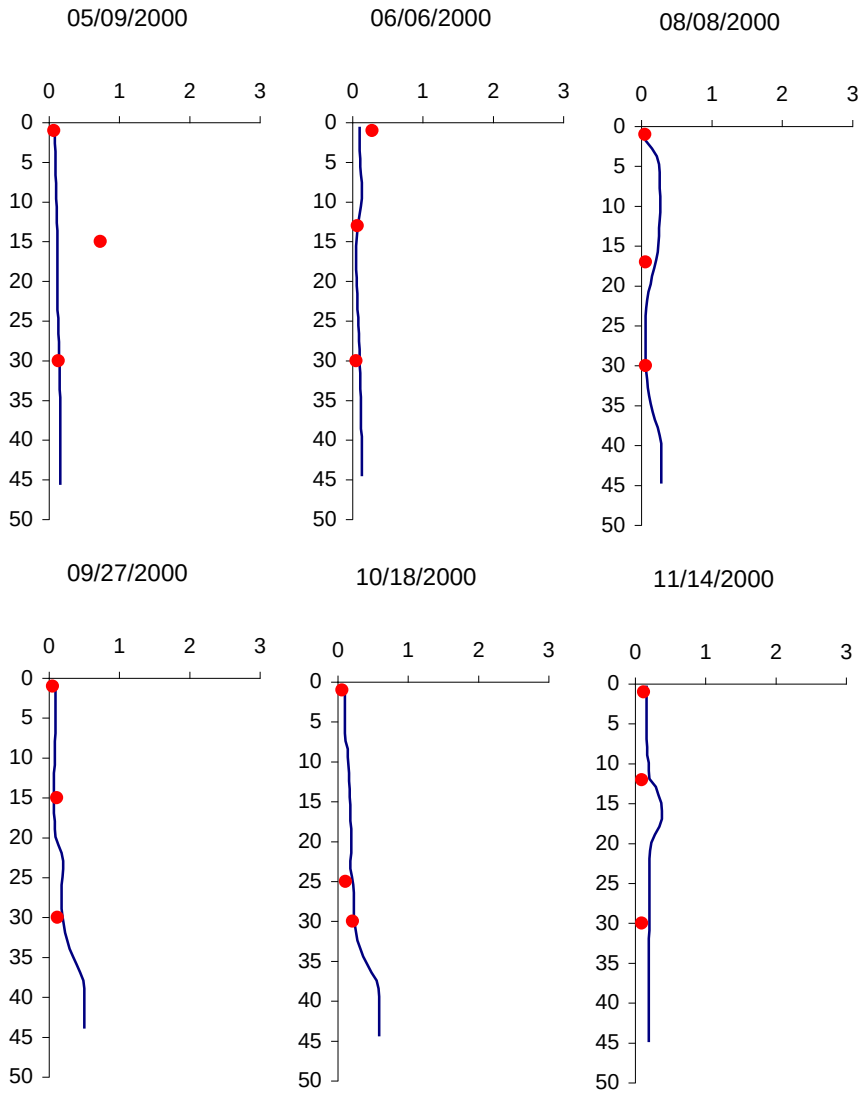

Figure J-4. NH_4 profile calibration results at Iron Gate Reservoir (2000) [X-axis NH_4 (mg/L) vs. Y-axis Depth (m)].

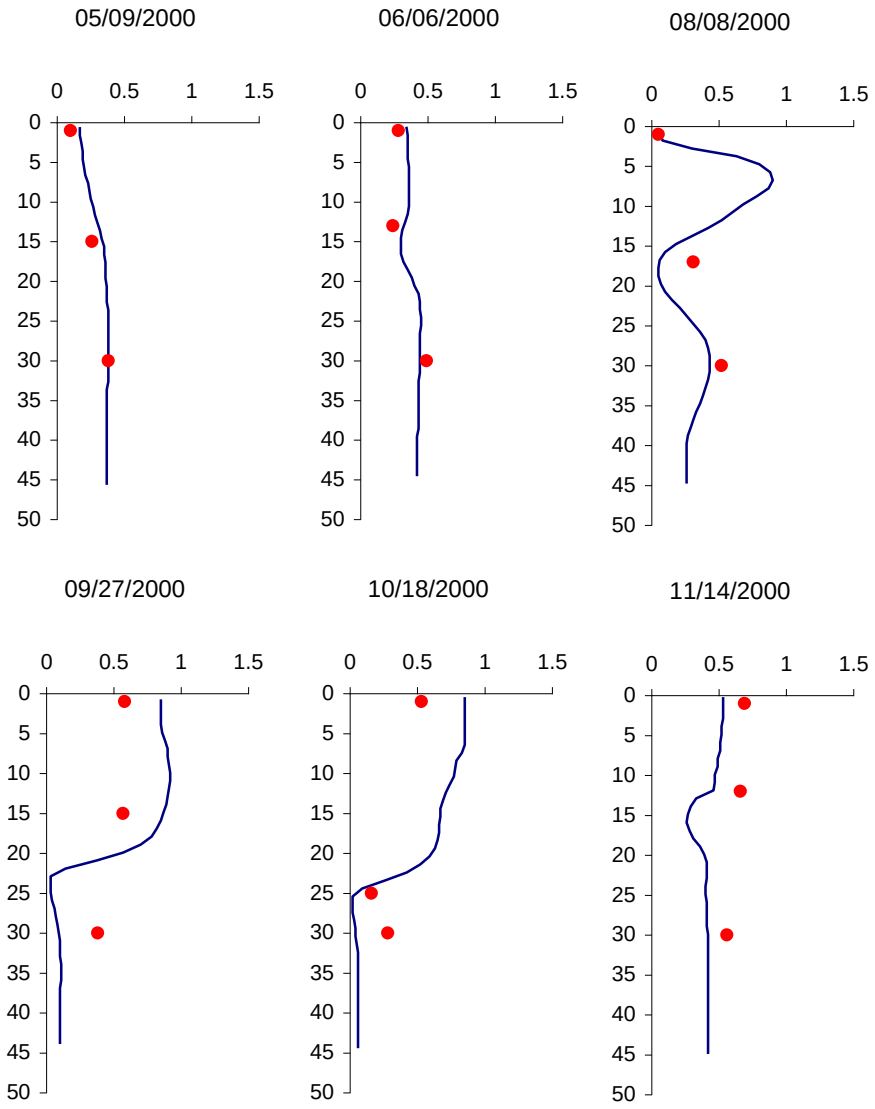

Figure J-5. NO_3 profile calibration results at Iron Gate Reservoir (2000) [X-axis NO_3 (mg/L) vs. Y-axis Depth (m)].

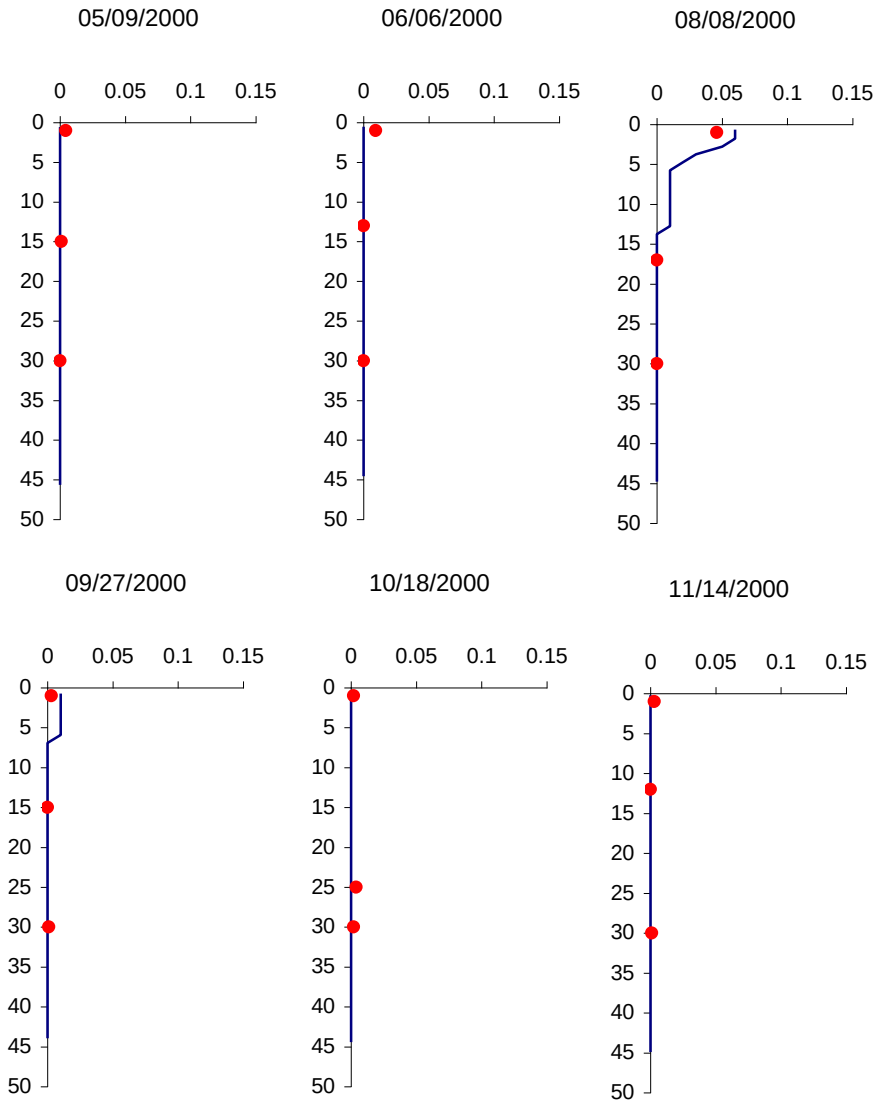

Figure J-6. Chlorophyll *a* profile calibration results at Iron Gate Reservoir (2000) [X-axis Chlorophyll *a* (mg/L) vs. Y-axis Depth (m)].

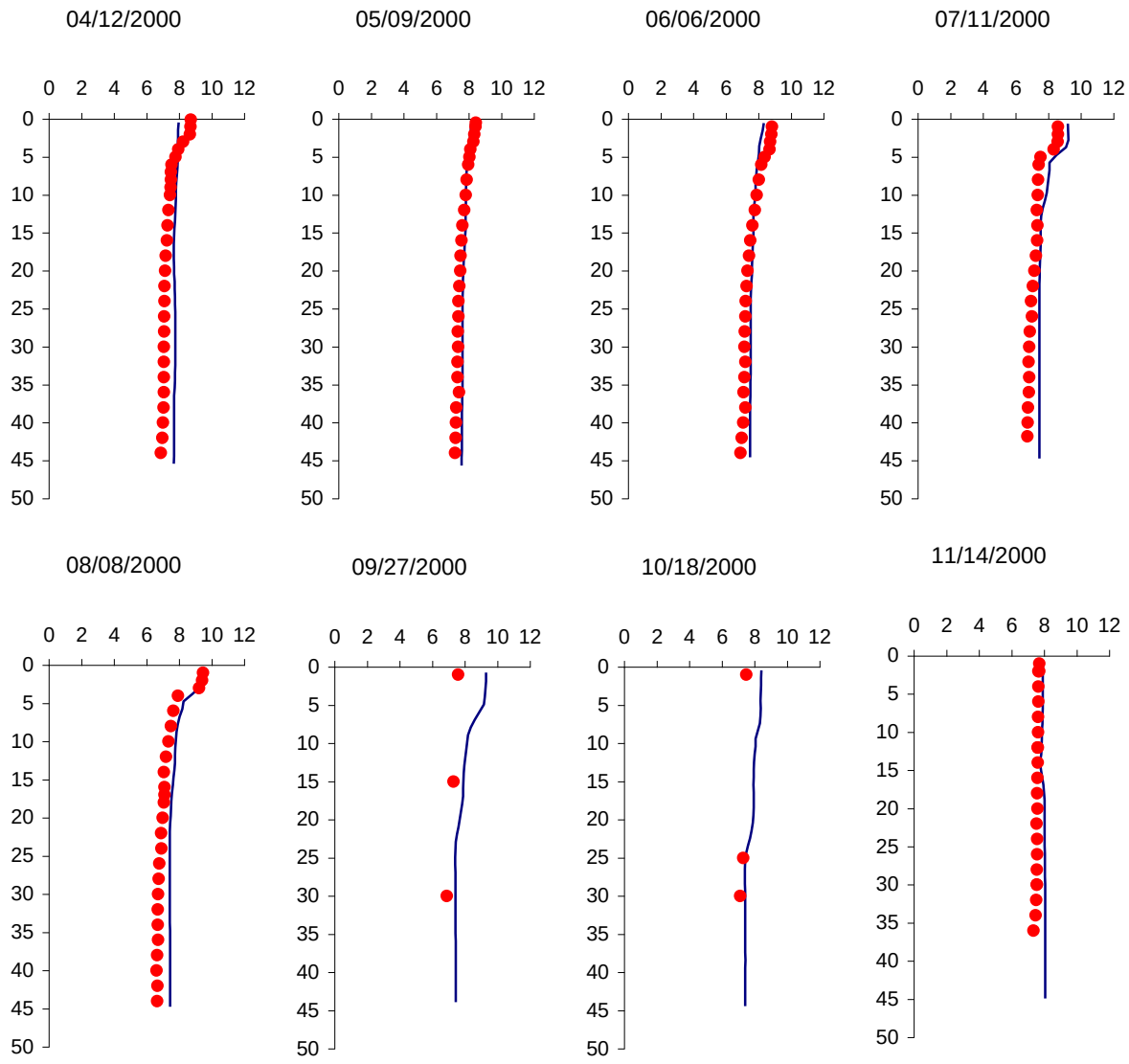

Figure J-7. pH profile calibration results at Iron Gate Reservoir (2000) [X-axis pH vs. Y-axis Depth (m)].

Appendix K

Calibration Results for Iron Gate Dam to Turwar (Modeling Segment 8)

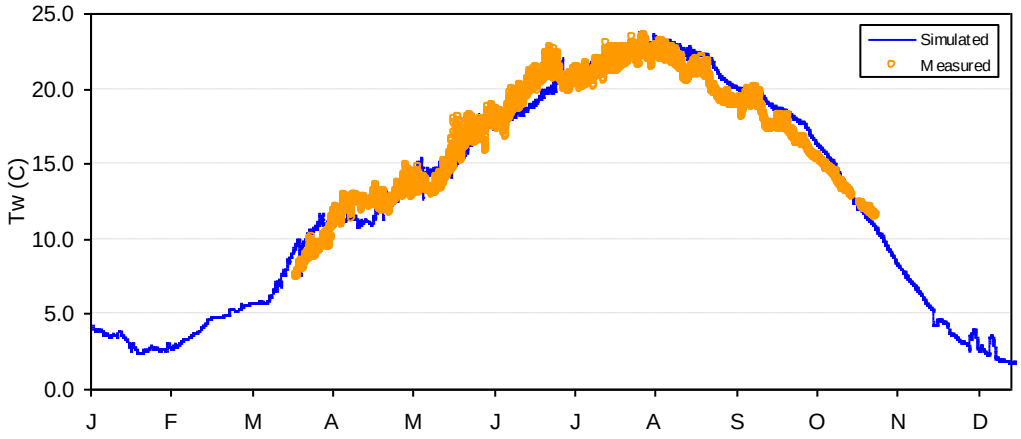

Figure K-1. Temperature calibration at Klamath River below Iron Gate Dam (Hatchery Br.) (2000).

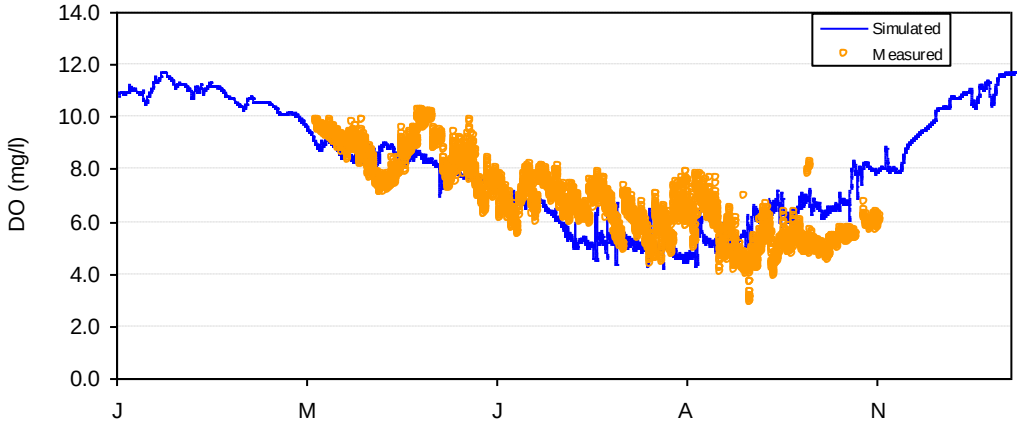

Figure K-2. Dissolved oxygen calibration at Klamath River below Iron Gate Dam (Hatchery Br) (2000).

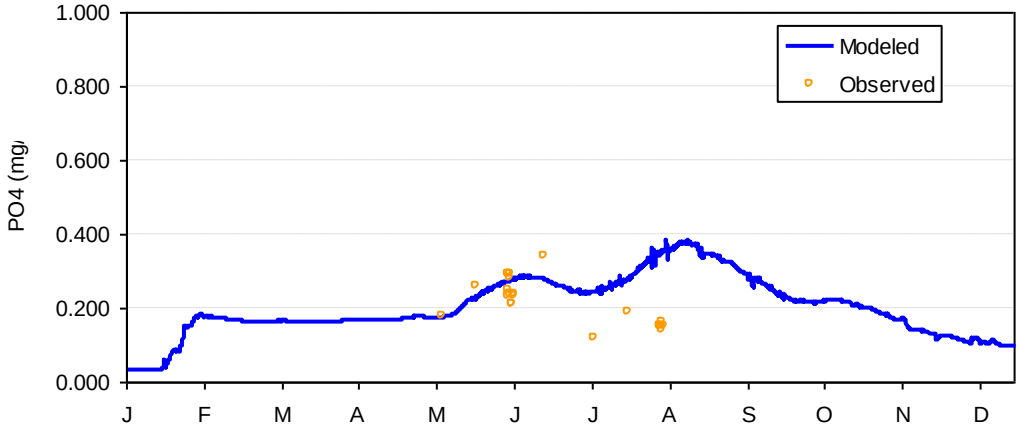

Figure K-3. PO_4 calibration at Klamath River below Iron Gate Dam (Hatchery Br) (2000).

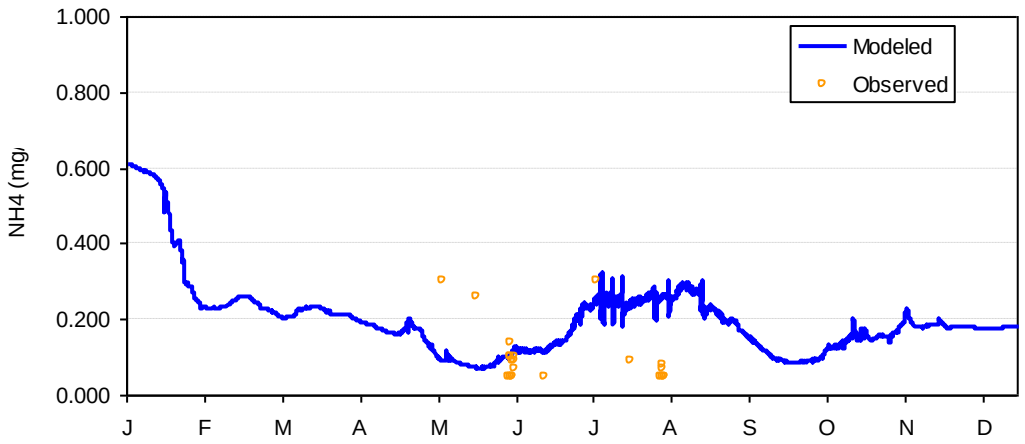

Figure K-4. NH_4 calibration at Klamath River below Iron Gate Dam (Hatchery Br) (2000).

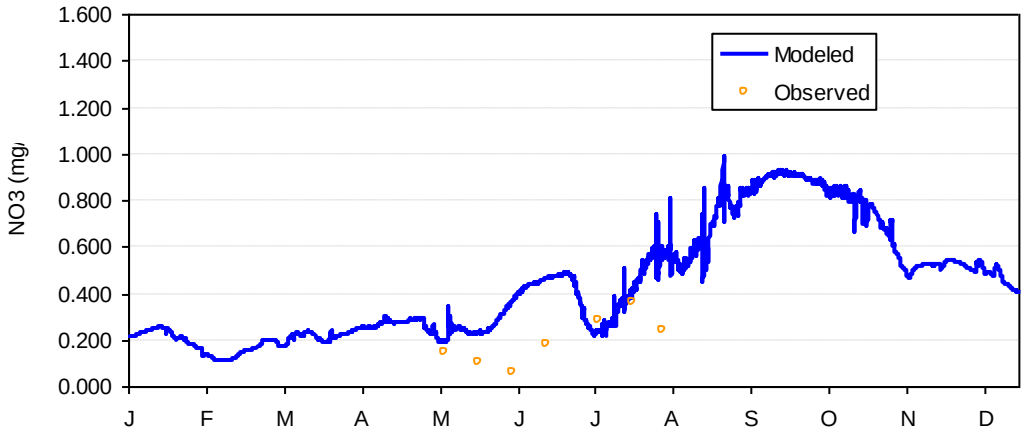

Figure K-5. NO_3 calibration at Klamath River below Iron Gate Dam (Hatchery Br) (2000).

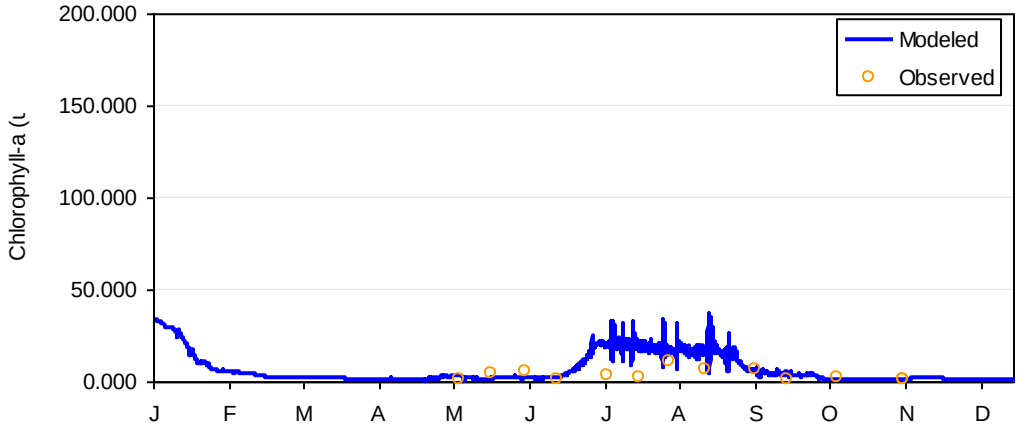

Figure K-6. Chlorophyll-a calibration at Klamath River below Iron Gate Dam (Hatchery Br) (2000).

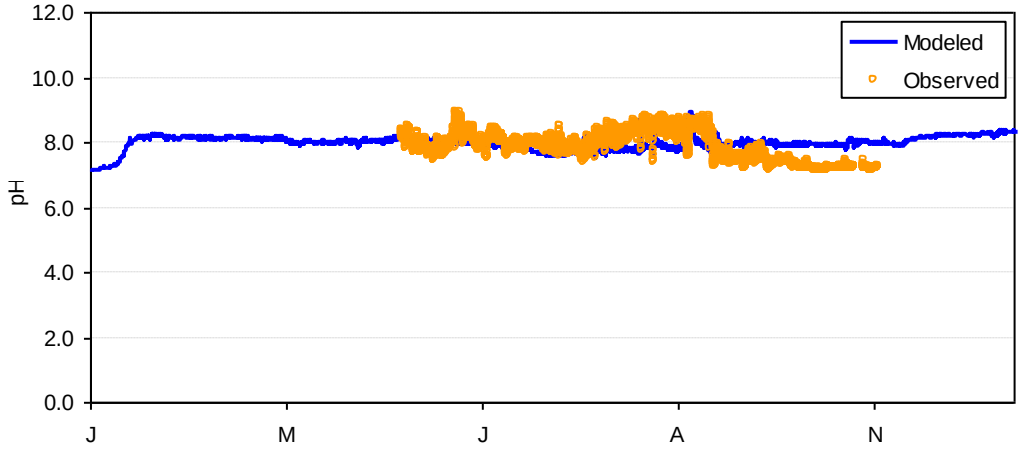

Figure K-7. pH calibration at Klamath River below Iron Gate Dam (Hatchery Br) (2000).

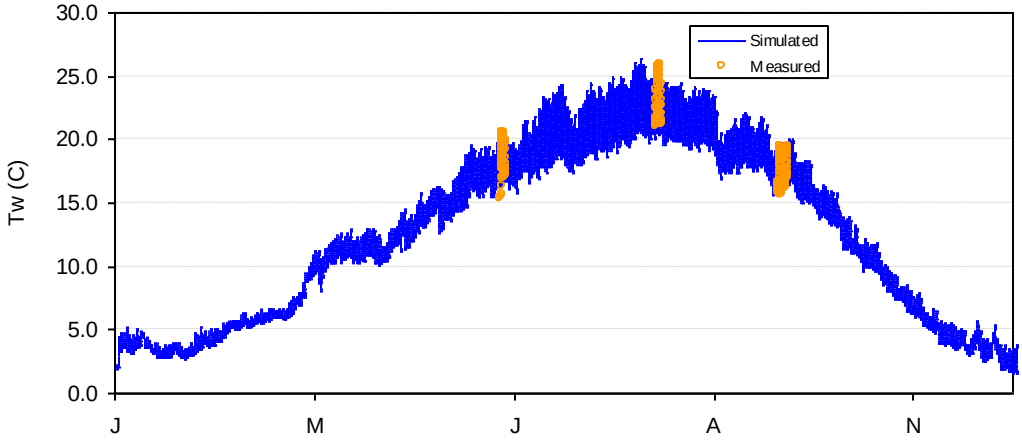

Figure K-8. Temperature calibration at Klamath River above Shasta River (2000).

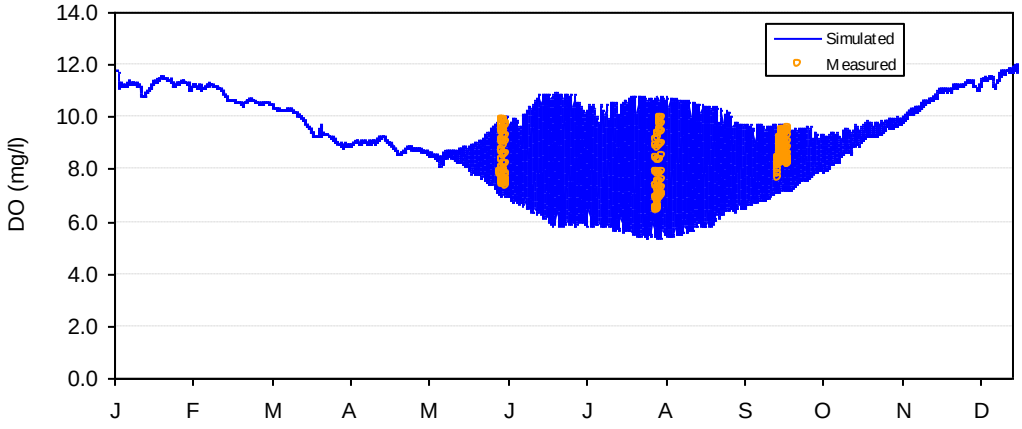

Figure K-9. Dissolved oxygen calibration at Klamath River above Shasta River (2000).

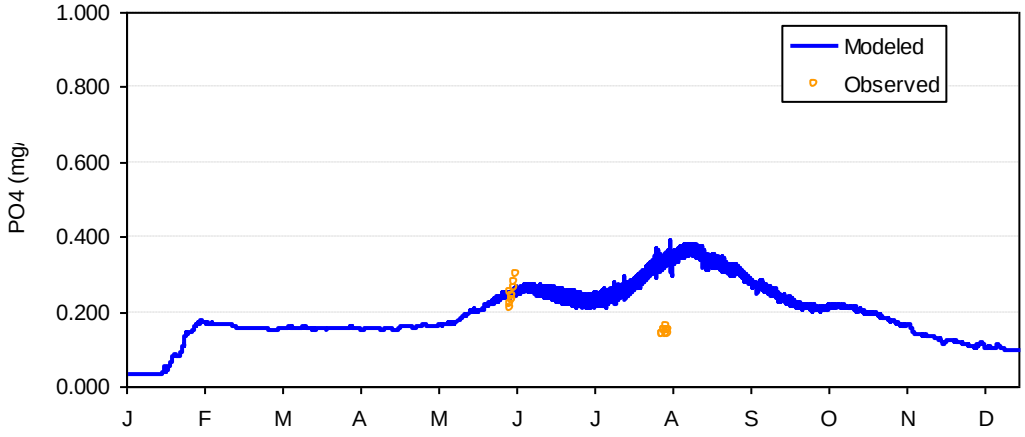

Figure K-10. PO_4 calibration at Klamath River above Shasta River (2000).

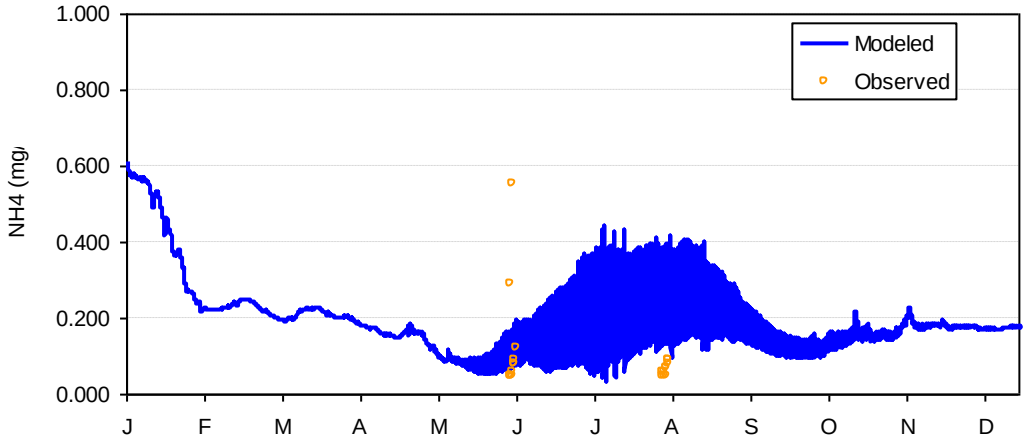

Figure K-11. NH_4 calibration at Klamath River above Shasta River (2000).

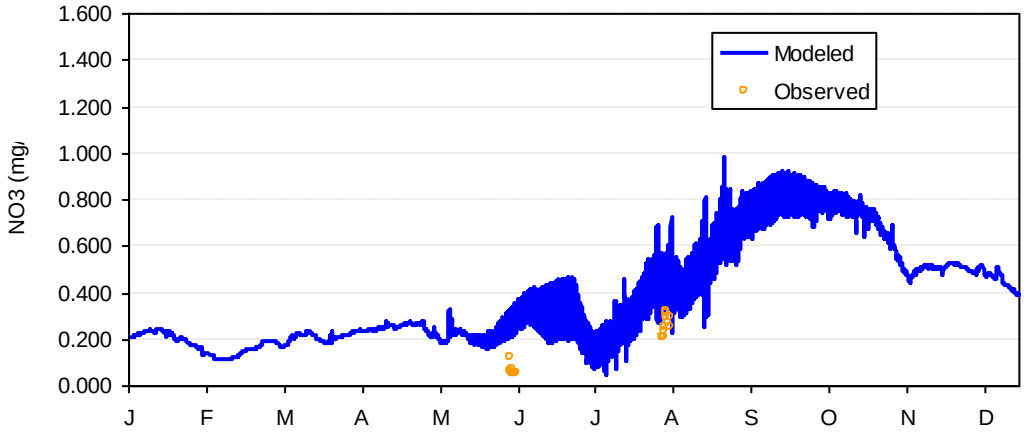

Figure K-12. NO_3 calibration at Klamath River above Shasta River (2000).

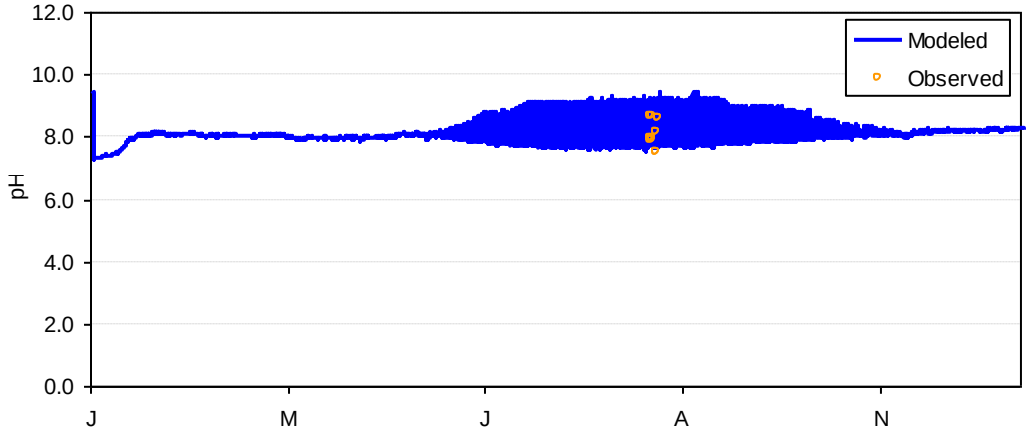

Figure K-13. pH calibration at Klamath River above Shasta River (2000).

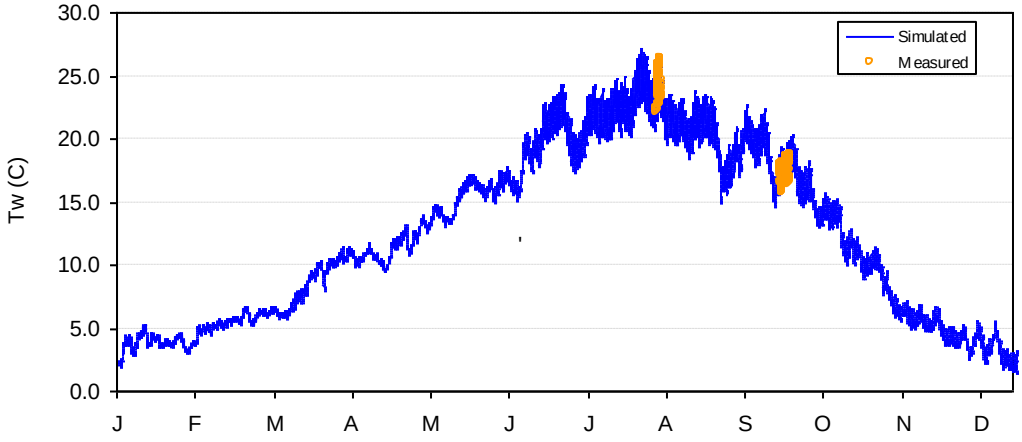

Figure K-14. Temperature calibration at Klamath River above Scott River (2000).

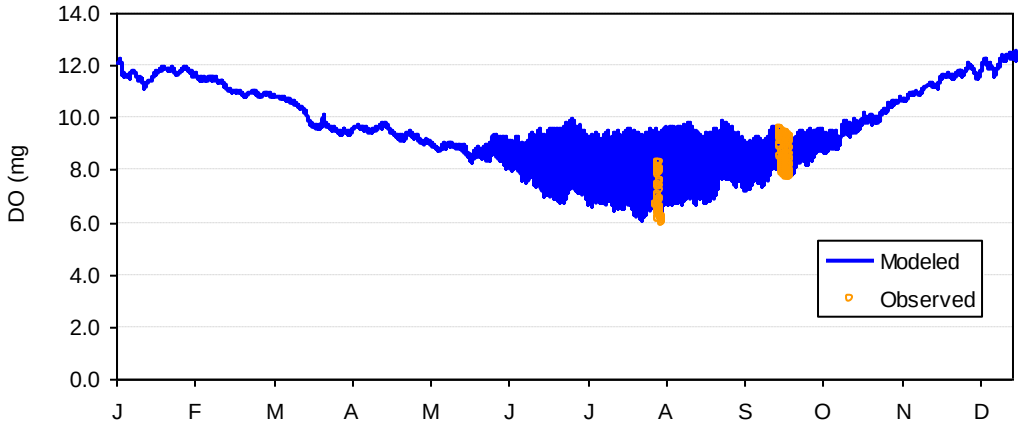

Figure K-15. Dissolved oxygen calibration at Klamath River above Scott River (2000).

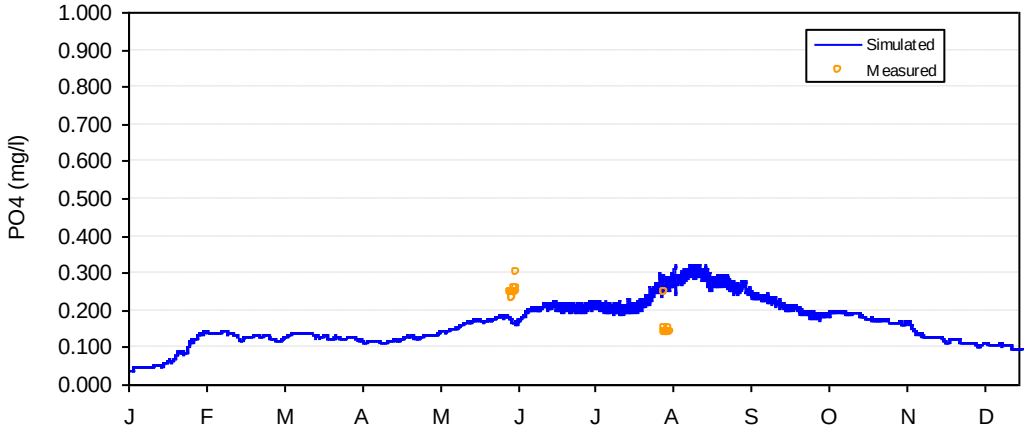

Figure K-16. PO_4 calibration at Klamath River above Scott River (2000).

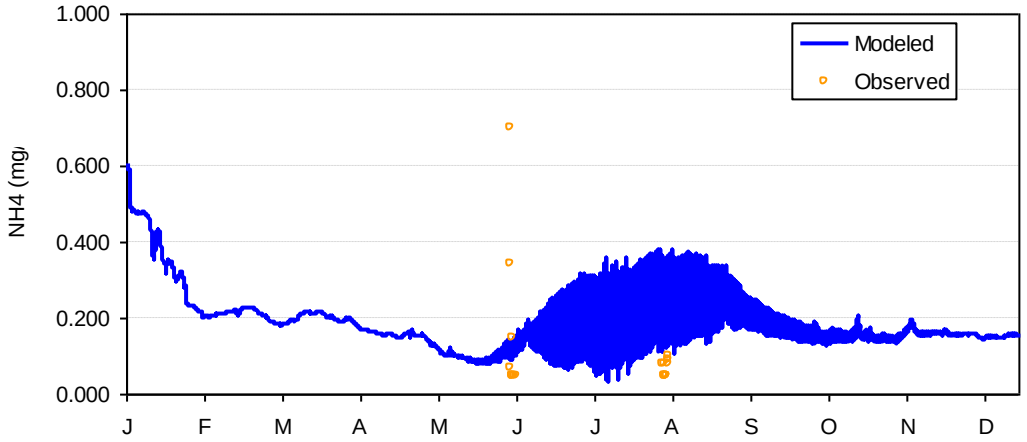

Figure K-17. NH_4 calibration at Klamath River above Scott River (2000).

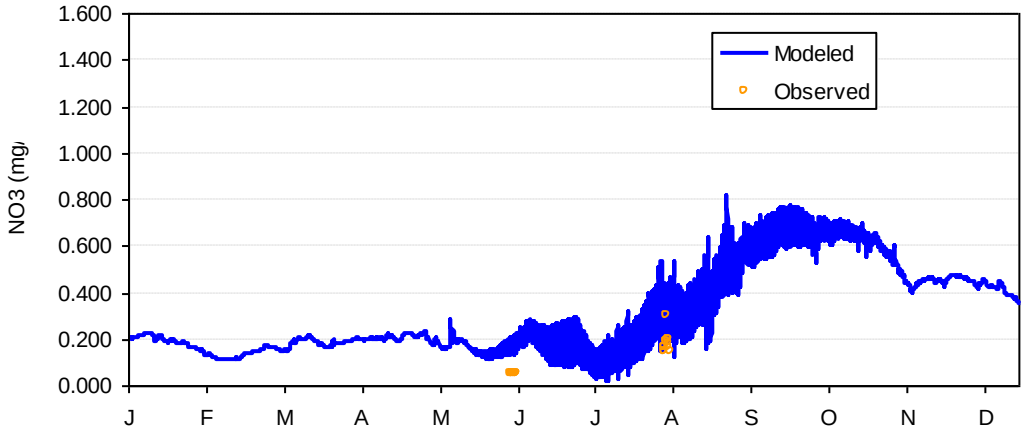

Figure K-18. NO_3 calibration at Klamath River above Scott River (2000).

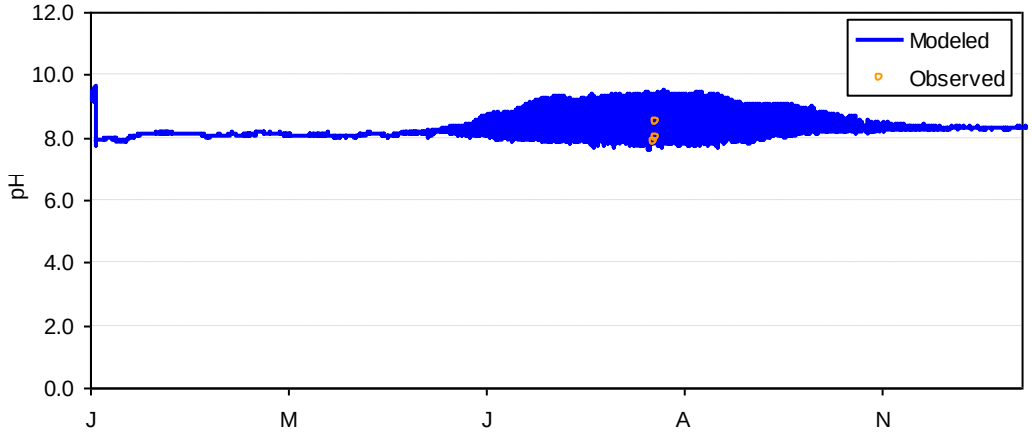

Figure K-19. pH calibration at Klamath River above Scott River (2000).

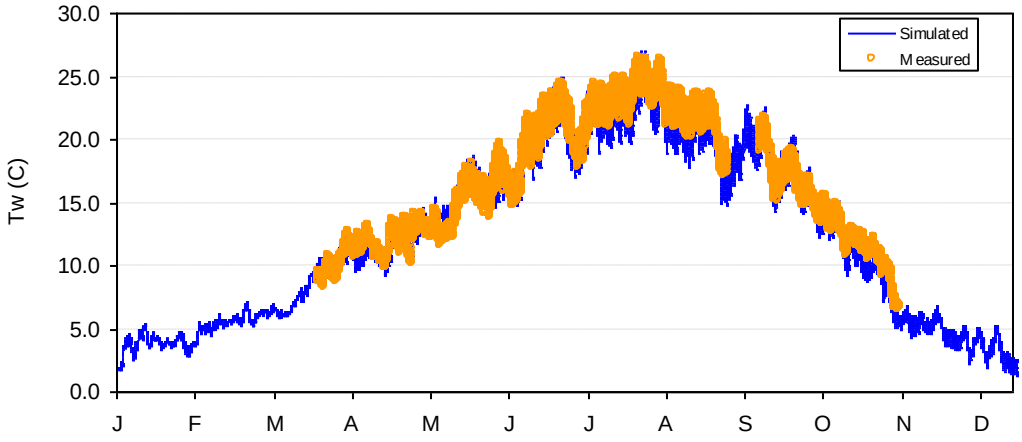

Figure K-20. Temperature calibration at Klamath River above Seiad Valley (2000).

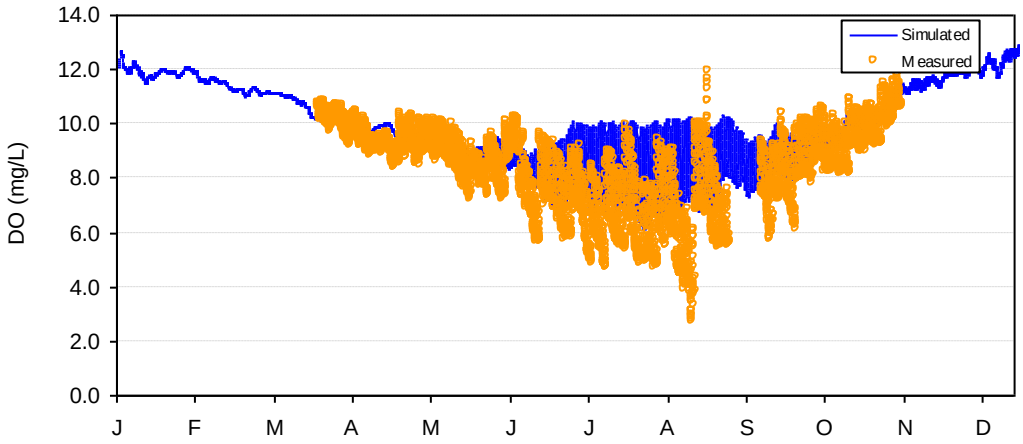

Figure K-21. Dissolved oxygen calibration at Klamath River above Seiad Valley (2000).

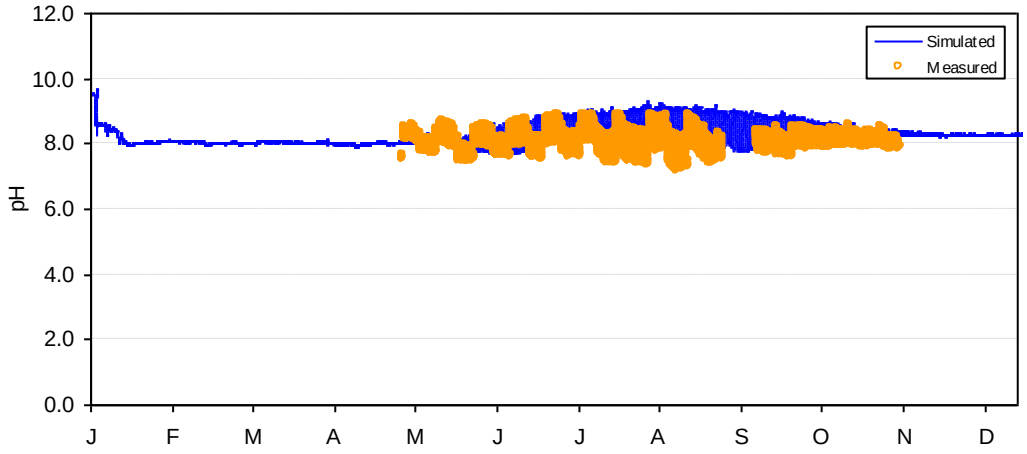

Figure K-22. pH calibration at Klamath River above Seiad Valley (2000).

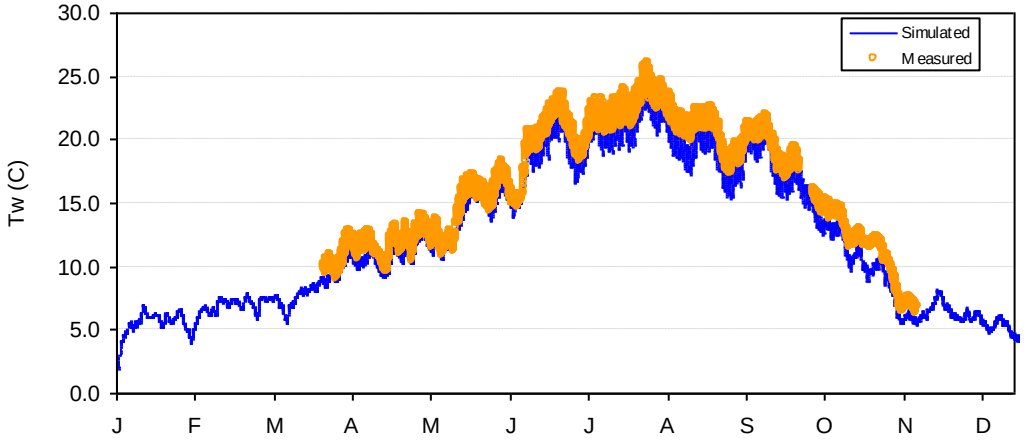

Figure K-23. Temperature calibration at Klamath River at Youngs Bar (2000).

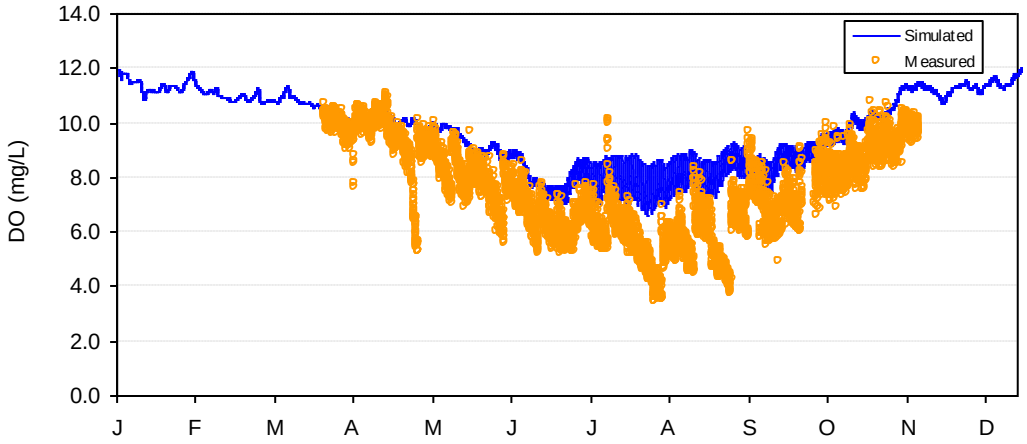

Figure K-24. Dissolved oxygen calibration at Klamath River at Youngs Bar (2000).

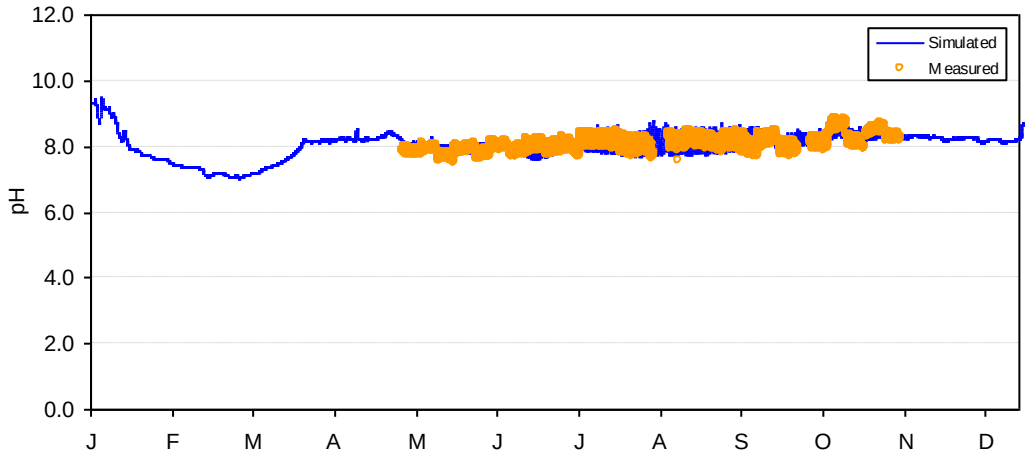

Figure K-25. pH calibration at Klamath River at Youngs Bar (2000).

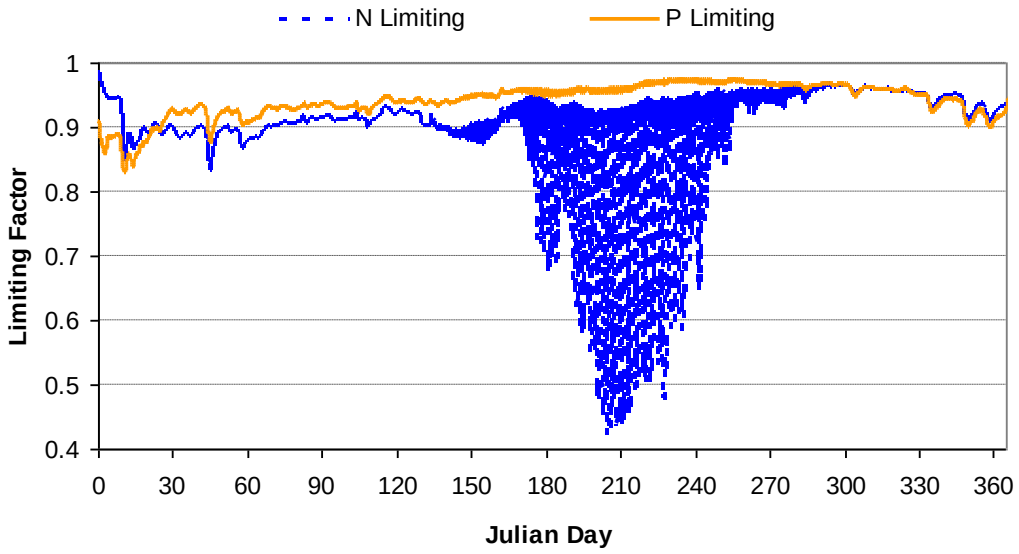

Figure K-26. Simulated Nutrient Limiting Condition at Klamath River at Turwar (2000).

Appendix L

Calibration Results for Turwar to the Pacific Ocean (Modeling Segment 9)

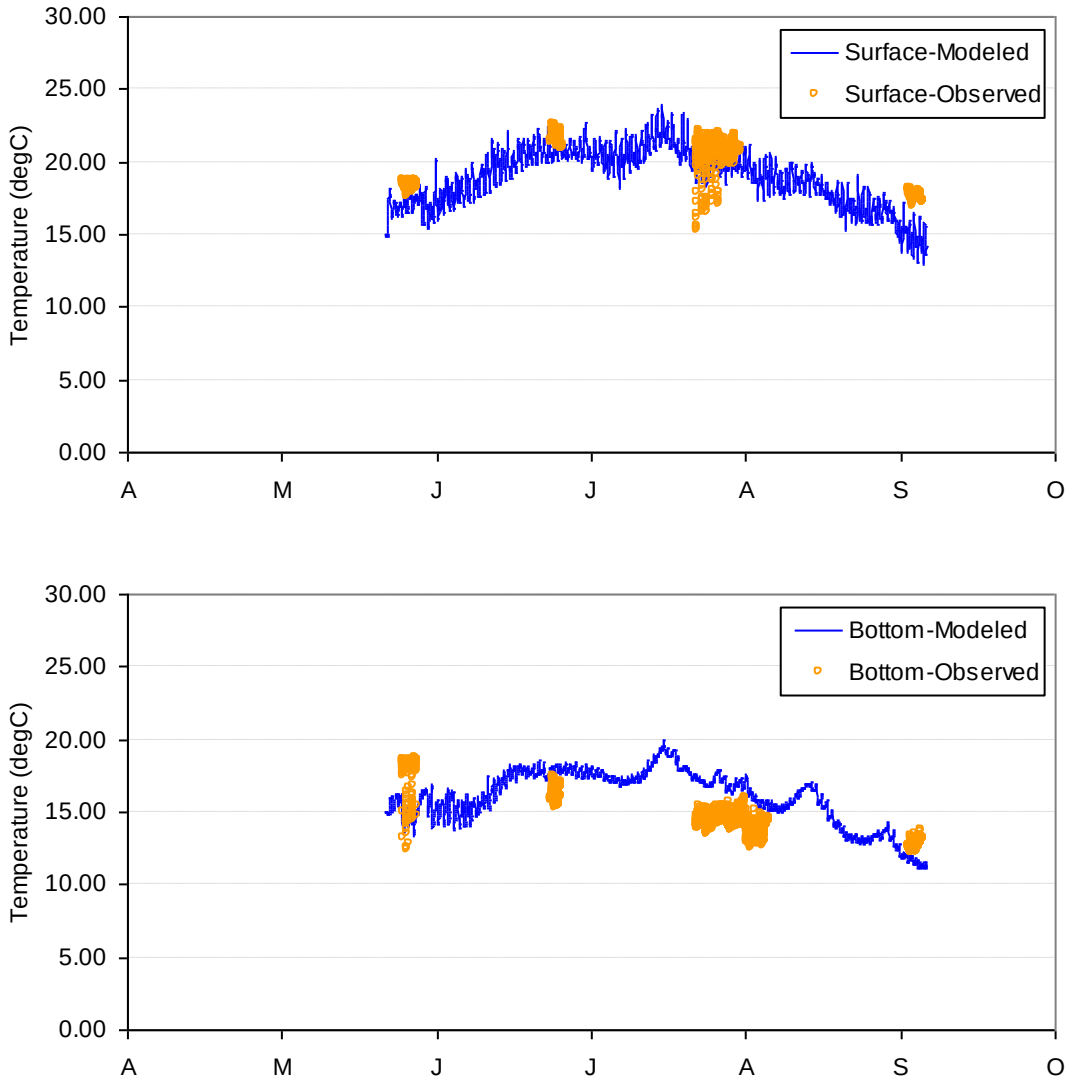

Figure L-1. Lower estuary temperature calibration (2004).

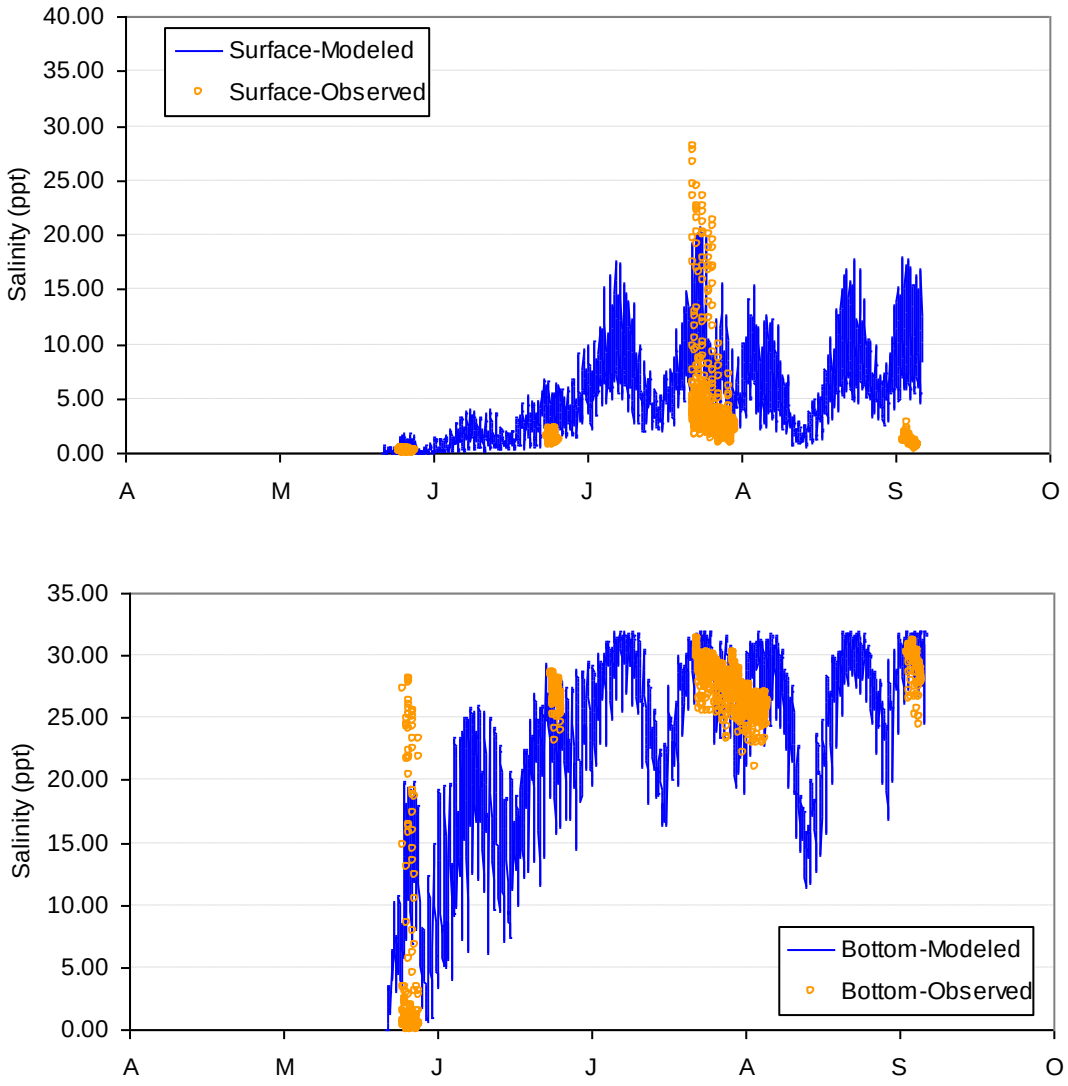

Figure L-2. Lower estuary salinity calibration (2004).

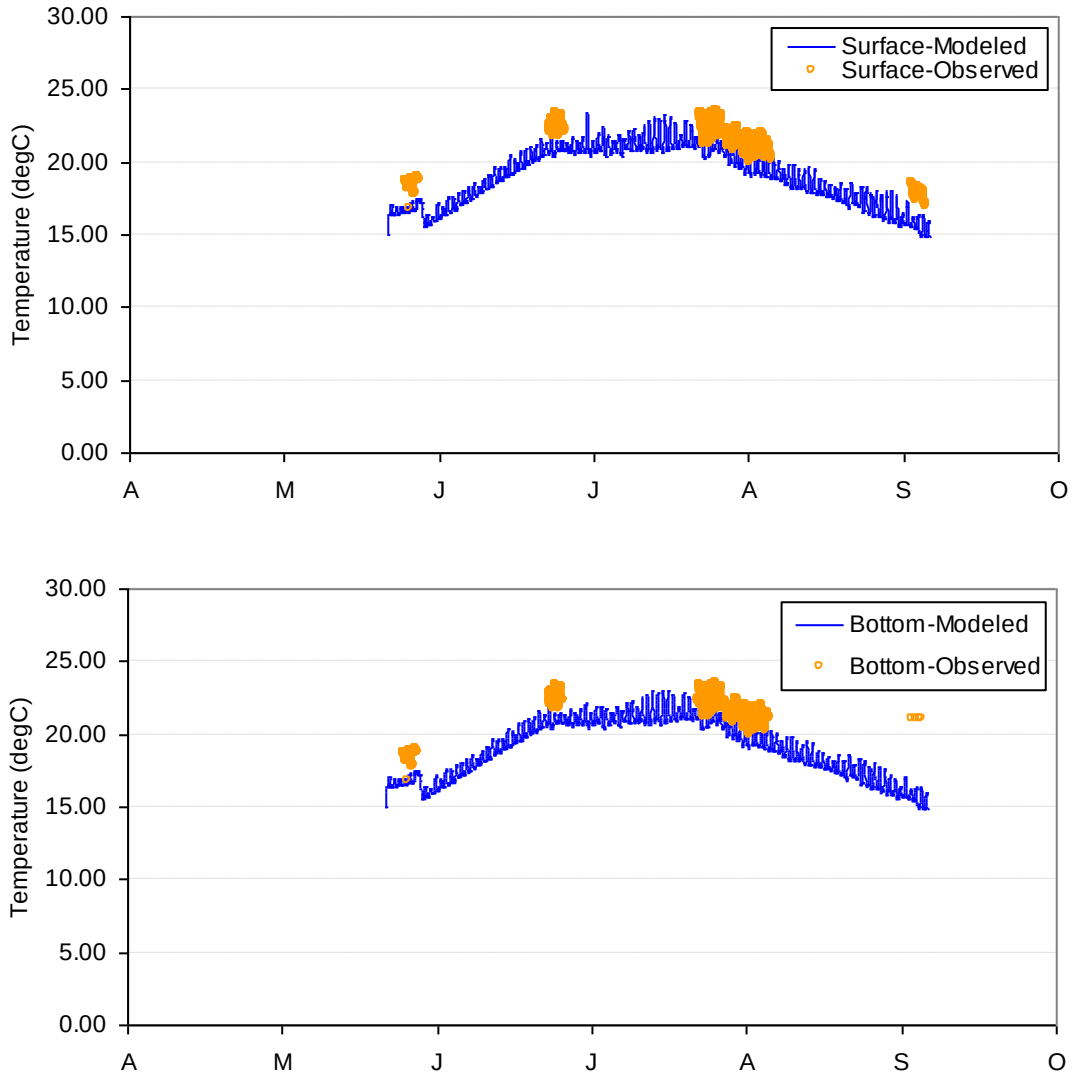

Figure L-3. Middle estuary temperature calibration (2004).

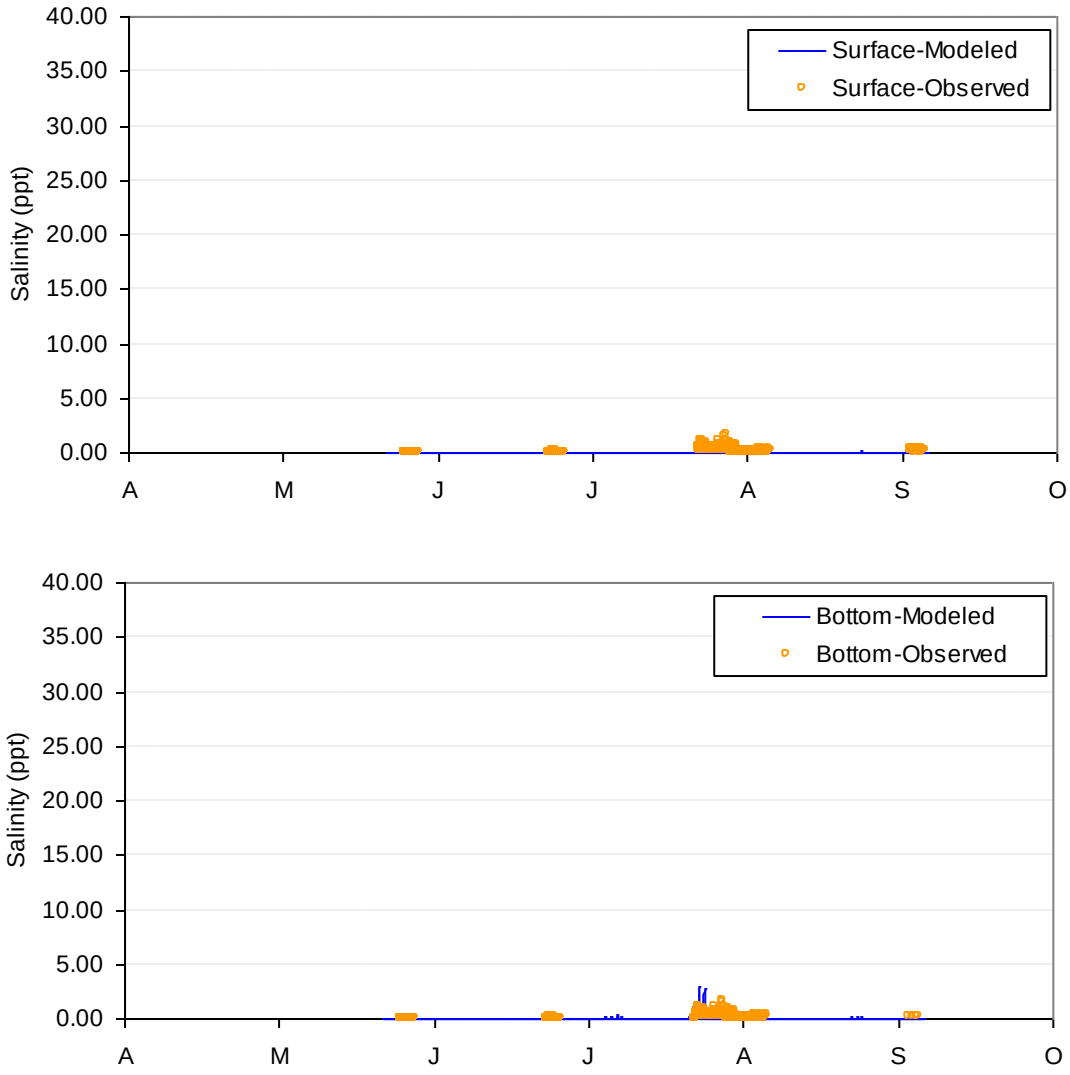

Figure L-4. Middle estuary salinity calibration (2004).

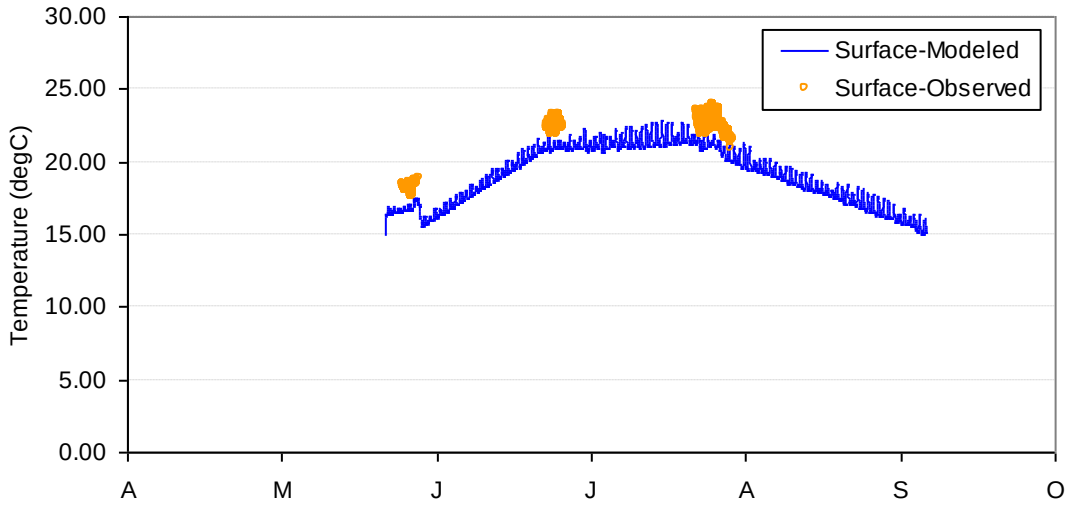

Figure L-5. Upper estuary temperature calibration (2004).

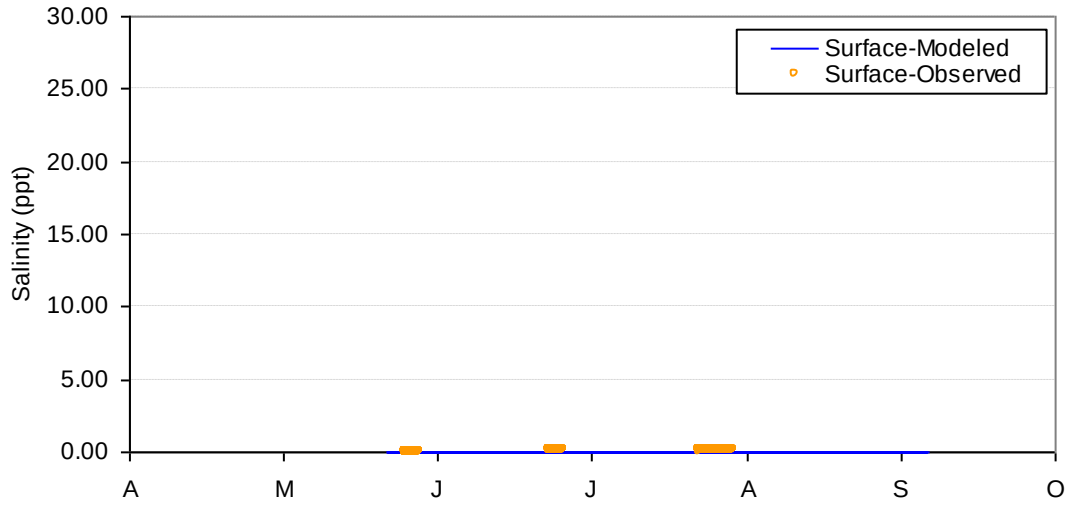

Figure L-6. Upper estuary salinity calibration (2004).

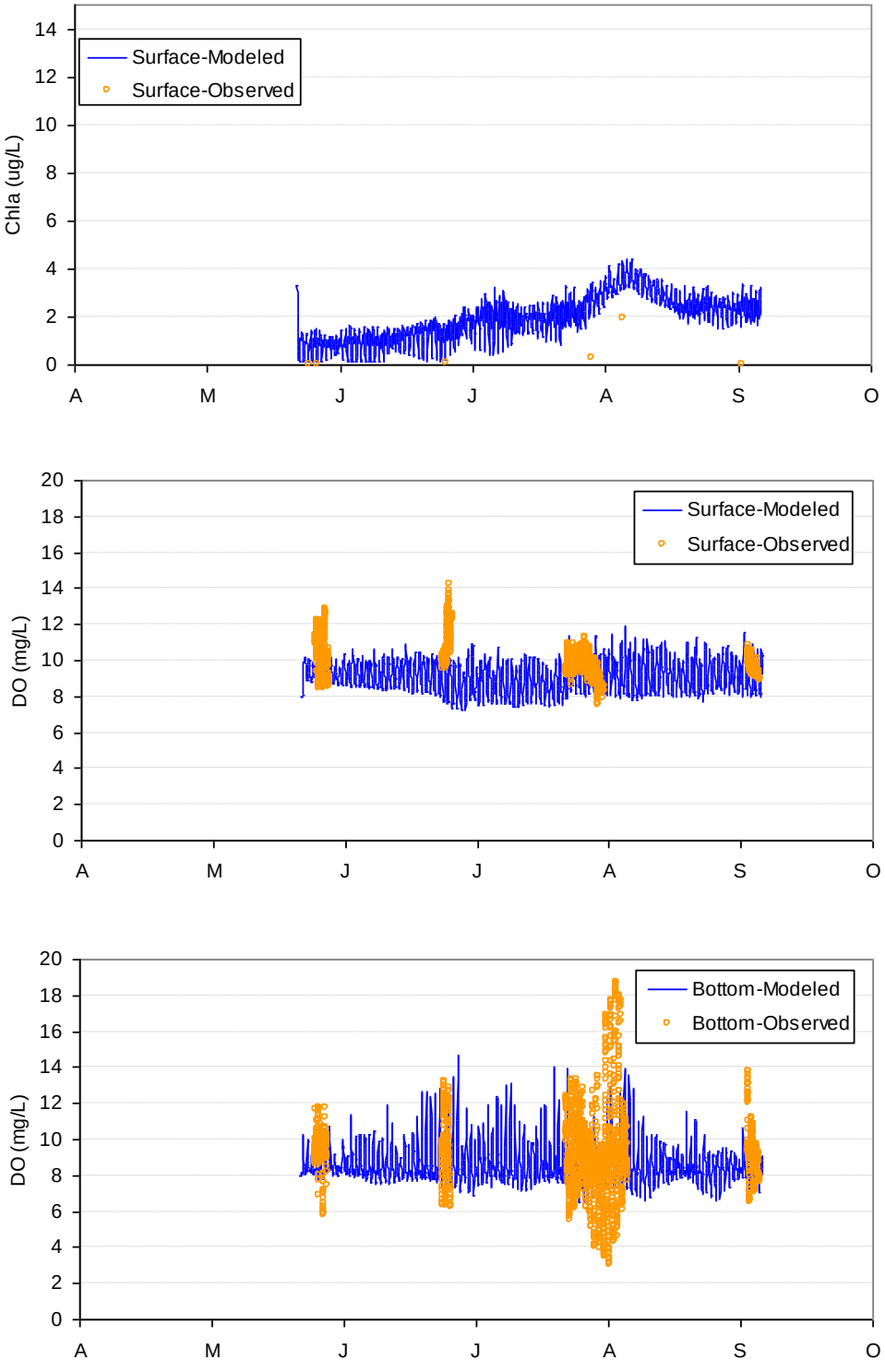

Figure L-7. Chlorophyll *a* and dissolved oxygen calibration results at the lower estuary water quality station (2004).

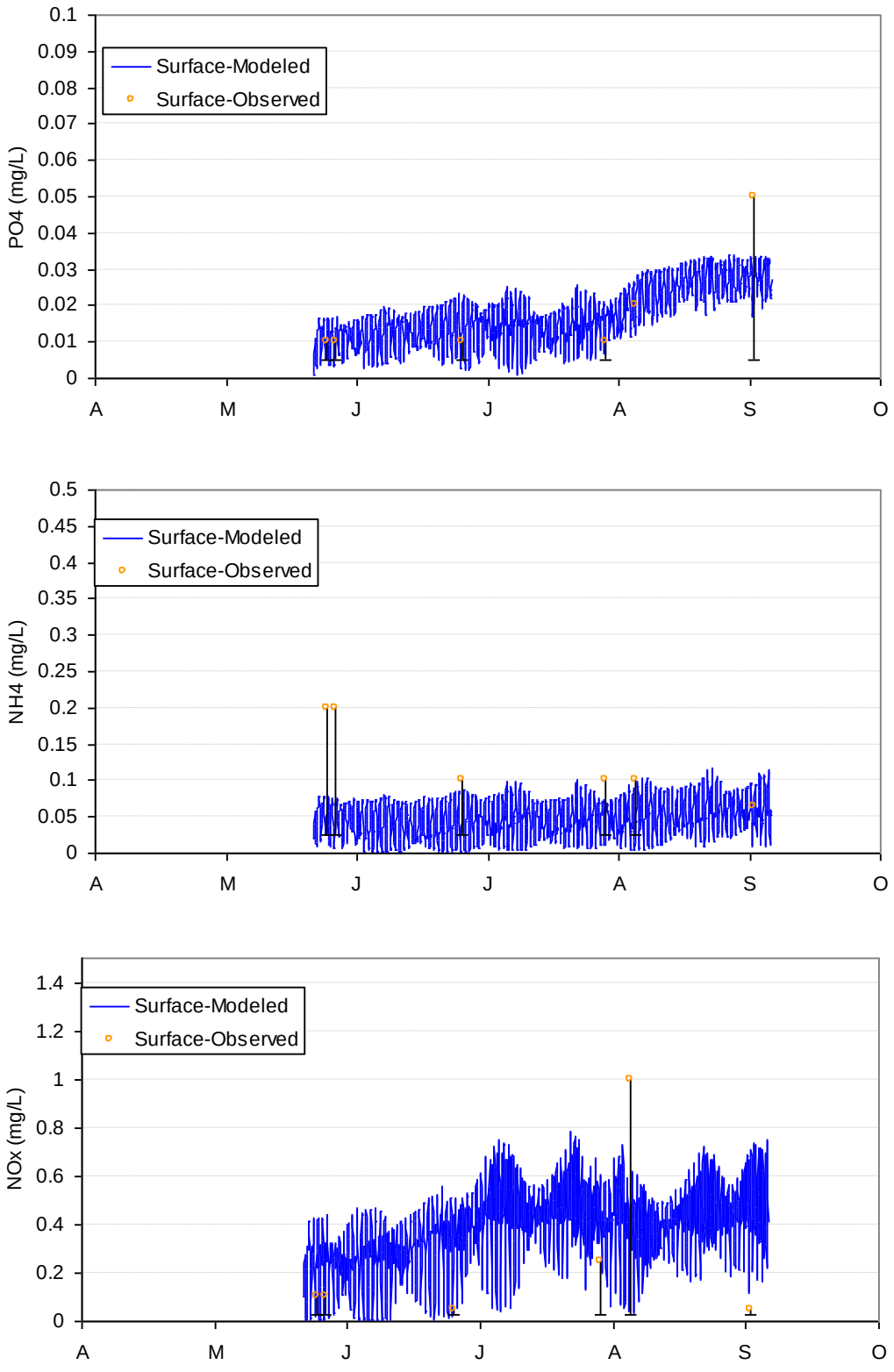

Figure L-7 (continued). PO_4, NH_4, and NO_x calibration results at the lower estuary water quality station (2004).

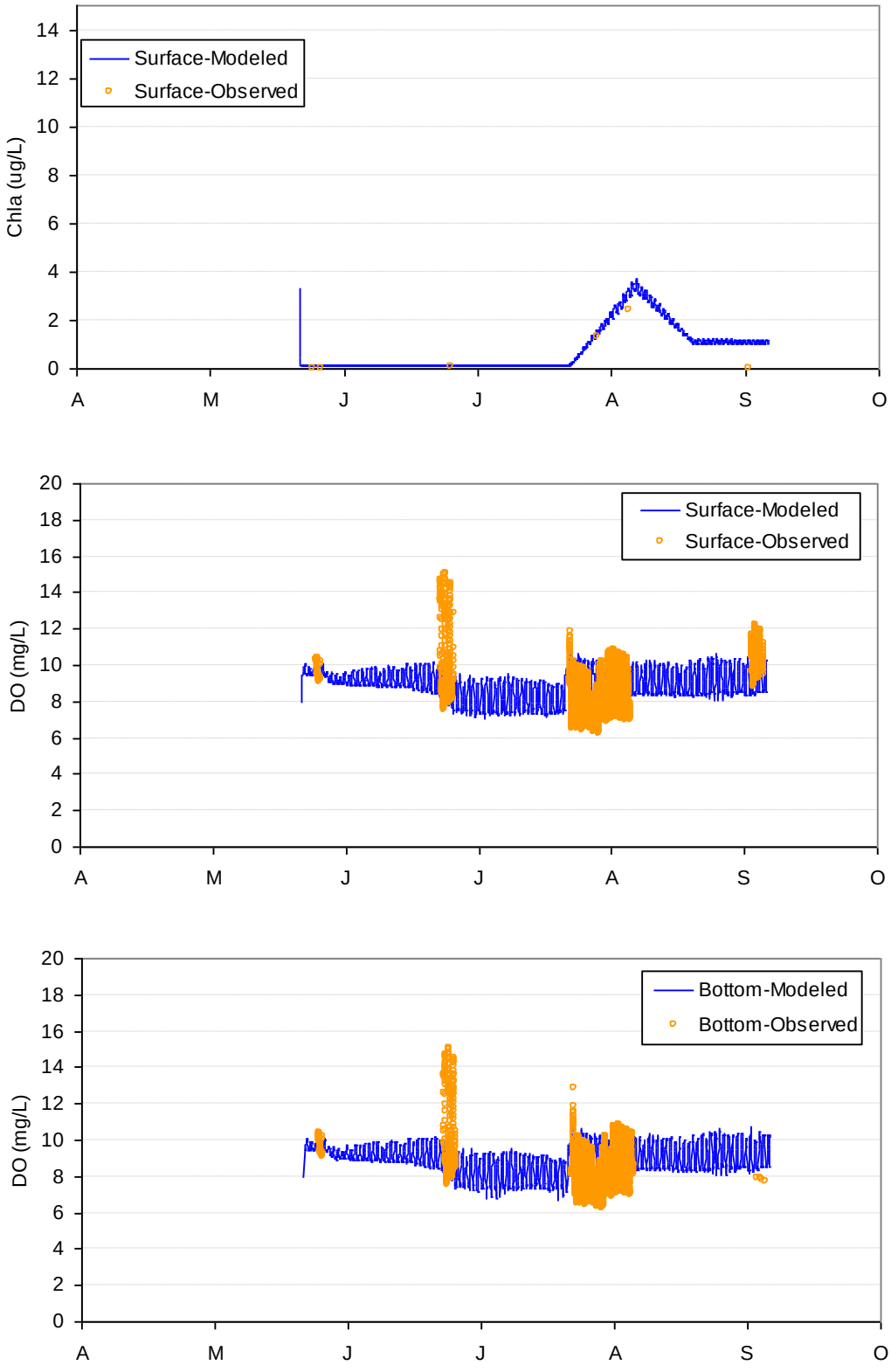

Figure L-8. Chlorophyll *a* and dissolved oxygen calibration results at the middle estuary water quality station (2004).

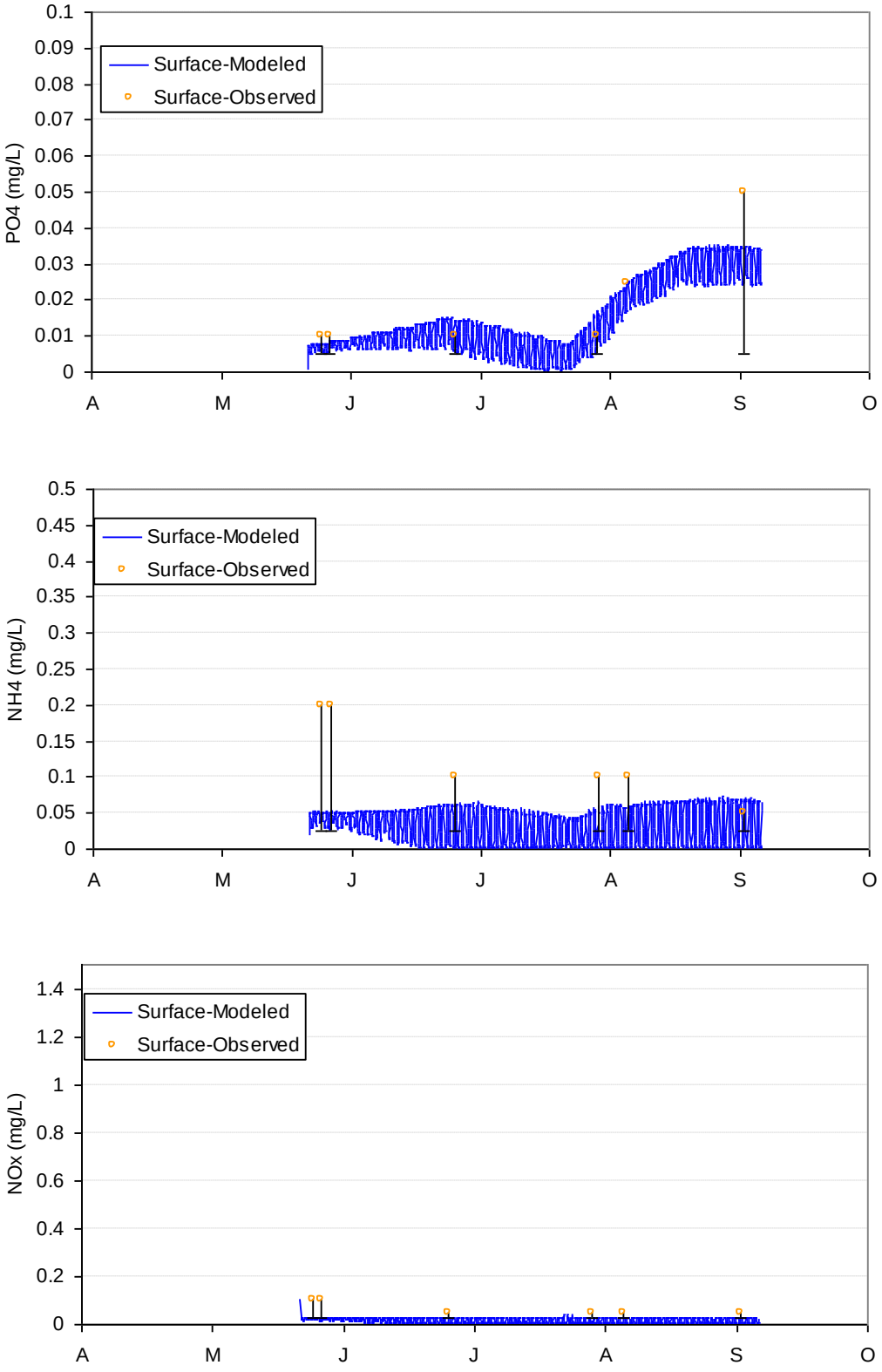

Figure L-8 (continued). PO_4, NH_4, and NO_x calibration results at the middle estuary water quality station (2004).

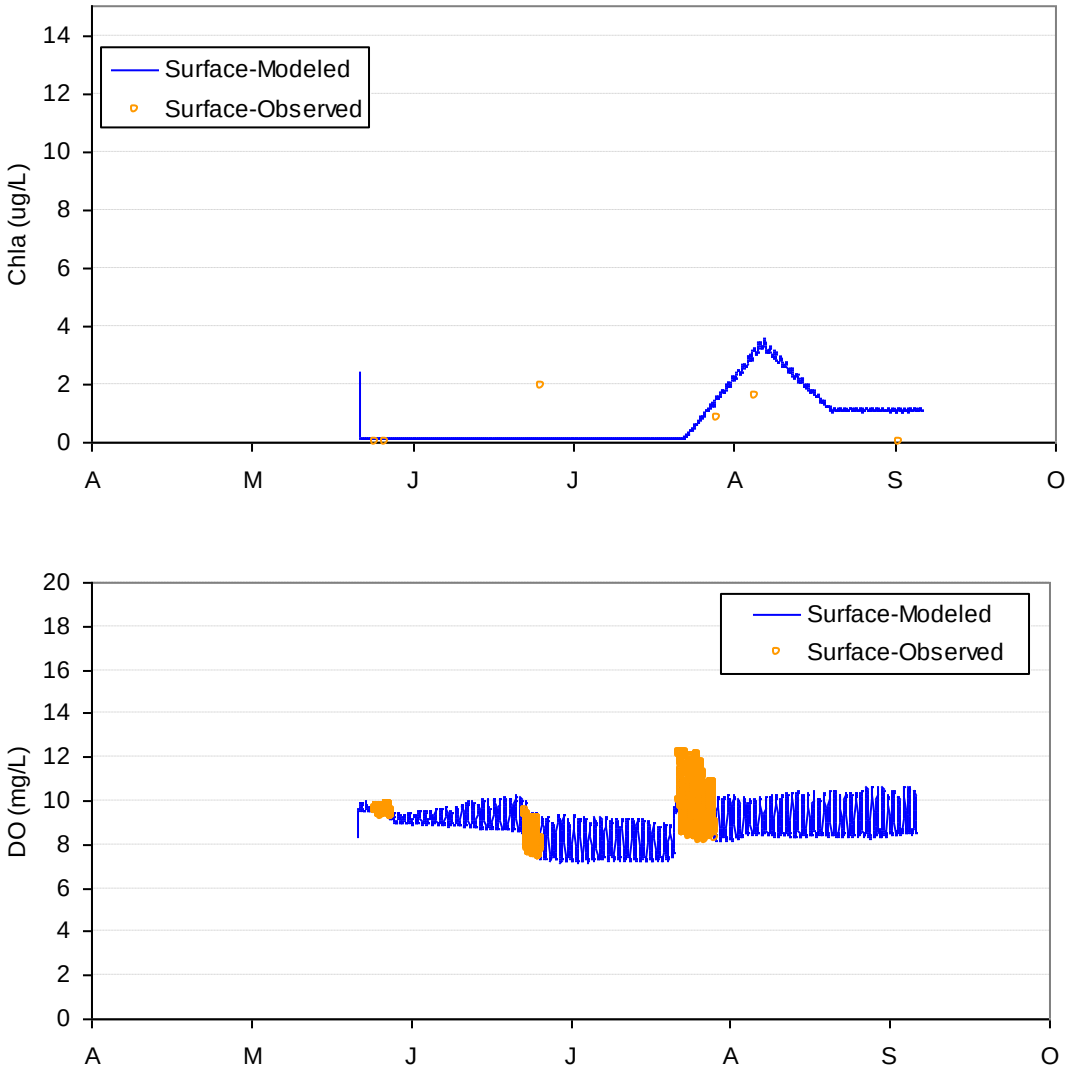

Figure L-9. Chlorophyll *a* and dissolved oxygen calibration results at the upper estuary water quality station (2004).

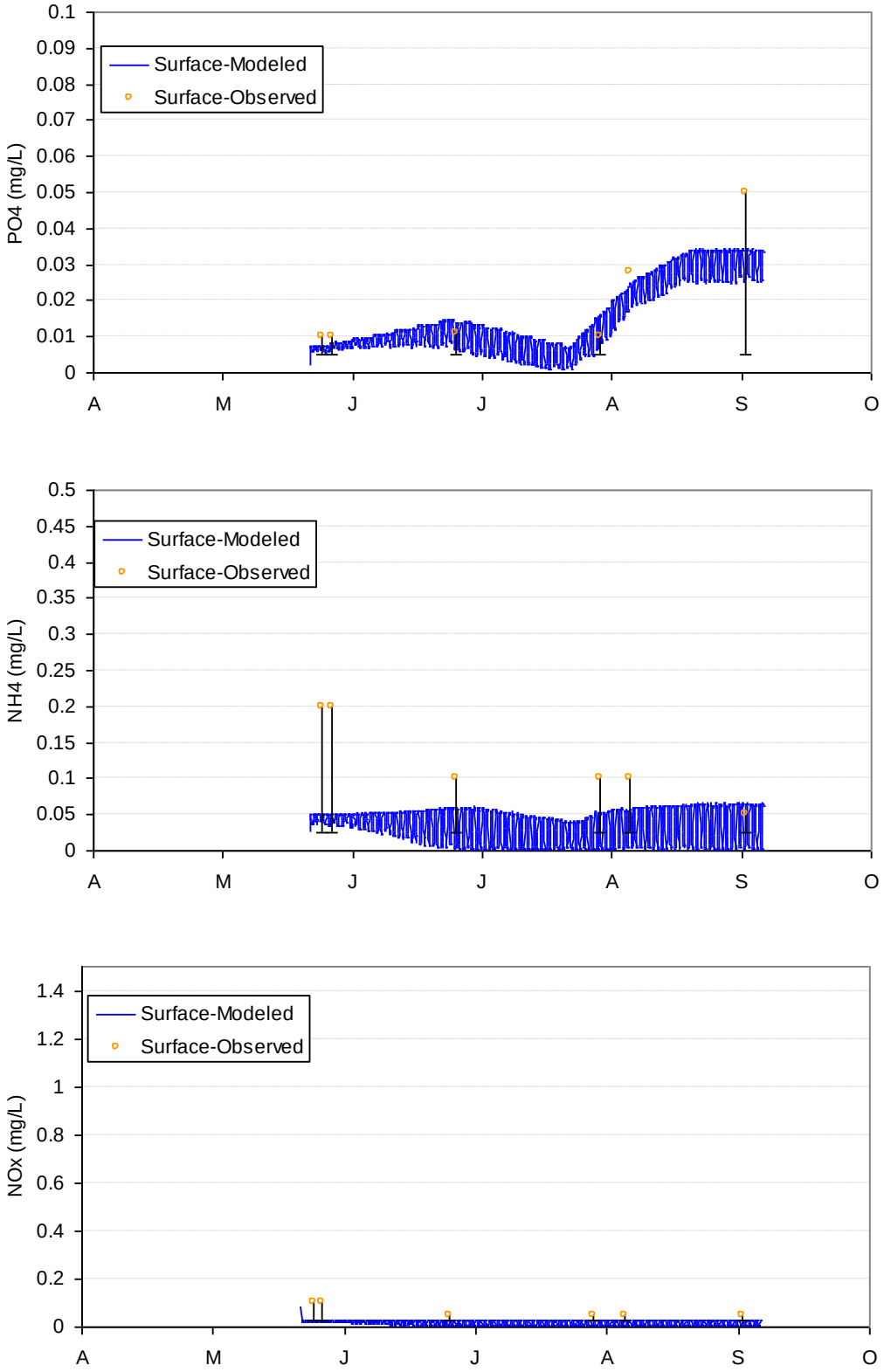

Figure L-9 (continued). PO_4, NH_4, and NO_x calibration results at the upper estuary water quality station (2004).